

Table of Contents - Issue 28, 2009

Full papers:

Fireworks on the Sumida River <i>Damien Liu-Brennan and Tadao Yoshida</i>	3
Metal–Fluorocarbon Pyrolants: IX. Burn rate and Radiometric Performance of Magnesium/Teflon/Viton (MTV) Modified with Zirconium <i>Ernst-Christian Koch</i>	16
Effects of Variation of Component Content on the Colored Flame of Firework Star Compositions <i>Kazuomi Itoh, Hideo Watanabe, Dayu Ding and Tadao Yoshida</i>	19
A New And Fast Method Of Evaluating Powder Energy <i>Andrew Tang, Hilary Chen and Andy Tang</i>	37
Characteristics of the Red Colored Flame of Firework Compositions <i>Dayu Ding, Daichi Tabata and Tadao Yoshida</i>	51
Pyrotechnically Relevant Salts of 1-(2-Chloroethyl)-5-nitriminotetrazole – Synthesis and Coloring Properties <i>Thomas M. Klapötke, Jörg Stierstorfer and Karina R. Tarantika</i>	61
Emissions of Reaction Products and Sound from Outdoor and Indoor Firework Displays <i>Andreas Dutschke, Stefan Seeger, Lutz Kurth, Ulrich Pannea, and Christian Lohrer</i>	78
Hazard Assessment and Effect of Nano-Sized Oxidizer on Sound Level Analysis of Firecrackers <i>T. L. Thanulingam, A. Jeya Rajendran, P. Karlmarx, K. Subramanian and A. Azhagurajan</i>	95
Ergonomic Hazards in Local Fireworks Factories <i>Stanley Azzopardi</i>	112
Information for authors	122
Sponsors	123

Journal of Pyrotechnics

Policy Board Members

Ettore Contestabile

Canadian Explosive Research
Lab
555 Booth Street
Ottawa, Ontario KA1 0G1
Canada

Per Alenfelt

Nammoliab AB
Sweden

Rutger Webb

TNO Defence, Security and
Safety
P.O. Box 45
NL-2280 AA Rjswijk
The Netherlands

Alexander van Oertzen

Unter den Eichen 87
12205 Berlin
Germany

Tadao Yoshida

Ashikaga Institute of Technology
268-1 Omae-cho, Ashikaga-shi,
Tochigi 326-8558, Japan

Matthew Davies

Health & Safety Laboratory
Harpur Hill, Buxton
Derbyshire
SK17 9JN, UK

Bonnie Kosanke

PyroLabs Inc
1775 Blair Road
Whitewater
CO 81527, USA

Tom Smith

Davas Ltd
8 Aragon Place, Kimbolton
Huntingdon, Cambs.
PE28 0JD, UK

Technical Editors for this issue

Mark Williams**Scot Anderson****Christian Lohrer****Tony Cardell****EC Koch****John Perriam****Stanislaw Cudzilo****Martin Guest****Georg Steinhauser**

Production Team

Publisher**Tom Smith**

Davas Ltd
8 Aragon Place, Kimbolton
Huntingdon, Cambs
PE28 0JD, UK

Phone: +44 1480 860124

Fax: +44 1480 861108

email: toms@davas.co.uk

Production Editor**Helen Saxton**

Davas Ltd
8 Aragon Place, Kimbolton
Huntingdon, Cambs
PE28 0JD, UK

Phone: +44 1480 860124

Fax: +44 1480 861108

email: helens@davas.co.uk

Publishing Consultant**Bonnie Kosanke**

1775 Blair Road,
Whitewater
CO 81527, USA

Phone: +1-970-245-0692

Fax: +1-970-245-0692

email: bonnie@jpyro.com

Fireworks on the Sumida River

Damien Liu-Brennan^{a*} and Tadao Yoshida^b

^aMacquarie University (Japanese Studies), Sydney, NSW, Australia, 2109

Email: damien.liu-brennan@students.mq.edu.au

^bAshikaga Institute of Technology, 286-1 Omae-cho, Ashikaga-shi, Tochigi-ken, 326-8558, Japan

Tel: +81 284 62 0605, fax: +81 284 62 0976, email: yoshida@ashitech.ac.jp

Abstract: *Fireworks (hanabi) were originally displayed on the Sumida River in 1733 as a memorial service for the victims of starvation due to crop failures and plague, and an epidemic of cholera. The fireworks display originated as the “Ryōgoku Kawabiraki Hanabi” (Ryōgoku River-Opening Fireworks) with only 20 fireworks displayed. Although the display has experienced several interruptions historically, it has evolved into what is known today as the “Sumidagawa Hanabi Taikai” (Sumida River Fireworks Display). Currently, a total of about twenty thousand hanabi shells are displayed from two separate firing locations on the river, and in conjunction with this, a fireworks competition is held at one of the locations. This paper describes the history, evolution, and current status of the display.*

Keywords: *Sumida River; fireworks history, Japanese fireworks, hanabi, Kagiya, Tamaya, Ryōgoku*

Introduction

Fireworks (*hanabi*) were introduced to Japan over 400 years ago and have since established a significant position in Japanese society and culture. The Sumida River stands testament to this with a continuing tradition of fireworks for over 275 years. Ironically, the historical documentation of fireworks in Japan is sporadic and somewhat incomplete, whilst documentation in English is minimal and usually confined to one or two paragraphs of general content consubstantially recounted in book chapters or seasonal articles. This can be exemplified by the reputable Sumida River Fireworks Festival, which, whilst arguably the most recognized fireworks festival in Japan, has only some aspects of its history known, with consideration rarely going beyond a brief account and handing down of the Kagiya and Tamaya legend; and perhaps a general understanding of the circumstances behind the origins of the festival, with little or no reference to recent or current

events.

Taking this into consideration, this paper intends to collate the history and evolution of Sumida River fireworks, increase the scope of current understanding with further annexation, and update the status of Sumida River fireworks history with the addition of recent and current events.

Origin of Ryōgoku River-opening fireworks

In 1732, Japan was devastated by nationwide crop failures and a plague in which nearly one million people died from the ensuing famine. Furthermore, in Edo (now Tokyo), a cholera epidemic broke out infecting many people and causing many further deaths and it was said that many corpses were discarded on the streets.¹

The following year, to alleviate superstition associated with these tragic incidences, Tokugawa Yoshimune,² the 8th Tokugawa Shogun, held a

Article Details

Manuscript Received:- 19/01/2009

Publication Date:-19/03/2009

Article No: - 0071

Final Revisions:- 19/03/2009

Archive Reference:-805

suijin festival (water god ritual) at Ryōgoku, where prayers were offered to the *suijin* (water god) to ward off evil spirits and assuage the souls of the dead. This coincided with the annual *kawabiraki* (a river or port opening festival) which was held in the cool of the evening on 28 May, 1733 (based on the old Japanese calendar), the first evening of the summer season. The *kawabiraki* signaled the opening of the river for boating activities and prayers were offered for safety on the river and at sea throughout the summer season (May 28 to August 28). During the summer season, people relaxed along the riverbanks or on various types of boats while enjoying the cool breeze of the summer evenings. The *misemonokoya* (show booths) around Ryōgoku were crowded and *yataimise* (portable stalls) along the riverbanks were allowed to open until late in the night. Also, on May 28, the riverside restaurants at Ryōgoku held a *kawasegaki* (a special memorial service for those who had drowned in the river).

As part of the memorial and *kawabiraki*, fireworks were displayed at Ryōgoku by the 6th generation master of the Kagiya (house), and the number of fireworks displayed was said to be about 20. Black powder consisting of saltpeter, sulfur, and charcoal, was used for fireworks but was not able to give such bright colors as seen today. Nevertheless, the citizens of Edo at that time were delighted by the fireworks display.

1733 thus marks the commencement of the *Ryōgoku kawabiraki hanabi* (Ryōgoku River-Opening Fireworks), which has since evolved into the Sumida River Fireworks Display.

Emergence of Kagiya and Tamaya

The Kagiya name began in 1659 when Kagiya Yahei, from Shinohara-mura (located in the present Nara Prefecture), came to Edo and opened a fireworks shop (house)³ at Yokoyama-chō, thus founding what would become the Kagiya dynasty. Fireworks were already popular in Edo before the arrival of Kagiya, however, due to the impending hazard of fire amongst the large numbers of wooden houses and shops, several official notices had been issued (notably in 1648, 1652, 1655, 1670, and 1680)^{4,5} forbidding fireworks to be displayed in most areas and outlining harsh penalties such as expulsion from the city for anyone responsible for

causing fire damage. Despite this, Kagiya obtained a good reputation earned by making specialized fireworks, like Roman candles, that shot out two or three stars.⁴

In about 1700, the 4th generation master of the Kagiya (house) was appointed as a purveyor to the Tokugawa Shogunate and was officially recognized as the first private fireworks manufacturer. By this time, fireworks usage was restricted to the surrounds of the Sumida River which had become somewhat of a playground for fireworks. Many river craft such as *chokibune* (small open boats), *yanebune* (roofed boats), and *yakatabune* (larger specialized roofed pleasure ships) appeared on the waters in the cool of the summer evenings hosting patrons who would relish in the festivities. During this period, the nobility and rich merchants of Edo often rivaled each other by financing Kagiya to display fireworks for them.

In 1808, a talented apprentice in the Kagiya (house) by the name of Seishichi emerged, demonstrating excellent skills. The 8th generation master of the Kagiya (house) helped Seishichi set up his own business at Yoshikawa-cho, thus branching out from the Kagiya (house). Seishichi took on the name Tamaya Ichibei and after not too long his reputation exceeded that of his former master.⁶ Consequently, the Ryōgoku *kawabiraki* saw both Kagiya and Tamaya preparing separate ships of fireworks at the upper and lower streams of the Ryōgoku Bridge and competing with each other by displaying their new creations. Both houses were renowned as the most outstanding *hanabishi* (fireworks masters) of the time and shouts of encouragement: “*Tamaya! Kagiya!*” were echoed across the Sumida River as each launched their creations, and it could be said that this event united people from the two domains on either side of the river.

On 14 October, 1843, a fire broke out in the Tamaya storehouse and the conflagration destroyed many houses in the neighborhood. This was considered unfavorable fortune as it occurred the day before Tokugawa Ieyoshi, the 12th Tokugawa Shogun, was to visit and pay respects at the ancestral Tōshōgū Shrine in Nikkō (enshrining the founder of the Tokugawa Shogunate, Tokugawa Ieyasu). As a result, Tamaya was banished from Edo and the Tamaya (house) lapsed from existence.

Meanwhile, the Kagiya (house) continued and evolved into a lasting dynasty. After 12 generations, however, it was succeeded by the Amano family when, in 1949, Amano Hutoshi took control and became the 13th generation master of the Kagiya (house). The Kagiya dynasty still continues today although in a different capacity as the tradition of manufacture has been discontinued and the company, whilst maintaining the Kagiya name (Sohke Hanabi Kagiya Co.), concentrates on fireworks design and event management. Currently the Kagiya (house) is in its 15th generation with Amano Akiko succeeding her father, Amano Osamu, in 2000 to become the first female director of the Kagiya dynasty.⁷ This year, 2009, marks the 350th anniversary of the Kagiya dynasty.

Despite the foregoing fate of the Tamaya (house) and the continuing success of the Kagiya (house), their exploits have significantly contributed to Japanese culture and both the names ‘Kagiya and Tamaya’ have become immortalized in Sumida and Japanese history.

Fireworks of the Edo period (1603–1868)

During the Edo period, fireworks which had previously been expensive entertainment for the nobility became available to the common people. Shops in Edo opened to sell fireworks to the general public and fireworks specifically made for children to play with were also available. Fireworks vendors called “*hanabi! hanabi! nezumi, tebotan, konguruma, karakurihanabi, hanabi!*” indicating the various types of fireworks available. A *nezumi hi* (rat fire), was a firework that scuttled along the ground like a rat; a *konguruma* one that spins on the ground; *tebotan* (hand peony) similar to the present day *senkō hanabi* (hand held sparkler); and *karakuri* (mechanism) akin to set piece fireworks.

A fireworks display program *ca.* 1800 displayed further names that appeared as fireworks in the Edo period such as *ryūsei, uchidashi, tsunabi utsushi kanagasa*, and *uchiage*.

A *ryūsei* (rising dragon/shooting star) would shoot skyward with a tail, emulating a dragon flying through the sky; an *uchidashi* was a ground shooting firework; *tsunabi utsushi kanagasa* was perhaps a firework like a traditional Japanese *tsunabi* (rope fire) firework; and an *uchiage*

(launched firework/skyrocket) was a new firework of the time that may have been a prototype for the modern day round shell.

Prior to the Edo period, Japan was at one stage the world leader in gun manufacture,⁴ however, under the Tokugawa Shogunate, gunnery was abolished and the necessity for gunnery craftsmen diminished, thus many of these craftsmen turned to making fireworks. The *daimyō* (feudal lords) who had residences along the Sumida River could view fireworks from their mansions and were inspired by the displays, thus many *daimyō* promoted these craftsmen and employed them to develop and display fireworks for them. Fireworks made under the *daimyō* were known as *buke hanabi* (warrior fireworks) and were often displayed in competitions with other *daimyō*. Of particular note was the development of *noroshi hanabi* (signal fire fireworks) for warriors that could be shot high into the sky as beacons. These were the likely prototype for the round Japanese firework shells of today. Figure 1 shows a structural picture of a round signal shell, as described in a secret hand written document by the Yasumori School dating back to 1756.

Fireworks in *ukiyo-e*

In the 19th century, fireworks on the Sumida River became the subject of *ukiyo-e* (literally, pictures of the transient world) and *nishiki-e* (literally, multicolor pictures), types of wood block prints. The area around Ryōgoku had become renowned as a pleasure quarters and the everyday frivolities of the area, such as teahouse and restaurant activity, sumo wrestling, indulgence with geisha, and river life, were often depicted in prints. As fireworks were a prominent part of the river life, depictions of fireworks featured in many prints, often showing the various styles of fireworks of the time (Figures 2 and 3).

One of the most famous color prints depicting fireworks and the river life at Ryōgoku is “*Meisho Edo hyakkei Ryōgoku hanabi*” (100 Famous Views of Edo: Fireworks at Ryōgoku) by Utagawa Hiroshige (Figure 2), which depicts a shooting *ryūsei* and the burst of an aerial shell next to Ryōgoku bridge, whilst onlookers are represented crowding on the bridge and in watercraft (*chokibune, yanebune* and a *yakatabune*) along

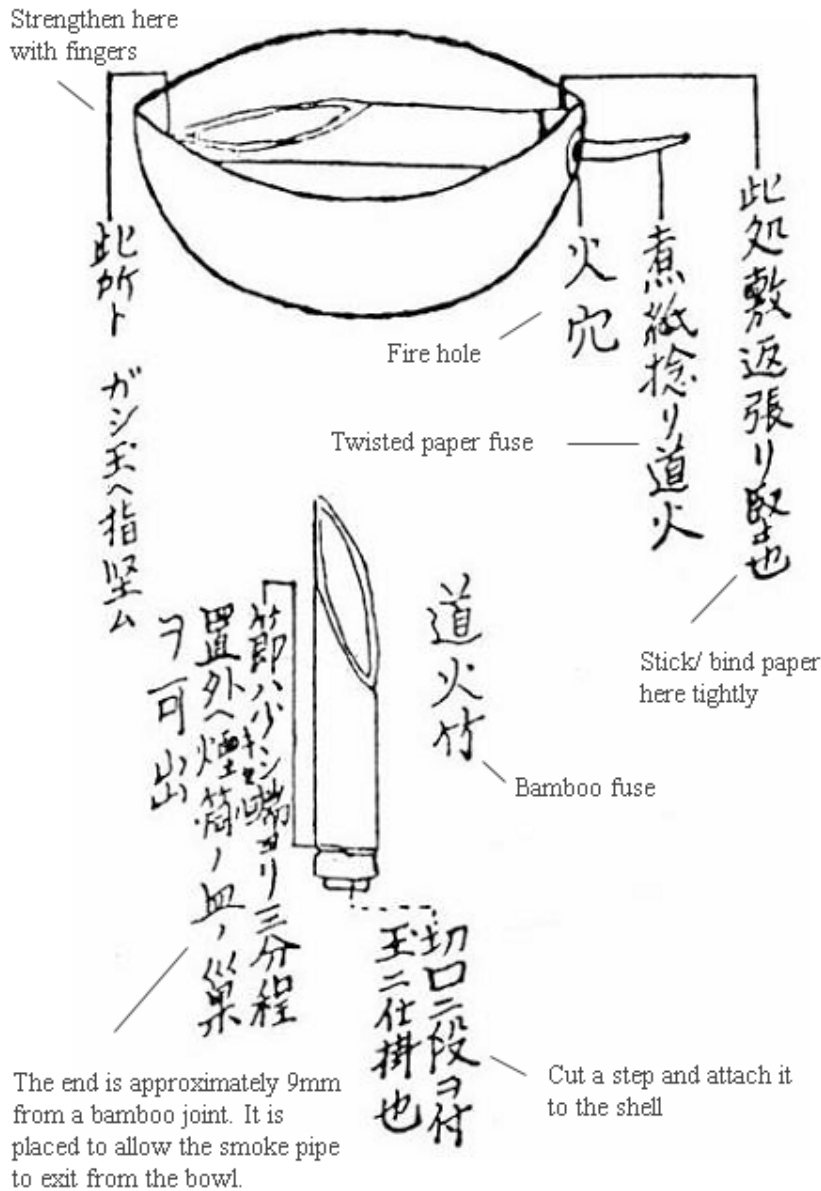


Figure 1. A round signal shell and its fuse developed by the Yasumori School, 1756 (Translation by T. Yoshida).⁸

both sides of the bridge.

Another such example (Figure 3) from a *kusazōshi* (a type of illustrated woodblock print book from the Edo period) shows *hanabishi* entertaining the patrons with different styles of fireworks whilst on a small river boat.

Further depictions of river life, festivities, and fireworks along the Sumida River continued to appear in *ukiyo-e*, *nishiki-e*, and other types of

woodblock print media throughout the Meiji period (1868–1912).

Development of fireworks from the Meiji era (1868–1912) to the present time

Though round shells were displayed in the Edo period, it is said that fireworks with completely round bursts have only been seen since about



Figure 2. “*Meisho Edo hyakkei Ryōgoku hanabi*” (*100 Famous Views of Edo: Fireworks at Ryōgoku*) by Utagawa Hiroshige.

1874.¹ This was achieved by the efforts of the 10th generation master of the Kagiya (house) and highlights the desire for perfection and progression of fireworks sought by the *hanabishi*.

Originally, black powder was used for fireworks, in which saltpeter (potassium nitrate) was used as the oxidizer. As a consequence, the combustion temperature of the powder was too low to give bright colored flames and only dark red or amber could be achieved.⁹ From about 1879, potassium chlorate was imported into Japan (along with

the safety match) which signified a turning point and allowed rapid advancements in fireworks technology. Using potassium chlorate as the oxidizer produced a significant increase in the combustion temperature allowing shells to burst with a higher velocity as well as allowing much brighter and colored flames. Metals such as magnesium, aluminium, and titanium were added to achieve higher brilliancy of light and effects such as sparkles and glitter; whilst various colored flames could be obtained by adding compounds containing sodium, strontium, barium, and copper.

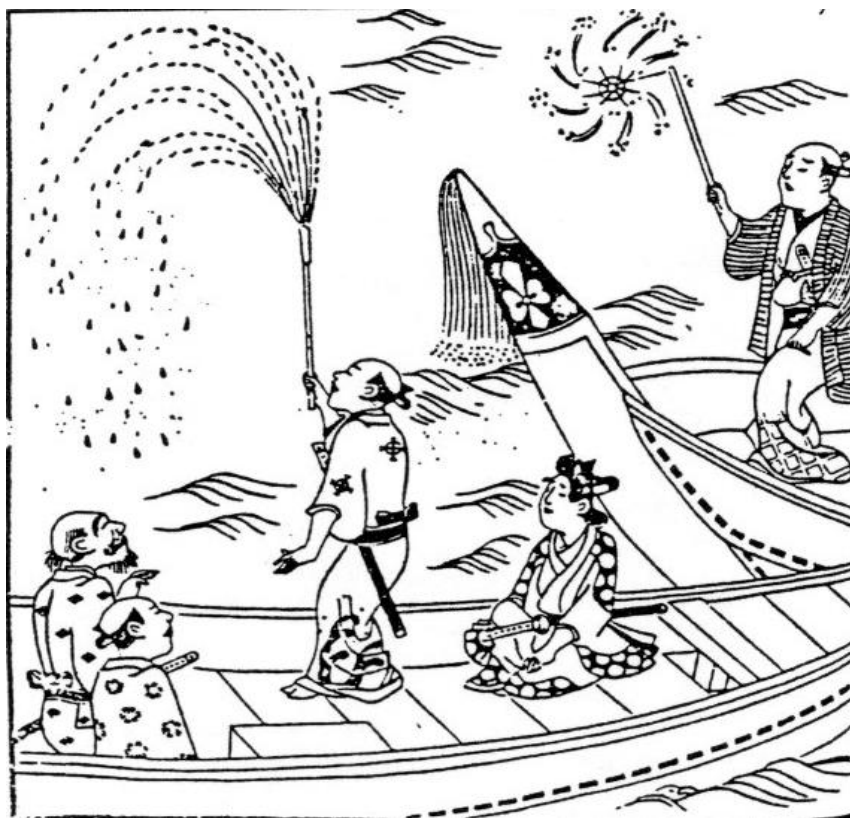


Figure 3. Fireworks play during the Edo period depicted in a *kusazōshi*.

Research is still being conducted in Japan today with new colors and effects continually being developed and perfected.

Traditionally, Japanese fireworks displays were enjoyed by shooting round shells into the sky one by one; a practice still implemented today in many locations throughout Japan. However, in other countries, many fireworks were shot successively in a short time. In 1904, the 11th generation master of the Kagiya (house) went to Manila in the Philippines and witnessed such a rapid firing of shells. Subsequently, this concept was brought back and applied at the Ryōgoku Kawabiraki Fireworks Display and is commonly known today throughout Japan as a “star mine”.

The Taishō era (1912–1926) saw further advancements and refinements of aerial shell fireworks and in 1926 the *shin iri kiku* (chrysanthemum with a single pistil) was finally perfected, whilst 1928 saw the success of *yaeshin kiku hanabi* (double pistil chrysanthemum)¹⁰ demonstrating the high level of precision

and skill that Japanese pyrotechnicians had acquired (Figure 4). These kinds of multi core chrysanthemum shells have come to be regarded as the representative fireworks of Japan.⁹ Despite the usage of star mines at the Sumida River Fireworks Display, it is still these types of aerial shells that are the highlight; however, due to the narrow display area of the river, which is lined with buildings (Figure 5), size restrictions have been applied for safety purposes and shells larger than 4-*gō* (0.12 m) are prohibited from the display.

Oodama (large size shells), such as 10-*gō* (0.30 m) and larger, can be displayed in more spacious sites and are the main shells used for single shot events in other displays throughout Japan. Again *yaeshin kiku* and other multi-core chrysanthemum shells are typical of the fireworks that are displayed at these events.

‘Set piece’ fireworks have been used for a long time, especially in Europe; however, in Japan they only became popular during the Meiji period when colored flame compositions could be used in



Figure 4. *Yaeshin kiku (double pistil chrysanthemum)*^{#10} (DLB 2008).

fireworks. ‘Frame set pieces’ arranged on wooden frames with various patterns and/or *kanji* (Chinese characters) and ‘wire set pieces’ arranged along ropes in the shape of Niagara Falls or Mount Fuji have been used often. The Niagara Falls set piece is still a popular inclusion at many fireworks displays today, although other set pieces have declined in popularity in Japan compared to the excitement of star mines.

Fireworks launching flags or floating figures suspended from parachutes were also once popular. Prior to the Second World War, floating figures such as ‘gold fish’ and ‘flowing fire’ could be seen, but these are no longer used in current Sumida River Fireworks displays due to the

inconvenience of tangling in overhead power lines or on buildings, and because of the inherent danger to children or others who may be injured whilst chasing them. Parachute fireworks can still be seen in some displays elsewhere in Japan.

Recent Sumida River fireworks displays

Due to the disarray at the end of the Edo period as the Tokugawa Shogunate collapsed the Ryōgoku Kawabiraki Fireworks Display underwent a period of dormancy from 1863 until June 8, 1868, when it was revived with much excitement from the people. Furthermore, fireworks as a culture on the Sumida River continued to increase in popularity,



Figure 5. *The narrow Sumida River lined with buildings with modern yakatabune taking position. A fireworks barge can be made out under the centre arch of the Umayu Bridge (DLB 2008).*

as demonstrated by the scheduling of extra trains in 1874 to accommodate crowds, and by the sheer number of spectators crowding onto the wooden Ryōgoku Bridge in 1897 causing it to split and break apart.⁶

The Kagiya (house) continued to manage the Ryōgoku Kawabiraki Fireworks until just before the Second World War. However, with the onset of war, most fireworks craftsmen were subjugated into military service and/or their businesses closed or used for military purposes. Fireworks underwent another period of dormancy from 1938 to 1947 as the events of the war transpired.

August 1, 1948 saw the post-war revival of fireworks on the Sumida River and a display was once again held near the Ryōgoku Bridge. Following this, on September 18 of the same year,¹¹ the first *zenkoku hanabi konkuru* (All Japan Fireworks Competition) was held and *hanabishi* were once again able to display their skills. From 1949, the Ryōgoku Kawabiraki Fireworks Display was held simultaneously with the All Japan Fireworks Competition, co-managed by Hosoya Kakou Co.

(now Hosoya Enterprise Co.) and Marutamaya Ogatsu Fireworks Co., and saw many successful displays. However, after the display in 1961, the Ryōgoku Kawabiraki Fireworks were again suspended, this time due to traffic congestion and pollution in Tokyo.

In 1978, the display was once again revived, although on a small scale, with the new name of *Sumidagawa Hanabi Taikai* (Sumida River Fireworks Display). The display site also moved upstream from the original site near the Ryōgoku Bridge to two new firing locations: the first between Sakura Bridge and Kototoi Bridge, and the second between Umayu Bridge and Komagata Bridge. This possibly served the dual purpose of alleviating traffic and pedestrian congestion as well as perhaps symbolizing the two firing sites of the two great historical masters, Kagiya and Tamaya, from the Edo period. Hosoya Enterprise Co. and Marutamaya Ogatsu Fireworks Co. separately take charge of each firing site in rotation every year. The two companies currently display about ten thousands shells each, and modern day *yakatabune* can still be seen on the river maintaining the



Figure 6. *Simultaneous launching from the two separate firing locations with modern yakatabune along the water (DLB 2008)*

tradition of old (Figures 5 and 6). Various aerial shell fireworks displayed at Sumida are shown in Figures 6 to 10.

The Sumida River Fireworks Competition

Since 1978, The Sumida River Fireworks Competition has been held in conjunction with the Sumida River Fireworks Display. The competition is held during an interlude of the main display at the previously mentioned first firing location (between Sakura Bridge and Kototoi Bridge). The competition comprises ten competitors, of which seven are regular exhibitors and the remaining three are fireworks companies that have previously been awarded prizes at famous fireworks competitions such as the National Japan Fireworks Competitions at Tsuchiura in Ibaraki Prefecture, and Ōmagari in Akita Prefecture.



Figure 7. *A baby's-breath.*



Figure 8. *Many weeping willows.*



Figure 9. *All flowers garden.*

As previously stated, aerial shells are considered a highlight at Sumida and it is the creative variety of these fireworks that are judged at the competition. Each competing company launches 4-gō (0.12 m) shells successively for one minute and such things as the construction, technical attributes, and creativity are judged. The Sumida River Fireworks Competition is adjudicated by a select panel of judges (Figure 11) representing a cross section of prominent people in their respective fields. There are two judging locations, at Kōtō-ku and Sumida-ku, used in rotation each year. Judges consist of chairmen and members, including representatives of the local community. Currently the chairmen are famous Japanese artists: Ōyama Chusaku and Hirayama Ikuo. The members comprise: a man of academic standing, a master of Japanese wrestling, and an entertainer; whilst representatives of the local community come from: Tokyo-to, Yomiuri Newspaper, Tokyo Broadcasting, and Mitsui Construction Co.¹²

There are no strict criteria for adjudicating



Figure 10. *Twinkling stars.*

the competition and points are awarded at the discretion of the individual judges. Some attributes considered are such things as: how well the pattern is formed, how well the firework sits in the sky before explosion, the intensity of colors, new colors, and how evenly the stars disappear. The final ranking of the competitors is based on the accumulative scores of points awarded by the judging panel. So far, adjudicating with a panel of judges in this manner has worked well for the competition.

The most popular type of firework used for the competition is the *katamono* (pattern firework). A pattern firework that displays a more perfect shape in the sky is ranked accordingly by the judges. Examples of pattern fireworks that have been awarded prizes at previous Sumida fireworks competitions can be seen in the video freeze frame captures in Figures 12 to 14. Freeze frame capture allows a precise visualization of the firework as it bursts and opens, which may be a better method for adjudicating pattern fireworks and has been used



Figure 11. Judges at the Sumida River Fireworks Competition.

by judges at prior Sumida River competitions.¹³

Conclusion

The Sumida River has enjoyed a long history of fireworks and has been a breeding ground for the development of fireworks and a fireworks culture that is historically significant to Japan and unique to the world. Originating as a memorial to honor the deceased and to ward off bad spirits, fireworks displays on the Sumida River have continued to

evolve, largely attributable to the two great artisans, Kagiya and Tamaya, whose names are synonymous with fireworks and have been immortalized in Sumida and Japanese history. With only a small number of historical interruptions, the culture of fireworks on the Sumida River has persisted and continues to symbolize the resplendent days of Edo so vividly depicted in *ukiyo-e* artworks.

Due to the narrowness of the Sumida River, the physical size of fireworks displayed is limited;

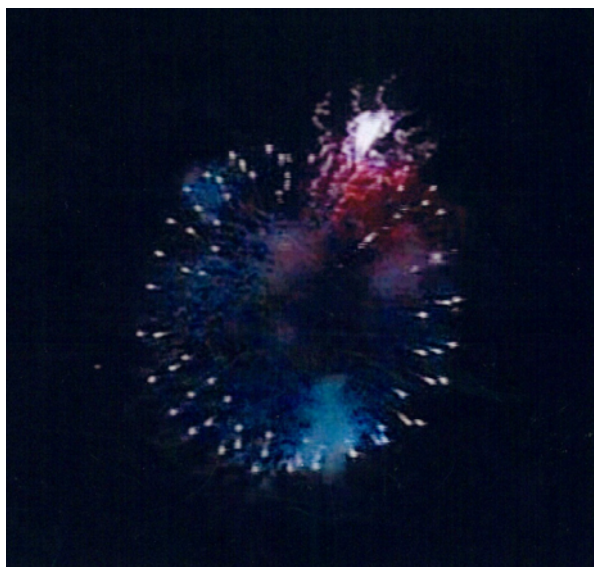


Figure 12. A diamond ring.



Figure 13. A new moon.

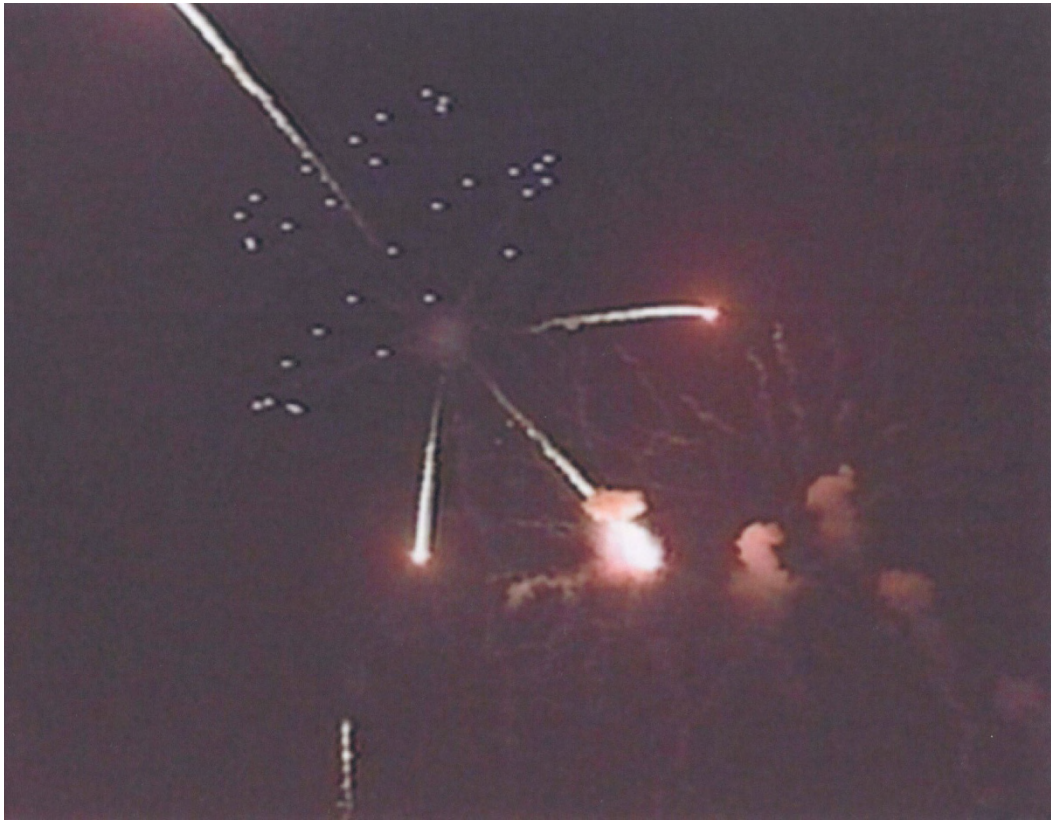


Figure 14. *The New Tokyo Tower.*

however, this lends itself to highlight the skills required by modern day *hanabishi* to work within these narrow limits and still continue to provide high quality displays of fireworks. As fireworks technology continues to progress, new colors and patterns are still being developed and perfected, and can be seen in the innovative works displayed at the Sumida River competition.

Whilst not the most elaborate or biggest fireworks display in Japan today, the *Sumidagawa hanabi taikai* is symbolic of fireworks culture in Japan and is certainly one of the most celebrated and highly regarded fireworks displays and competitions on the Japanese fireworks calendar.

Acknowledgements

The authors are grateful to Mr T. Matsumoto for photos in Figures 7–10 and Miss M. Watanabe for the freeze frame video captures in Figures 12–14.

References and Notes

1 T. Yoshida, “Fireworks Display on the

Sumida River”, *Journal of the Illuminating Engineering Institute of Japan*, Vol. 92(7), 2008, pp. 386–389.

2 Japanese names are traditionally written with the family name first.

3 The Japanese translation of *ya* in the case of Kagiya and Tamaya is equivalent to house, shop, or guild. For clarity, the addition of “(house)” has been included after these names as an explanatory aid.

4 “*Hanabi-gaku Nyuumon*” (*Introduction to Fireworks*), Eds T. Yoshida and D. Ding, Pleiades Publishing, 2006.

5 G. Plimpton, *Fireworks: a History and Celebration*, Doubleday and Company Inc., Garden City, New York, 1984.

6 JICC, *Hanabi: The Fireworks of Japan*, Japan Publications, 1986.

7 Y. Hani, “Touched by the Hand of the Fire God”, *The Japan Times*, Sunday, August 4, 2002.

- 8 The original Japanese text is written in the classical language and whilst all care has been taken, the proposed translation may have some inaccuracies.
- 9 T. Shimizu, *Fireworks, the Art, Science, and Technique*; Pyrotechnica Publications, Austin, Texas, USA, 1996.
- 10 The Japanese term *shin* (芯) from *yaeshin* means “core” or “heart” and in terms of fireworks refers to concentric inner layers of a break or a central core (*yae* means “double”). In Japan, *shin* is often translated into English as “pistil” with the terms: double-pistil, triple-pistil, quadruple-pistil, and 5-pistil often used.

The definition of a pistil as outlined by Kosanke¹⁴ describes a pistil as a dense symmetrical pattern of stars within a break and implies that a pistil spreads no more than 1/3 the size of the break, with anything larger being a petal. Petals are further described as concentric spherical layers but also include the outermost layer of the break (anything smaller than 1/3 of the break being a pistil).

A double-pistil chrysanthemum (describing only the two inner cores) is therefore equivalent in concept to a double-petal chrysanthemum with a pistil (describing the two outer layers and an inner core).

Whilst the term double-pistil, may perhaps be incorrect according to Western terminology, this term corresponds with the Japanese concept and is used in this text to maintain a Japanese sense.

- 11 Ryogoku Fireworks Association, Yanagibashi, Tokyo.
- 12 The executive Committee for the Sumida River Fireworks Display, “Fireworks/Down Town/Sumida River”, 1983.
- 13 M. Watanabe, “A Study on the Recording Method for Fireworks Display”, Master’s Thesis, School of Fireworks, Ashikaga Institute of Technology, 2008.
- 14 K. L. Kosanke, B. J. Kosanke and E. Contestabile, *The Illustrated Dictionary of Pyrotechnics (Pyrotechnic Reference Series No.1)*, Journal of Pyrotechnics Inc. 1st edn, March 1995.

Metal–Fluorocarbon Pyrolants: IX.† Burn rate and Radiometric Performance of Magnesium/Teflon/Viton (MTV) Modified with Zirconium

Ernst-Christian Koch‡

Abstract: The burn rate, u (mm s^{-1}) of fuel rich magnesium/Teflon/Viton (MTV) is increased by 65% upon addition of zirconium whereas the spectral efficiency $E\beta$ ($\text{J g}^{-1} \text{sr}^{-1}$) is reduced by 15%.

Keywords: Burn rate, zirconium, magnesium, MTV, polytetrafluoroethylene, radiometry, TeflonTM, VitonTM

Metal–fluorocarbon pyrolants such as MTV play an important role as both igniter materials for rocket propellants (type N-35)^{1,2} and infrared decoy flares to protect flying platforms.^{3–5} Recently the author reported the increase in the burn rate of MTV upon addition of graphite.⁶ Another method for modifying the burn rate of MTV has been disclosed by Kuwahara and Ochiai. They observed an increase in the burn rate of fuel rich MTV (65/30/5) upon the addition of zirconium.⁷

However it is unclear if the addition of zirconium to MTV would also affect the spectral efficiency of such compositions. Hence in the present investigation a fuel rich MTV composition (65/30/5) was modified with various amounts of zirconium.

The compositions were prepared in 500 g batches with conventional mixing in a 0.5 l blender. The following materials were used: magnesium (non ferrum Metallpulver, A-5111 St. Georgen, ECKA Mg-Pulver LNR-61, mean particle radius 20 μm), PTFE (Dyneon, D-84505 Burgkirchen, TF-9205, mean particle radius: 2 μm), Viton (Mach I Inc. King of Prussia, USA, FC-2175), zirconium (Chemetall GmbH, Special Metals Division,

D-60487 Frankfurt, Zirconium-GH, Blaine mean particle size 5.5 μm). Magnesium and zirconium were wetted with acetone and mixed in a blender until a uniform grey mass resulted. Addition of PTFE powder and Viton dissolved in acetone followed. The mass was mixed until small granules had formed. These were screened through a 3.5 mm sieve and dried on stainless steel drying pans at reduced pressure at 40 °C for 12 h.

The compositions were pressed in a 24.5 mm cylindrical die with 250 MPa pressing pressure and 6 s hold time to give consolidated strands of ~39 g mass and ~42 mm height. The lateral surfaces of the strands were painted with polyurethane lacquer and to the top face was applied an ignition dip from a boron, potassium nitrate, nitrocellulose (12/84/4) mix.

The pellets were placed between steel split pins on a brass cylinder and ignited by an electric igniter enhanced with a quickmatch fixed with adhesive tape on top of the strands.

The burn rate and radiometric performance were determined in the range 3.0–5.1 μm with an IR radiometric system (RM 6600 and uncooled pyroelectric detector RkP 575 both from Laser Probe USA). The radiometer was calibrated with a black body (SR-32, CI Electro-Optical Systems, Haifa/Israel) at $T = 1000 \text{ K}$.

Kuwahara had noted that the burn rate of MTV (65/30/5) increases upon addition of zirconium of

†For Part VIII see ref. 6.

‡ Current address: NATO Munitions Safety Information Analysis Center (MSIAC), Boulevard Leopold III, B-1110 Bruxelles, Belgium. e-c.koch@msiac.nato.int

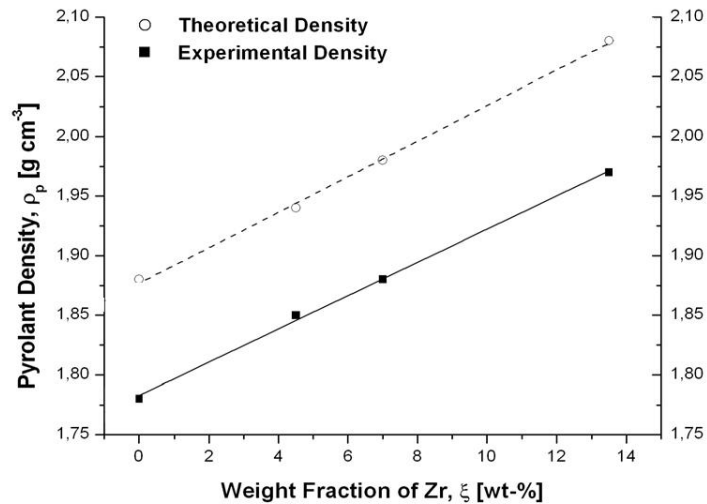
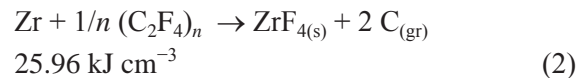
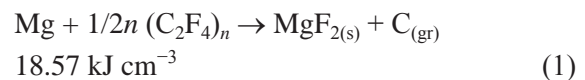


Figure 1. Theoretical maximum density and experimental density of pyrolants.

unspecified particle size. Now the present pyrolant was modified such that the MTV ratio was kept nearly constant with increasing zirconium content. Table 1 gives the actual stoichiometries. The experimental density of the pellets was ~ 94% theoretical maximum density (TMD) in all cases as can be seen from Figure 1.

Upon addition of zirconium the burn rate of the pyrolant increases to a range with a maximum at ~7% Zr, and thereafter it decreases again. This is in quite good accord with earlier findings.⁷ However the burn rate increase is more pronounced than that reported by Kuwahara. This may be due to different particle size distributions. This work: MTZ (20/2/5.5) vs. Kuwahara: MTZ (60/600/?).⁷

The decrease in the burn rate at higher Zr contents is indicative of a minimum of two propagation mechanisms in the condensed phase. At first Zr imparts a higher volumetric exothermicity with PTFE as can be seen from the following equations:



This accounts for the observed increase in burn rate at lower zirconium percentages. The thermal diffusivity of zirconium, $\alpha(\text{Zr}) = 1.28 \times 10^{-5} (\text{m}^2 \text{s}^{-1})$, is by a factor of 10 lower than the corresponding magnesium value, $\alpha(\text{Mg}) = 1.15 \times 10^{-4} (\text{m}^2 \text{s}^{-1})$. As a consequence with increasing Zr content the overall diffusivity drops by ~5% and the burn rate slows down again. A similar effect has been measured by Kuo with boron modified fuel rich MTV (50/50) pyrolant.⁸

Although the burn rate increases upon addition of Zr it lowers the spectral efficiency as can be seen from the nearly exponential decrease in Figure 2.

At first hand this is quite unexpected as zirconium based flare compositions are known to have high

Table 1. Composition details (wt%).

	1	2	3	4
Magnesium	65	62	59	56.5
Polytetrafluoroethylene	30	29	27	26
Hexafluoropropene-co-vinylidene fluoride polymer	5	4.5	5	4.5
Zirconium	0	4.5	7	13.5

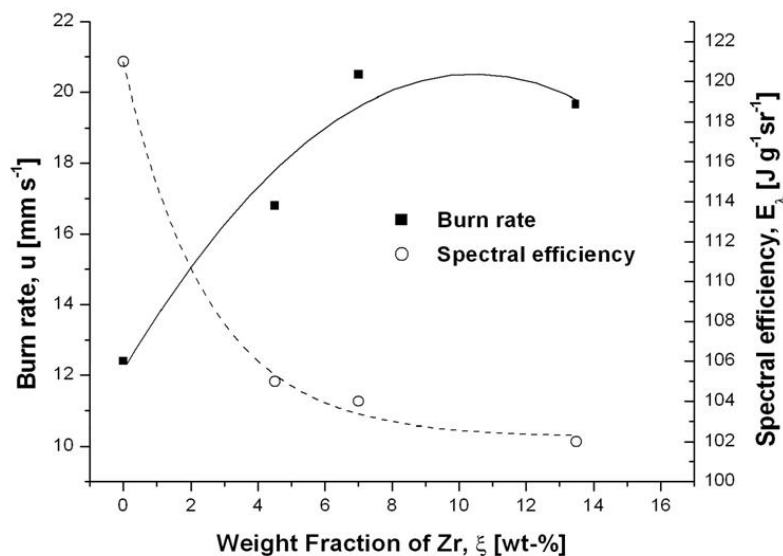


Figure 2. Burn rate and spectral efficiency of pyrolants.

radiant intensity.⁹

The fluorination of zirconium according to Glassman's criteria for metal combustion occurs entirely in the condensed phase.¹⁰ Thus the aerobic diffusion flame responsible for the radiative heat feedback to the primary carbon rich zone cannot be altered by zirconium. As the magnesium content decreases linearly from 65 wt% to 56.6 wt% the decrease in performance can be explained.³ Now the non-linear decrease of the spectral efficiency requires additional explanation. However this is not presently available.

References

- 1 Ignition Pellets, Magnesium-Fluorocarbon, MIL-PRF-82736A(OS), 16. November 1988, Naval Sea Systems Command, Indian Head, USA; accessed at <http://www.assist.online.com>
- 2 E. C. Julian, F. G. Crescenzo and R. C. Meyers, Igniter Composition, *U.S. Patent 3.753.811*, 1973, USA.
- 3 E.-C. Koch and A. Dochnahl, IR Emission Behaviour of Magnesium/Teflon/Viton (MTV), *Propellants, Explosives and Pyrotechnics*, Vol. 25, 2000, p. 37.
- 4 E.-C. Koch, Review on Pyrotechnic Aerial Infrared Decoys, *Propellants, Explosives and Pyrotechnics*, Vol. 26, 2001, p. 3.
- 5 E.-C. Koch, Metal-Fluorocarbon Pyrolants: III. Development and Application of Magnesium/Teflon/Viton (MTV), *Propellants, Explosives and Pyrotechnics*, Vol. 27, 2002, p. 262.
- 6 E.-C. Koch, Metal-Fluorocarbon Pyrolants: VIII. Behavior of Burn rate and Radiometric Performance of two Magnesium/Teflon/Viton (MTV) Formulations, *Journal of Pyrotechnics*, No. 27, 2008, p. 38.
- 7 T. Kuwahara and T. Ochiai, Burning rate of Mg/TF Pyrolants, *18th International Pyrotechnics Seminar*, Breckenridge, CO, July 13–17, 1992, p. 539.
- 8 B. L. Fetherolf, T. S. Snyder, M. D. Bates, A. Peretz and K. Kuo, Combustion Characteristics and CO₂ Laser Ignition behaviour of Boron/Magnesium/PTFE Pyrotechnics, *14th International Pyrotechnics Seminar*, 18–22 September 1989, Jersey, UK, p. 691.
- 9 C. A. Knapp, *New Infrared Flare and High-Altitude Igniter Compositions*, Feltman Research and Engineering Laboratories, Picatinny Arsenal, Dover, N.J., July 1959.
- 10 I. Glassman and R. Yetter, *Combustion*, 4th edn, Academic Press, 2008, p. 459.

Effects of Variation of Component Content on the Colored Flame of Firework Star Compositions

Kazuomi Itoh,^a Hideo Watanabe,^b Dayu Ding^{a*} and Tadao Yoshida^a

^a Ashikaga Institute of Technology, 268-1 Omae-cho, Ashikaga-shi, Tochigi 326-8558, Japan
Email: *dding@ashitech.ac.jp

^b Pyrotechnica Co. Ltd. 4179 Shimoakima, Annaka-shi, Gunma 379-0104, Japan

Abstract: *The spectra of the colored flames of firework compositions were measured with a spectrometer and processed into chromaticity coordinates. The change in color purity as a function of composition is shown using chromaticity diagrams. Firework star compositions of red, yellow, green and blue were tested. The components of the compositions were altered to investigate the influence of color agents, chlorine donors and high energy agents on the colored flames.*

Keywords: *firework composition, combustion, colored flame, chromaticity diagram*

Introduction

The light and color of fireworks are major effects in firework displays. These come mainly from the combustion of firework star compositions. Many colored flames of firework star compositions are formed by color generating chemical species which are produced by the combustion of firework stars.

To give insight into the relative importance and roles of some of the components, the effects of variation of single component content such as color agent, chlorine donor or high energy agent used in reference firework compositions on the colored flame of firework compositions were investigated

in this study. Compositions used in the experiment are those of red, yellow, green and blue stars.

Experimental

Materials

Reference compositions were selected from a book¹ and are listed in Table 1. Hereafter, reference compositions in Table 1 are abbreviated as RC.

Magnalium (MgAl) is an alloy of magnesium (Mg) and aluminium (Al) and it is usually used as a high energy agent in firework compositions because of its high heat of combustion.

The experiments were carried out on the

Table 1 Reference compositions (wt%).

Component	Red	Yellow	Green	Blue	Role
Potassium perchlorate (KClO ₄)	54	50	20	63	Oxidant
Strontium carbonate (SrCO ₃)	12				Color agent
Sodium oxalate (Na ₂ C ₂ O ₄)		15			Color agent
Barium nitrate (Ba(NO ₃) ₂)			37		Color agent
Cupric oxide (CuO)				10	Color agent
Magnalium (MgAl)	15	15	16	16	Fuel
Phenolic resin	8	7.5	6	12	Fuel
Chlorinated gum	6	7.5	16	10	Chlorine donor
Rice granules	5	5	5	5	Binder

Article Details

Manuscript Received:-02/03/09

Publication Date:-27/05/09

Article No: - 0076

Final Revisions:-27/05/09

Archive Reference:-902

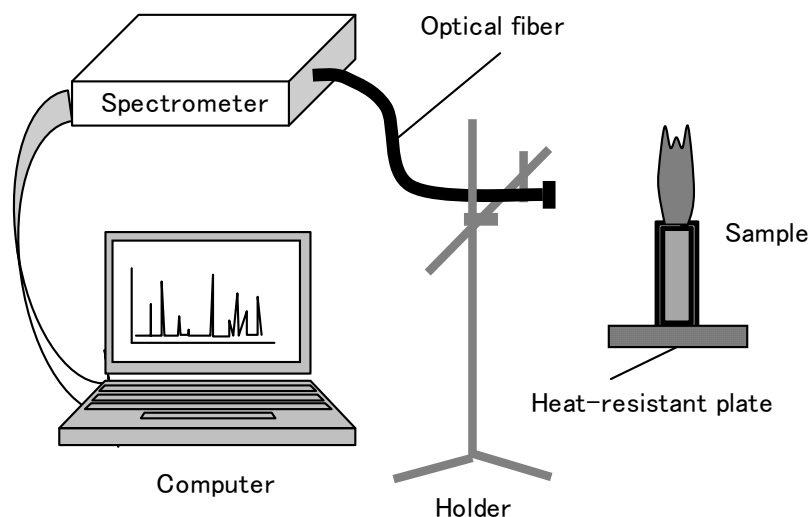


Figure 1 Schematic diagram of the experimental setup.

compositions by changing the content of specific components based on reference compositions and the ratios of other components were kept constant.

For all experiments, chemicals were used as supplied from Sunaga Fireworks Co. Ltd. The samples of compositions were prepared by mixing the chemicals as dry powders. About 1.4 g of the mixture was poured into a paper tube of 8.0 mm inner diameter, 0.2 mm thick and 30 mm long.

Methods

A schematic diagram of the experimental setup used in this work is shown in Figure 1. A PMA-11C7473-36 spectrometer from Hamamatsu Photonics Co. Ltd was used for measuring the spectrum of the firework flame. When a sample at the top was ignited which was placed vertically on a heat-resistant plate, the light of the flame was transmitted to the spectrometer through an optical fiber and the spectral data were recorded on a personal computer. The experiments were conducted in a dark room and the chamber in which samples were burned was painted flat black to avoid reflections. Three samples for each formula were prepared and tested under the same conditions.

Results and discussion

Experimental data reduction

From the spectra measured, we can understand the properties and features of colored firework flames in which there are various desired or undesired emitters, and there is further discussion later. On the other hand, color sensations are not uniquely related to one wavelength of light, but related to the combinations of many wavelengths of light entering one's eyes. Firework flame is one kind of colored light source and light of various wavelengths is emitted. In order to quantify colored firework flames, the CIE1931 color system developed in 1931 by the International Commission on Illumination was used in the research. Using this color system, the color of a firework flame can be quantitatively evaluated with color coordinates x and y in a two-dimensional diagram called a chromaticity diagram, see Figure 2. Monochromatic light colors lie on the outer periphery of the tongue-shaped region called the monochromatic light line and for which the corresponding wavelengths are listed. The white light point ICI illuminant "C" lies at the center of the diagram.

In this study, all of the firework flame spectra were taken and saved to the computer. With the measured spectra and color-matching functions in the XYZ chromatic system, we calculated the color coordinates x and y . For an instance, the color coordinates x and y of a firework flame are calculated, then a color point A for the data is

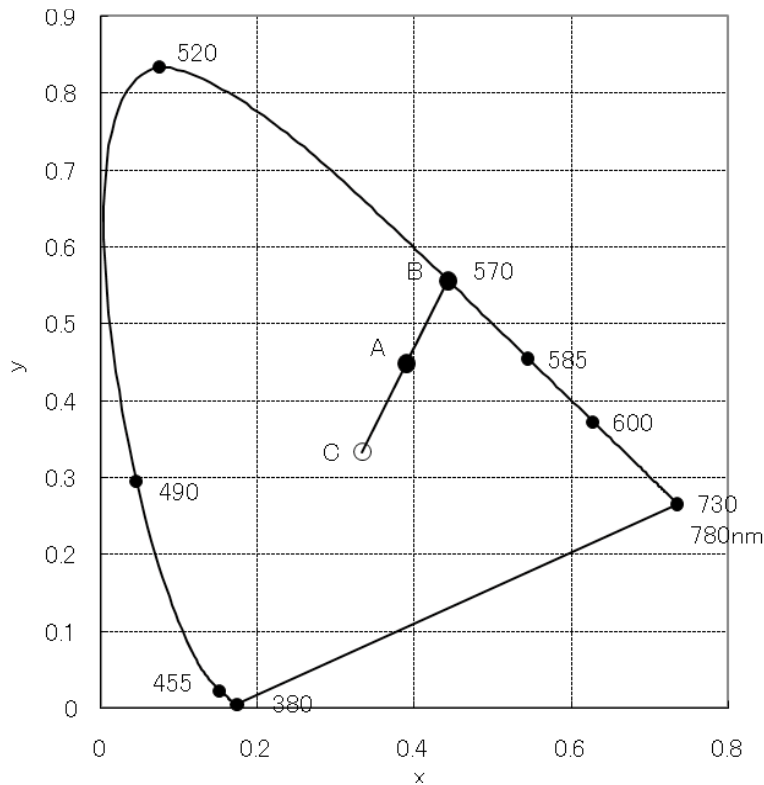


Figure 2 Chromaticity diagram.

plotted in the chromaticity diagram. The straight line that connects point A with C extends to a point B on the monochromatic light line. The wavelength of monochromatic light point B is called the dominant wavelength of color point A. The percentage of the distance along the straight

line CB from point C is called the excitation purity or purity, with white light point C having 0% purity and monochromatic light point B having 100% purity.

The spectrometer used in our experiments can

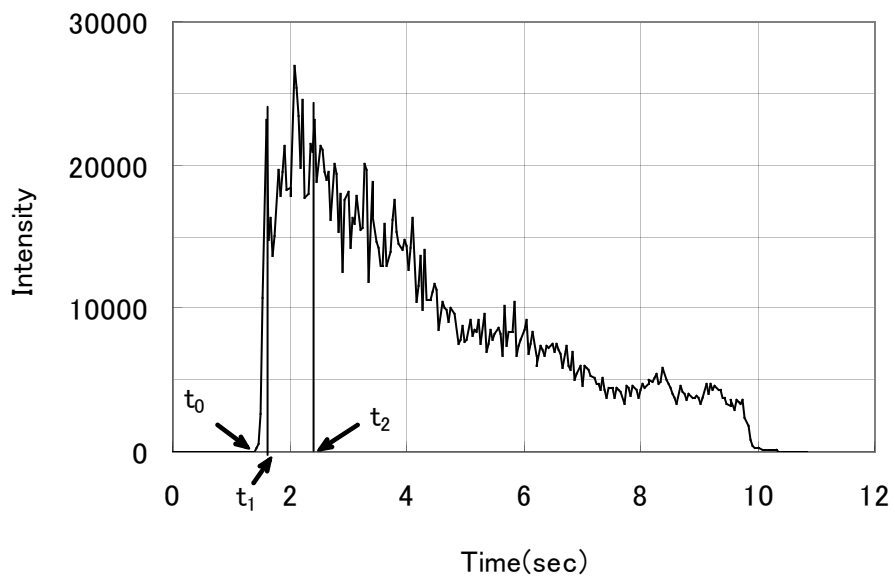


Figure 3 Change of the spectrum with time.

measure the change in the spectrum with time with a repeated measurement function. An example of spectral change with time (light emission at a particular wavelength) is shown in Figure 3. After ignition at time t_0 , the sample began to burn and radiate light, and the flame reached approximate stability at time t_1 . But after t_1 , the intensity profile changed with time because of flickering of the flame as the air surrounding the flame was heated and movement of the air resulted. To eliminate the effects of flame flickering and to correctly evaluate the colored firework flame, the average intensity between t_1 and t_2 for each wavelength was used to calculate the CIE coordinates. The time between t_1 and t_2 was set to about one second for data reduction of all wavelength intensities of firework flames.

Red composition flame spectra

The spectrum of the red composition flame in Figure 4 shows several peaks of light intensity in the wavelength range 600–700 nm. The red color is responsible for characteristics of these peaks such as their position, width, and intensity. If the peaks are located at longer wavelengths, or the peaks are higher-intensity or sharper, a deeper red colored flame will be formed. The peak at 606 nm is due to strontium monohydroxide (SrOH) emissions and the peaks at 635, 660, and 673 nm are due to

strontium monochloride (SrCl) emissions. SrCl is a desired emitter for forming a deeper red flame because the peak intensity of SrCl is higher than that of SrOH.

There was a ubiquitous sodium atomic emission at 589 nm, which contributed an undesirable yellow or orange-yellow light. Sodium or sodium compounds were not used in the red compositions, but they existed in the chemicals as impurities.

The very high peak at 767 nm was produced by potassium, which was also an undesired emitter, but there was little effect on the red color sensation because the peak was near the infrared range.

(1) Effects of SrCO₃

Experiments were carried out to vary the color agent SrCO₃ based on the red reference composition (see Table 1). The SrCO₃ content was changed in 5% increments and the formulas are shown in Table 2. The chromaticity results of the compositions are shown in Figure 5.

The chromaticity coordinates of the formula move towards the red region with increasing SrCO₃ content. A reason for this is likely that the concentration of SrCl in the flame increased with SrCO₃ content. However, when the SrCO₃ content is about 17%, on adding more SrCO₃ the color movement towards the red region becomes

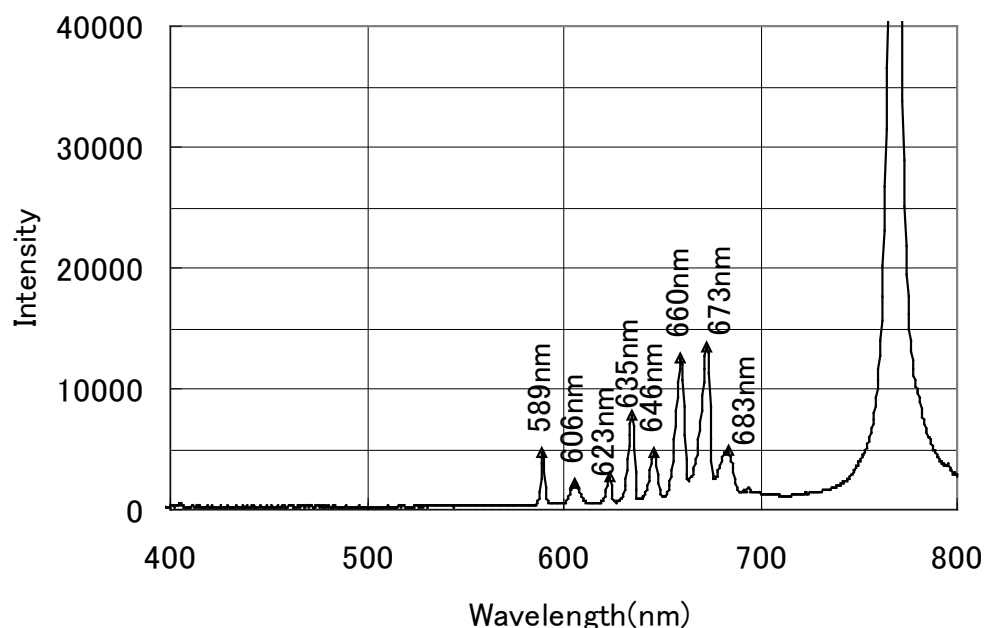


Figure 4 Spectrum of red flame.

Table 2 Variation of color agent based on red formula (wt%).

Component	Formula				
	R-1	R-2	R-3 (RC)	R-4	R-5
KClO ₄	60.1	57.1	54	50.9	47.9
SrCO ₃	2.0	7.0	12	17.0	22.0
MgAl	16.7	15.9	15	14.1	13.3
Phenolic resin	8.9	8.5	8	7.5	7.1
Chlorinated gum	6.7	6.3	6	5.7	5.3
Rice granules	5.6	5.3	5	4.7	4.4

very slight. Adding SrCO₃ to the red reference composition can improve the red colored flame, but once a certain amount of the color agent is attained, adding more does not improve the red flame.

(2) Effects of chlorinated gum

The percentage of chlorinated gum in the red reference composition was varied, and the formulas are listed in Table 3. The results of those experiments are shown in Figure 6. There is a tendency for the chromaticity coordinates

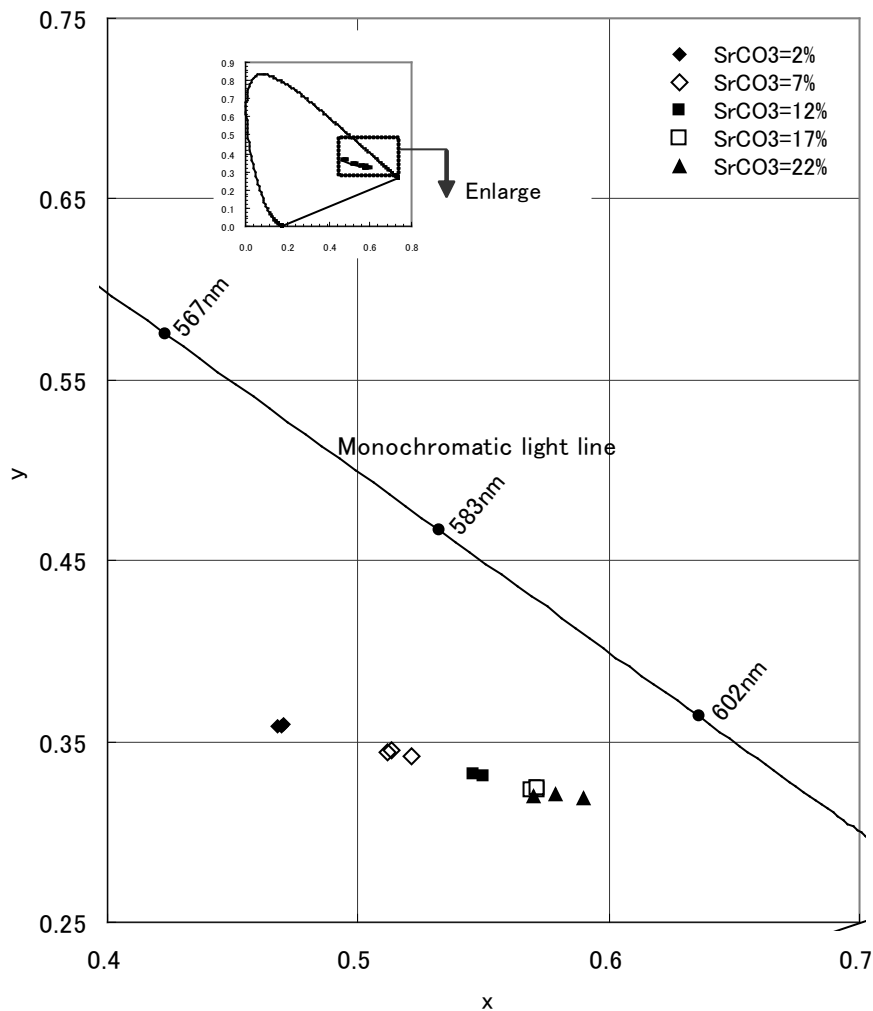


Figure 5 Chromaticity of variation of color agent based on red formula.

Table 3 Variation of chlorinated gum based on red formula (wt%).

Component	Formula				
	R-6	R-7	R-3 (RC)	R-8	R-9
KClO ₄	56.3	55.1	54	52.9	51.7
SrCO ₃	12.5	12.3	12	11.7	11.5
MgAl	15.6	15.3	15	14.7	14.4
Phenolic resin	8.3	8.2	8	7.8	7.7
Chlorinated gum	2.0	4.0	6	8.0	10.0
Rice granules	5.2	5.1	5	4.9	4.8

to move towards the red region with increasing chlorinated gum content. The predominant peaks in the spectrum are the emissions from SrCl and a chlorinated gum added to the composition will provide Cl and so the amount of SrCl will increase.

(3) Effects of MgAl

To assess the effect of MgAl, experiments were conducted to vary the amount of MgAl based on the red reference formula. The percentage of MgAl was changed in 5% increments and the formulas are listed in Table 4. The chromatic performance

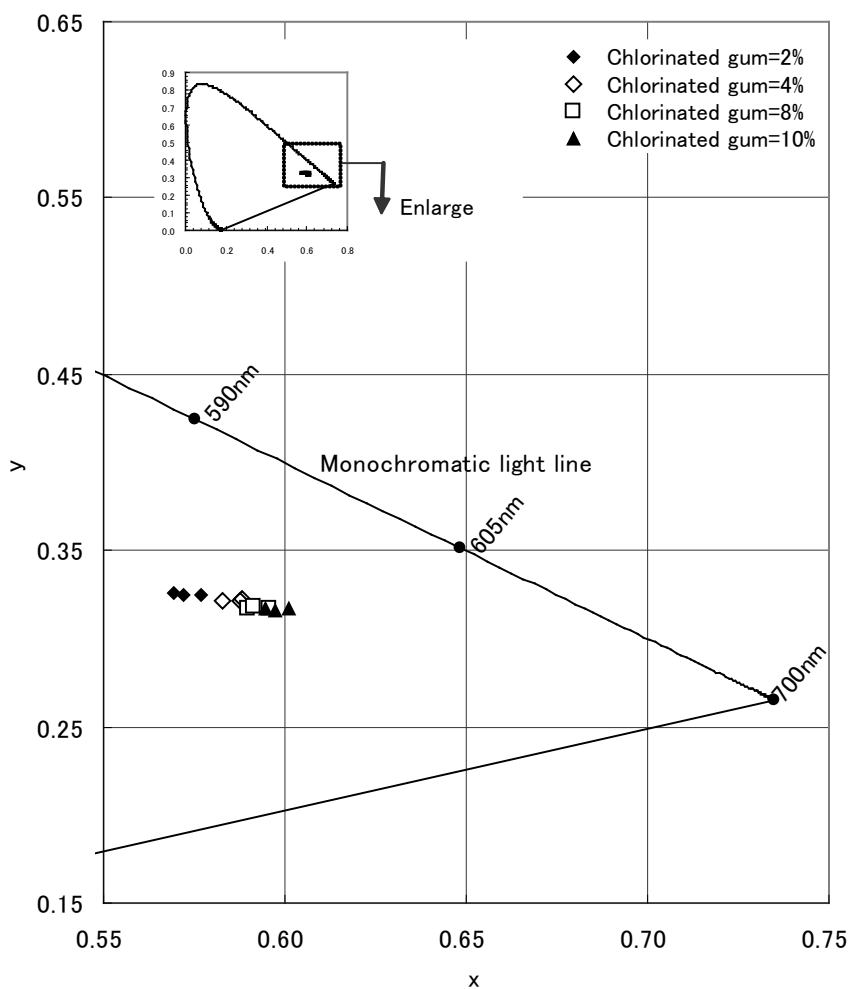


Figure 6 Chromaticity of variation of chlorinated gum based on red formula.

Table 4 Variation of MgAl based on red formula (wt%).

Component	Formula				
	R-10	R-11	R-3 (RC)	R-12	R-13
KClO ₄	60.4	57.2	54	50.8	47.6
SrCO ₃	13.4	12.7	12	11.3	10.6
MgAl	5.0	10.0	15	20.0	25.0
Phenolic resin	8.9	8.5	8	7.5	7.1
Chlorinated gum	6.7	6.4	6	5.6	5.3
Rice granules	5.6	5.3	5	4.7	4.4

data of the compositions are shown in Figure 7.

MgAl is used in most modern firework stars as a bright agent. When the amount of MgAl increased from 5% to 10%, the chromatic performance improved a little. A likely reason for this is that

as more MgAl is added, the heat generated by the composition increases, heating the flame towards the optimum temperature for emission from SrCl excitation. However, once the percentage of MgAl exceeds 10%, the chromatic performance will

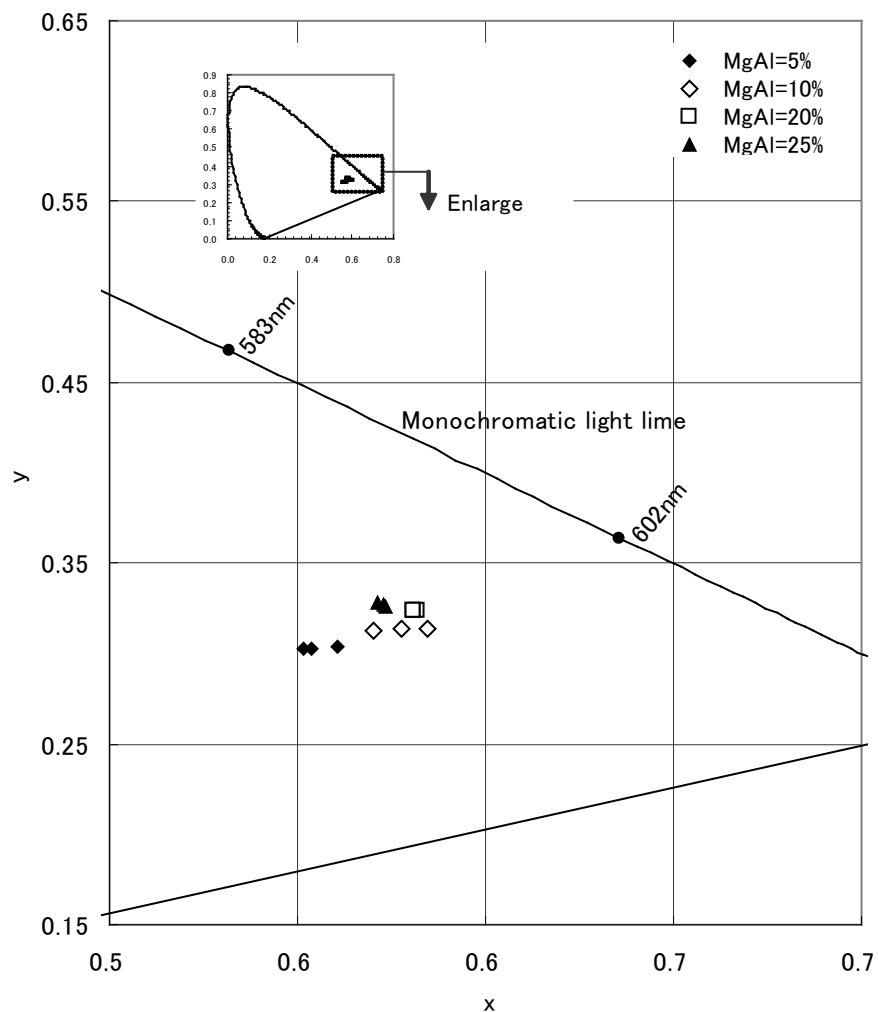


Figure 7 Chromaticity of variation of MgAl based on red formula.

decrease.

Yellow composition flame spectra

The spectrum of a flame of yellow composition is shown in Figure 8. In forming a yellow flame, the atomic emitter sodium (Na) is responsible for the deep yellow flame, with emission at 589 nm. There are only two intensity peaks in the wavelength range 380–780 nm. One (desired) peak is at 589 nm due to sodium (Na) emission, and the other (undesired) peak is at 767 nm due to potassium (K) emission.

(1) Effects of $\text{Na}_2\text{C}_2\text{O}_4$

Experiments were carried out to vary the color agent $\text{Na}_2\text{C}_2\text{O}_4$ based on the yellow reference composition (see Table 1). The percentage of $\text{Na}_2\text{C}_2\text{O}_4$ was changed in 5% increments and the formulas are shown in Table 5. The chromaticity results of the compositions are shown in Figure 9.

The results show that the yellow flame attained an optimum chromatic performance when the percentage of color agent $\text{Na}_2\text{C}_2\text{O}_4$ was about 15% in the yellow formula, and the chromatic performance would decrease if the amount of $\text{Na}_2\text{C}_2\text{O}_4$ was below or above this level. When only a little color agent was added, the atomic emitter

sodium (Na) of the yellow color in the flame was not enough, and as more color agent was added, the heat of combustion was lost in heating the excess color agent, cooling the flame temperature for the emitting sodium (Na) excitation.

(2) Effects of MgAl

The percentage of MgAl was changed in 5% increments based on the yellow reference composition and the formulas are listed in Table 6. The experiment results are shown in Figure 10.

The chromatic coordinates shifted to a monochromatic light line at wavelength 589 nm when the percentage of MgAl increased. The chromatic performance of the yellow flame can be improved by adding MgAl. But once the amount of MgAl was at or over 15%, the effect of MgAl on the performance was very slight.

Green composition flame spectra

A typical spectrum of green composition flame is shown in Figure 11. The molecular emitter barium monochloride (BaCl) is responsible for emissions at 514 and 525 nm, and the emitter barium monohydroxide (BaOH) is responsible for emissions at 487, 515, and 527 nm.² According to Kosanke and Kosanke,³ barium monohydroxide is

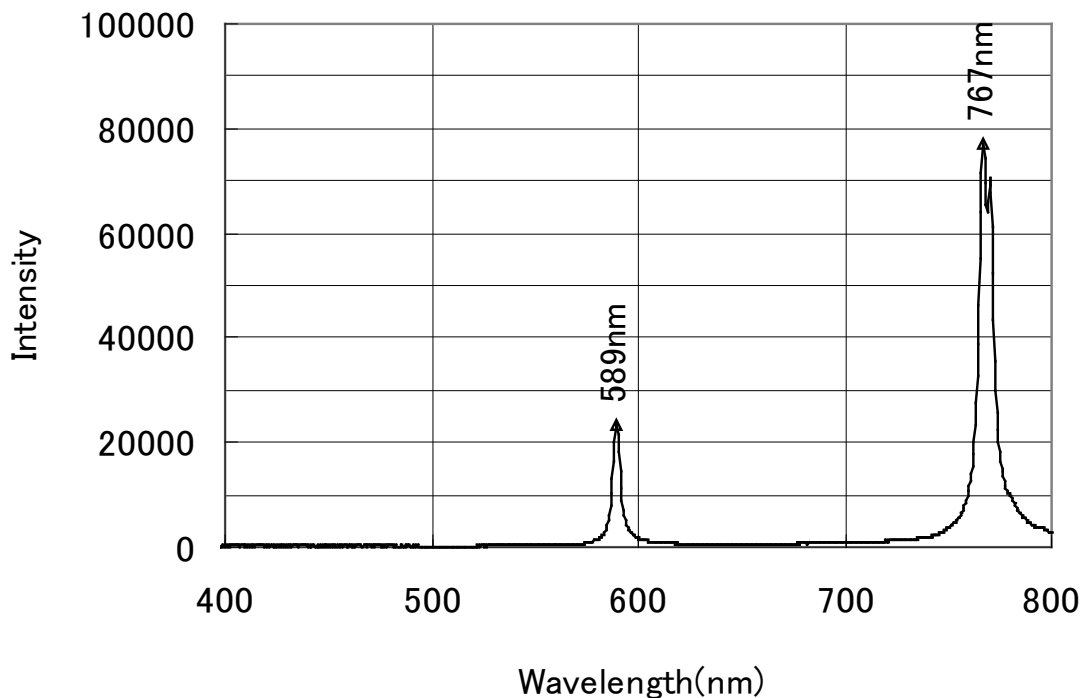


Figure 8 Spectrum of yellow flame.

Table 5 Variation of $\text{Na}_2\text{C}_2\text{O}_4$ based on yellow formula (wt%).

Component	Formula				
	Y-1	Y-2	Y-3 (RC)	Y-4	Y-5
KClO_4	55.9	52.9	50	47.1	44.1
$\text{Na}_2\text{C}_2\text{O}_4$	5.0	10.0	15	20.0	25.0
MgAl	16.8	15.9	15	14.1	13.2
Phenolic resin	8.4	7.9	7.5	7.1	6.6
Chlorinated gum	8.4	7.9	7.5	7.1	6.6
Rice granules	5.6	5.3	5	4.7	4.4

quite a weak emitter by comparison with barium monochloride, so the desired emitter in a green firework flame is barium monochloride. There is a relatively strong interfering emission at 589 nm, originating from atomic sodium (Na). There are also interfering emissions from the glowing matter

in the flame. When the temperature of the matter is high enough, it can emit light across the entire visible wavelength 380–780 nm, but the intensity of light becomes high with increasing wavelength. If the interfering or undesired emissions between 550 and 780 nm are decreased or eliminated, the

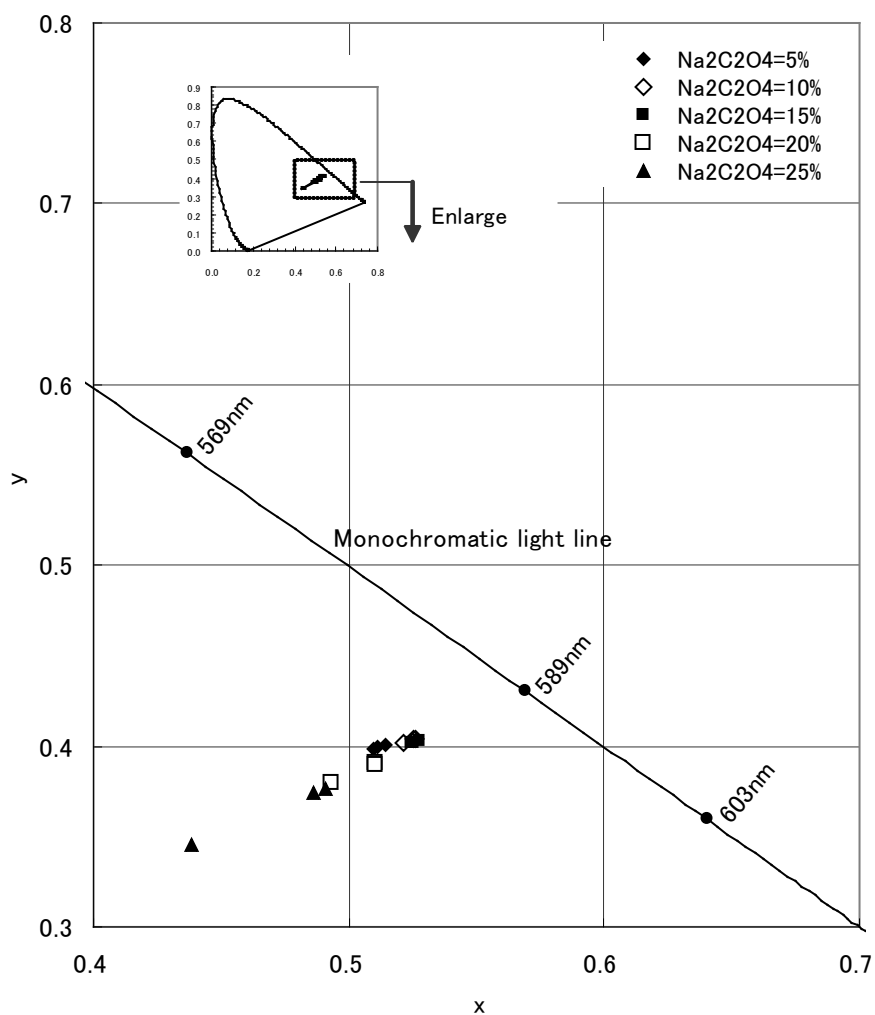


Figure 9 Chromaticity of variation of $\text{Na}_2\text{C}_2\text{O}_4$ based on yellow formula.

Table 6 Variation of MgAl based on yellow formula (wt%).

Component	Formula				
	Y-10	Y-11	Y-3 (RC)	Y-12	Y-13
KClO ₄	55.9	52.9	50	47.1	44.1
Na ₂ C ₂ O ₄	16.8	15.9	15	14.1	13.2
MgAl	5.0	10.0	15	20.0	25.0
Phenolic resin	8.4	7.9	7.5	7.1	6.6
Chlorinated gum	8.4	7.9	7.5	7.1	6.6
Rice granules	5.6	5.3	5	4.7	4.4

color will be favorably moved toward the center of the green area of the chromaticity diagram, and the performance of the green flame will be significantly improved.

(1) Effects of Ba (NO₃)₂

The experiments were conducted by changing the

percentage of Ba(NO₃)₂ in 5% increments and the formulas are listed in Table 7. The chromaticity results of the compositions are shown in Figure 12.

As can be seen, the chromatic data shifted slightly toward the green area with increasing Ba(NO₃)₂

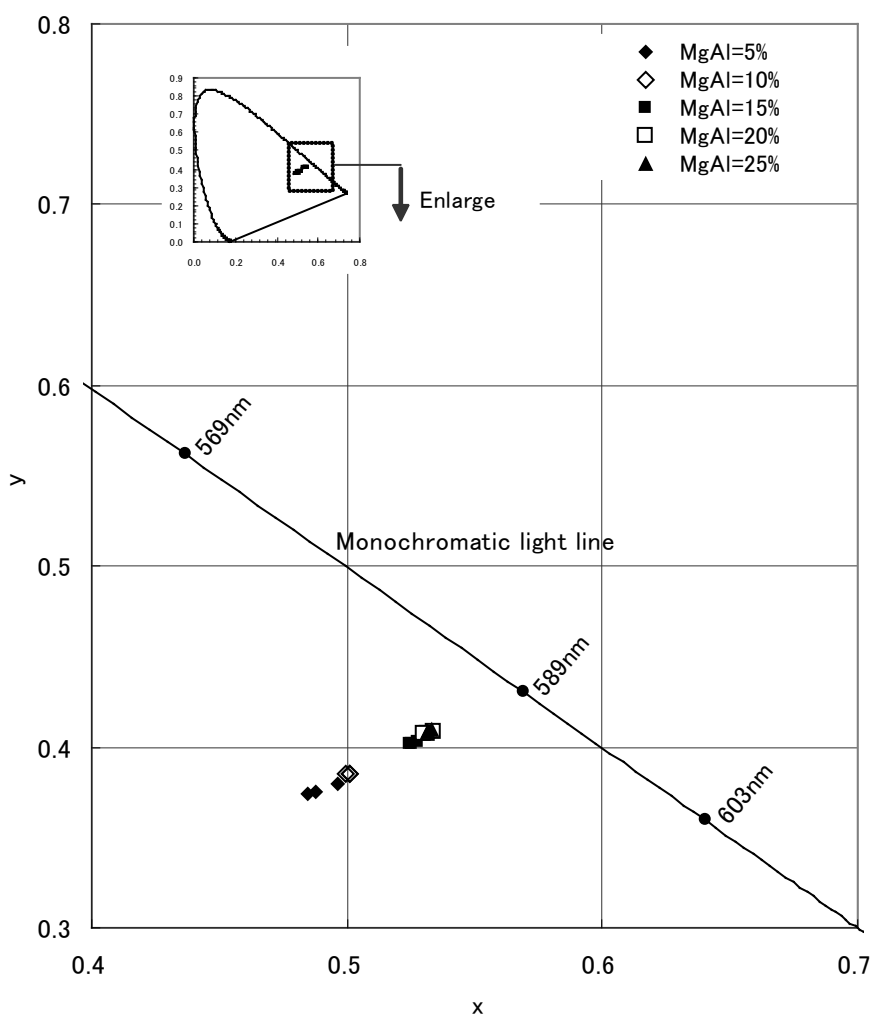


Figure 10 Chromaticity of variation of MgAl based on yellow formula.

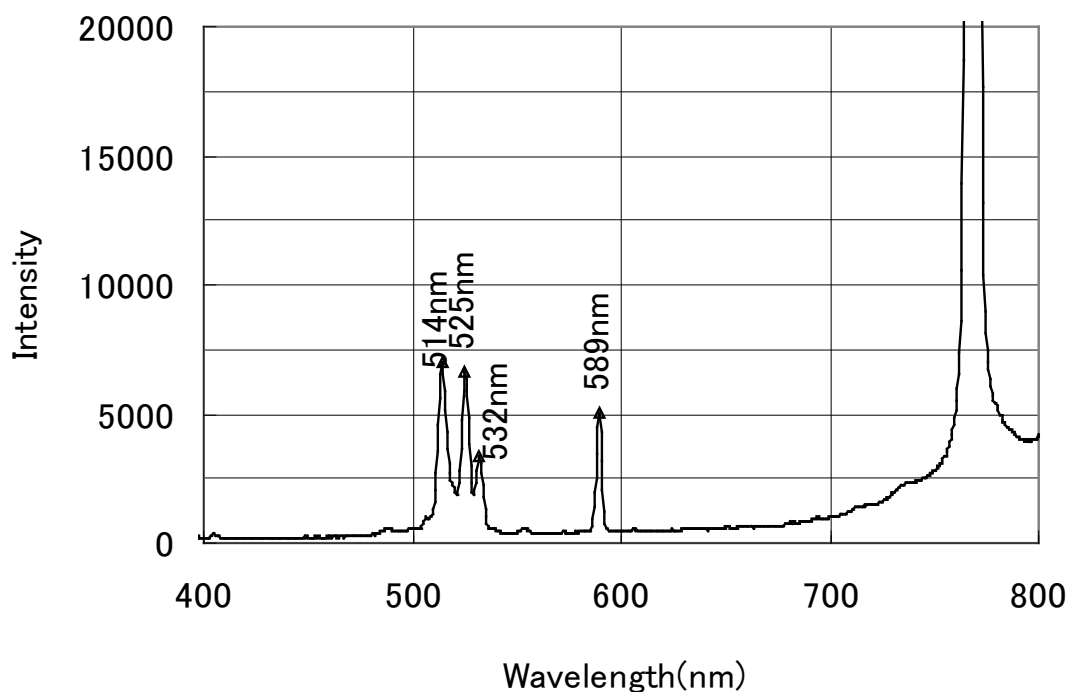


Figure 11 Spectrum of green flame.

content. The results possibly indicate that the color agent does not have a great effect on the chromatic performance.

(2) Effects of chlorinated gum

Experiments were done according to the formulas listed in Table 8. The percentage of chlorinated gum in the green formula was varied in 5% increments. The results of these experiments are shown in Figure 13.

When the amount of chlorinated gum was varied from 6% to 16%, the chromatic data showed a very slight change. But once the chlorinated gum content was above 16%, the performance decreased obviously. This may indicate that the flame temperature decreased with increasing chlorinated gum content because the combustion heat was lost in heating excess chlorinated gum.

(3) Effects of MgAl

The percentage of MgAl was changed in 5% increments based on the green reference composition and the formulas are listed in Table 9. The flame spectra were collected and analyzed. Those results are shown in Figure 14.

When the amount of MgAl increased from 6% to

21%, the chromatic coordinates moved towards the green region. However, when the MgAl content was above 21%, the chromatic coordinate changes were very slight.

Note that when the MgAl amount was below 16%, the chromatic coordinates quickly moved towards the orange-yellow region. A reason for this may be that as the MgAl amount decreased, the heat generated by MgAl burning decreased and there was not enough heat for the desired emitter excitation. The results suggest that a high energy agent such as MgAl is necessary for forming a deep green firework flame.

Blue composition flame spectra

A blue composition flame spectrum is shown in Figure 15. There were several peaks from approximately 400 to 560 nm which were from emissions of copper monochloride (CuCl) and copper hydroxide (CuOH). According to other researchers,² the molecular emitter copper monochloride (CuCl) is responsible for the emissions at 430, 436, 484, 489, and 527 nm. The emission at 465 nm is also from the emitter CuCl. Either emitter CuCl or emitter CuOH emits light over a wider wavelength range. The collection of emissions from 400 to 480 nm is recognized

Table 7 Variation of $Ba(NO_3)_2$ based on green formula (wt%).

Component	Formula				
	G-1	G-2	G-3 (RC)	G-4	G-5
KClO ₄	23.2	21.6	20	18.4	16.8
Ba(NO ₃) ₂	27	32	37	42	47
MgAl	18.5	17.3	16	14.7	13.5
Phenolic resin	7	6.4	6	5.6	5
Chlorinated gum	18.5	17.3	16	14.7	13.5
Rice granules	5.8	5.4	5	4.6	4.2

as violet-blue, and that from 480 to 560 nm is recognized as greenish-yellow. The dominant wavelength is possibly in the blue region, but it is difficult to improve the purity of the blue flame. Therefore, as long as compounds of copper are used as color agents in firework compositions, it is

very difficult to produce a deepest blue flame. In addition, the presence of the strong sodium peak at 589 nm and a continuum extending throughout longer wavelength region deteriorate the purity of the blue flame.

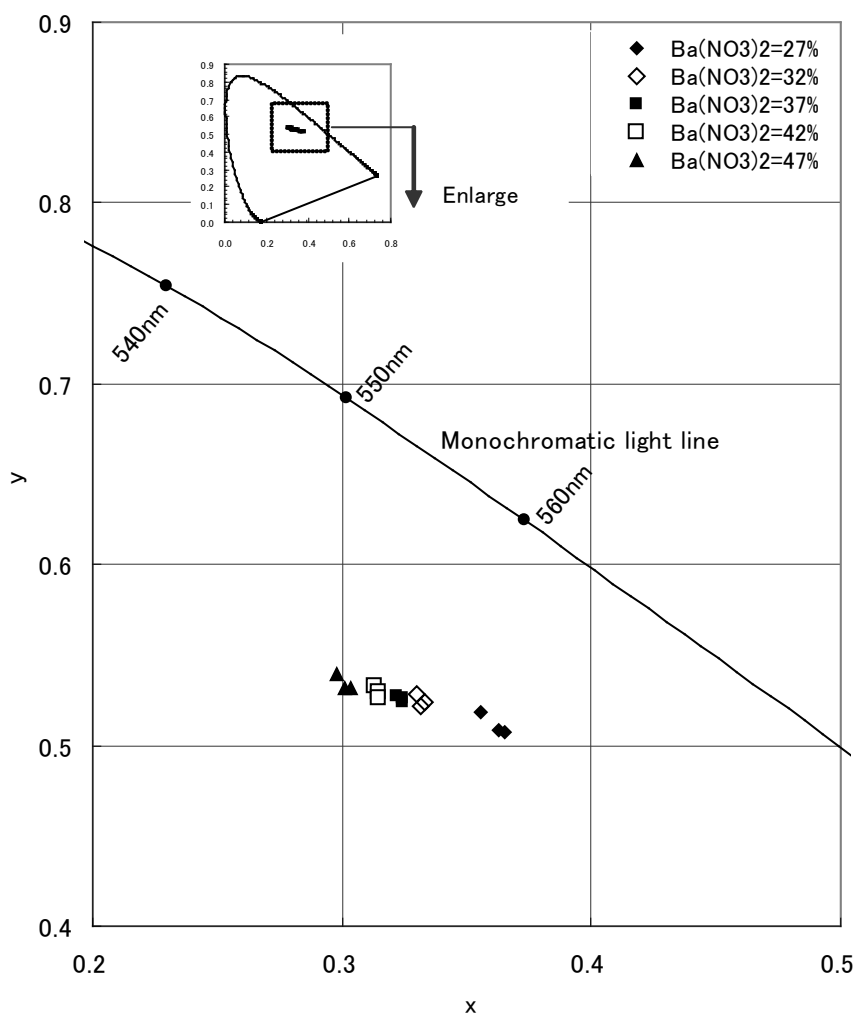


Figure 12 Chromaticity of variation of $Ba(NO_3)_2$ based on green formula.

Table 8 Variation of chlorinated gum based on green formula (wt%).

Component	Formula				
	G-6	G-7	G-3 (RC)	G-8	G-9
KClO ₄	22.4	21.2	20	18.8	17.6
Ba(NO ₃) ₂	41.4	39.2	37	34.8	32.6
MgAl	17.9	17	16	15.1	14.1
Phenolic resin	6.7	6.3	6	5.6	5.3
Chlorinated gum	6	11	16	21	26
Rice granules	5.6	5.3	5	4.7	4.4

Effects of CuO

The formulas with varying contents of the color agent CuO are listed in Table 10. The experimental results for these formulas are shown in Figure 16.

The results show that the chromatic coordinates

moved towards the blue region when the CuO content was increased, but once the amount of CuO was above 6%, the color performance hardly changed. It indicates that there is not a great dependence of the color performance on the amount of CuO.

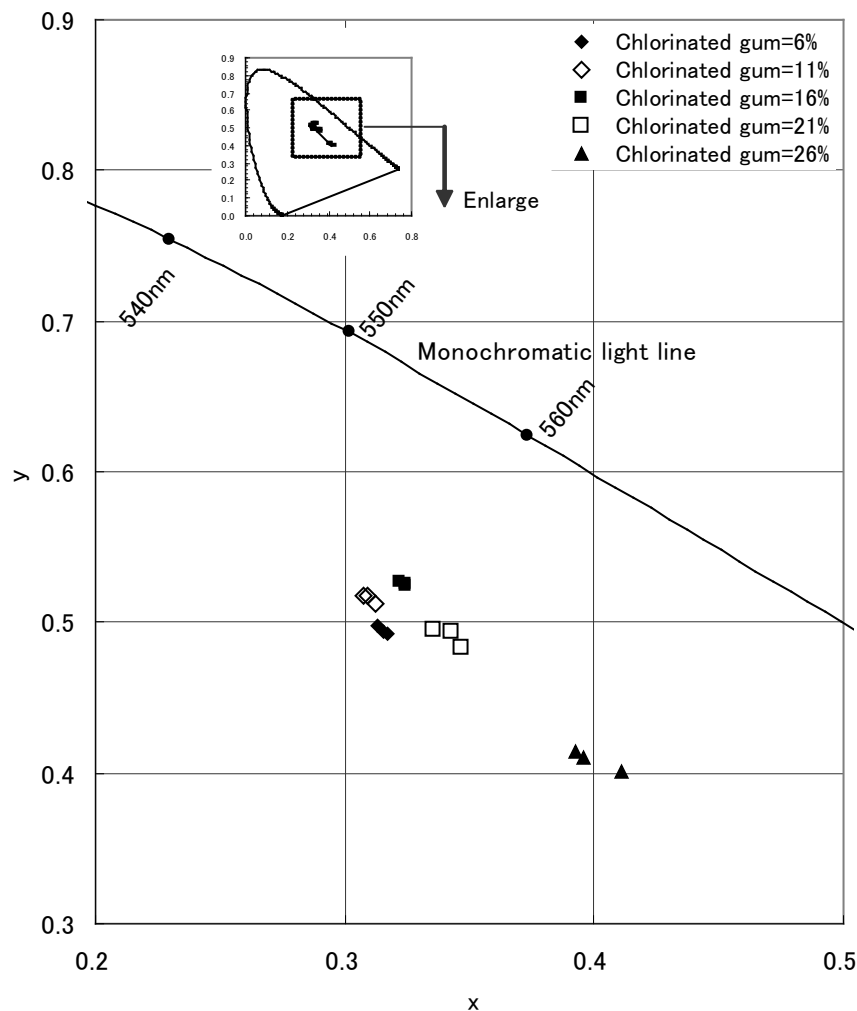


Figure 13 Chromaticity of variation of chlorinated gum based on green formula.

Table 9 Variation of MgAl based on green formula (wt%).

Component	Formula				
	G-10	G-11	G-3 (RC)	G-12	G-13
KClO ₄	22.4	21.2	20	18.8	17.6
Ba(NO ₃) ₂	41.4	39.2	37	34.8	32.6
MgAl	6	11	16	21	26
Phenolic resin	6.7	6.4	6	5.7	5.3
Chlorinated gum	17.9	16.9	16	15	14.1
Rice granules	5.6	5.3	5	4.7	4.4

Effects of chlorinated gum

The percentage of chlorinated gum in the blue reference composition was varied, and the formulas are shown in Table 11. The experimental results are shown in Figure 17. The results show that the chromaticity coordinates shift towards

the blue region with increasing chlorinated gum content. The predominant peaks in the spectrum are the emissions from CuCl. Therefore, adding a chlorinated gum to the composition will provide more Cl and will result in an increase in the amount of CuCl. But once the amount of chlorinated gum

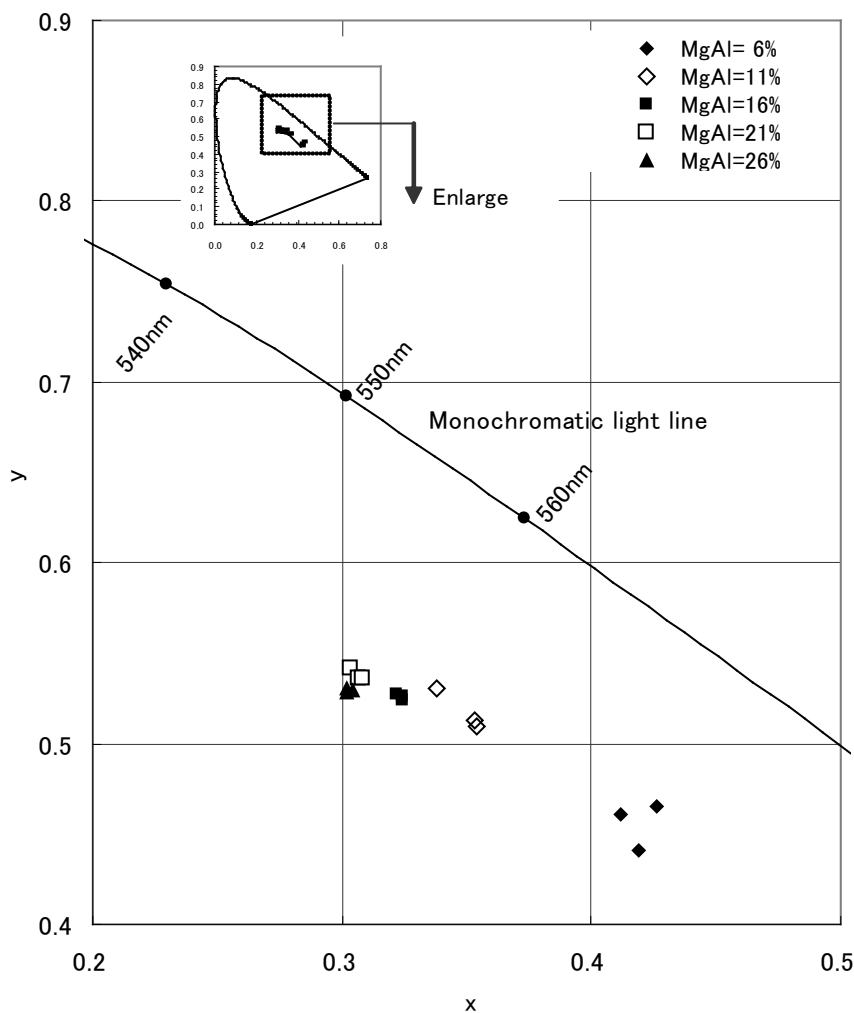


Figure 14 Chromaticity of variation of MgAl based on green formula.

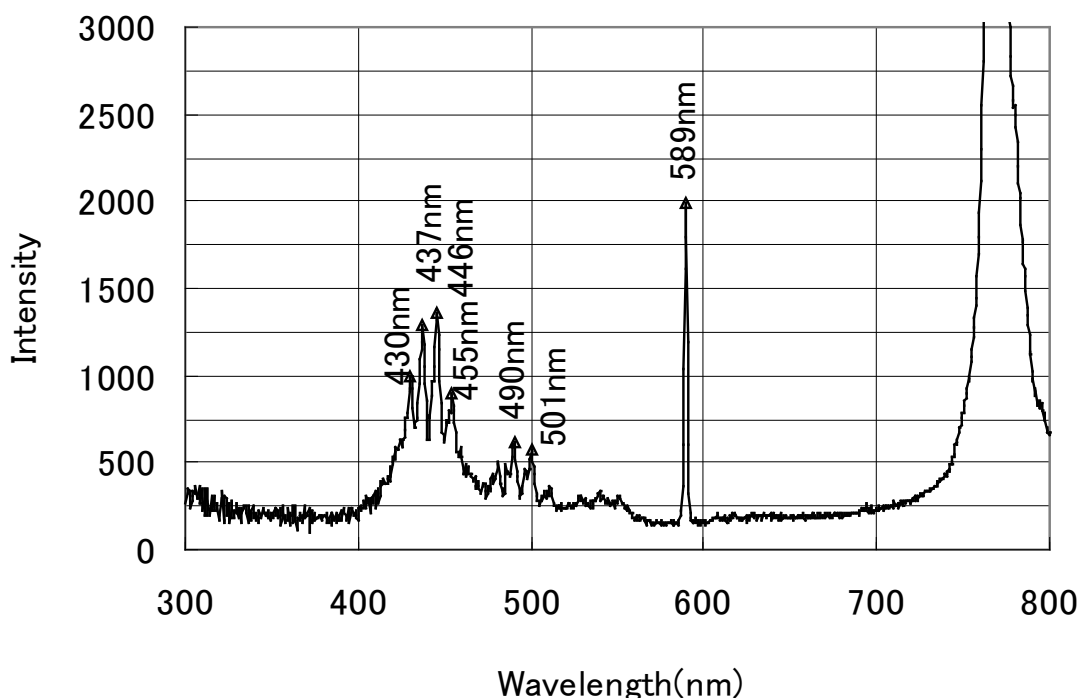


Figure 15 *Spectrum of blue flame.*

is at or above 14%, the chromaticity coordinates shift back to the white light region.

Effects of MgAl

MgAl powder was added to the blue reference composition with 5% increments from 5% to 25%, respectively, and the experiments were conducted. Those experimental results are plotted in Figure 18. For the comparison, the results for the blue reference composition are also plotted in the same figure. The point C indicates the ICI white light chromatic coordinate.

The results show that as MgAl metal powder above 5% was added to the blue reference composition, the chromatic coordinates would move towards the white light region and the purity of the blue flame would deteriorate. In fact, the flame could not be perceived as blue if above 5% metal powder MgAl was added to the blue reference composition. The reason is that the intensity of the sodium peak at 589 nm and continuous emission of light extending throughout the longer wavelength region will increase due to the high combustion heat of MgAl.

Conclusions

The effects of variation of content of color agent, chlorine donor or high energy agent on the colored flame of firework compositions have been investigated in this study. The quality of a colored flame mainly depends on the competition between desired emitters and undesired emitters. From the spectra measured, the emitting light peak and wavelength information due to the emitters is obtained. The atomic sodium peak at 589 nm is an undesired emission when forming a deep red, green or blue flame, but not for a yellow flame. Continuous radiation extending throughout the longer wavelength region is also undesirable for all colored flames. It is easier to form a deep red or yellow flame with the proper formula, but it is difficult to form a deep blue flame. In particular, a firework formula to which a metal powder such as MgAl is added cannot form a deep blue flame.

Table 10 Variation of CuO based on blue formula (wt%).

Component	Formula				
	B-1	B-2	B-3 (RC)	B-4	B-5
KClO ₄	68.6	65.8	63	60.2	57.4
CuO	2.0	6.0	10	14.0	18.0
Phenolic resin	13.1	12.5	12	11.5	10.9
Chlorinated gum	10.9	10.4	10	9.6	9.1
Rice granules	5.4	5.2	5	4.8	4.6

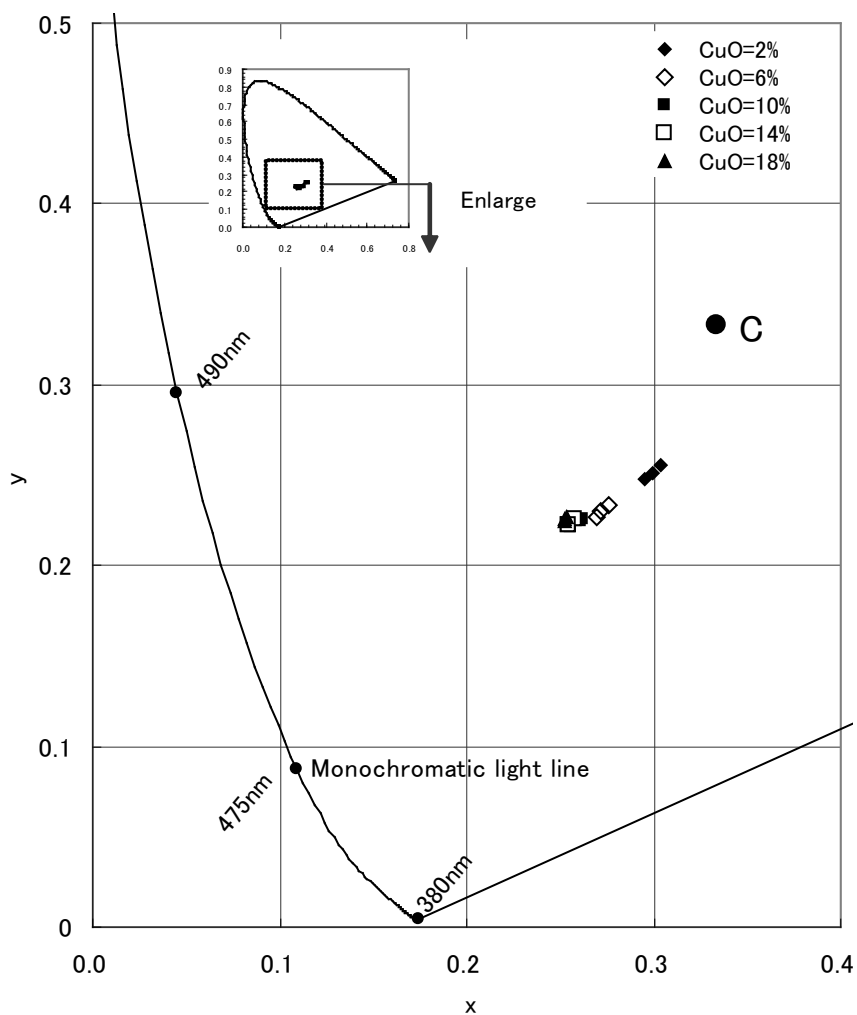


Figure 16 Chromaticity of variation of CuO based on blue formula (● sign indicates white light point ICI illuminant “C”).

Table 11 Variation of chlorinated gum based on blue formula (wt%).

Component	Formula				
	B-6	B-7	B-3 (RC)	B-8	B-9
KClO ₄	68.6	65.8	63	60.2	57.4
CuO	10.9	10.4	10	9.6	9.1
Phenolic resin	13.1	12.5	12	11.5	10.9
Chlorinated gum	2.0	6.0	10	14.0	18.0
Rice granules	5.4	5.2	5	4.8	4.6

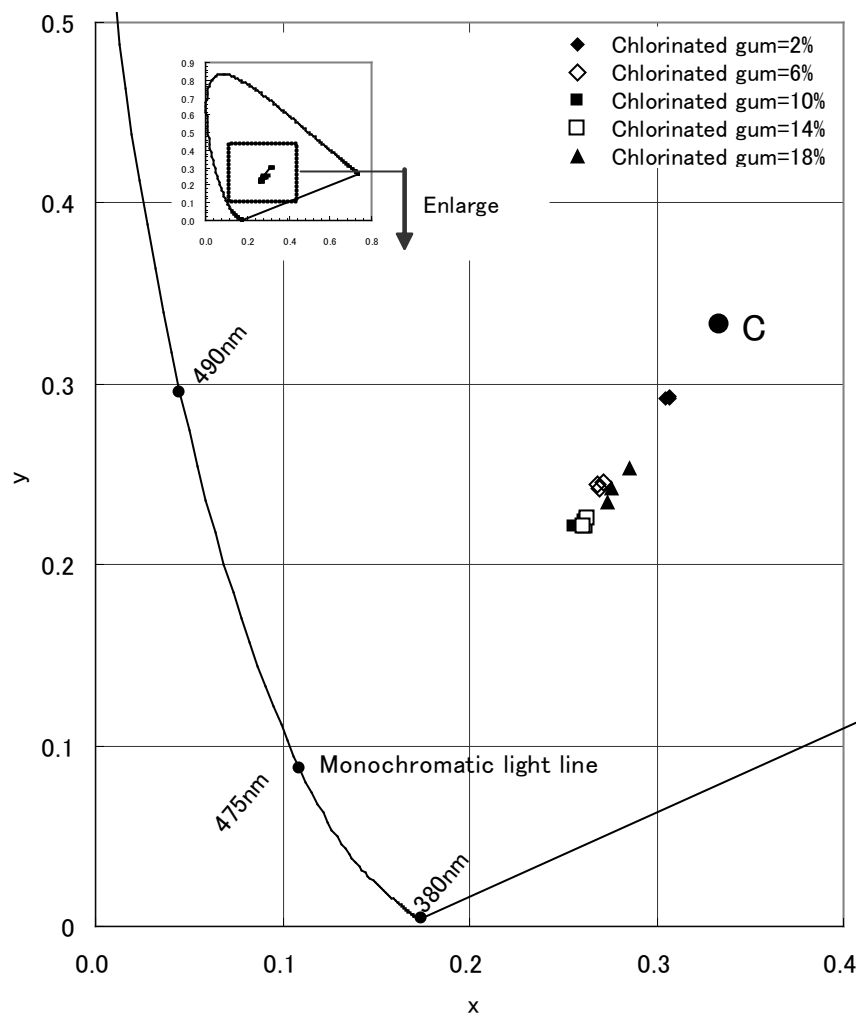


Figure 17 Chromaticity of variation of chlorinated gum based on blue formula (● sign indicates white light point ICI illuminant “C”).

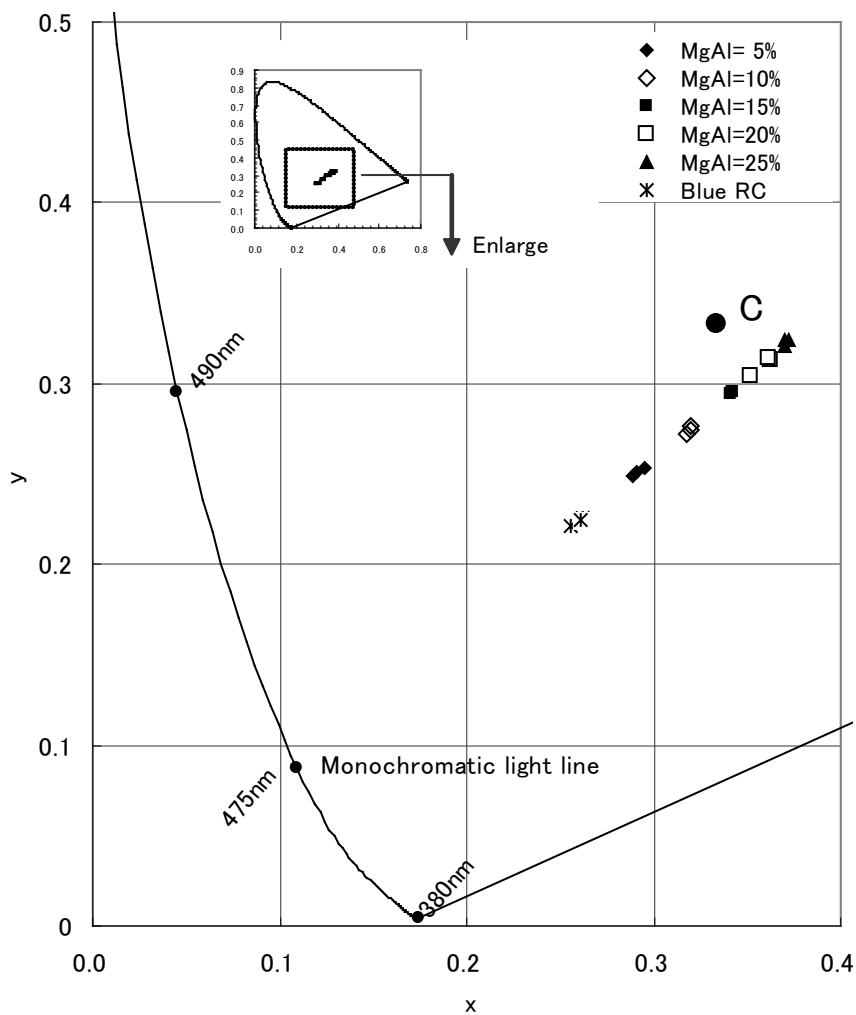


Figure 18 Chromaticity of variation of MgAl added to blue reference formula (● sign indicates white light point ICI illuminant “C”).

References

- 1 Y. Sashimura, Fireworks, Personal publication, Printed by Nanfudo, Japan, Feb. 1, 2007, pp.166-173
- 2 Brian V. Ingram, “Color Purity Measurement of Traditional Pyrotechnic Star Formulas”, *Journal of Pyrotechnics*, Issue 17, Summer 2003, pp. 1–18.
- 3 K. L. Kosanke and B. J. Kosanke, “The Chemistry of Colored Flames”, *Pyrotechnic Chemistry*, Ch. 9, pp. 42–44, Journal of Pyrotechnics Inc., 2004.
- 4 K. Itoh, D. Ding, Y. Sashimura, H. Watanabe and T. Yoshida, “Effect of Composition on Color Values of Green Star Flame”, 11th International Symposium on Fireworks, Puerto Vallarta, México, April 20-24, 2009, pp.115-126.

A New And Fast Method Of Evaluating Powder Energy

Andrew Tang, Hilary Chen and Andy Tang

Tian Cheng Pyrotechnics Laboratory

Liuyang, Hunan, China

atang@tcpyrolab.org, www.tcpyrolab.org

Abstract: *In the fireworks or pyrotechnics industry, black powder (nitrate–sulphur–charcoal) is a traditional and commonly used base for creating other chemical compositions. Due to the large variety of pyrotechnic effects, the creation of such different compositions that meet so many needs has led to many different formulations. The energetic status of such formulations can easily be confused, for instance the break charge used in a breaking aerial shell can produce a tremendous audible sound like flash powder. Nowadays manufacturers may also develop their own chemical compositions by replacing and/or adding different chemical substances in order to give a “perfect” function such as large break. It is always the breaking energy that dominates the display color effect and it may generate unnecessary pressure causing danger to the operators or the audience. European standard UN default classification controls the use of metal alloys in black powder formulations, i.e. flash powder. The time/pressure test is very tedious. In the United States, the usage of flash powder is limited to 50 milligrams for ground items or 130 milligrams for aerial items for consumer fireworks. Sometimes manufacturers add non-metallic chemicals such as perchlorate and benzoate to create a formulation that can still create unnecessary pressure and cause danger. It is necessary to develop a fast and simple test method to evaluate the powder energy no matter what the chemical formulation is. Such a method can be used by manufacturing industry quality control personnel on-the-spot to evaluate the powder energy.*

The method uses a simple test fixture which is composed of a steel tube acting as mortar and a standard “weight” steel ball. The powder energy is “evaluated” by the height to which the steel ball is ejected by the explosion of the powder confined in a standard plastic vial sitting inside the mortar. By plotting a graph of steel ball height vs amount of powder used, the graph shows a straight line with a gradient called Energy Return On Powder (EROP value). A market survey reviews powders of different chemical compositions with different EROP values.

Keywords: *powder energy, black powder, flash powder, EROP value, mesh size, mortar height*

Introduction

Black powder (chemical composition potassium nitrate : sulphur : charcoal in a ratio of approximately 60 : 25 : 15), which in Chinese is called *Hei yue*, is the base of most chemical formulations in fireworks manufacturing. Factory personnel often modify its composition by changing the percentages of these three chemical substances, replacing or substituting them with other chemical substances in order to obtain the intended effect. However the

energy of the black powder will then be modified to a extent not known to the factory personnel, unless a good experienced worker might possibly be able to predict it. The only way to ensure its energy performance is to prepare a final production sample to run a test of the prototype product, so that one will know whether the powder energy is good or not. In order to provide a practical and cheaper way to “evaluate” the powder energy, we are trying to develop an alternative method for such on-the-spot factory personnel to use.

Article Details

Manuscript Received:-28/05/2009

Publication Date:-28/07/2009

Article No: - 0078

Final Revisions:-28/07/2009

Archive Reference:-936

At the same time, international requirements, including the EU and American markets, are very concerned about the usage of metal alloys mixed with black powder to make flash powder (a definition that usually means metallic chemicals added to black powder). The energy of such modified flash powder can generate a much greater effect than black powder on its own. Furthermore, due to limitations of the usage of flash powder,¹ manufacturers also invented non-metallic powder mixed with black powder which can generate similar effects to flash powder.

European authorities and experts have started to adopt the time/pressure test such as the UN Test Series 2(c)(i) time/pressure test as the definition of flash powder,² but the test requires expensive equipment as well as an experienced engineer to carry it out. Therefore it is not practical for on-the-spot factory personnel to follow such a time/pressure test procedure. Furthermore, a recent study³ shows the time/pressure test is not a good reliable testing method.

Theory

The height of the steel ball ejected from the steel tube (mortar) is directly proportional to the weight of the powder confined in the standard test vials.⁴

Among the three laws of motion of Sir Isaac Newton,⁵ the second law, the Law of Momentum, is the most applicable one in this study. The law states: *If a particle is subjected to a force, the particle will accelerate. The acceleration of the particle will be in the direction of the force, and the magnitude of the acceleration will be proportional to the force and inversely proportional to the mass of the particle.* In simple terms, the acceleration of an object is proportional to the resultant force acting on it and is in the direction of this force, or

$$\text{Momentum} = mV \quad (1)$$

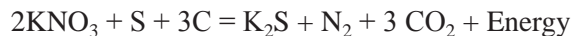
For an object of mass m subjected to a resultant force F , the law may be stated mathematically as

$$F = ma \quad (2)$$

where F denotes force in newtons; m , mass in Kg; and a , acceleration in ms^{-2} .

Most of the powder used in the fireworks or pyrotechnics industry uses black powder as the

basis of the formulation. Its chemical reaction has been studied and can be summarized as the following reactions.



The energy generated evolves as a force that expands from the standard confined vial that contains a sample of black powder. The release of energy expels the steel ball from the opening of the steel tube upwards to a height, as shown in Figure 1. The ball is ejected upwards and then falls down towards the ground.⁶

Force is defined as a quantity that is capable of producing motion or a change in motion that is a change in velocity, or constant acceleration.

Force, $F = ma$,

where F is the force of the ball,

m is the mass of the ball,

a is the acceleration of the ball.

In a more real case, the force is expressed as

$$F = ma = m(V_2 - V_1)/t \quad (3)$$

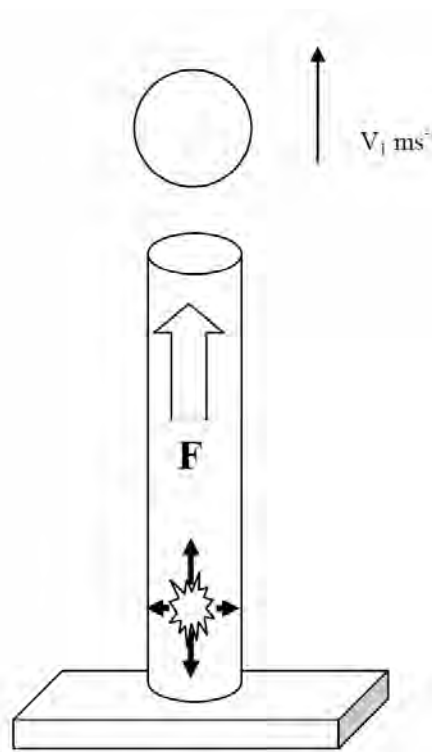


Figure 1. Sketch diagram of test fixture.

where V_2 is the final velocity of the ball,

V_1 is the initial velocity of the ball.

Therefore, $F \propto (V_2 - V_1) \propto$ velocity V .

Neglecting air resistance, an example of questions and answers is introduced by using the Equations of Motion⁷ for uniformly accelerated motion that comes from elementary physics, to explain the theory, where

V_1 is initial velocity

V_2 is final velocity

S is displacement

a is uniform acceleration

t is time of travel

(i) How high does the ball rise with velocity V_1 ?

From the equation for a free falling ball,

$$V_2^2 - V_1^2 = 2aS \quad (4)$$

$\rightarrow S = (V_2^2 - V_1^2)/2a = V_1^2 / 2 \times 9.8,$
where $V_2 = 0$ and $a = 9.8 \text{ ms}^{-1}$

$$\rightarrow S = V_1^2/19.6$$

$$\rightarrow S \propto V_1^2 \propto V_1$$

(ii) How long does it take to rise up and return to ground?

From the equation for a free falling ball,

$$S = V_1t + at^2/2 \quad (5)$$

$$\rightarrow 0 = (V_1 + at/2)t,$$

where $S = 0,$

$$\rightarrow t = 0 \text{ or } t = -2V_1/a$$

The ball takes the same time to and from the ground but this is not of interest at this point.

(iii) With what speed does the ball hit the ground?

From the equation for a free falling ball,

$$V_2 = V_1 + at \quad (6)$$

$$\rightarrow V_2 = V_1 + a(-2V_1/a) = V_1$$

Work W is defined as the transfer of energy occurring when the point of application of force F newtons moves through a distance S metres, with,

$$W = FS \text{ newton metres (Nm) or joules (J)}$$

When work is expended in accelerating a ball,

mass m , from rest to a velocity V the force F being applied to give the acceleration a , is

$$F = ma \text{ newtons (N)}$$

and the distance S through which the point of application moves is given by $V^2 = 2aS$. Thus the work done is

$$FS = (ma)(1/2 V^2/a) = (1/2) mV^2 \text{ Nm}$$

Energy has been transferred to the object and it is said to be have gained kinetic energy.

KE of the ball is,

$$(1/2) mV^2 \text{ joules (J)}$$

When work is expended in slowly raising an object of mass m through a vertical height h , the force mg has its point of application moved through distance (or height) h and so the work done is mgh . Energy has been transferred to the object and it is said to have gained potential energy.

PE of the ball is,

$$mgh \text{ joules (J)}$$

As we have seen, energy changes form one form to another, and it does so without a net loss or net gain. It is one of the most basic scientific principles.

Initial Energy = Final Energy

$$(KE + PE)_I = (KE + PE)_F \quad (7)$$

Newton's first law, the conservation of energy: Kinetic Energy and Potential Energy⁸

$$KE \rightarrow PE$$

$$1/2 mV \rightarrow mgh \quad (8)$$

where m is the mass of the ball,

g is gravity

h is the ejected height of the ball.

Assuming zero air resistance and perfect aerodynamics, therefore at the highest point,

$$\text{Total Energy} = 1/2 (mV^2) = mgh \quad (9)$$

$$\rightarrow V = \sqrt{(2g \Delta h)}$$

When the powder generates energy and transfers it to the steel ball by ejecting it to a height, the power within the steel ball becomes,

$$P = W/t = FS/t = FV$$

Where **velocity, $V \propto$ height, h** because mass, m and gravity, g are constant for a given amount of powder used.

Power $P \propto V \propto h$

Experiment

The experiment is designed to show the height of the steel ball, m grams, has a relationship with the force generated by the powder confined in the steel tube. With constant mass of the ball and dimensions of the tube, it is also assumed the air resistance is neglected and experiments are therefore designed as the following parts:

- I. Relationship between mesh size of black powder and height of mortar tube.

The experiment is designed to study the different heights of stainless steel ball D, ejected by using different mesh size black powders P1, P2 and P3 with different mortar

tubes T1, T2 and T3.

- II. Relationship between mesh size of black powder and weight of stainless steel ball.

The experiment is designed to study the different heights of the stainless steel ball ejected by using fixed mortar tube T2 with mesh size black powders P1, P2 and P3.

- III. Relationship between weight of black powder and height of stainless steel ball

The experiment is designed to study the effect on stainless steel ball D, ejected by using fixed mortar tube T2 with different weights of black powder P3 that was collected from a fireworks manufacturer.

- IV. Relationship between weight of break charge powder and height of stainless steel ball

The experiment is designed to study the



Figure 2. Steel tube (mortar) (from left to right, A, B and C) and steel balls (shell) (from left to right, A to F).

effect on stainless steel ball D, ejected by using fixed mortar tube T2 with different weights of break charge powder that was collected from a fireworks manufacturer.

- V. Relationship between weight of flash powder and height of stainless steel ball
The experiment is designed to study the effect on stainless steel ball D, ejected by using fixed mortar tube T2 with different weights of flash powder that was collected from a fireworks manufacturer.

- VI. Repeatability test using black powder
The experiment is designed to study the repeatability of the test by using black powder.

Test apparatus

1. Specially made steel tubes of following dimensions (length, ID), see Figure 2:
T1 : 82.5 mm × 44 mm
T2 : 165.0 mm × 44 mm
T3 : 330.0 mm × 44 mm
2. Specially made stainless steel balls of following dimensions (weight, OD), see Figure 2.
Ball A : 208 grams, 48 mm
Ball B : 371 grams, 45 mm
Ball C : 513 grams, 50 mm

Ball D : 639 grams, 54 mm

Ball E : 777 grams, 58 mm

Ball F : 879 grams, 60 mm

3. Powders, see Figure 3.
Black powder P1 of mesh size +40
Black powder P2 of mesh size +60
Black powder P3 of mesh size -120
Break charge powder B1, mesh size -100
Flash powder F1
4. Electrical igniter with power supply
5. Standard test vials, PP material, 5.0 ml, see Figure 4.
6. Measuring slide, 3 metres
7. Video camera

Procedures

1. Measure 1.0 grams of powder and place into standard test vial.
2. Place standard test vial into the bottom of mortar tube.
3. Set the stainless steel ball sitting on top of the mortar tube.
4. Fire the igniter and record the motion by video recorder.



Figure 3. Powders collected from market (left: break charge, right: flash powder).

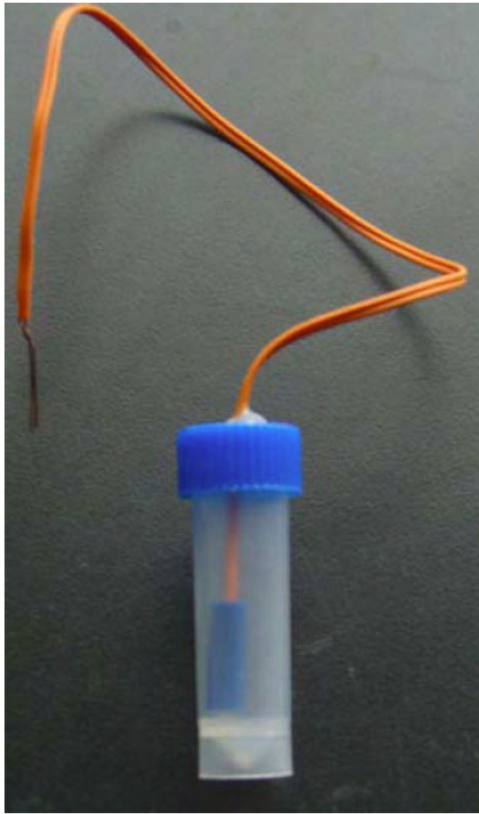


Figure 4. Standard test vials with electric igniter inside.

- Review the video recorder to observe the height to which the stainless steel ball is ejected.

Note: All sample powders were conditioned for 24 hours in a dry chamber before use.

Results and discussion

I. Relationship between mesh size black powder using a steel tube and height of mortar tube

Conditions: 1.0 gram powder with mortars T1, T2 and T3 using ball D

Discussion: Black powder P1 is mesh size +40, P2 is mesh size +60 and P3 is mesh size -120. Different mesh size black powders show different energy profiles using different height mortars (Figure 5). This proves that the force generated inside the mortar tube is different which proves that the finer the powder, the higher the energy it generates and so the greater the height to which the stainless steel ball is ejected. Thus the energy generated by these three powders is

energy of P1 < energy of P2 < energy of P3

though the direct relationship of the mortar height (length), or of its internal volume, to the energy is

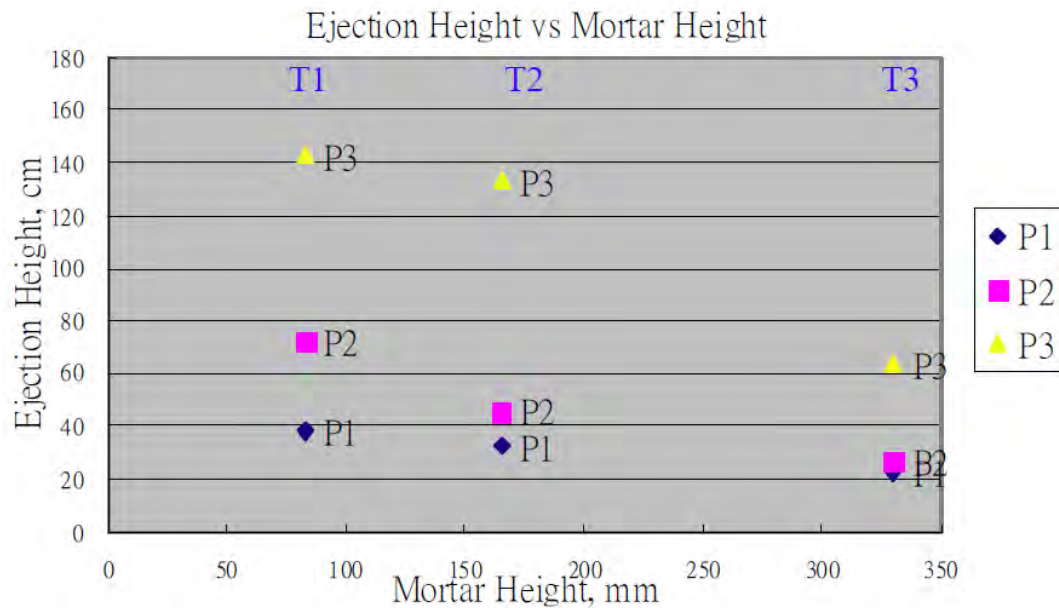


Figure 5. Ejection height of steel ball from different mortar heights using different mesh size black powder.

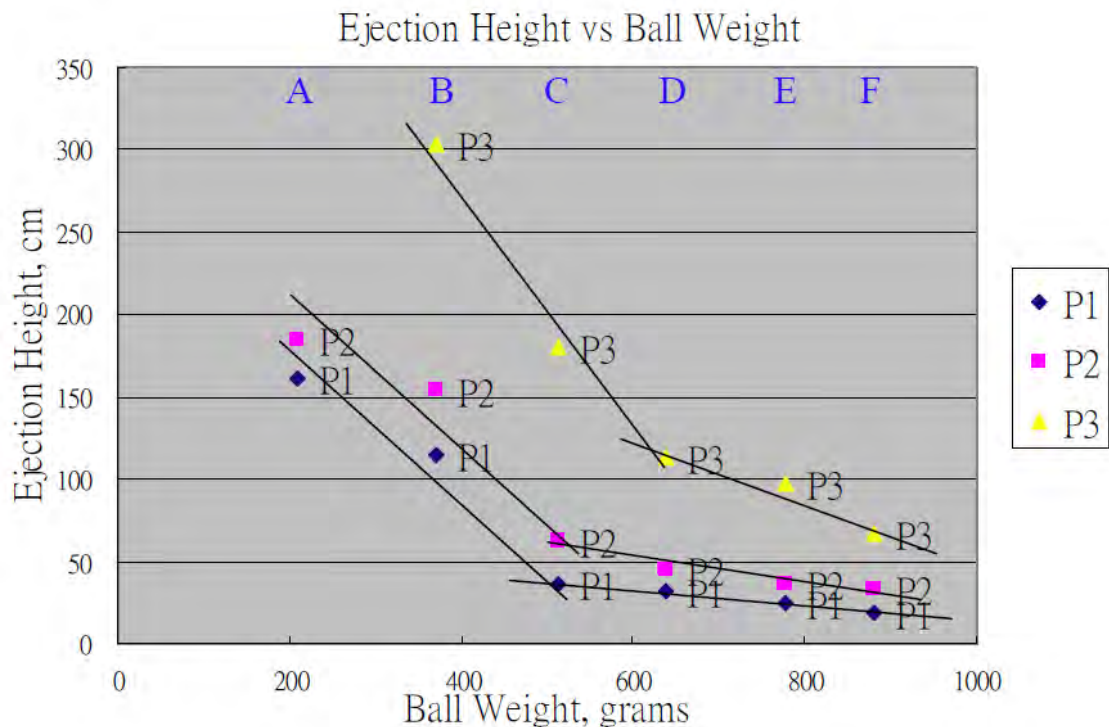


Figure 6. Ejection height vs weight of steel ball using different mesh size black powder.

unknown at this moment. However it is possible to show that the shorter the tube, the greater will be the energy transferred to the ball. Thus the energy transferred by using these three mortar tubes is,

energy transfer by T1 > energy transfer by T2 > energy transfer by T3

II. Relationship between mesh size black powder and weight of stainless steel ball

Conditions: 1.0 gram powder with mortar T2 using balls A to D.

Discussion: The three different curves in Figure 6 correspond to three different mesh sizes of black powder P1, P2 and P3 by using different balls (A to F). The height of ejection is inversely proportional to the ball weight, i.e. the lighter the ball the higher is the ejection.

Note: Only two points were measured for ball A because the result was too high to be recorded.

The weight of the ball is

$$A < B < C < D < E < F$$

The height to which the ball is ejected, using the

same amount of powder and test conditions, is

$$A > B > C > D > E > F$$

Furthermore the diameters of the balls lie between 45 mm and 60 mm. The smallest is ball B and the biggest is ball F. Among balls C, D, E and F, the height is mostly inversely proportional to its diameter which may be caused by air resistance. To continue the study, it is appropriate to take the middle weight which is ball D for further studies.

III. Relationship between weight of black powder P3 and height of stainless steel ball

Conditions: x grams of powder with mortar T2 using ball D

Discussion: For a given amount of powder, there were three trial tests done and the height was recorded in centimetres (Table 1).

The graph (Figure 7) shows an almost linear relationship between the weight of black powder and the ejection height of the stainless steel ball. The slope of the line is 137.6 cm g^{-1} .

If we calculate the best fit line (Figure 8) and its

Table 1. Relationship between weight of black powder P3 and height of stainless steel ball.

Powder weight/g	Height/cm			Average height/cm	Standard deviation	Relative standard deviation (%)
	Trial 1	Trial 2	Trial 3			
0.3	40	42	40	41	1.2	3
0.5	62	72	60	65	6.4	10
1.0	116	160	120	132	24.3	18
1.5	168	220	260	216	46.1	21
2.0	252	278	272	267	13.6	5

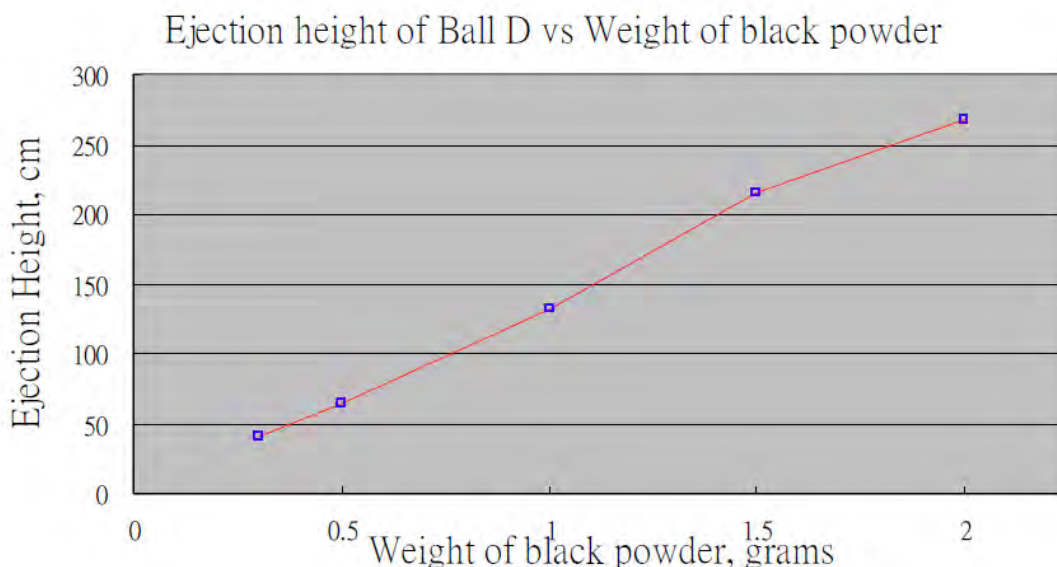


Figure 7. Ejection height of ball vs weight of black powder P3, using ball D/T2

respective energy generated by using total energy equation (9), the energies are calculated as shown in Table 2.

a fixed amount of powder which is here termed as Energy Return On Powder (EROP), calculated as 8.58 joules per gram ($J g^{-1}$).

The slope therefore becomes energy generated by

Table 2. Relationship between weight of black powder P3 and energy of stainless steel ball.

Powder weight/g	Energy/J			Average energy/J
	Trial 1	Trial 2	Trial 3	
0				0
0.3	2.5049	2.6301	2.5049	2.547
0.5	3.8826	4.5088	3.7573	4.050
1.0	7.2642	10.020	7.5146	8.266
1.5	10.521	13.777	16.282	13.53
2.0	15.781	17.409	17.033	16.74

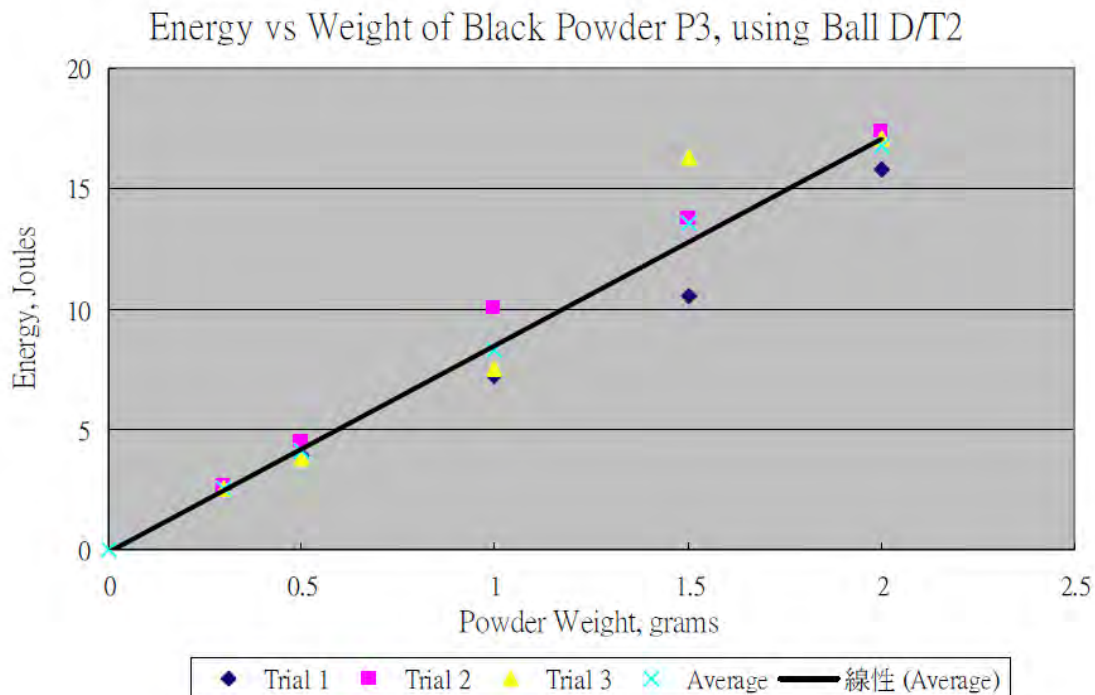


Figure 8. Energy vs weight of powder P3, using ball D/T2.

IV. Relationship between weight of break charge powder B1 and height of stainless steel ball

Condition: x grams of powder with mortar T2 using ball D

Discussion: For a given amount of powder, there were three trial tests done and the height was recorded in centimetres (Table 3).

The graph (Figure 9) shows an almost linear relationship between weight of break charge powder and ejection height of the stainless steel

ball. The slope of the line is 248.0 cm g^{-1} .

If we calculate the best fit line (Figure 10) and its respective energy generated by using total energy equation (9), the energies are calculated as shown in Table 4.

The slope therefore becomes energy generated by a fixed amount of powder which is here termed as Energy Return On Powder (EROP), calculated as $15.53 \text{ joules per gram (J g}^{-1}\text{)}$.

V. Relationship between weight of flash powder F1 and height of stainless steel ball

Table 3. Relationship between weight of break charge powder B1 and height of stainless steel ball.

Powder weight/g	Height/cm			Average height/cm	Standard deviation	Relative standard deviation (%)
	Trial 1	Trial 2	Trial 3			
0	0	0	0	0		
0.1	18	18	18	18.0	0.00	0
0.3	66	48	38	50.7	14.19	28
0.5	122	124	84	110.0	22.54	20
0.7	142	208	154	168.0	35.16	21
1.0	240	218	240	232.7	12.70	5

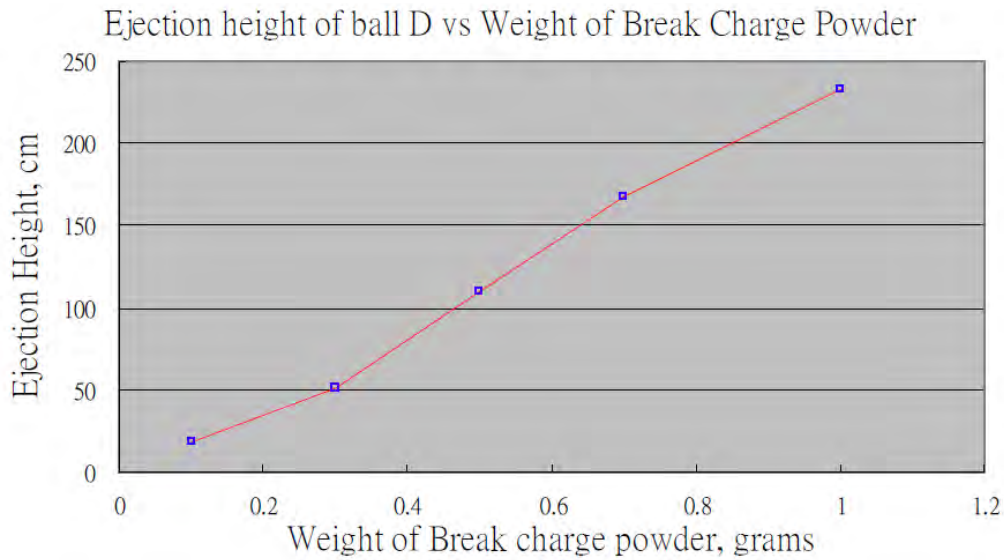


Figure 9. Ejection height vs weight of break charge, using ball D/T2.

Table 4. Relationship between weight of break charge powder B1 and energy of stainless steel ball.

Powder weight/g	Energy/J			Average energy/J
	Trial 1	Trial 2	Trial 3	
0	0	0	0	0
0.1	1.127	1.127	1.127	1.127
0.3	4.133	3.006	2.380	3.173
0.5	7.640	7.765	5.260	6.888
0.7	8.892	13.025	9.644	10.52
1.0	15.029	13.652	15.029	14.57

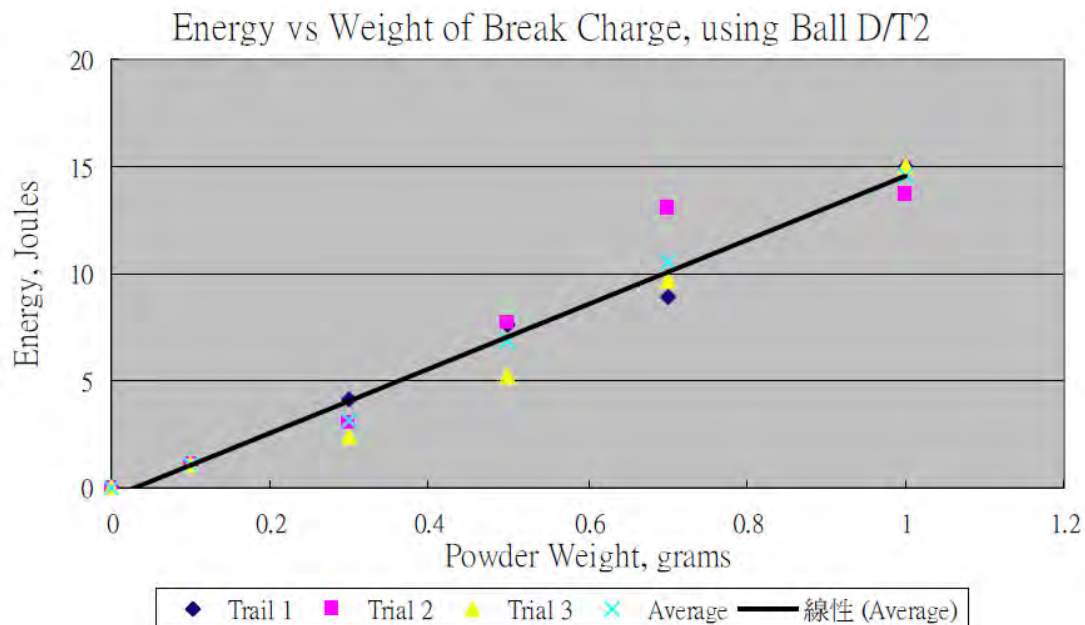


Figure 10. Energy vs weight of break charge powder, using ball D/T2.

Table 5. Relationship between weight of flash powder F1 and height of stainless steel ball.

Powder weight/g	Height/cm			Average height/cm	Standard deviation	Relative standard deviation (%)
	Trial 1	Trial 2	Trial 3			
0	0	0	0	0		
0.1	50	52	56	52.7	3.06	6
0.3	162	154	158	158.0	4.00	3
0.5	248	222	230	233.3	13.32	6
0.7	312	308	294	304.7	9.45	3
1.0	416	408	378	400.7	20.03	5

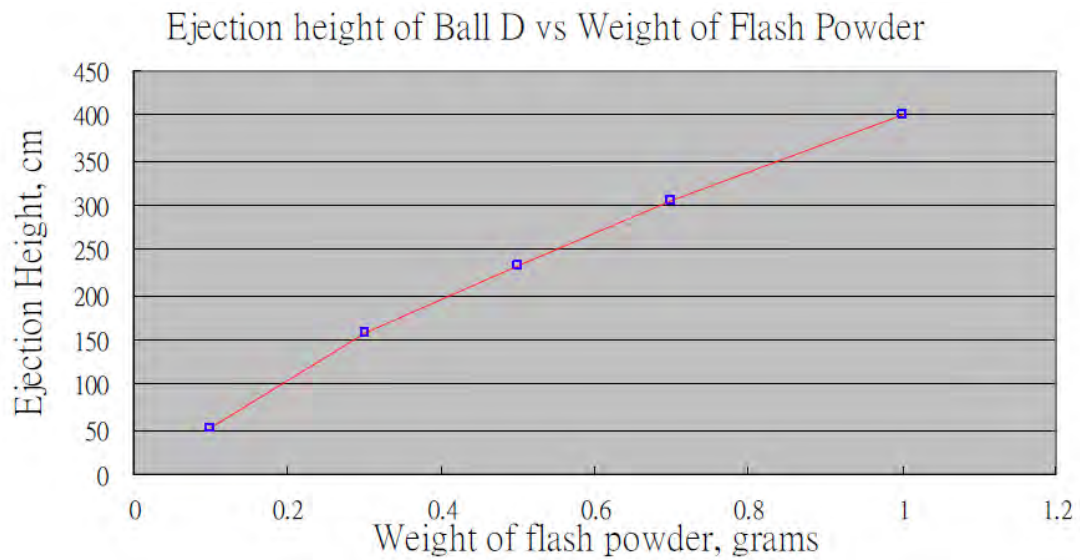


Figure 11. Ejection height vs weight of flash powder, using ball D/T2.

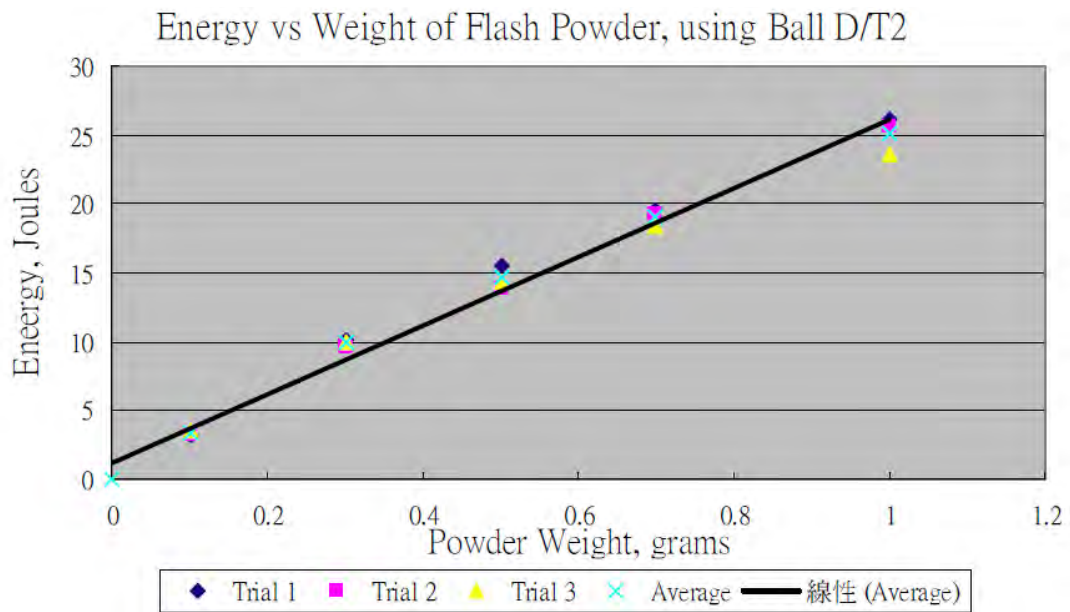


Figure 12. Energy vs weight of flash powder, using ball D/T2.

Condition: x grams of powder with mortar T2 using ball D

Discussion: For a given amount of powder, there were 3 trial tests done and the height was recorded in centimetres (Table 5).

The graph (Figure 11) shows another linear relationship between the weight of flash powder and the ejection height of the stainless steel ball. The slope of the line is 380.4 cm g^{-1} .

If we calculate the best fit line (Figure 12) and its respective energy generated by using total energy equation (9), the energies are calculated as shown in Table 6.

The slope therefore becomes the energy generated by a fixed amount of powder which is here termed as Energy Return On Powder (EROP), calculated

as $23.82 \text{ joules per gram (J g}^{-1}\text{)}$.

VI. Repeatability study of black powder

Condition: 1.0 gram of black powder, P3 with mortar T2 using ball D

Discussion: The graph (Figure 13) shows 20 trial tests result with average height of 109.4 cm, standard deviation of 29.95 and relative standard deviation of 27%.

Conclusion

The alternative method using a simple test fixture and a stainless steel ball may be used to evaluate the energy generated by the powder. The results of experiment I and II are useful in understanding

Table 6. Repeatability study on black powder.

Powder weight/g				Average energy/J
	Trial 1	Trial 2	Trial 3	
0				0
0.1	3.1311	3.2563	3.5068	3.298
0.3	10.145	9.6438	9.8943	9.894
0.5	15.530	13.902	14.403	14.61
0.7	19.538	19.288	18.411	19.08
1.0	26.051	25.550	23.671	25.09

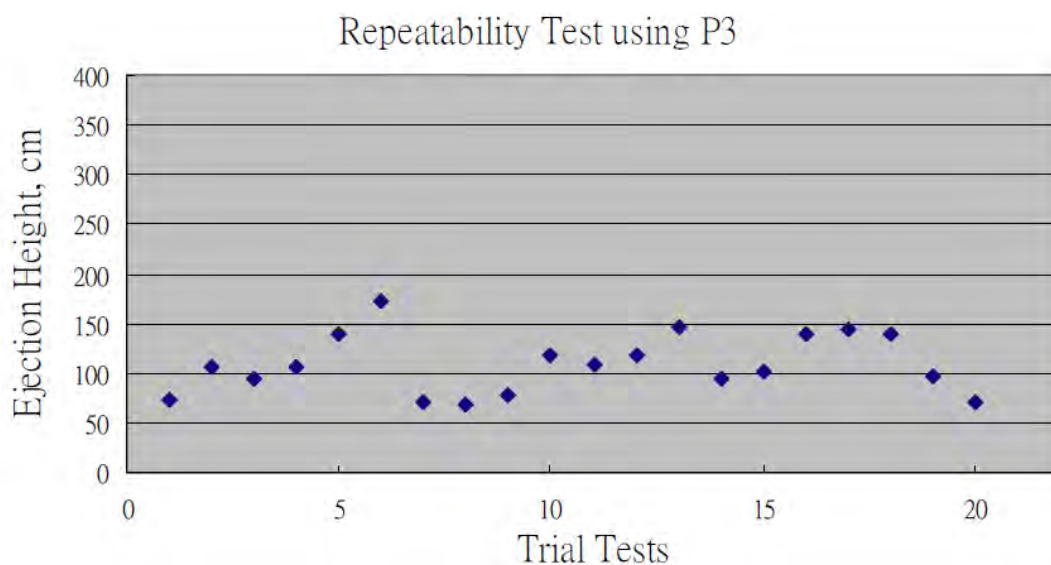


Figure 13. Repeatability test of black powder P3, using ball D/T2.

Table 7. Comparison of EROP of different powders.

Powders	Slope of graph/ cm g ⁻¹	EROP/J g ⁻¹
Black powder	137.6	8.58
Break charge	248.0	15.53
Flash powder	380.4	23.82

the effect of using mortar tubes of different dimensions and stainless steel balls of different weights. It appears that the smaller the volume of the mortar tube, the larger the energy of the powder generated. The lighter the stainless steel ball, the higher the ejection height. It is necessary that a lot of tests be performed in order to understand the relationship between the mesh size of the powder and the dimensions of the mortar tube and ball. The powder P3 shows a better proportional relationship than powders P2 and P1 with the turning point at ball D.

Experiments III, IV and V show the ejection height is directly proportional to the amount of powder used. There is a good linear relationship between the weight of powder and ejection height. All three curves show a different slope. By using the linear equation, integrating these three curves will produce a slope factor of 137.6 cm g⁻¹, 248.0 cm g⁻¹, and 380.4 cm g⁻¹. The higher the

figure is, the higher the energy. In an alternative expression for the energy generated by different powders under these test conditions with the standard test fixture, we can use

$$PE = mgh$$

$$EROP = PE/\text{mass of powder} \quad (10)$$

The method is very simple and practical for non-technical personnel to evaluate the amount of energy stored in the powder. By using this principle, we have a good practical technique to separate those powerful formulated powders from traditional black powder formulations. The different slopes of different powders generate different EROP values, from equation (10), calculated and shown in Table 7. These index values are a good indication of energy produced by the powders.

Following the experiment, several samples were collected from the market and tested. The results are listed as Table 8.

The EROP is a good index value and shows that black powder lies below 10 J g⁻¹. Break charges lie between 10 and 20 J g⁻¹. There are some exceptions because of its wide usage in the industry, depending whether it is used in breaking shells or breaking insert tubes. Flash powder is the most powerful among these three types of powder,

Table 8. Comparison of EROP of different brands of powders.

Powders		Mesh Size	EROP/J g ⁻¹
Formulation	Source		
Black powder	(Brand A)	-120	6.8
	(Brand B)	-120	6.9
	(Brand C)	-120	5.5
	(Brand B)	60	4.6
	(Brand B)	40	3.7
	Unknown	Unknown	8.6
Break charge	(Brand QC)	Unknown	4.4
	(Brand DS)	Unknown	14.3
	Unknown	Unknown	15.5
Flash powder	(Brand EZ)	Unknown	14.0
	(Brand HB)	Unknown	26.1
	Unknown	Unknown	23.8

and the EROP values lie between 20 and 30 J g⁻¹.

Further study is still required in order to better describe the energy level by using this alternative evaluation method. Such studies should also extend to consider air resistance, mortar volume etc.

References

- 1 Title 16, Code of Federal Regulation, Parts 1500.17 (requirement regarding pyrotechnic composition in consumer fireworks).
- 2 UN ADR Annex A: General Provisions and Provisions Concerning Dangerous Substances and Articles, Part 2 Classification, Chapter 2.2.1.1.7.5, *UN Default Fireworks Classification Table*, 2008.
- 3 Takuro Mitsuya *et al.*, *Japanese "Wariyaku", is it a flash composition or not?* The 11 International Symposium of Fireworks, Mexico, 2009.
- 4 A. Tang, *An Alternative Method of Evaluating Powder Energy*, The 11th International Symposium of Fireworks, Mexico, 2009.
- 5 A. Morre and F. Cajori, *Newton's Principia*, translated and reproduced in Great Books, Volume 34, pages 1–372, Encyclopaedia Britannica, Inc., Chicago, IL.
- 6 Shipman Wilson Todd, *An Introduction to Physical Science*, Tenth Edition, Houghton Mifflin.
- 7 T. A. O. Ping Kee and L. E. E. Hong Moon, *New Physics at Work*, Second Edition, Oxford, 2008.

Characteristics of the Red Colored Flame of Firework Compositions

Dayu Ding,* Daichi Tabata and Tadao Yoshida

Ashikaga Institute of Technology, 268-1 Omae-cho, Ashikaga-shi, Tochigi 326-8558, Japan

* Email: dding@ashitech.ac.jp

Abstract: *Experiments have been conducted varying the oxygen balance of firework compositions and adding a chlorine donor to compositions in order to understand how or why a red flame is affected by the oxygen balance and presence of chlorine in the composition. The results show that with a negative oxygen balance, i.e., a fuel-rich composition, the flame extends longer, so a deep red flame is easily formed. The results also show that strontium containing species SrO, SrOH and SrCl can form a red flame. SrO or SrOH is responsible for a deeper red light, SrCl is responsible for a deepest red color. Emissions due to SrO and SrOH can be diminished by the emissions due to SrCl. For forming a red flame, a favorable chlorine donor is not an oxidant like potassium perchlorate but a fuel like chlorinated gum.*

Keywords: *firework composition, red colored flame, chromaticity diagram, oxygen balance*

Introduction

Light and color from firework flames are important effects in firework displays. It has been an enduring goal of pyrotechnists to produce a deep, saturated colored flame in a firework application.

Firework compositions are powder mixtures of several agents such as fuel, oxidant, and color agent etc. To understand the factors affecting the performance of colored flames, many studies have been conducted by other researchers.¹⁻⁴

When a firework composition burns, the combustion products in the flame emit radiation or light. Some products emit light at or near the hue intended in the flame, and they are called desirable emitters. Other products emit light in the visible spectrum that will hinder the performance of the colored flame and they are called undesirable emitters. The desirable or undesirable emitters are atomic or molecular species in the flame. Also present are some incandescent solid and/or liquid combustion products emitting black body, gray body, or continuous radiation. In colored flames, they emit undesirable broadband radiation across a very large wavelength range, even across the

entire visible spectrum when the temperature is high.

Strontium compounds are usually used as color agents in red flame firework compositions. Shimizu¹ qualitatively researched the red flames of firework compositions and concluded that the molecular emitter strontium oxide (SrO) is responsible for the red color, and the red flame will become deeper in colour if some chlorine agent is added to the composition.

Since Shimizu's research, optical measurement technology and computer technology have advanced greatly. Therefore, further studies, which use advanced measurement technology to quantitatively show spectral information and to correlate the data with emitters in the flame, are ongoing.

Some research results show that if a chlorine agent is used in a firework composition, a higher quality red flame can be formed by molecular band emitters such as strontium monochloride (SrCl) and strontium monohydroxide (SrOH).

The purpose of this study is quantitatively to investigate the effects of factors such as the

Article Details

Manuscript Received:-23/07/2009

Publication Date:-19/10/2009

Article No: - 0079

Final Revisions:-17/10/2009

Archive Reference:-989

oxygen balance and chlorine donors in firework compositions on the performance of red flames by acquiring spectra with a spectrometer, and to give insight into the relative importance and roles of those factors.

Experimental

Materials

To investigate the influence of oxygen balance and chlorine (element Cl), the formulas of red flame firework compositions were designed separately as four groups listed in Table 1. The oxygen balance (OB) for each formula was calculated by the method explained in the next section. In each group except group 1 the formulas were designed with a positive, near zero and a negative oxygen balance, respectively. The oxygen balance of one formula in group 1 was near zero and the formula would be difficult to ignite if the oxygen balance was below zero. The amount of hydrogen (element H) contained in the charcoal used in group 1 was lower compared with the rice granules used in group 2. Chlorine was not contained in the materials used in group 1 and group 2, but chlorine was contained in the fuel used in group 3 and the oxidant used in group 4.

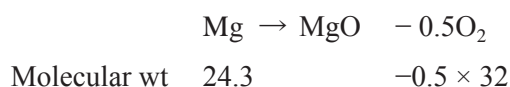
Magnesium (Mg metal powder) was used as a high energy agent in this experiment to improve the ignition performance.

For all compositions, chemicals except for strontium nitrate ($\text{Sr}(\text{NO}_3)_2$) were used as supplied from Sunaga Fireworks Co. Ltd. The compound strontium nitrate ($\text{Sr}(\text{NO}_3)_2$) (JIS special grade reagent) was purchased from Wako Pure Chemical Industries, Ltd. The samples of compositions were prepared by mixing the dry powders of the chemicals. About 2.5 g of the mixture was poured

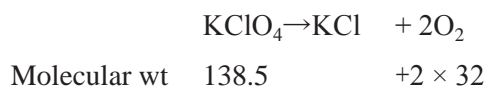
into a steel tube of 13.0 mm inner diameter, 1.0 mm thick and 20 mm long.

Calculation of oxygen balance

The oxygen balance is the amount of oxygen available within an explosive material in grams when 1 g of the material burns or explodes as a result of complete conversion of the explosive material to CO_2 , H_2O , KCl , MgO , Al_2O_3 , etc. For example, the oxygen balances of magnesium (Mg) and potassium perchlorate (KClO_4) are calculated as follows.



$$\text{OB of Mg} = -16/24.3 = -0.658$$



$$\text{OB of KClO}_4 = +64/138.5 = +0.462$$

Therefore, the oxygen balance of a mixture of Mg and KClO_4 (mix ratio = 40 : 60) can be calculated as:

$$\begin{aligned} \text{OB} &= (-0.658) \times 40\% + (+0.462) \times 60\% \\ &= +0.014 \end{aligned}$$

For the calculation of oxygen balance, the chemical formula of charcoal was approximately expressed in carbon (element C) as its main ingredient is carbon. Similarly rice granules are approximately expressed in the chemical formula $(\text{C}_6\text{H}_{10}\text{O}_5)_n$ of starch because the main ingredient is starch. The chemical formula $(\text{C}_{10}\text{H}_{11}\text{Cl}_7)_n$ of chlorinated gum is cited from Sturman.⁵ A negative oxygen balance means the oxygen within the material is deficient for complete reaction, and zero or a positive oxygen balance identifies that the material has

Table 1. Red colored flame firework formulations (wt%).

Component	Group1	Group 2			Group 3			Group 4		
Strontium nitrate	80%	80%	70%	60%	80%	70%	60%	40%	35%	30%
Potassium perchlorate								40%	35%	30%
Magnesium	10%	10%	10%	10%	10%	10%	10%	10%	10%	10%
Charcoal	10%									
Rice granules		10%	20%	30%				10%	20%	30%
Chlorinated gum					10%	20%	30%			
OB	-0.03	0.12	-0.04	-0.19	0.14	0.01	-0.12	0.18	0.04	-0.09

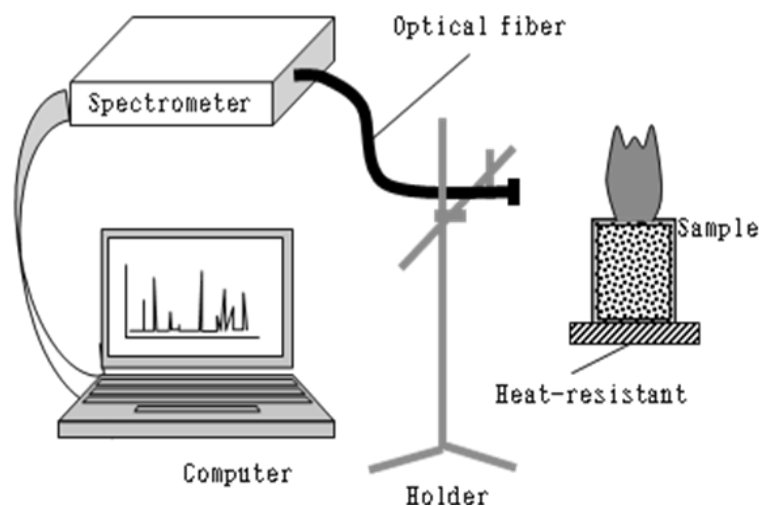


Figure 1. Schematic diagram of the experimental setup.

sufficient available oxygen within itself to enable the combustion to go to completion. It is known that an explosive or a firework composition with an oxygen balance close to zero is the most powerful during combustion or explosion.

Methods

A schematic diagram of the experimental setup used in this work is shown in Figure 1. A spectrometer named PMA-11C7473-36 from Hamamatsu Photonics Co. Ltd was used for measuring the spectrum of light from the firework flame. Once the sample at the top, which was vertically placed on a heat-resistant plate, was ignited, the light of the flame was transmitted to the spectrometer through an optical fiber and the spectral data were recorded on a personal computer. The photographs of the flame were taken by a camera with the same conditions for each test. The experiments were conducted in a dark room and the chamber in which samples were burned was painted flat black to avoid reflections. Two samples for each formula were prepared and tested under the same conditions.

Results and discussion

Experimental data reduction

The CIE1931 Chromaticity Diagram, which is a two-dimensional diagram with x and y coordinate axes shown in Figure 2, is used for quantifying colored firework flames in this

work. The outside boundary of the tongue-shape is called the monochromatic light line, which defines perfect purity and complete saturation at a given wavelength. ICI illuminant "C" locates at $x = 0.33$, $y = 0.33$ and defines perfectly balanced white light.

The color coordinates (x, y) were calculated from measured spectra and were plotted on the chromaticity diagram. For example, color point A is plotted with calculated coordinates (x, y) in Figure 2. The straight line that connects point A with C extends to a point B on the monochromatic light line. The wavelength of monochromatic light point B is called the dominant wavelength of color point A. The percentage of the distance along the straight line CB from point C is called excitation purity or purity, with white light point C having 0% purity and monochromatic light point B having 100% purity.

In our experiments, the change of the spectrum with time was measured using a spectrometer with a repeat measurement function. After ignition, the sample began to burn and light radiated from the flame. The light intensity changed noisily with time because of the flickering of the flame, and it decreased with time due to the presence of smoke. To eliminate the effects of flame flickering and smoke, and to correctly evaluate colored firework flames, the time-average intensity within one second after ignition, before the smoke had spread widely, for each wavelength was used to calculate

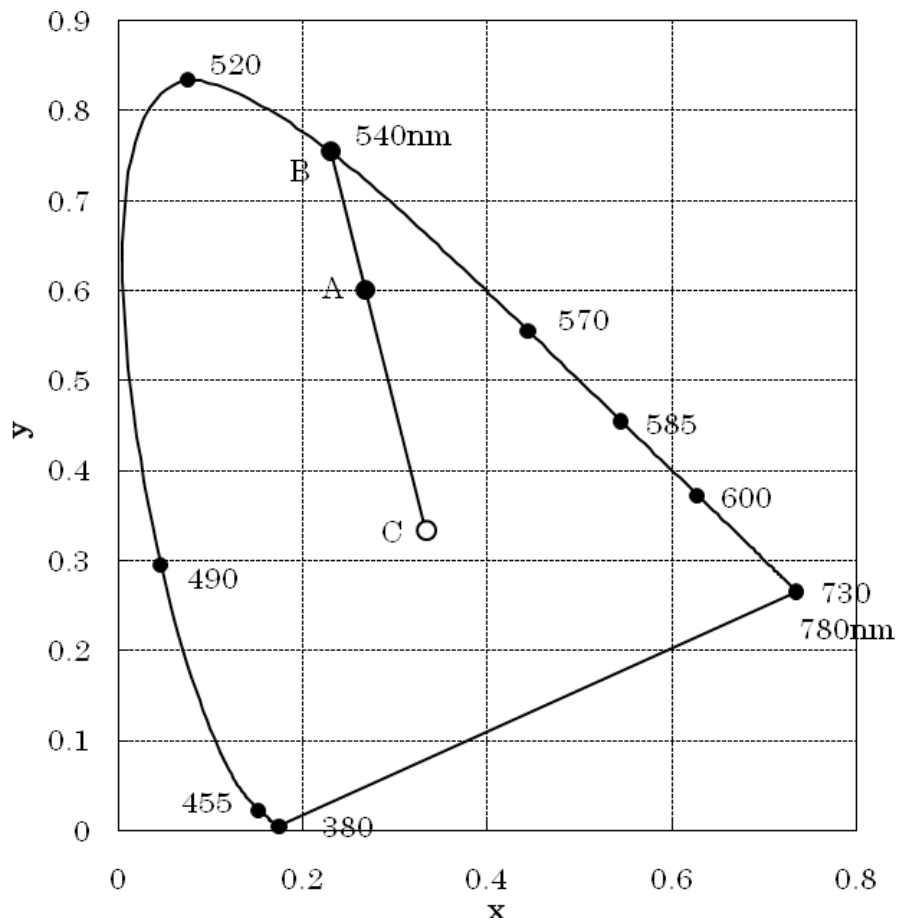


Figure 2. Chromaticity diagram.

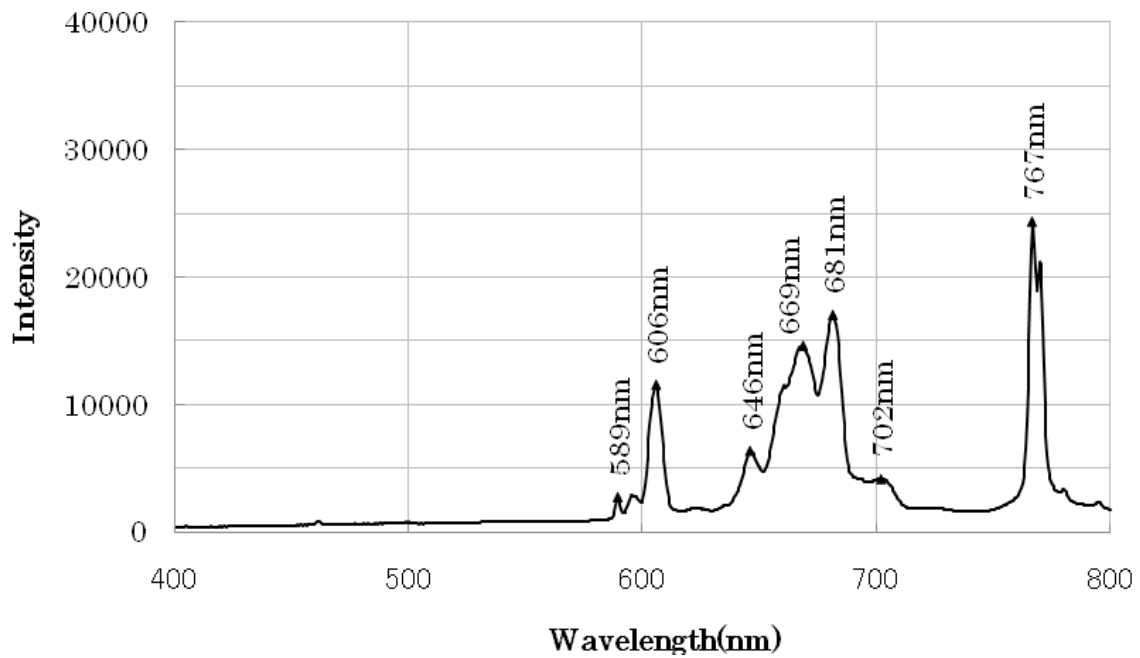


Figure 3. Spectrum of group 1.

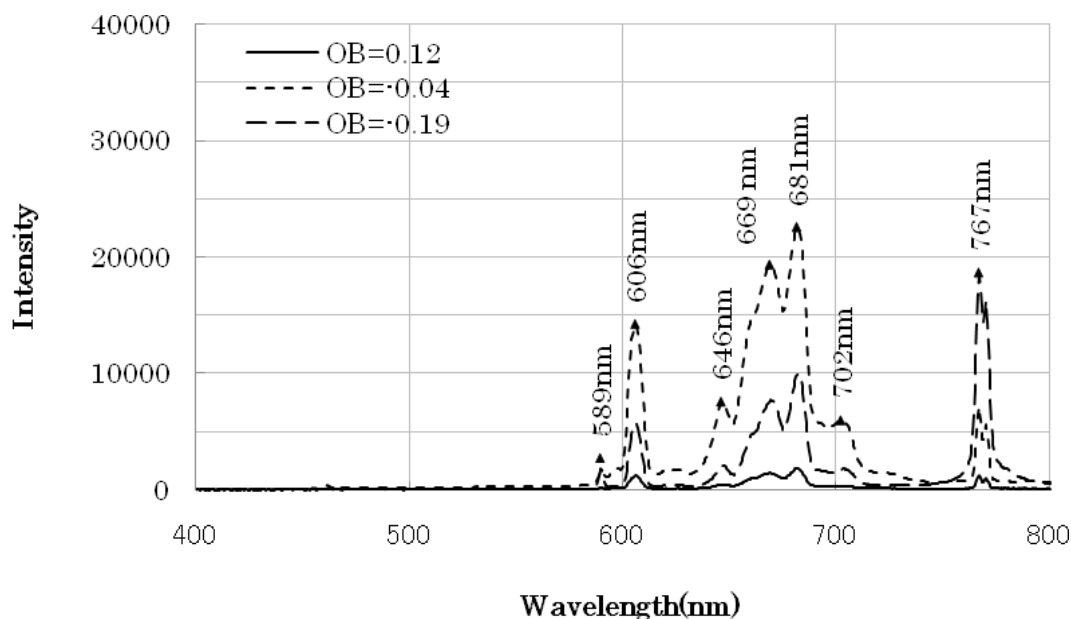


Figure 4. Spectrum of group 2.

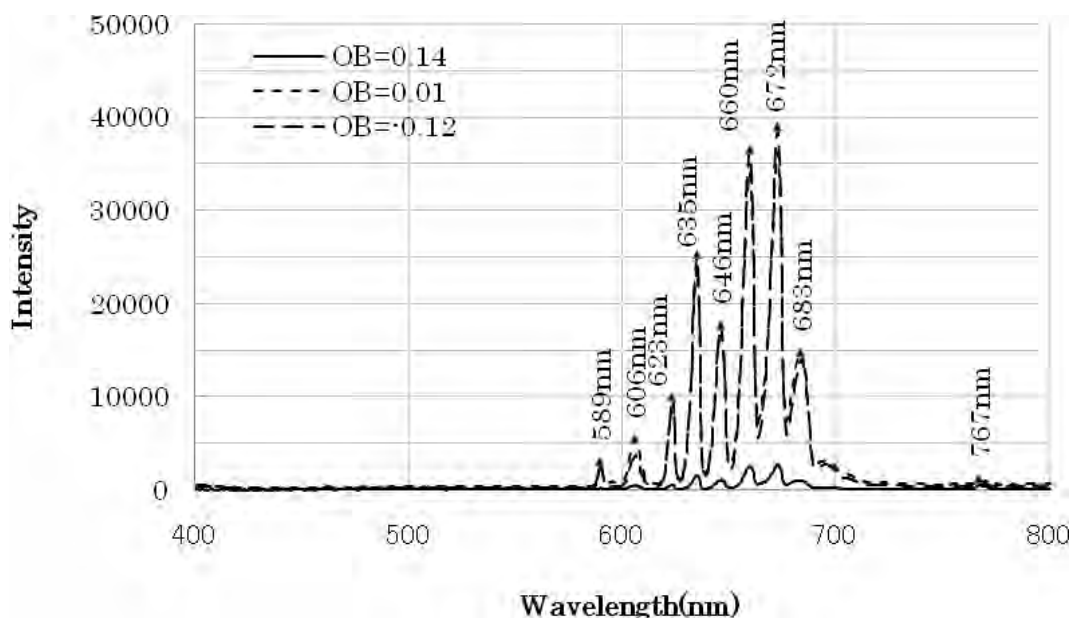


Figure 5. Spectrum of group 3.

CIE coordinates.

Characteristics of red flame spectra

The experiments were performed varying the oxygen balance of the compositions and adding a chlorine donor to the compositions for the four groups listed in Table 1. The measured spectra are shown in Figures 3 through 6.

As can be seen from the measured spectra shown in Figures 3 through 6, the flame of each composition

shows some band emissions in the wavelength range 600–700 nm. The quality of the red color is mainly responsible for the performance of those band emissions such as their position, width, and intensity.

The patterns of band emissions of compositions of group 1 are similar to those of group 2. The patterns of band emissions of group 3 are also similar to those of group 4. But the patterns of band emissions of group 1 and group 2 are very

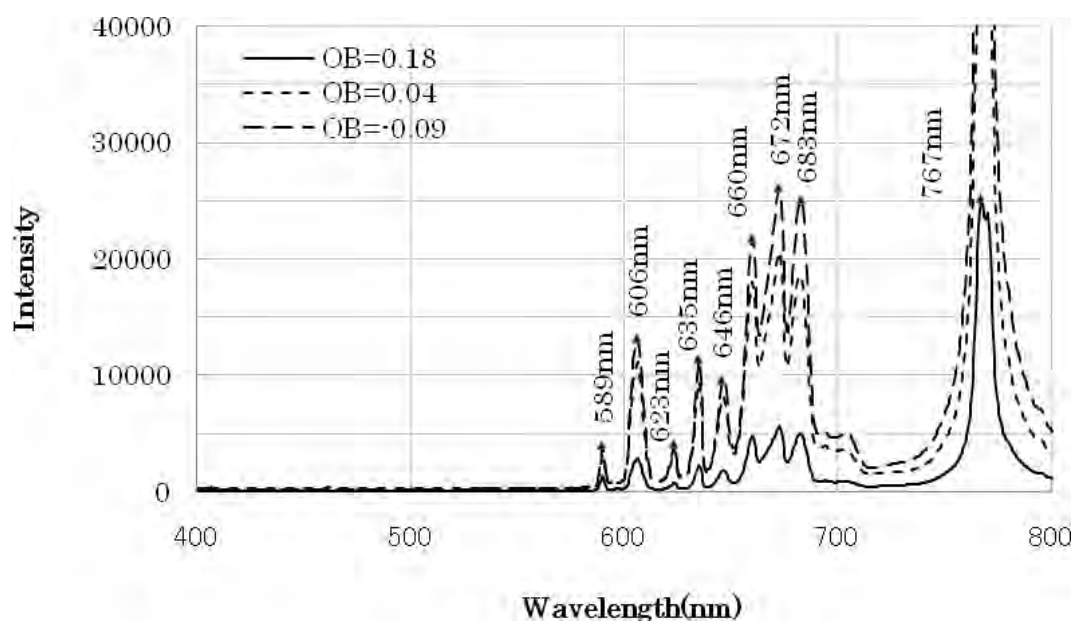


Figure 6. Spectrum of group 4.

different from those of group 3 and group 4.

For the compositions of groups 1 and 2, in which no chlorine (Cl element) is contained, the spectra displayed in Figure 3 and Figure 4 show that there is one narrow band emission with a peak at 606 nm and another wide band emission in the wavelength range 630–700 nm with some peaks at 646 nm, 669 nm and 681 nm.

According to Pearse and Gaydon,⁶ strontium salts give bright red banded radiation in a flame, but the flame bands are mostly due to strontium monohydroxide (SrOH). Also, strontium oxide emits light with strong bands near 595 nm and 605 nm and a stronger complex structure between 640 nm and 685 nm. The strong band due to SrOH is centered at 605 nm.

Also according to the spectrum graphs provided by Meyerriecks and Kosanke,³ strontium oxide (SrO) emits light near 600 nm, and strontium monohydroxide (SrOH) displays a similar

spectrum in the wavelength range 630–700 nm like that shown in Figure 3 or 4.

For the compositions in groups 3 and 4, in which chlorine (Cl element) is contained, the spectra in Figure 5 and Figure 6 show that the structure of the spectrum between 600 nm and 700 nm is very different from that of non-chlorine compositions and displays several separated narrow band emissions.

The narrow band emissions with peaks at 635 nm, 660 nm and 672 nm are stronger than that of other band emissions. According to Ingram,³ those band emissions are due to strontium monochloride (SrCl).

For each composition, there are a sodium atomic emission at 589 nm and a potassium atomic emission at 767 nm in the flame. The sodium atomic emission contributes an undesirable yellow or orange-yellow light to the red flame. The potassium atomic emission is also an undesired

Table 2. Identification of spectra shown in Figures 3–6.

Wavelength/nm	Emitter	Wavelength/nm	Emitter
589	Na	660	SrCl
606	SrO, SrOH	672	SrCl
623	SrCl	681	SrOH
635	SrCl	683	SrOH
646	SrOH	767	K

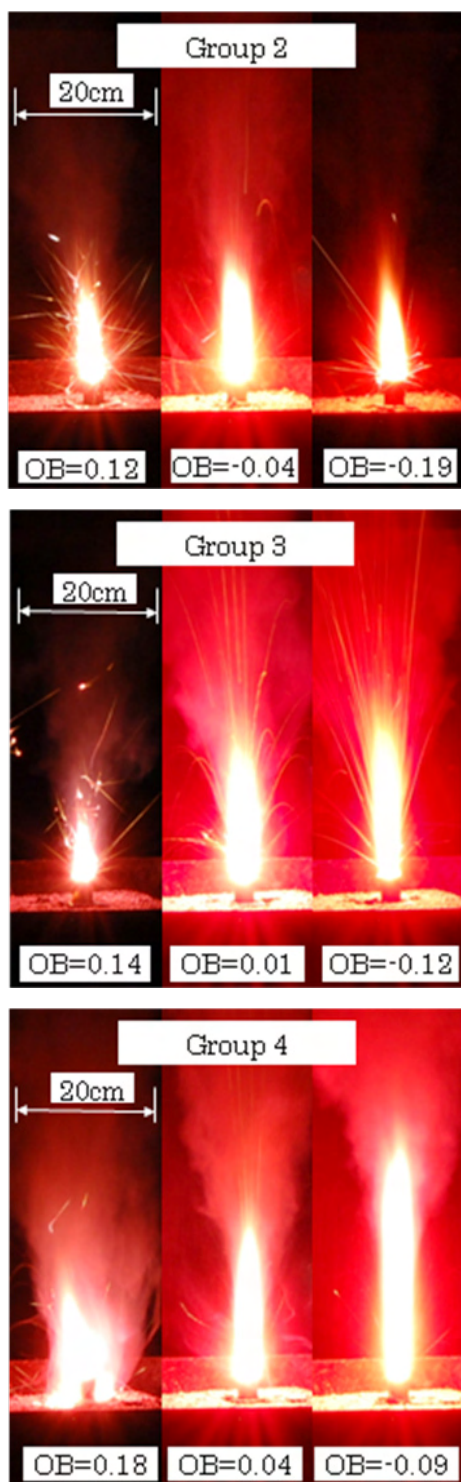


Figure 7. Pictures of the combustion flames.

emitter, but there is little effect on the red color because the emission is near the infrared range.

Sodium and potassium probably existed in the strontium nitrate as impurities because neither sodium nor sodium compounds were used in any

composition. Potassium or potassium compounds were also not used in the compositions except for the compositions in group 4.

By referring to some spectral data in references 2–4, the emitters with emissions at wavelengths in the spectra indicated in Figures 3–6 can be determined and the information is listed in Table 2.

Effects of oxygen balance

The measured spectra of compositions with varying oxygen balance show that the emissions are weak for compositions with a positive (oxidant-poor) oxygen balance and the emissions become stronger with a negative (fuel-rich) or near zero oxygen balance.

Photographs of the combustion flames taken by a camera are shown in Figure 7. The same distance between sample and camera is kept for all the pictures and the pictures show the same area. As can be seen, there is a tendency for the height of flames to become greater as the oxygen balance decreases from positive to negative, possibly indicating that there is a strong dependence of color performance on the oxygen balance. It suggests that the combustion zone and flame structure are largely influenced by the oxygen balance.

The chromaticity coordinates of the tested compositions were calculated with the measured spectra, and their color performance plotted on a chromaticity diagram is shown in Figure 8. Meanwhile, dominant wavelength (corresponding to hue) and purity (corresponding to color quality) were calculated with the chromaticity coordinates. The results are listed in Table 3.

As the oxygen balance changes from positive to negative, the chromaticity coordinates of the compositions in each group move towards the red region in the chromaticity diagram. It can be seen that the tendency of the change in the height of the flames corresponds to the change in the chromaticity coordinates with the change of the oxygen balance for compositions of groups 3 and 4.

If the oxygen balance varies from positive to negative, the combustion zone of the flame extends longer and the emissions become stronger, because the emitters SrO, SrOH and SrCl emit light only while they exist in a gas or vapor

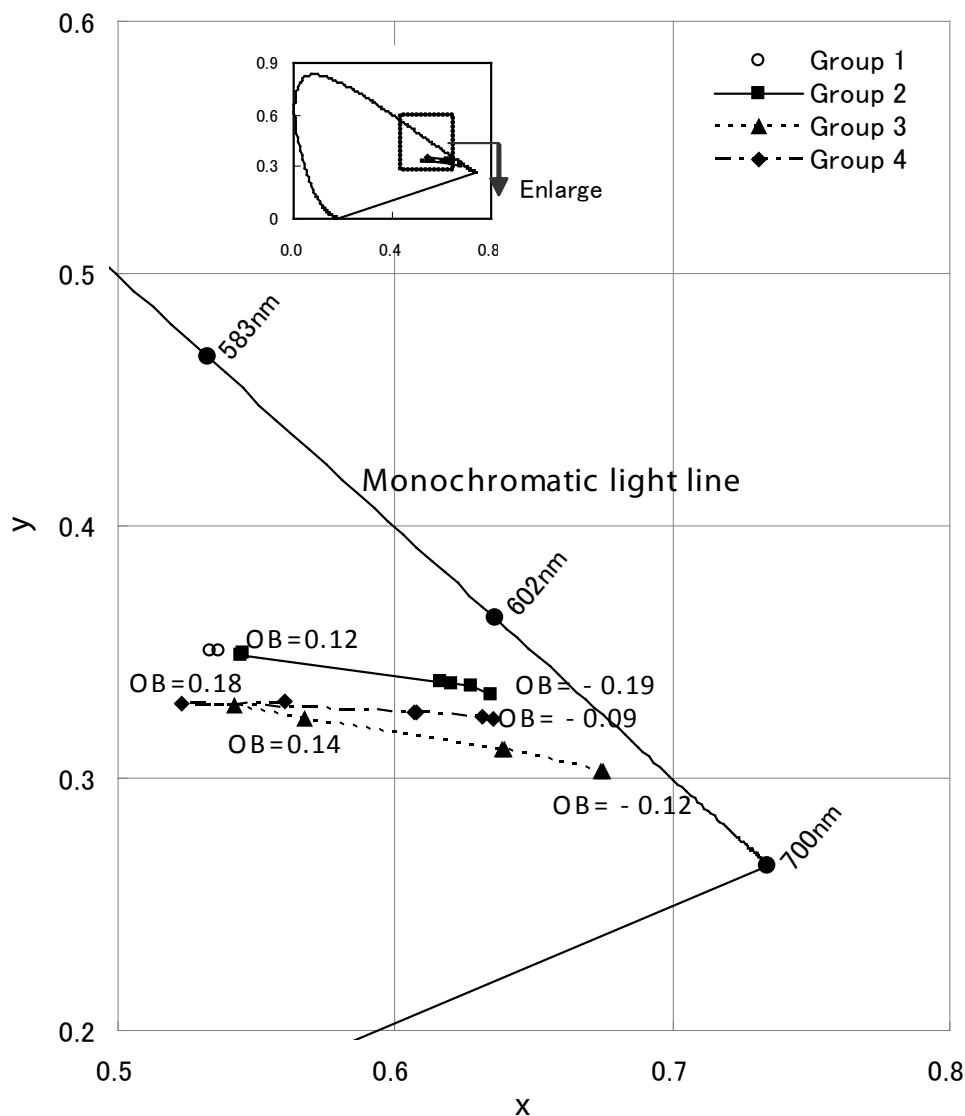


Figure 8. Chromaticity of red colored flame for tested compositions.

Table 3. Dominant wavelength and purity of red colored flame.

	OB	Dominant wavelength/nm	Purity (%)
Group 1	-0.03	603	66
	0.12	604	68
Group 2	-0.04	609	87
	-0.19	610	90
Group 3	0.14	614	64
	0.01	620	85
	-0.12	624	93
Group 4	0.18	612	61
	0.04	613	80
	-0.09	614	87

state. The experiments suggest that if the oxygen balance of the composition is negative, SrO, SrOH and SrCl are easily formed in the vapor states as the combustion zone is longer. Conversely, if the oxygen balance is positive, SrO, SrOH and SrCl will be difficult to form in the vapor state, and many combustion products concerning strontium maybe do not exist in the gas or vapor states as the combustion zone of the flame is narrow.

Therefore, the experimental results suggest that the color saturation of a red flame is possibly improved with a negative oxygen balance.

Effects of chlorine

For non-chlorine containing compositions, the red color of the flame is mainly due to emissions from emitters SrO and SrOH in the flame.

The charcoal used in the compositions of group 1 contains mainly carbon and a small amount of hydrogen. Rice granules, which mainly contain carbohydrate, are used in the compositions in group 2 as the fuel. Therefore, when the compositions of group 1 and group 2 are burning, the strontium-containing emission species in the flame are mostly strontium oxide (SrO) and strontium monohydroxide (SrOH).

Either SrO or SrOH emits light near 606 nm. The band emission at 606 nm in Figure 3 or Figure 4 is strong.

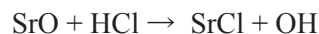
The complex band emissions in the range 630–700 nm are almost continuous, which is mostly due to SrOH.

For a chlorine donor such as chlorinated gum or potassium perchlorate added to the composition of group 3 and group 4, the emitter SrCl is present in the flame besides the emitters SrO and SrOH.

Any of the emission species SrO, SrOH and SrCl can form a red flame, but the red color purities due to these species are different. SrO or SrOH is responsible for an orange-red light, but SrCl is responsible for a deepest red color.

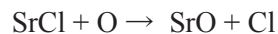
The experimental results in Figure 5 or 6 show that the emission at 606 nm, which contributes an orange-red light, becomes weak when a chlorine donor is used in the compositions. This suggests that if a source of chlorine atoms is available in the flame, the emissions due to SrO and SrOH can be diminished by the emitter SrCl. The reason is

probably due to strontium monochloride (SrCl) which may form from the chemical reaction as follows:⁴



Further, by comparison of Figure 5 and Figure 6, it can be seen that to diminish the light due to the emission at 606 nm, a chlorine donor serving as the fuel such as chlorinated gum is more effective than potassium perchlorate, which serves as an oxidant.

For the compositions of group 3, chlorinated gum (= chlorine donor) serving as fuel is rich with a negative oxygen balance, so that the deeper red colored flame is formed. In contrast, for the compositions in group 4, potassium perchlorate (= chlorine donor) serving as oxidant decreases to the negative oxygen balance, but the red colored flame is deeper than that with a positive oxygen balance. This probably can be explained by the following chemical reaction.⁴



In this equation, the loss of strontium monochloride (SrCl) due to the formation of SrO can be diminished by decreasing the amount of oxygen in the flame with a fuel-rich composition, i.e., with a negative oxygen balance composition. Therefore, it can be concluded that it is advantageous to form SrCl in the flame when the oxygen balance of the composition is negative, and a deeper red colored flame can be formed.

Conclusions

The effects of varying the oxygen balance of compositions and chlorine on the colored flame of fireworks compositions have been investigated in this study. Some conclusions are obtained as follows.

- (1) The red color saturation can be improved with a negative oxygen balance, i.e., a fuel-rich composition.
- (2) Strontium concerning species SrO, SrOH and SrCl can form a red flame, but SrO and SrOH are responsible for an orange-red light, whereas SrCl is responsible for a deepest red color.
- (3) Emissions due to SrO and SrOH can be diminished by the emissions due to SrCl.

- (4) To form a red flame, a suitable chlorine donor is not an oxidant like potassium perchlorate but a fuel like chlorinated gum.

References

- 1 T. Shimizu, "Studies on Colour Flame Composition of Fireworks 4. On Flame Spectra of Red, Yellow and Green Colour Compositions", *Selected Pyrotechnic Publications of Dr. Takeo Shimizu, Part 3. Studies on Fireworks Colored Flame Compositions* (translated from Japanese), Journal of Pyrotechnics, Inc., 1999.
- 2 W. Meyerriecks and K. L. Kosanke, "Color Values and Spectra of the Principal Emitters in Colored Flames", *Journal of Pyrotechnics*, Issue 18, Winter 2003, pp. 1–22.
- 3 B. V. Ingram, "Color Purity Measurement of Traditional Pyrotechnic Star Formulas", *Journal of Pyrotechnics*, Issue 17, Summer 2003, pp. 1–18.
- 4 K. L. Kosanke and B. J. Kosanke, "The Chemistry of Colored Flames", *Pyrotechnic Chemistry*, Journal of Pyrotechnics Inc., 2004, Chapter 9.
- 5 B. T. Sturman, "Notes on chlorinated rubber and some other chlorine donors", *Journal of Pyrotechnics*, Issue 22, Winter 2005, pp. 63–66.
- 6 R. W. B. Pearse and A. G. Gaydon, *The Identification of Molecular Spectra*, Chapman and Hall Ltd., 4th edn, 1976, pp. 334–340.

Pyrotechnically Relevant Salts of 1-(2-Chloroethyl)-5-nitriminotetrazole – Synthesis and Coloring Properties

Thomas M. Klapötke,^{*a,b} Jörg Stierstorfer^a and Karina R. Tarantik^a

^a Department of Chemistry and Biochemistry, University of Munich (LMU), Butenandtstr. 5-13, D-81377 Munich, Germany

e-mail: tmk@cup.uni-muenchen.de

^b Center for Energetic Concepts Development, CECD, University of Maryland, UMD, Department of Mechanical Engineering, College Park, MD 20742, USA

Abstract: Alkaline and alkaline earth metal salts are widely used in pyrotechnic formulations as colorant agents. Salts of strontium are responsible for a red flame color, barium salts, mostly $\text{Ba}(\text{NO}_3)_2$, for a green one and copper salts, only combined with a chlorine donor, are able to yield a blue flame color. To investigate the possibility of reducing the amount of metal in pyrotechnic formulations producing colored flames, the strontium and barium salts of 1-(2-chloroethyl)-5-nitriminotetrazole, *trans*-[diaqua-bis{1-(2-chloroethyl)-5-nitriminotetrazolato- $\kappa^2\text{N}^4, \text{O}^5$ }copper(II)] dihydrate, copper(II) 1-(2-chloroethyl)-5-nitriminotetrazolate and *trans*-[diammine-bis{1-(2-chloroethyl)-5-nitriminotetrazolate- $\kappa^2\text{N}^4, \text{O}^1$ }copper(II)] were synthesized and characterized using IR and Raman spectroscopy, elemental analysis, and differential scanning calorimetry (DSC). Their sensitivities towards shock, friction, and electric discharge and the solubility in H_2O at ambient temperature were determined. Heats of formation were calculated using bomb calorimetric measurements. Crystal structures of all compounds have been determined by single crystal X-ray diffraction and a detailed description is given. Last but not least, all salts were tested with regard to their color performance.

Keywords: pyrotechnics, coloring agent, tetrazoles, perchlorate-free.

Introduction

Nitrogen-rich compounds and in particular their metal salts and copper(II) compounds play a key role in the development of environmentally benign pyrotechnics.¹⁻³ Smokeless combustion, caused by the formation of mainly gaseous products, is one reason nitrogen-rich substances seem to be a good alternative. Furthermore, this class of substances gains its energy from high heats of formation rather than from the oxidation of a carbon backbone or a fuel. Even more promising seem to be tetrazoles, which exhibit energetic nitrogen-oxygen containing functional groups such as nitro groups ($\text{R}-\text{NO}_2$),^{4,5} nitrate esters ($\text{R}-\text{O}-\text{NO}_2$)⁶ or nitramine functionalities ($\text{R}_2\text{N}-\text{NO}_2$),⁷⁻⁹ since these compounds have balanced oxygen contents.

5-Nitriminotetrazoles have been known for a long

time, since they are obtainable via facile synthetic routes.¹⁰ 1-Substituted 5-nitriminotetrazoles, e.g. 1-methyl-5-nitriminotetrazole and 1-ethyl-5-nitriminotetrazole, were first described in 1957.¹¹ Another advantage of these substances is that they can be deprotonated yielding thermally stable anions or serve as ligands in several metal complexes.¹²

Colors in pyrotechnics are obtained by the addition of chemicals that produce substances that combine in the flame and emit the desired radiation. Emission of green light is achieved by the addition of barium nitrate, which acts as both coloring agent and oxidizer. This is true for strontium nitrate, the agent for intensive red colors. The corresponding light emitting species (in the gas phase) are the monohydroxides, SrOH and BaOH, and the monochlorides, SrCl and BaCl,

Article Details

Manuscript Received:-28/05/2009

Publication Date:-16/11/2009

Article No: - 0077

Final Revisions:-16/11/2009

Archive Reference:-1011

respectively. If a blue flame is desired, usually copper or copper compounds are combined with a chlorine donor like PVC (poly vinyl chloride). This is necessary, since the formation of CuCl is responsible for the emitting of blue light.¹³ If no chlorine is present or the temperature rises above 1200 °C in an oxygen-rich flame, CuOH and CuO – light emitting species of green and red, respectively – are formed.¹⁴ Chlorine containing species like potassium perchlorate are widely added to common fireworks for red, green or blue flame colors on this account, besides its property as an oxidizer.

Recently, several strontium salts of different 5-nitriminotetrazoles and their properties as coloring agents to find application in pyrotechnic compositions were presented.¹⁵ The same is true for different barium tetrazole derivatives.¹⁶

Pyrotechnic applications and fireworks cause manifold environmental pollution, as shown in several studies.¹ One main pollutant is perchlorate which is added as an oxidizer in most pyrotechnic compositions. It is a high energy oxidizer with good thermal and chemical stability. However, the presence of potassium perchlorate, like all perchlorates, in drinking water is a cause of concern, because of their known ingestion to inhibit iodide uptake by the thyroid gland. Therefore, in our research group concentrated efforts are spent on the substitution of perchlorate in pyrotechnic compositions. An alternative is presented in a recently published paper.² Another study in which potassium perchlorate is replaced by potassium, sodium or strontium nitrate is known in the literature.¹⁷ In the cases where these salts are used

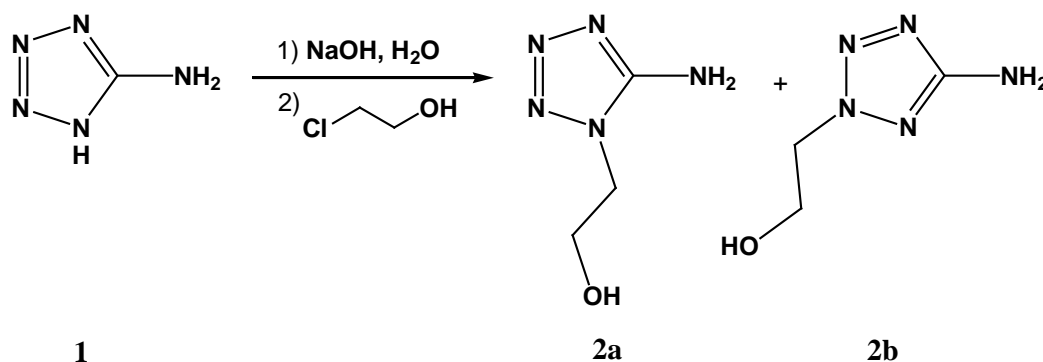
as oxidizers, there is a lack of a chlorine donor, which guarantees a more intense flame color, especially in the combination with strontium (red), barium (green) or copper (blue) salts. Therefore, the strontium and barium salts of 1-(2-chloroethyl)-5-nitriminotetrazole, *trans*-[diaqua-bis{1-(2-chloroethyl)-5-nitriminotetrazolato- κ^2N^4, O^5 } copper(II)] dihydrate, copper(II) 1-(2-chloroethyl)-5-nitriminotetrazolate and *trans*-[diammine-bis{1-(2-chloroethyl)-5-nitriminotetrazolato- κ^2N^4, O^1 } copper(II)] were prepared. In addition to the syntheses a comprehensive characterization of the chemical as well as the energetic properties is given. Furthermore, all compounds were tested with regard to their color performance and some pyrotechnic compositions are presented in this work.

Results and discussion

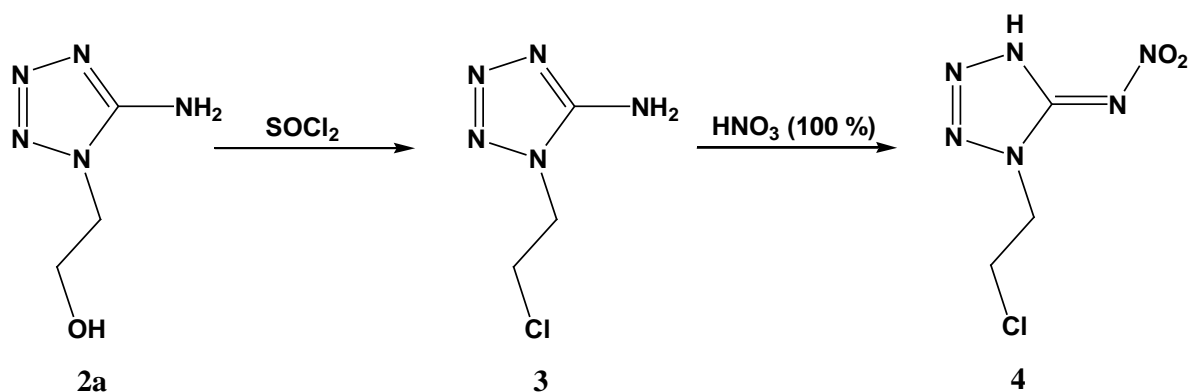
Syntheses

The alkylation of 5-amino-1*H*-tetrazole (**1**) with 2-chloroethanol was performed according to the literature (Scheme 1).^{18,19} Both isomers 1- and 2-(2-hydroxyethyl)-5-aminotetrazole could be isolated. Since the work up of the 2-isomer (**2b**) is extremely time-consuming, further reaction steps were only realized with 1-(2-hydroxyethyl)-5-aminotetrazole (**2a**).

1-(2-Chloroethyl)-5-aminotetrazole (**3**) could be obtained *via* chlorination of **2a** with thionyl chloride according to Finnegan and Henry (Scheme 2).²⁰ The nitration of **3** was performed in HNO₃ (100%), which procedure is well known in the literature.^{7,19} Therefore, compound **3** was slowly added to an ice-cooled solution of HNO₃



Scheme 1. Preparation of 1- and 2-(2-hydroxyethyl)-5-aminotetrazole (**2a**, **b**), starting from 5-amino-1*H*-tetrazole (**1**).



Scheme 2. Preparation of 1-(2-chloroethyl)-5-aminotetrazole (3) and 1-(2-chloroethyl)-5-nitriminotetrazole (4).

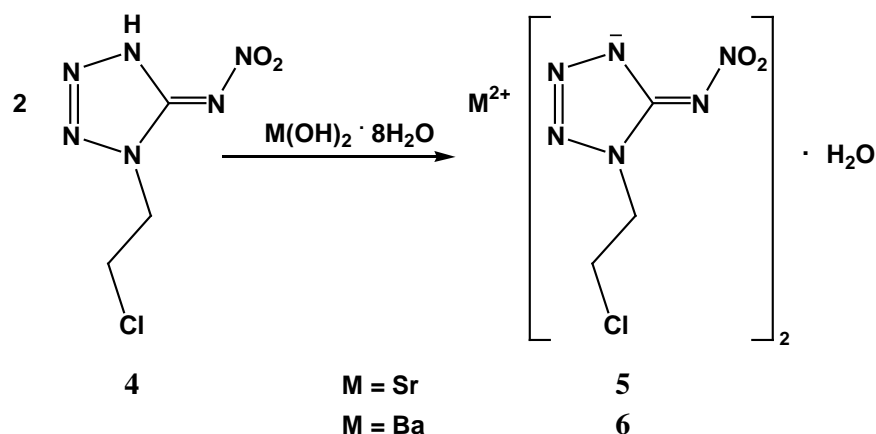
(100%) and stirred for at least 17 hours. Afterwards the colorless solution was poured on to ice. After recrystallization from H_2O 1-(2-chloroethyl)-5-nitriminotetrazole (4) could be obtained in a yield of 93%.

For preparation of strontium 1-(2-chloroethyl)-5-nitriminotetrazolate monohydrate (5) and barium 1-(2-chloroethyl)-5-nitriminotetrazolate monohydrate (6) compound 4 was reacted with the corresponding hydroxides in H_2O (Scheme 3). Both salts 5 and 6 could be obtained in very good yields of 91% and 95%, respectively.

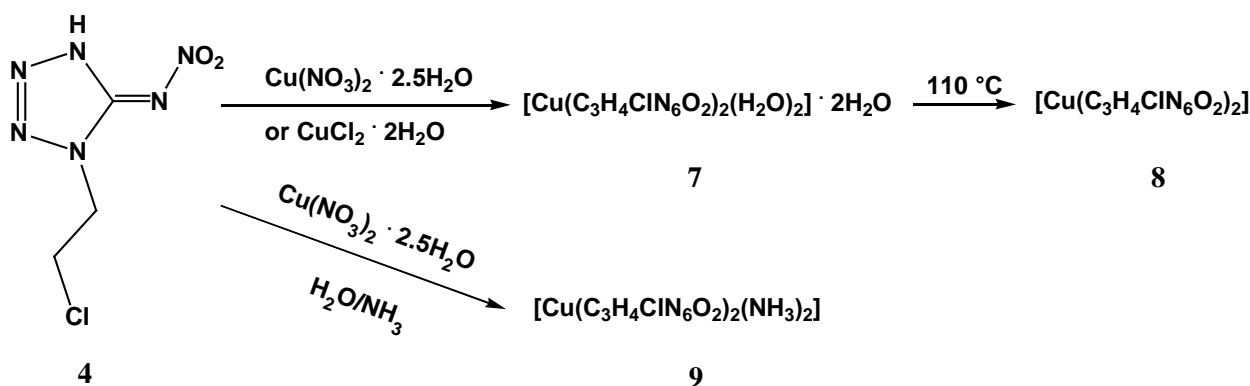
The copper(II) complex diaqua *trans*-[diaqua-bis{1-(2-chloroethyl)-5-nitriminotetrazolato- κ^2N^4, O^5 }copper(II)] dihydrate (7) is described in the

literature.¹⁹ It could be obtained by the reaction with either copper(II) chloride dihydrate or copper(II) nitrate pentahemihydrate (Scheme 4). The water free copper salt copper(II) 1-(2-chloroethyl)-5-nitriminotetrazolate (8) was prepared by removing the coordinated water of powdered 7 at 110 °C in almost quantitative yields.

In the presence of diluted ammonia solution *trans*-[diammine-bis{1-(2-chloroethyl)-5-nitriminotetrazolato- κ^2N^4, O^1 }copper(II) (9) was obtained from 4 and the copper(II) nitrate solution. Deep violet crystals formed after storing the solution for a few days at ambient temperature.



Scheme 3. Synthesis of strontium 1-(2-chloroethyl)-5-nitriminotetrazolate monohydrate (5) and barium 1-(2-chloroethyl)-5-nitriminotetrazolate monohydrate (6).



Scheme 4. Synthesis of the copper compounds 7–9.

Molecular structures

After recrystallization from H₂O crystals of salts **5** and **6** suitable for X-ray diffraction could be obtained. Crystals of **8** were grown from half-concentrated HNO₃ (35%). Suitable crystals of **9** were formed in the mother liquor. All crystals were picked from the crystallization mixture and

mounted in Kel-F oil and transferred to the N₂ stream of an Oxford Xcalibur3 diffractometer with a Spellman generator (voltage 50 kV, current 40 mA) and a KappaCCD detector. The data collections were performed using the CrysAlis CCD software,²¹ the data reduction with the CrysAlis RED software.²² The structures of **5**,

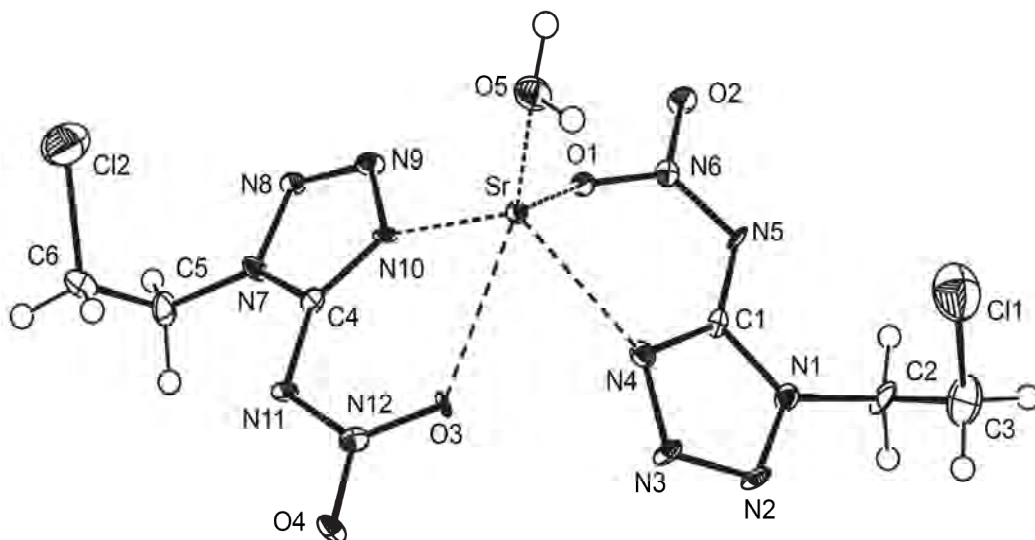


Figure 1. Molecular unit of **5**. Hydrogen atoms shown as spheres of arbitrary radius and thermal displacements set at 50% probability. Selected geometries: distances (Å) N1–N2 1.346(7), N7–N8 1.357(6), N2–N3 1.295(7), N8–N9 1.304(7), N3–N4 1.367(7), N9–N10 1.358(7), N5–N6 1.311(7), N11–N12 1.314(7), N4–C1 1.323(8), N10–C4 1.321(8), N1–C1 1.344(8), N7–C4 1.355(7), N5–C1 1.381(7), N11–C4 1.376(7), O1–N6 1.279(6), O3–N12 1.281(6), O2–N6 1.251(6), O4–N12 1.253(6), Sr–N4 2.788(5), Sr–N10 2.728(5), Sr–O1 2.699(4), Sr–O3 2.684(4), Sr–O5 2.597(5), N1–C2 1.462(7), N7–C5 1.470(8), C2–C3 1.485(10), C5–C6 1.497(9), C11–C3 1.767(8), C12–C6 1.826(7); angles (°) N6–N5–C1 116.0(5), N12–N11–C4 115.7(5), O1–N6–N5 123.7(4), O3–N12–N11 124.2(5), O2–N6–O1 118.9(5), O4–N12–O3 118.7(5), N4–Sr–O1 67.5(1), N10–Sr–O3 67.0(1); torsion angles (°) N6–N5–C1–N4 –7.1(1), C1–N5–N6–O1 –0.2(8).

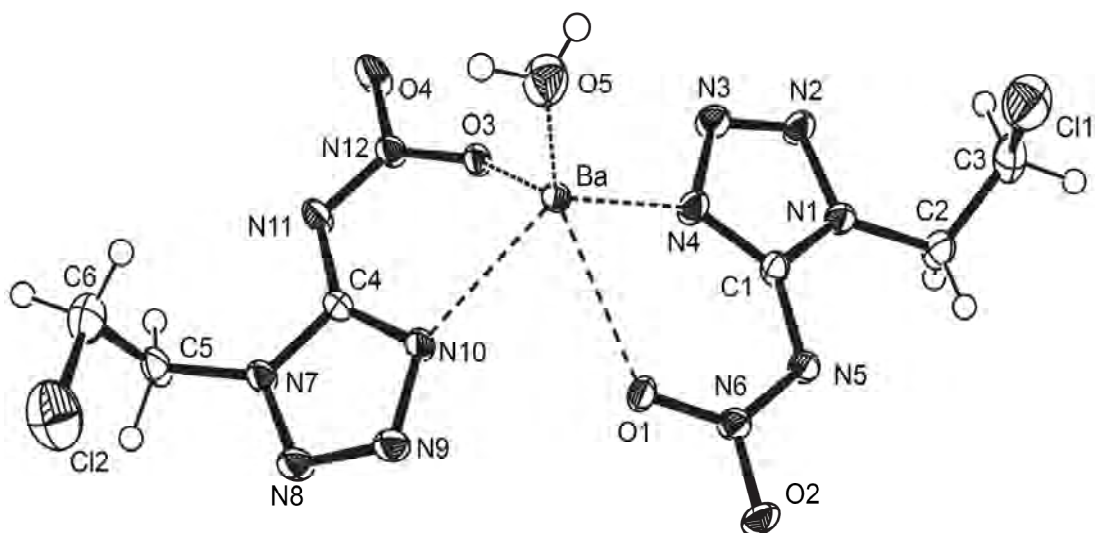


Figure 2. Molecular unit of **6**. Hydrogen atoms shown as spheres of arbitrary radius and thermal displacements set at 50% probability. Selected geometries: distances (Å) N1–N2 1.353(5), N7–N8 1.348(5), N2–N3 1.287(5), N8–N9 1.292(5), N3–N4 1.369(5), N9–N10 1.373(5), N5–N6 1.296(5), N11–N12 1.306(5), N4–C1 1.331(5), N10–C4 1.320(5), N1–C1 1.350(5), N7–C4 1.349(5), N5–C1 1.381(5), N11–C4 1.382(5), O1–N6 1.273(4), O3–N12 1.266(4), O2–N6 1.268(4), O4–N12 1.258(4), Ba–N4 2.908(4), Ba–N10 2.944(3), Ba–O1 2.864(3), Ba–O3 2.841(3), Ba–O5 2.767(4), N1–C2 1.463(5), N7–C5 1.463(5), C2–C3 1.514(6), C5–C6 1.510(7), C11–C3 1.783(5), C12–C6 1.794(6); angles (°) N6–N5–C1 116.7(3), N12–N11–C4 116.2(3), O1–N6–N5 125.0(3), O3–N12–N11 124.8(3), O2–N6–O1 117.9(3), O4–N12–O3 118.5(3), N4–Ba–O1 129.68(9), N10–Ba–O3 128.13(8); torsion angles (°) N6–N5–C1–N4 8.9(7), C1–N5–N6–O1 –0.2(6).

6 and **9** were solved with SIR-92,²³ **8** with SIR-97²⁴ and refined with SHELXL-97²⁵ and finally checked using the PLATON software.²⁶ The non-hydrogen atoms were refined anisotropically and the hydrogen atoms were located and freely refined. The absorptions were corrected by the SCALE3 ABSPACK multi-scan method.²⁷ All relevant data and parameters of the X-ray measurements and refinements are given in Table 1. Further information on the crystal-structure determinations has been deposited with the Cambridge Crystallographic Data Centre (CCDC)²⁸ as supplementary publications 718890 (**5**), 718891 (**6**) 733993 (**8**) and 733994 (**9**). The structure of **7** (CCDC 704305) is discussed in Klapötke *et al.*¹⁹

The strontium salt **5** crystallizes with one molecule of water of crystallization in the orthorhombic space group *Pbca*. One unit cell contains eight formula units (Figure 1). The calculated density is 2.033 g cm⁻³. The strontium cation is coordinated by the atoms O1, O2, O3, O4, N3, N4, N9, N10 and the oxygen atom of the

crystal water (O5). The oxygen atoms O1 and O3 are each coordinated to two different strontium atoms. Three different hydrogen bonds can be observed. In each case O5 is the donor atom (H⋯A (Å): H1a⋯N2ⁱ 2.40(6), H1a⋯O2ⁱⁱ 2.51(7), H1b⋯N5ⁱⁱ 2.49(4); D⋯A (Å): O5⋯N2ⁱ 3.233(7), O5⋯O2ⁱⁱ 2.936(6), O5⋯N5ⁱⁱ 3.250(7); angle DHA (°): O5H1aN2ⁱ 173(8), O5H1aO2ⁱⁱ 113(6), O5H1bN5ⁱⁱ 151(8); *i*: *x* + 1/2, –*y* + 1/2, –*z* + 1, *ii*: *x* + 1/2, –*y* + 3/2, –*z* + 1). The nitrimino group of both anions follows the planarity of the tetrazole ring with a twist angle of ~0° (C1–N5–N6–O1) and ~1° (C4–N11–N12–O3), respectively.

By analogy with strontium 1-methyl-5-nitrimino-tetrazolate monohydrate¹⁵ the packing of **5** is strongly influenced by the formation of stacks. The crystal water molecules effect no bridging and are coordinated alternately up and down.

The barium salt **6** crystallizes in the monoclinic space group *P* $\bar{1}$ with only two formula units per unit cell (Figure 2). Its density of 2.180 g cm⁻³ is comparable to that of **5**. The atoms coordinated to the barium atoms are analogous to those of the

Table 1. Crystallographic data of **5**, **6**, **8** and **9**.

	5	6	8	9
Formula	C ₆ H ₁₀ Cl ₂ N ₁₂ O ₅ Sr	C ₆ H ₁₀ BaCl ₂ N ₁₂ O ₅	C ₆ H ₈ Cl ₂ CuN ₁₂ O ₄	C ₆ H ₁₄ Cl ₂ CuN ₁₄ O ₄
<i>M</i> [g mol ⁻¹]	488.78	538.50	446.68	480.75
Crystal system	orthorhombic	triclinic	monoclinic	monoclinic
Space group	<i>Pbca</i> (61)	<i>P</i> $\bar{1}$ (2)	<i>P</i> 2 ₁ / <i>c</i> (14)	<i>P</i> 2 ₁ / <i>c</i> (14)
Color/habit	colorless blocks	colorless plates	green disks	blue pads
Size [mm]	0.12 × 0.11 × 0.07	0.10 × 0.10 × 0.03	0.32 × 0.25 × 0.03	0.4 × 0.2 × 0.01
<i>a</i> [Å]	12.9331(4)	8.5674(2)	11.273(6)	14.4769(5)
<i>b</i> [Å]	8.3175(3)	9.0807(3)	6.451(3)	5.5805(2)
<i>c</i> [Å]	29.6896(10)	11.8239(3)	9.685(5)	10.7259(5)
α [°]	90	98.756(3)	90	90
β [°]	90	96.802(2)	90.925(5)	101.154(4)
γ [°]	90	113.050(3)	90	90
<i>V</i> [Å ³]	3193.74(19)	820.38(5)	704.2(7)	850.16(6)
<i>Z</i>	8	2	2	2
ρ_{calc} [g cm ⁻³]	2.033	2.180	2.107	1.878
μ [mm ⁻¹]	3.765	2.798	1.981	1.651
<i>F</i> (000)	1936	520	446	486
$\mu\text{MoK}\alpha$ [Å]	0.71073	0.71073	0.71073	0.71073
<i>T</i> [K]	200	200	100	200
θ min–max [°]	3.99, 26.0	3.88, 26.0	3.79, 28.7	3.86, 26.0
Dataset [<i>h</i> , <i>k</i> , <i>l</i>]	–10:15; –9:10; –36:36	–10:10; –11:11; –14:14	–13:13; –7:7; –11:11	–17:11; –3:6; –13:11
Reflections collected	15296	18013	4557	3194
Independent reflections	3120	3205	1371	1661
<i>R</i> _{int}	0.0756	0.0327	0.0345	0.0237
Observed reflections	1862	2849	1138	1284
No. parameters	243	243	115	136
Restraints	3	0	0	0
<i>R</i> ₁ (obs)	0.0428	0.0265	0.0409	0.0254
<i>wR</i> ₂ (all data)	0.1358	0.0691	0.1285	0.0573
GooF	1.047	1.118	1.142	0.922
Resd. dens. [e Å ⁻³]	–1.242, 1.635	–0.734, 1.392	–1.014, 0.710	–0.244, 0.353
Device type	Oxford Xcalibur3 CCD	Oxford Xcalibur3 CCD	Oxford Xcalibur3 CCD	Oxford Xcalibur3 CCD
Solution	SIR-92	SIR-92	SIR-97	SIR-92
Refinement	SHELXL-97	SHELXL-97	SHELXL-97	SHELXL-97
Absorption correction	multi-scan	multi-scan	multi-scan	multi-scan
CCDC	718890	718891	733993	733994

strontium atoms in **5**. Furthermore, the nitrimino group is not twisted out of the tetrazole ring plane. One hydrogen bond with the parameters ($H\cdots A$ (Å): $H1b\cdots O2^i$ 2.047; DHA (°): 166.98; $D\cdots A$ (Å): $O5\cdots O2^i$ 2.858; $i: x, y - 1, z.$) can be found. Both **5** and **6** show similar bond lengths and angles of their anions.

The packing of **6** is also dominated by stacks, formed along the a axis with the crystal water molecules coordinated alternately up and down.

The copper salt **8** crystallizes analogously to *trans*-[diaqua-bis{1-(2-chloroethyl)-5-nitrimino-tetrazolato- κ^2N^4, O^5 }copper(II)] dihydrate (**7**) in the monoclinic space group $P2_1/c$ with two molecular units per unit cell.¹⁹ As expected, the calculated density of **8** (2.107 g cm⁻³) is higher than that of **7** (1.871 g cm⁻³).¹⁹ The copper(II) atoms are located on the center of inversion, whereby the 1-(2-chloroethyl)-5-nitriminotetrazole anions act as bidentate ligands (Figure 3). A Jahn–Teller-distorted octahedral coordination of the copper cations is observed. Interestingly, the Cu–N4 and Cu–O1 distances are equal to 1.954 Å and the distance between the copper cation and O2 of 2.602 Å is the longest. No hydrogen bonds could be observed.

Copper(II) complex **9** also crystallizes in the space group $P2_1/c$ with two molecular units per unit cell (Figure 4). The calculated density of 1.878 g cm⁻³ is comparable with that of **7**. Analogous to **8**, the copper(II) cations are located on the center of inversion and are coordinated by the 5-nitriminotetrazole anions and neutral ammonia ligands forming a Jahn–Teller-distorted octahedron. The copper nitrogen distances are comparable in length (Cu–N4 2.011(2) Å and Cu–N7 2.005(2) Å), but the Cu–O1 distance is clearly longer at 2.352(2) Å, which is in agreement with the coordination sphere in **7**.

Energetic properties

The energetic properties, such as decomposition temperature (T_{dec}), sensitivity towards shock (E_{dt}), friction (F_r) and electric discharge (E_{ei}), and combustion energy ($\Delta_c U$), were determined or adopted from the literature. Furthermore, the solubility in H₂O at ambient temperature of each compound was defined. An overview of the energetic properties of **5–9** is given in Table 2.

The thermal behavior of *ca.* 2 mg of the compounds **5–9** was determined *via* differential scanning calorimetry (DSC) in the temperature range

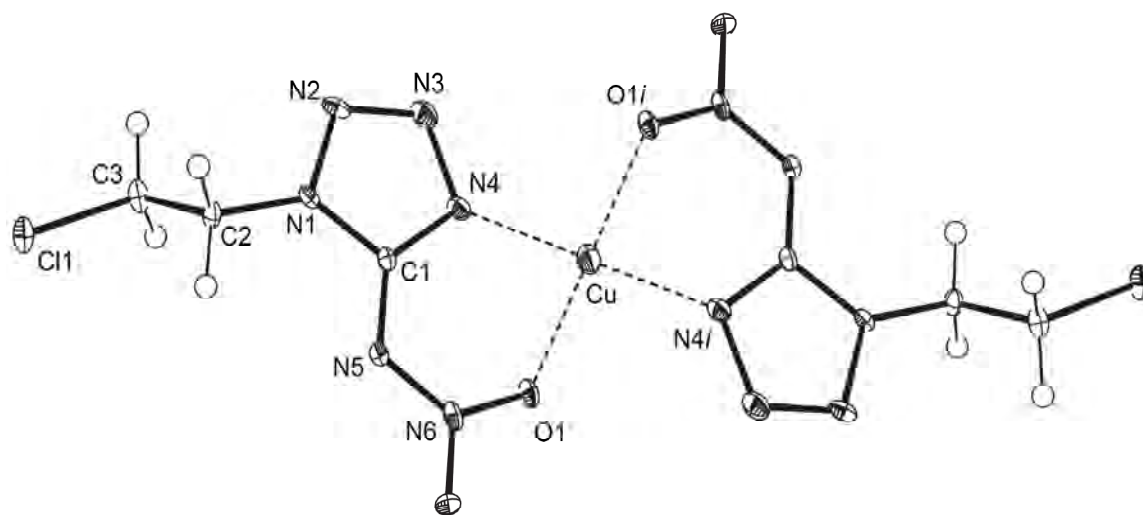


Figure 3. Molecular unit of **8**. Hydrogen atoms shown as spheres of arbitrary radius and thermal displacements set at 50% probability. Selected geometries: distances (Å) N1–N2 1.362(4), N2–N3 1.280(5), N3–N4 1.381(5), N5–N6 1.308(5), N4–C1 1.329(5), N1–C1 1.347(5), N5–C1 1.362(5), O1–N6 1.293(4), O2–N6 1.245(4), Cu–N4 1.954(3), Cu–O1 1.954(3), N1–C2 1.463(5), C2–C3 1.515(5), Cl1–C3 1.785(4); angles (°) N6–N5–C1 117.1(3), O1–N6–N5 124.8(3), O2–N6–O1 117.9(3), N4–Cu–O1 84.81(13); torsion angles (°) N6–N5–C1–N4 –10.6(6), C1–N5–N6–O1 –3.4(5).

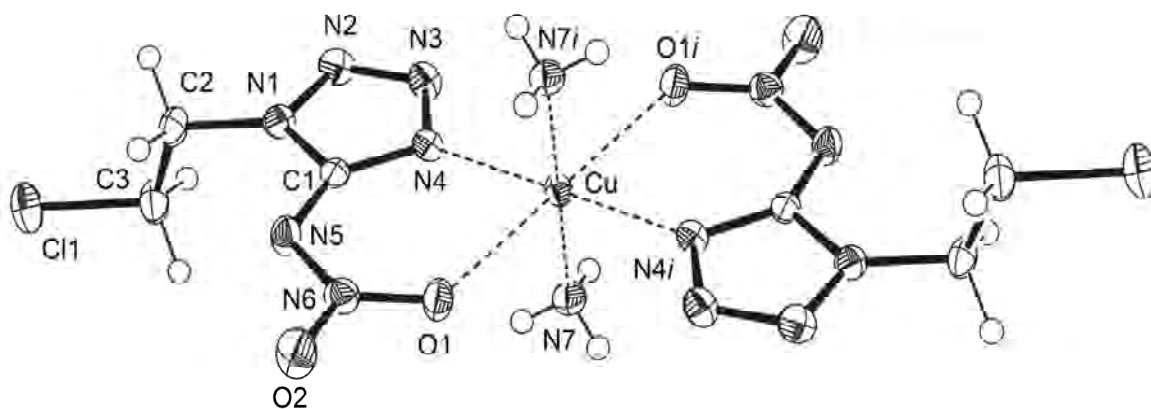


Figure 4. Molecular unit of **9**. Hydrogen atoms shown as spheres of arbitrary radius and thermal displacements set at 50% probability. Selected geometries: distances (Å) N1–N2 1.343(2), N2–N3 1.286(2), N3–N4 1.362(2), N5–N6 1.318(2), N4–C1 1.332(3), N1–C1 1.356(2), N5–C1 1.359(3), O1–N6 1.262(2), O2–N6 1.241(2), Cu–N4 2.011(2), Cu–O1 2.352(2), Cu–N7 2.005(2), N1–C2 1.456(2), C2–C3 1.509(3), Cl1–C3 1.788(2); angles (°) N6–N5–C1 117.3(2), O1–N6–N5 123.6(2), O2–N6–O1 118.8(2), N4–Cu–O1 76.04(6), N4–Cu–N7 88.81(9), N7–Cu–O1 90.05(8); torsion angles (°) N6–N5–C1–N4 –8.4(4), C1–N5–N6–O1 –2.4(3).

from 50 °C to 400 °C. All prepared substances decompose above 200 °C, whereby the copper(II) compounds **7** and **8** offer the highest decomposition temperatures of 242 °C and 238 °C, respectively. In

view of this fact and that **7** loses H₂O at 103 °C, it was possible to obtain **8** by removing the chemical water of **7**. In the case of copper(II) complex **9** no loss of ammonia could be observed.

Table 2. Overview of the physico-chemical properties of **5–9**.

	5	6	7	8	9
Formula	C ₆ H ₁₀ Cl ₂ N ₁₂ O ₅ Sr	C ₆ H ₁₀ BaCl ₂ N ₁₂ O ₅	C ₆ H ₁₆ Cl ₂ CuN ₁₂ O ₈	C ₆ H ₈ Cl ₂ CuN ₁₂ O ₄	C ₆ H ₁₄ Cl ₂ CuN ₁₄ O ₄
<i>M</i> [g mol ⁻¹]	488.78	538.50	518.72	446.68	480.75
<i>E</i> _{dr} [J] ^a	10	3.0	>50	6.0	6.0
<i>F</i> _r [N] ^b	>360	144	>360	192	>360
<i>E</i> _{el} [J] ^c	0.75	1.0	0.60	0.50	0.50
<i>N</i> [%] ^d	34.4	31.2	32.4	37.6	40.8
<i>Ω</i> [%] ^e	-39	-36	-37	-43	-53
<i>T</i> _{dec} [°C] ^f	208	207	242	238	205
<i>ρ</i> [g cm ⁻³] ^g	2.03	2.18	1.87 ¹⁹	2.11	1.89
<i>Δ</i> _c <i>U</i> [kJ kg ⁻¹] ^h	-7030	-6330	-7042	-8797	-10238
<i>Δ</i> _c <i>H</i> ^o [kJ mol ⁻¹] ⁱ	-3416	-3389	-3633	-3908	-4893
<i>Δ</i> _r <i>H</i> ^o [kJ mol ⁻¹] ^j	-863	-846	-1068	346	474
<i>Δ</i> _r <i>U</i> [kJ kg ⁻¹] ^k	-1691	-1504	-1969	775	987
H ₂ O sol. [wt%] ^l	14 (21 °C)	0.8 (21 °C)	0.9 (23 °C)	0.7 (23 °C)	0.4 (23 °C)

^a BAM drop hammer. ^b BAM methods. ^c Electric spark tester. ^d Nitrogen content. ^e Oxygen balance. ^f Decomposition temperature from DSC ($\beta = 5 \text{ °C min}^{-1}$). ^g Determined by X-ray crystallography. ^h Combustion energy. ⁱ Enthalpy of combustion. ^j Molar enthalpy of formation. ^k Energy of formation. ^l Solubility in H₂O (H₂O temperature).

The compounds **5**, **6**, **8**, and **9** are sensitive to shock according to the literature.²⁹ Salt **5** shows the lowest sensitivity (10 J), but it is insensitive towards friction. The barium salt **6** is very sensitive towards shock (3.0 J) and sensitive towards friction (144 N). The copper(II) complexes **7** and **9** are insensitive towards friction. Salt **7** is also insensitive towards shock, whereas **9** offers a impact sensitivity of 6.0 J and the water free compound **8** is sensitive towards both stimuli (E_{dr} : 6 J, F_r : 192 N). This is a verification that the inclusion of crystal water decreases the sensitivity.

All determined values for the electrostatic sensitivity are in the range of 0.5–1.0 J (**8**, **9**: 0.50 J; **7**: 0.60 J; **5**: 0.75 J; **6**: 1.0 J). These results are consistent with the sensitivities of other insensitive energetic materials.

The reported values of the combustion energy ($\Delta_c U$) are the average of three single bomb calorimetry measurements. The standard molar enthalpy of combustion ($\Delta_c H^\circ$) was derived from equation (1).

$$\Delta_c H^\circ = \Delta_c U + \Delta n RT \quad (1)$$

$$\Delta n = \sum n_i (\text{gaseous products}) - \sum n_i (\text{gaseous starting materials})$$

n_i = molar amount of gas i .

The enthalpy of formation ($\Delta_f H^\circ$) for each compound **5–9** was calculated at 298.15 K using the Hess thermochemical cycle and the following combustion reactions (Scheme 5). The heats of formation of the combustion products $\text{H}_2\text{O}_{(l)}$ (-286 kJ mol^{-1}), $\text{CO}_{2(g)}$ (-393 kJ mol^{-1}), $\text{HCl}_{(g)}$ ($-92.3 \text{ kJ mol}^{-1}$), $\text{SrO}_{(s)}$ (-592 kJ mol^{-1}), $\text{BaO}_{(s)}$ (-548 kJ mol^{-1}), and $\text{CuO}_{(s)}$ (-157 kJ mol^{-1}) were

adopted from the literature.³⁰

Except for **8** and **9** all compounds were calculated to be formed exothermically. Copper complex **7** shows the highest negative value for the heat of formation ($-1068 \text{ kJ mol}^{-1}$). In contrast to that, the copper compounds **8** and **9** offer the highest positive ones. The calculated values of **5** and **6** are comparable.

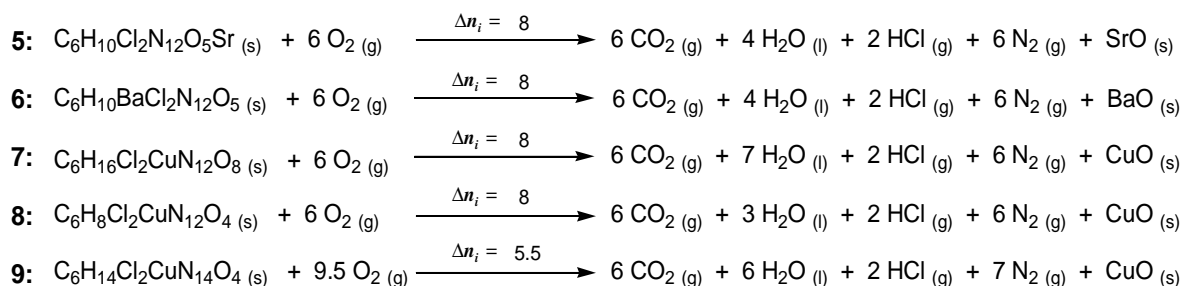
For determining the solubility of **5–9**, each compound was added to 1 mL H_2O at the noted temperature until the solution was saturated. The solubilities of **5–9** are given in weight percent (wt%) and were calculated according to equation (2).

$$\text{wt}\% = \frac{m_{\text{dissolvedCompound}}}{m_{\text{dissolvedCompound}} + m_{\text{Solvent}}} \cdot 100 \quad (2)$$

The strontium salt **5** offers the highest solubility with 14 wt%. All other compounds **6–9** are almost insoluble in H_2O under these conditions with solubilities below 1.0 wt%.

Coloring properties and some pyrotechnic compositions

All compounds **5–9** show the expected flame color – with regard to their corresponding cations – in the flame of a Bunsen burner (Figure 5). Furthermore, their combustion occurs without smoke production. The strontium salt **5** combusts with a very intense red flame, significantly more intense than the other nitrogen-rich salts strontium 5-nitriminotetrazolate dihydrate, strontium (5-nitrimino-1*H*-tetrazolate) tetrahydrate,



Scheme 5. Combustion equations of **5–9**.



Figure 5. Color performance of (top to bottom) 5–9 in the flame of a Bunsen burner.

strontium (1-methyl-5-nitriminotetrazolate) monohydrate and strontium (2-methyl-5-nitriminotetrazolate).¹⁵ A very intense green flame is shown by 6, also significantly more intense than other barium salts like barium tetrazolate,

barium 5-aminotetrazolate tetrahydrate, barium 5-nitriminotetrazolate dihydrate, barium bis(5-nitrimino-1*H*-tetrazolate) tetrahydrate, barium 1-methyl-5-nitriminotetrazolate monohydrate, or barium 2-methyl-5-nitriminotetrazolate dihydrate.¹⁶

Since the copper salts contain chlorine, 7 combusts with a bright blue flame and the water free 8 deflagrates fast (but subsonically) with the formation of a bright blue flame. The ammine complex 9 shows an analogous combustion behaviour to 7. All salts feature no solid residues after their combustion.

The compounds 5–7 were chosen as coloring agents for some pyrotechnic compositions. They offer the possibility of the formation of SrCl, BaCl, and CuCl, respectively – their corresponding light emitting species in the gas phase – without additional chlorine donors. (All other cations used do not need any chlorine for a more intense flame color.) No composition was prepared with 8 and 9, because of their higher sensitivity and the fast deflagration of 8. Furthermore, 9 shows the lowest decomposition temperature. In Table 3 the results of the two best formulations are listed. The performance of each composition has been evaluated with respect to the following categories:

- color emission (subjective impression)
- smoke generation
- morphology and amount of solid residues
- thermal stability
- moisture sensitivity

The US Army red flare composition # 126 A1 (red parachute), 39% Sr(NO₃)₂, 30% Mg, 13% KClO₄, 8% VAAR, was a measure of the red light composition performance. The performance of the compositions for green light were compared to the barium nitrate-based US Army composition # 125 A1 (green parachute): 50% Ba(NO₃)₂, 30% Mg, 15% PVC, 5% VAAR (mass percent). The compositions for blue light were compared with Shimizu's:³¹ 15% Cu, 17% PVC, 68% KClO₄, 5% starch.

The composition 5_1 with the strontium salt 5

Table 3. General summary of the performance of the pyrotechnic composition.

Pyrotechnic composition	Color emission	Smokeless combustion	Amount of solid residues	Thermal stability	Moisture stability	Environmental compatibility
5_1	+++	++	++	---	-	+++
5_2	+	+	+	---	-	+++
# 126 A1	++	---	++	+++	+++	---
6_1	++	++	++	-	-	-
6_2	+++	+	++	---	-	-
# 125 A1	++	---	++	+++	+++	---
7_1	++	+	+	---	+	++
7_2	+	++	-	-	++	++
Shimizu ³¹	+++	-	++	+++	+++	---

as coloring agent consists of 11% **5**, 44% ADN (ammonium dinitramide), 34% 5-aminotetrazole (**1**) and 11% VAAR. The observed flame color is significantly more intense red compared to that of # 126 A1. Furthermore, the combustion occurs very fast and smokeless. The composition shows high sensitivities towards shock (4.5 J), friction (54 N) and electric discharge (0.75 J). It has a lack in thermal stability ($T_{\text{dec}} = 167\text{ }^{\circ}\text{C}$) and is slightly sensitive towards moisture, but its coloring properties are very good. The mixture **5_2** contains 14% **5**, 68% NH_4NO_3 , 7% Mg and 11% VAAR. The observed flame is intense red, but smaller compared to # 126 A1. The combustion velocity is significantly slower than that of **5_1**. Almost no smoke is produced, but some magnesium sparks could be observed. A very small amount of solid residues was obtained. The decomposition temperature is comparable to **5_1** (165 $^{\circ}\text{C}$), but **5_2** is less sensitive towards shock (6 J), friction (240 N) and electric discharge (1.2 J). Furthermore, it is more stable towards moisture. Figure 6 shows the burn down of all red burning compositions.

The pyrotechnic composition **6_1** containing the barium salt **6** consists of 25% **6**, 45% ADN, 10% **1** and 20% VAAR. It combusts with a very intense green flame (more intense than # 125 A1) and without smoke production. The reaction velocity is comparable to # 125 A1. The sensitivities towards shock (2 J), friction (160 N) and electric discharge (0.65 J) are very high, but similar to **5_1**. Also the decomposition occurs below 180 $^{\circ}\text{C}$ ($T_{\text{dec}} = 175^{\circ}\text{C}$) and the mixture is slightly sensitive towards moisture. Composition **6_2** was made up with 20% **6**, 60% NH_4NO_3 , 4% **1**, 7% magnalium and 9% VAAR. Its flame color is comparably intense to **6_1**, but the burning

**Figure 6.** Burn down of the US Army composition # 126 A1 (top), the compositions **5_1** (middle) and **5_2** (bottom).

velocity is a little slower. As in the case of **5_2** some magnesium sparks and no smoke production could be observed. The combustion occurred completely without solid residues. **6_2** shows the lowest decomposition temperature of 154 °C. It is very sensitive towards shock (4.5 J) and electric discharge (1.0 J), but insensitive towards friction (> 360 N). A comparison of the combustion behavior of the green burning mixtures can be found in Figure 7.

For the preparation of composition **7_1** the copper compound **7** was used (43% **7**, 43% ADN, 4%

starch and 10% VAAR). The observed flame color is comparably intense to that of Shimizu (Figure 8). This is true for the combustion velocity. Smoke could be detected during combustion but less than that of Shimizu and a small amount of solid residues was yielded. The composition **7_1** decomposes at temperatures above 150 °C and is very sensitive towards shock (<1.0 J) and friction (108 N). A marginal sensitivity towards moisture was observed. The pyrotechnic composition **7_2** (24% **7**, 12% ADN, 43% NH₄NO₃, 4% boron and 17% VAAR) shows a less brilliant blue flame color compared to Shimizu's. However, its combustion



Figure 7. Burn down of the US Army composition # 125 A1 (top), the compositions **6_1** (middle) and **6_2** (bottom).



Figure 8. Burn down of Shimizu's composition (top), the compositions **7_1** (middle) and **7_2** (bottom).

occurs smokelessly and with a marginal amount of solid residues. The combustion velocity is slower compared to **7_1**. Composition **7_2** offers no sensitivity towards moisture. Its decomposition point is at 159 °C. The sensitivities towards impact and friction were determined to be 2.5 J and 192 N.

Experimental

All chemicals and solvents were employed as received (Sigma-Aldrich, Fluka, Acros). ¹H and ¹³C NMR spectra were recorded using a Jeol Eclipse 270, Jeol EX 400 or a Jeol Eclipse 400 instrument. The chemical shifts quoted in ppm in the text refer to typical standards, such as tetramethylsilane (¹H, ¹³C). To determine the decomposition points of the described compounds a Linseis PT 10 DSC (heating rate β : 5 °C min⁻¹) was used. Raman spectra were recorded with a Perkin-Elmer Spektrum 2000R NIR FT-Raman instrument, which uses a Nd:YAG laser with a wavelength of 1064 nm. Infrared (IR) spectra were recorded using a Perkin-Elmer One FT-IR instrument with an ATR unit at 25 °C. To measure Elemental Analyses a Netsch STA 429 Simultaneous Thermal Analyzer was employed. The impact sensitivity (E_{dr}) tests were carried out according to STANAG 4489³² modified according to instructions³³ using a BAM (Bundesanstalt für Materialforschung³⁴) drop hammer.³⁵ The friction sensitivity (F_r) tests were carried out according to STANAG 4487³⁶ modified according to instructions³⁷ using the BAM friction tester. The electrostatic sensitivity (E_{el}) tests were carried out using an electric spark tester ESD 2010EN (OZM Research) operating with the “Winspark 1.15 software package”³⁸ For all calorimetric measurements a Parr 1356 bomb calorimeter (static jacket) equipped with a Parr 1108CL oxygen bomb for the combustion of highly energetic materials were used.³⁹

The compounds 1- and 2-(2-hydroxyethyl)-5-aminotetrazole (**2a**, **b**) were prepared according to the literature,^{17,19} as were 1-(2-chloroethyl)-5-aminotetrazole and 1-(2-chloroethyl)-5-nitriminotetrazole.^{19,20}

A solution of 25% vinyl alcohol acetate resin (VAAR) was used as binder (for the pyrotechnic compositions).

Strontium 1-(2-chloroethyl)-5-nitriminotetrazolate monohydrate (**5**)

A solution of 1.31 g (6.8 mmol) 1-(2-chloroethyl)-5-nitriminotetrazole (**4**) and 0.90 g (3.4 mmol) strontium hydroxide octahydrate in 25 mL H₂O was refluxed for 15 minutes. The solvent was removed under high vacuum to obtain a colorless powder. Recrystallization from H₂O yielded 1.51 g of colorless needles suitable for X-ray determination. Yield: 91%.

Mp 208 °C (dec.). **Raman** (200 mW, 25 °C, cm⁻¹): 3016 (6), 2967 (15), 1647 (5), 1542 (3), 1507 (100), 1462 (6), 1438 (6), 1380 (6), 1344 (24), 1291 (7), 1261 (3), 1245 (2), 1205 (3), 1111 (10), 1031 (37), 995 (3), 875 (4), 766 (10), 743 (3), 653 (6), 507 (2), 473 (2), 371 (3), 306 (5), 196 (5). **IR** (Diamond-ATR, cm⁻¹): 3501 (w), 3015 (vw), 2966 (vw), 2852 (vw), 2363 (vw), 2340 (vw), 1640 (w), 1508 (m), 1462 (m), 1421 (w), 1380 (s), 1340 (s), 1310 (s), 1257 (m), 1236 (s), 1130 (w), 1109 (m), 1027 (m), 996 (w), 954 (w), 904 (w), 871 (w), 771 (w), 764 (w), 740 (w), 708 (vw), 677 (w), 653 (w). **¹H NMR** (DMSO-*d*₆): 4.39 (*t*, 2H, ³*J* = 5.9 Hz, CH₂), 3.98 (*t*, 2H, ³*J* = 5.9 Hz, CH₂), 3.32 (*s*, 2H, H₂O). **¹³C NMR** (DMSO-*d*₆): 157.7 (CN₄), 47.8 (CH₂), 42.1 (CH₂). **EA** C₆H₁₀Cl₂N₁₂O₅Sr (488.75 g mol⁻¹): calc.: C, 14.74; H, 2.06; N, 34.39; found: C, 14.85; H, 2.20; N, 34.62%. E_{dr} >10 J. F_r >360 N. E_{el} >0.75 J. $\Delta_c U = -1679$ cal g⁻¹.

Barium 1-(2-chloroethyl)-5-nitriminotetrazolate monohydrate (**6**)

A solution of 1.31 g (6.8 mmol) 1-(2-chloroethyl)-5-nitriminotetrazole (**4**) and 1.07 g (3.4 mmol) barium hydroxide octahydrate in 25 mL H₂O was refluxed for 15 minutes. The solvent was evaporated to obtain a colorless powder. Recrystallization from H₂O–ethanol (1:1) yielded 1.75 g of colorless needles suitable for X-ray diffraction. Yield: 95%.

Mp 207 °C (dec.). **Raman** (200 mW, 25 °C, cm⁻¹): 3022 (5), 2974 (12), 1538 (2), 1496 (100), 1460 (4), 1383 (7), 1351 (26), 1315 (6), 1293 (6), 1258 (2), 1199 (1), 1108 (11), 1028 (35), 999 (3), 872 (3), 758 (5), 677 (5), 646 (4). **IR** (Diamond-ATR, cm⁻¹): 3607 (w), 3406 (w), 3025 (w), 3002 (vw), 2363 (vw), 2341 (vw), 1783 (vw), 1629 (w), 1496 (m), 1458 (w), 1444 (m), 1429 (m), 1340 (s), 1315 (s), 1258 (m), 1242 (m), 1229 (m),

1136 (w), 1106 (m), 1025 (m), 1000 (w), 961 (vw), 942 (w), 909 (w), 870 (w), 768 (w), 755 (w), 746 (w), 738 (w), 710 (vw), 672 (w), 655 (w), 646 (w). $^1\text{H NMR}$ ($\text{DMSO-}d_6$): 4.39 (t, 2H, $^3J = 5.9$ Hz, CH_2), 3.98 (t, 2H, $^3J = 5.9$ Hz, CH_2), 3.32 (s, 2H, H_2O). $^{13}\text{C NMR}$ ($\text{DMSO-}d_6$): 157.7 (CN_4), 47.8 (NCH_2), 42.1 (CH_2Cl). **EA** $\text{C}_6\text{H}_{10}\text{Cl}_2\text{N}_{12}\text{O}_5\text{Ba}$ ($538.45 \text{ g mol}^{-1}$): calc.: C, 13.38; H, 1.87; N, 31.22; found: C, 13.35; H, 1.85; N, 31.46%. $E_{\text{dr}} > 3.0 \text{ J}$. $F_r > 144 \text{ N}$. $E_{\text{el}} > 1.0 \text{ J}$. $\Delta_c U = -1512 \text{ cal g}^{-1}$.

***trans*-[Diaqua-bis{1-(2-chloroethyl)-5-nitriminotetrazolato- $\kappa^2\text{N}^4, \text{O}^5$ }copper(II)] dihydrate (7)**

A solution of 2.00 g (10.4 mmol) 1-(2-chloroethyl)-5-nitriminotetrazole (4) in 20 mL H_2O and a solution of 1.21 g (5.2 mmol) copper(II) nitrate pentahydrate in 10 mL H_2O were combined. Deep blue crystals formed after one day of storing at room temperature. Yield: 85%.

Mp 103 °C (loss of H_2O), 242 °C (dec.). **IR** (Diamond-ATR, cm^{-1}): 3649 (w), 3588 (m), 3497 (w), 3168 (s, br), 3031 (s), 2392 (vw), 2286 (vw), 1515 (s), 1463 (s), 1435 (w), 1425 (w), 1383 (s), 1349 (s), 1297 (s), 1268 (s), 1253 (s), 1211 (m), 1138 (w), 1111 (m), 1036 (w), 1010 (w), 959 (w), 904 (w), 872 (w), 810 (w), 772 (w), 764 (w), 740 (m), 684 (w), 662 (w). **EA** $\text{C}_6\text{H}_{16}\text{Cl}_2\text{CuN}_{12}\text{O}_8$ ($518.72 \text{ g mol}^{-1}$): calc.: C, 13.89; H, 3.11; N, 32.40; Cl, 13.67; found: C, 13.79; H, 2.90; N, 32.55; Cl, 13.68%. $E_{\text{dr}} > 50 \text{ J}$. $F_r > 360 \text{ N}$. $E_{\text{el}} > 0.60 \text{ J}$. $\Delta_c U = -1682 \text{ cal g}^{-1}$.

Copper(II) 1-(2-chloroethyl)-5-nitriminotetrazolate (8)

1.00 g (1.9 mmol) *trans*-[diaqua-bis{1-(2-chloroethyl)-5-nitriminotetrazolato- $\kappa^2\text{N}^4, \text{O}^5$ }copper(II)] dihydrate (7) was stored for 48 hours at 110 °C to remove the water of crystallization. 0.84 g of a green powder could be obtained. After recrystallization from half-concentrated HNO_3 bright green crystals suitable for X-ray diffraction could be obtained. Yield: 99%.

Mp 238 °C (dec.). **IR** (Diamond-ATR, cm^{-1}): 3033 (w), 3002 (vw), 2964 (vw), 2360 (w), 2331 (vw), 1739 (w), 1533 (m), 1488 (s), 1452 (m), 1436 (s), 1429 (m), 1388 (w), 1341 (m), 1304 (s), 1235 (s), 1133 (w), 1107 (w), 1047 (vw), 1001 (m), 873 (w), 793 (vw), 775 (vw), 740 (w), 730 (w), 708 (m), 687 (w). **EA** $\text{C}_6\text{H}_8\text{Cl}_2\text{CuN}_{12}\text{O}_4$

($446.66 \text{ g mol}^{-1}$): calc.: C, 16.13; H, 1.81; N, 37.63; found: C, 16.04; H, 1.85; N, 37.60%. $E_{\text{dr}} > 6.0 \text{ J}$. $F_r > 192 \text{ N}$. $E_{\text{el}} > 0.50 \text{ J}$. $\Delta_c U = -2245 \text{ cal g}^{-1}$.

***trans*-Diammine-bis{1-(2-chloroethyl)-5-nitriminotetrazolato- $\kappa^2\text{N}^4, \text{O}^1$ }copper(II) (9)**

At 50 °C 5.0 mL aqueous ammonia solution (25%) were added to a solution of 2.0 g (10.4 mmol) 1-(2-chloroethyl)-5-nitriminotetrazole in 25 mL H_2O . The mixture was combined with a solution of 1.2 g (5.2 mmol) copper(II) nitrate pentahydrate in 10 mL H_2O . The deep blue solution was stored at ambient temperature until deep blue crystals suitable for X-ray diffraction were formed. Yield: 81%.

Mp 205 °C (dec.). **IR** (Diamond-ATR, cm^{-1}): 3332 (w), 3264 (w), 3177 (vw), 1611 (vw), 1512 (m), 1459 (m), 1438 (w), 1396 (s), 1363 (w), 1342 (m), 1301 (w), 1283 (s), 1268 (m), 1234 (s), 1128 (w), 1106 (w), 1026 (w), 991 (vw), 873 (vw), 790 (vw), 766 (vw), 750 (vw), 732 (vw), 708 (w). **EA** $\text{C}_6\text{H}_{14}\text{Cl}_2\text{CuN}_{16}\text{O}_4$ ($480.72 \text{ g mol}^{-1}$): calc.: C, 14.99; H, 2.94; N, 40.79; found: C, 15.01; H, 3.13; N, 40.63%. $E_{\text{dr}} = 6.0 \text{ J}$. $F_r > 360 \text{ N}$. $E_{\text{el}} = 0.50 \text{ J}$. $\Delta_c U = -2495 \text{ cal g}^{-1}$.

Preparation of the pyrotechnic mixtures

For preparation of the pyrotechnic compositions all substances, except the binder, were carefully mixed in a mortar. Then the binder, dissolved in a few millilitres of ethyl acetate, was added. The mixture was formed by hand and dried under high vacuum for several hours. The controlled burn down was filmed with a digital video camera recorder.

Conclusion

In this paper the compounds strontium 1-(2-chloroethyl)-5-nitriminotetrazolate monohydrate (5), barium 1-(2-chloroethyl)-5-nitriminotetrazolate monohydrate (6), *trans*-[diaqua-bis{1-(2-chloroethyl)-5-nitriminotetrazolato- $\kappa^2\text{N}^4, \text{O}^5$ }copper(II)] dihydrate (7), copper(II) 1-(2-chloroethyl)-5-nitriminotetrazolate (8) and *trans*-[diammine-bis{1-(2-chloroethyl)-5-nitriminotetrazolato- $\kappa^2\text{N}^4, \text{O}^1$ }copper(II) (9) were presented and extensively characterized using vibrational and multinuclear magnetic resonance spectroscopy, elemental analysis, and differential scanning calorimetry (DSC). Furthermore, their sensitivities

towards shock, friction, and electric discharge and their solubility in H₂O at ambient temperature were determined. The heats of formation were calculated using bomb calorimetric measurements.

The crystal structures of **5**, **6**, **8** and **9** were determined and discussed.

The color performance and combustion properties of all salts **5–9** were analyzed with regard to their usage as potential coloring agents in pyrotechnic compositions.

Furthermore, several pyrotechnic compositions, containing the most promising compounds **5–7**, were prepared and compared to known formulations. They all show promising properties, especially regarding color performance and lower smoke production. The decomposition temperatures and sensitivities towards shock, friction and electric discharge of all prepared pyrotechnic compositions were determined.

Therefore, the prepared salts **5–9** are a step forward in preparing more environmentally benign pyrotechnic compositions without potassium perchlorate.

Acknowledgment

Financial support of this work by the Ludwig-Maximilian University of Munich (LMU), the Fonds der Chemischen Industrie (FCI), the European Research Office (ERO) of the US Army Research Laboratory (ARL) and the Armament Research, Development and Engineering Center (ARDEC) under contract nos. W911NF-09-2-0018, W911NF-09-1-0120 and W011NF-09-1-0056 is gratefully acknowledged. The authors acknowledge collaborations with Dr Mila Krupka (OZM Research, Czech Republic) in the development of new testing and evaluation methods for energetic materials and with Dr Muhamed Suceca (Brodarski Institute, Croatia) in the development of new computational codes to predict the detonation and propulsion parameters of novel explosives. We are indebted to and thank Drs Betsy M. Rice and Brad Forch (ARL, Aberdeen, Proving Ground, MD) and Dr Gary Chen (ARDEC, Picatinny Arsenal, NJ) for many helpful and inspired discussions and support of our work. Furthermore, special thanks to Mr Stefan Huber for determining the sensitivities and carrying out the calorimetric measurements.

References

- 1 G. Steinhauser and T. M. Klapötke, Green Pyrotechnics: a Chemists' Challenge, *Angewandte Chemie, International Edition*, Vol. 47, 2008, pp. 3330–3347.
- 2 T. M. Klapötke and K. Tarantik, *New Trends in Research of Energetic Materials*, Proceedings of the Seminar, 11th, Pardubice, Czech Republic, Pt. 2, 2008, pp. 586–597.
- 3 G. Steinhauser, K. Tarantik and T. M. Klapötke, Copper in Pyrotechnics. *Journal of Pyrotechnics*, Vol. 27, 2008, pp. 3–13.
- 4 (a) T. M. Klapötke, C. M. Sabatè and J. Stierstorfer, Neutral 5-nitrotetrazoles: easy initiation with low pollution, *New Journal of Chemistry*, Vol. 33, 2009, pp. 136–147; (b) T. M. Klapötke and C. M. Sabatè, Alkali metal 5-nitrotetrazolate salts: prospective replacements for service lead(II) azide in explosive initiators, *Dalton Transactions*, Issue 45, 2008, pp. 6372–6380.
- 5 G. Holl, T. M. Klapötke, K. Polborn and C. Rienäcker, Structure and bonding in 2-diazo-4,6-dinitrophenol (DDNP), *Propellants, Explosives, Pyrotechnics*, Vol. 28, 2003, pp. 153–156.
- 6 K. Karaghiosoff, T. M. Klapötke, A. Michailovski, H. Nöth and M. Suter, 1,4-Diformyl-2,3,5,6-tetranitratopiperazine: A new primary explosive based on glyoxal, *Propellants, Explosives, Pyrotechnics*, Vol. 28, 2003, pp. 1–6.
- 7 M. Klapötke and J. Stierstorfer, Nitration products of 5-amino-1H-tetrazole and methyl-5-amino-1H-tetrazoles – structures and properties of promising energetic materials, *Helvetica Chimica Acta*, Vol. 90, 2007, pp. 2132–2150.
- 8 (a) T. M. Klapötke, J. Stierstorfer, A. U. Wallek, Nitrogen-Rich Salts of 1-Methyl-5-nitriminotetrazole: An Auspicious Class of Thermally Stable Energetic Materials, *Chemistry of Materials*, Vol. 20, 2008, pp. 4519–4530; (b) S. Berger, K. Karaghiosoff, T. M. Klapötke, P. Mayer, H. Piotrowski, K. Polborn, R. L. Willer and J. J. Weigand, N-nitroso- and N-nitraminotetrazoles, *Journal of Organic Chemistry*, Vol. 71, 2006, pp. 1295–1305.
- 9 (a) J. Geith, G. Holl, T. M. Klapötke,

- J. J. Weigand, Pyrolysis experiments and thermochemistry of mononitrobiuret (MNB) and 1,5-dinitrobiuret (DNB), *Combustion and Flame*, Vol. 139, 2004, pp. 358–366;
- (b) J. Geith, T. M. Klapötke, J. J. Weigand and G. Holl, Calculation of the detonation velocities and detonation pressures of dinitrobiuret (DNB) and diaminotetrazolium nitrate (HDAT-NO₃), *Propellants, Explosives, Pyrotechnics*, Vol. 29, 2004, pp. 3–8.
- 10 E. Lieber, E. Sherman, R. A. Henry and J. Cohen, Reaction of nitrous acid with nitroaminoguanidine, *Journal of the American Chemical Society*, Vol. 73, 1951, pp. 2327–2329.
 - 11 J. A. Garrison and R. M. Herbst, Synthesis and characterization of nitraminotetrazoles, *Journal of Organic Chemistry*, Vol. 22, 1957, pp. 278–283.
 - 12 G. Geisberger, T. M. Klapötke and J. Stierstorfer, Copper bis(1-methyl-5-nitriminotetrazolate): a promising new primary explosive, *European Journal of Inorganic Chemistry*, Vol. 30, 2007, pp. 4743–4750.
 - 13 B. T. Sturman, On the emitter of blue light in copper-containing pyrotechnic flames, *Propellants, Explosives, Pyrotechnics*, Vol. 31, 2006, pp. 70–74.
 - 14 J. A. Conkling, *Chemistry of Pyrotechnics: Basic Principles and Theory*, Marcel Dekker, Inc., New York, 1985.
 - 15 T. M. Klapötke, J. Stierstorfer, K. R. Tarantik and I. D. Thoma, Strontium Nitriminotetrazolates: Suitable Colorants in Smokeless Pyrotechnic Compositions, *Zeitschrift für Anorganische Allgemeine Chemie*, Vol. 634, 2008, pp. 2777–2784.
 - 16 T. M. Klapötke, J. Stierstorfer and K. R. Tarantik, Barium Tetrazolates – Promising Colorants in Smokeless Pyrotechnic Compositions, *European Journal of Inorganic Chemistry*, 2009, submitted.
 - 17 G. T. Flegg, T. T. Griffiths, E. L. Charsley, H. M. Markham, J. J. Rooney and P. D. Howe, Elimination of perchlorate oxidizers from pyrotechnic incendiary compositions, *38th International Annual Conference of the ICT*, 2007, pp. 34/1–34/11.
 - 18 R. A. Henry and W. G. Finnegan, Monoalkylation of Sodium 5-Aminotetrazole in Aqueous Medium, *Journal of the American Chemical Society*, Vol. 76, 1954, pp. 923–926.
 - 19 T. M. Klapötke, J. Stierstorfer and K. R. Tarantik, New Energetic Materials: Functionalized 1-Ethyl-5-aminotetrazoles and 1-Ethyl-5-nitriminotetrazoles, *Chemistry – A European Journal*, 2009, DOI: 10.1002/chem.200802203.
 - 20 W. G. Finnegan and R. A. Henry, N-Vinyltetrazoles, *J. Org. Chem.* **1959**, *24*, 1565–1567.
 - 21 CrysAlis CCD, Oxford Diffraction Ltd., Version 1.171.27p5 beta (release 01-04-2005 CrysAlis171 .NET).
 - 22 CrysAlis RED, Oxford Diffraction Ltd., Version 1.171.27p5 beta (release 01-04-2005 CrysAlis171 .NET).
 - 23 A. Altomare, G. Cascarano, C. Giacovazzo and A. Guagliardi, SIR-92, A program for crystal structure solution. *Journal of Applied Crystallography*, Vol. 26, 1993, p. 343.
 - 24 A. Altomare, M. C. Burla, M. Camalli, G. Cascarano, C. Giacovazzo, A. Guagliardi, A. G. G. Moliterni, G. Polidori and R. Spagna, SIR-97, A program for crystal structure solution, *Journal of Applied Crystallography*, Vol. 27, 1994, pp. 435–435.
 - 25 G. M. Sheldrick, SHELXL-97. Program for the Refinement of Crystal Structures. University of Göttingen, Germany, 1997.
 - 26 A. L. Spek, PLATON, A Multipurpose Crystallographic Tool, Utrecht University, Utrecht, The Netherlands, 1999.
 - 27 SCALE3 ABSPACK – An Oxford Diffraction program (1.0.4,gui:1.0.3) 2005 Oxford Diffraction Ltd.
 - 28 Crystallographic data for the structures have been deposited with the Cambridge Crystallographic Data Centre. These data can be obtained free of charge via www.ccdc.cam.ac.uk/data_request/cif, or by emailing data_request@ccdc.cam.ac.uk, or by contacting The Cambridge Crystallographic Data Centre, 12, Union Road, Cambridge CB2 1EZ, UK; fax: +44 1223 336033.

- 29 E_{dr} : insensitive >40 J, less sensitive ≥ 35 J, sensitive ≥ 4 J, very sensitive ≤ 3 J;
 F_r : insensitive >360 N, less sensitive = 360 N, sensitive <360 N to > 80 N, very sensitive ≤ 80 N, extremely sensitive ≤ 10 N.
 According to the UN Recommendations on the Transport of Dangerous Goods.
- 30 <http://webbook.nist.gov/>
- 31 T. Shimizu, Studies on Blue and Purple Flame Compositions Made With Potassium Perchlorate, *Pyrotechnica*, Vol. 6, 1980, p. 5.
- 32 NATO standardization agreement (STANAG) on explosives, *impact sensitivity tests*, no. 4489, edn 1, Sept. 17, 1999.
- 33 WIWEB-Standardarbeitsanweisung 4-5.1.02, Ermittlung der Explosionsgefährlichkeit, hier der Schlagempfindlichkeit mit dem Fallhammer, Nov. 8, 2002.
- 34 <http://www.bam.de>
- 35 <http://www.reichel-partner.de/>
- 36 NATO standardization agreement (STANAG) on explosive, *Friction sensitivity tests*, no. 4487, edn 1, Aug. 22, 2002.
- 37 WIWEB-Standardarbeitsanweisung 4-5.1.03, Ermittlung der Explosionsgefährlichkeit oder der Reibeempfindlichkeit mit dem Reibeapparat, Nov. 8, 2002.
- 38 (a) <http://www.ozm.cz/testing-instruments/small-scale-electrostatic-discharge-tester.html>; (b) S. Zeman, V. Pelikan and J. Majzlik, *Central European Journal of Energetic Materials*, Vol. 3, 2006, p. 45; (c) D. Skinner, D. Olson and A. Block-Bolten, *Propellants, Explosives, Pyrotechnics*, Vol. 23, 1997, p. 3
- 39 <http://www.parrinst.de/>

Emissions of Reaction Products and Sound from Outdoor and Indoor Firework Displays

Andreas Dutschke,^a Stefan Seeger,^a Lutz Kurth,^a Ulrich Panne^{a,b} and Christian Lohrer^{a*}

^a BAM Federal Institute for Materials Research and Testing - Unter den Eichen 87, 12205 Berlin, Germany

Tel: +49 30 8104-3249; fax +49 30 8104-1237; email: christian.lohrer@bam.de

^b Humboldt-Universität zu Berlin - Unter den Linden 6, 10099 Berlin, Germany

Abstract: *This work presents results of investigations towards the emission of chemical reaction products and sound pressure during an outdoor and an indoor firework display. Potentially harmful and toxic gases, and aerosols, were measured as well as sound pressures. Aerosols were measured with a Differential Mobility Analyzer (DMA) as well as a Laser Particle Counter. The focus was on particles with diameters between 11 nm and 20 μm. A transportable Fourier Transform Infrared (FTIR) spectroscopy detector registered the concentrations of emitted reaction gases, simultaneously. During the outdoor firework display, peak particle concentrations of >550 000 particles cm⁻³, equivalent to a mass concentration of approximately 3.95 mg m⁻³, were detected, revealing a concentration maximum at approximately 175 nm particle diameter. The time-averaged particle mass concentration did not exceed 1.58 mg m⁻³ over 15 minutes. Due to the large distances (110 m) to the firing points, no significant harmful or toxic gas concentrations were measured during the entire firework display. In contrast, concentrations of sulphur dioxide (SO₂) rose after an indoor firework display in a large event hall. On two days, more than 23 000 particles cm⁻³ (which equates to a mass concentration of approximately 0.41 mg m⁻³) were detected when the hall ventilation was turned off, and more than 11 000 particles cm⁻³ (which equates to a mass concentration of approximately 1.18 mg m⁻³) when the hall ventilation was activated. Concentration maxima appeared at approximately 300 nm particle diameter. The time-averaged particle concentrations in this case did not exceed 0.56 mg m⁻³ (over 15 minutes).*

Keywords: *pyrotechnic articles, aerosols, combustion gases*

Introduction

Indoor and outdoor firework displays provide possible hazards to man and the environment. High sound pressure impacts can lead to hearing damage (such as acoustic trauma, tinnitus, drum head perforation or acute hearing loss; often irreparable) and fireworks which are not functioning correctly (e.g. “black shells” and “blind stars”) directly endanger the audience, and pyrotechnicians as well as third parties. Besides, gaseous and solid reaction products released by the fireworks can be potentially harmful. In recent years, some experimental investigations towards the impact of fireworks on the environment have been described in the literature.

Steinhauser and Klapötke¹ give an overview about possible hazards arising from (consumer)

fireworks. These possible hazards comprise the emission of heavy metals, perchlorates, polychlorinated organic compounds, aerosols, and combustion gases. As a result of this work, the authors suggest developing nitrogen rich compounds, and excluding perchlorates and heavy metals from future fireworks. A possible alternative to the conventional oxidiser potassium perchlorate could be the insertion of metal nanoparticles into the pores of nano-metal oxides. Steinhauser *et al.*² identified solid reaction products (heavy metals) after New Year’s Eve fireworks during snowfall in the Alps. It was found that combustion products are absorbed by snowflakes, and the concentration of barium in the snow increased rapidly. Therefore, the authors stated that an increase in the concentration of barium is a good indicator for the combustion of fireworks. Moreno *et al.*³

Article Details

Manuscript Received:-16/09/2009

Publication Date:-22/12/2009

Article No: - 0080

Final Revisions:-20/12/2009

Archive Reference:-1022

measured metalliferous particles from Las Fallas firework displays in Valencia, Spain, and Guy Fawkes celebrations in London, UK. An increase in various metal concentrations was observed (potassium, aluminium, titanium, magnesium, lead, barium, strontium, copper, and antimony). Van der Kamp *et al.*⁴ traced a fireworks plume generated by a pyrotechnic display with a lidar ceilometer. Thereby, the vertical height of the plume was measured (~100 m), as well as particulate matter (PM) concentrations of 30–40 $\mu\text{g m}^{-3}$. Wang *et al.*⁵ confirmed the emission of sulphur dioxide (SO_2), nitrogen dioxide (NO_2), and solid particles $\text{PM}_{2.5}$ and PM_{10} at a firework display in Beijing, China. In addition, chemical analyses of the particles showed amongst others, the existence of barium, potassium, strontium, lead, and magnesium. The influence of fireworks on the formation of particles was analysed by Vecchi *et al.*⁶ at the festivities in Milan, Italy, after the final of the soccer world cup 2006. Significant emissions of metals and metal ions (e.g. strontium, magnesium, potassium, barium, and copper) were measured. Drewnick *et al.*⁷ verified the generation of particles consisting of potassium, sulphates, and chlorides after a New Year's Eve firework display in Mainz, Germany. During the millennium fireworks in Leipzig, Germany, a rapid increase of particle and nitrogen monoxide (NO) concentrations was measured by Wehner *et al.*⁸ Perry⁹ investigated the influence of fireworks on the air quality in the west of Washington State, USA. Large concentrations of strontium, potassium, vanadium, titanium, barium, copper, lead, magnesium, aluminium, sulphur, manganese, and zinc were detected. Smith and Dinh¹⁰ tested the effects of the New Year's Eve fireworks in Honolulu (Hawaii), USA, on the emission of gaseous and solid reaction products. In this pioneering work, an average PM concentration of 2.15 mg m^{-3} was measured (with a maximum value of more than 3.8 mg m^{-3}) during 30 minutes around midnight. This study underlines with its spirometry data that inhalation of reaction products of fireworks can cause a change in human lung function. Hussain and Rees¹¹ published results for the measurements of gaseous reaction products from burning pyrotechnical substances using Fourier Transform Infrared (FTIR) spectroscopy. The experiments were carried out under different conditions. In an air atmosphere carbon dioxide

(CO_2) was identified as the main product, whereas NO_2 , NO, and carbon monoxide (CO) were mainly detected in a nitrogen atmosphere. SO_2 , however, was mostly determined under an oxygen atmosphere. Dutschke *et al.*¹² reported analysis of reaction gases under isolated conditions in a manometric bomb with FTIR spectroscopy. Thereby, the dependence of the reaction gas composition on the initial masses was determined for black powder, a pyrotechnical light, and a stage fountain. Main reaction products were CO and CO_2 . The ratio CO/ CO_2 increased with rising pyrotechnic mass, caused by the oxygen limitation in the manometric bomb. Furthermore, high concentrations of hydrogen sulphide (H_2S) and carbonyl sulphide (COS) were observed. The authors also measured particle emissions in a ventilated hall room at different locations during the combustion of single stage fireworks. After the ignition, particle concentrations immediately raised up to <550 000 particles cm^{-3} (which equates a mass concentration of 1.4 mg m^{-3}) and decreased exponentially afterwards. That fact was explained by sedimentation of the particles and room ventilation. Kreyling *et al.*¹³ reported the health risks caused by PM. It was stated that the particle size distribution has a major impact on the hazard potential. Particles with a diameter smaller than 100 nm can interfere with the alveolar system.

The objective of this work was to compare two different types of firework displays – indoor and outdoor – with regard to the possible hazards to the audience, pyrotechnicians, other third parties, and the environment. Therefore, continuous measurements of gaseous and solid reaction products, sound pressure levels, surrounding air temperature, pressure, and humidity, as well as wind speed and direction were carried out. The analysed firework displays were the 3rd Pyronale® World Championship of Fireworks (outdoor, September 5th and 6th, 2008, location Maifeld in Berlin, Germany) and the 26th international ADAC-Super-Motocross (opening indoor firework display; November 14th and 15th, 2008, location Martin-Schleyer Hall in Stuttgart, Germany).

Experimental investigations

Figure 1 and Figure 2 illustrate the locations of the festivals as well as the measuring points and

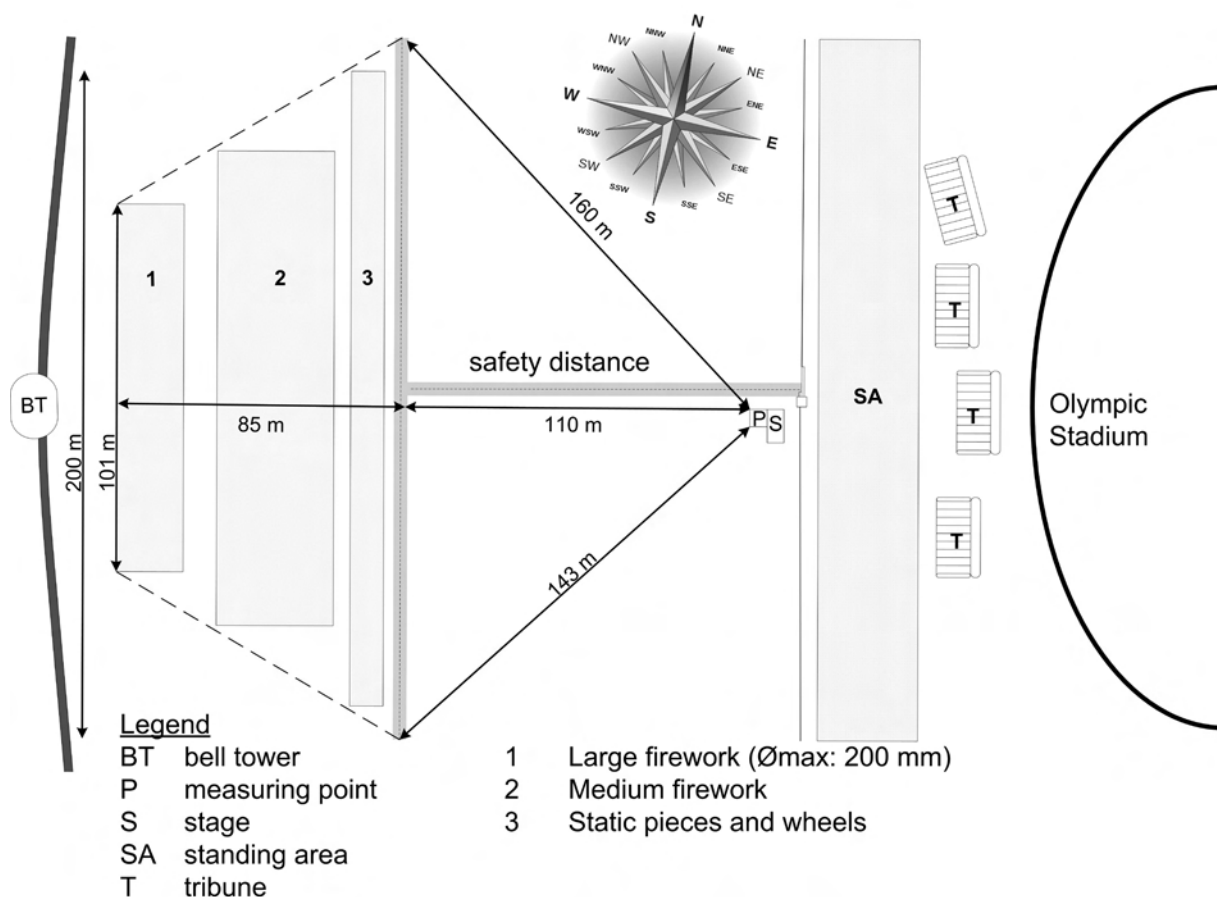


Figure 1. Map of the Maifeld (outdoor) in Berlin, Germany.

boundary conditions.

Tribunes and the standing area of the audience were located in front of the Olympic stadium. The standing area and the firework batteries were separated by a safety distance of more than 130 m. The measuring point was set at a horizontal distance to the first firework batteries of approximately 110 m inside the safety distance. It can be seen from Figure 1 that wind coming from west was necessarily needed to measure reaction products liberated by the firework displays. During the Pyronale®, 7 firework displays were performed, 1–3 on the first evening, and 4–7 on the second evening. Each display continued for about 15 minutes.

As illustrated in Figure 2, the ground level, where the indoor motocross show was performed, was surrounded by tribunes for the audience. The measuring point was located at the upper end of the tribunes, next to the ventilation outlet openings.

The ventilation inlet was realized by hall doors. This hall consists of a volume of approximately 200 000 m³, a ventilation rate of 446 000 m³ h⁻¹, and a total smoke vent surface of ca. 76 m². The hall ventilation was shut down on the first day (November 14th) and activated on the second day (November 15th).

Indoor pyrotechnic articles were placed at ground level in front of the audience (safety distance to the audience approximately minimum 10 m) and partly fixed to the ceiling construction. The indoor pyrotechnic articles contained airbursts, concussions, flash curtains, falling fires, water falls, mortar hits, mines, line rockets, flickering lights, saxons, and gerbs. All in all, 212 indoor pyrotechnic articles, with a net explosive content of 4.2 kg, were burned off on both show days. The overall length of the pyrotechnic show was about 9 minutes on both evenings and started at 20:00.

For continuous and simultaneous combustion gas

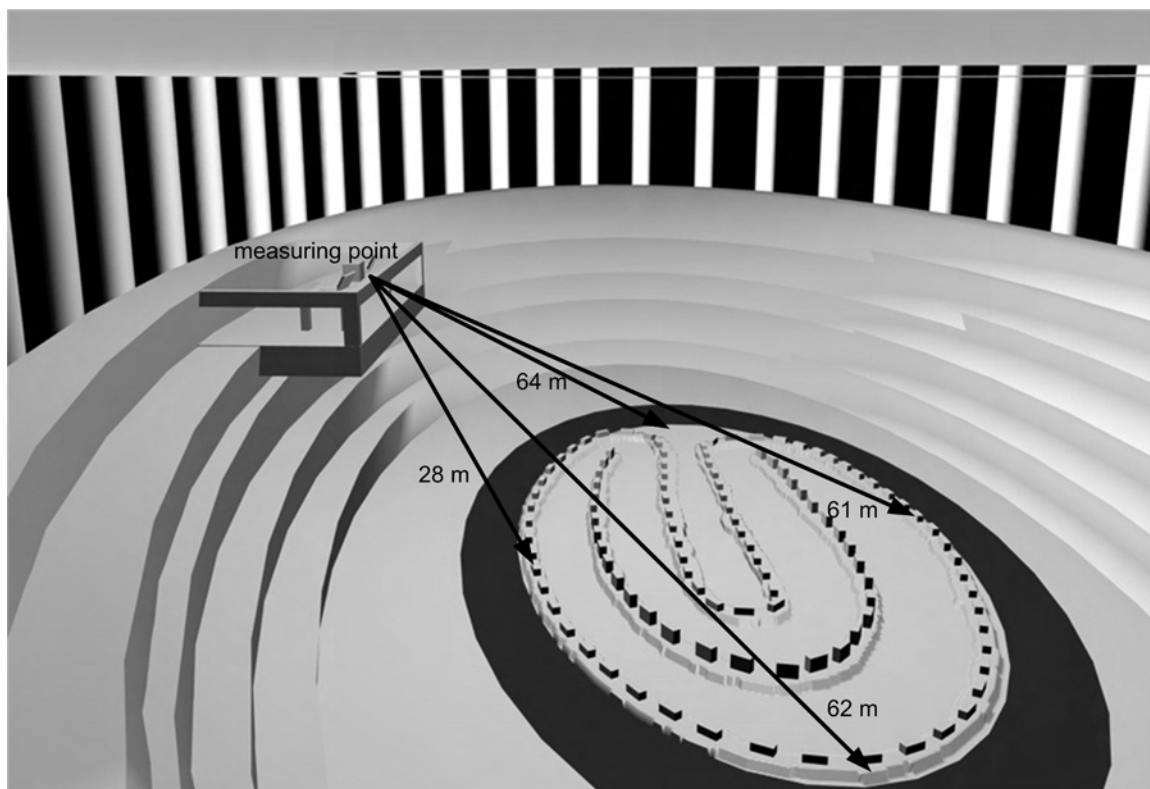


Figure 2. Map of the Martin-Schleyer Hall (indoor) in Stuttgart, Germany.

detection, the transportable FTIR spectrometer Gasmeter DX-4000N from Ansyco with an optical path range of 5 m was used (detection limit <10 ppm). It offers a wavelength range of 900 cm^{-1} to 6000 cm^{-1} , a resolution of 8 cm^{-1} , a sample volume of 0.5 L, a constant zero gas flow of 2.3 L min^{-1} , and measures at a temperature of $50\text{ }^{\circ}\text{C}$.

Aerosol measurements were carried out with two different devices with an overlapping particle diameter range:

SMPS (TSI 3936); the measurement range was set between 11 nm and 461 nm (with an aerosol flow rate of 1 L min^{-1} and a scan frequency of $0.5\text{ spectra min}^{-1}$, and 105 particle size channels), and

a laser particle counter (Grimm 1.108); measurement range between 300 nm and $20\text{ }\mu\text{m}$, aerosol flow rate of 1 L min^{-1} , and a scan frequency of $10\text{ spectra min}^{-1}$.

In addition, wind speed and direction were measured continuously at the Pyronale[®] by an

electrical cup anemometer and a weather vane at a height of 2 m. The measuring frequency was set to 1 Hz.

Sound pressure measurements were carried out at the outdoor location with a 2 channel real time analyzer type 830 (company Nortronic) with the following technical data: frequency range 50 Hz to 20 kHz, resolution third octave band width, time weighting impulse, frequency weighting LIN A. A $\frac{1}{2}$ " condenser microphone type MK 221 with a cartridge type 4190 of the company B&K was used (sensitivity 49.3 mV Pa^{-1} ; calibration unit type 4231 of the company B&K).

Results and discussion

3rd Pyronale[®] World Championship of Fireworks (outdoor)

Table 1 summarizes time-averaged results of the meteorological data such as air temperature, humidity, and pressure during the measurements.

Temperature, ambient pressure, and relative humidity were comparable on both days. The only major difference was the occurrence of continuous

Table 1. Meteorological data of September 5th and September 6th 2008 at the Maifeld in Berlin, Germany.

Date	September 5th 2008	September 6th 2008
(Measurement time)	(19:00–22:15)	(20:20–22:35)
Temperature/°C	18 ± 0.5	18 ± 0.5
Air pressure/hPa	1001	1002
Relative humidity (%)	70–75	70–80
Rain ?	No	Rain started after 21:06

rain, which started during the firework display on September 6th, 2008.

Detailed information about the wind conditions on September 5th and 6th, 2008, at the Maifeld in Berlin, Germany, is given in Figure 3 and Figure 4.

The left ordinate of Figure 3 and Figure 4 represents the wind speed at 2 m height; the right ordinate gives the corresponding wind direction with the following definitions:

- 0/360° = south,
- 90° = west;
- 180° = north, and
- 270° = east.

Figure 3 reveals that due to the wind conditions

on Friday September 5th, 2008, measurements of gaseous and solid reaction products liberated by the firework display were not possible. The prevailing wind direction was from the south/east, blowing the fume plume away from the location of instrumentation.

On Saturday September 6th, 2008, wind conditions changed significantly. As can be seen from Figure 4, comparatively low wind speeds (average over the evening < 0.8 m s⁻¹) were measured almost during the entire evening. Though, at around 21:15 to 21:30, wind squalls occurred with a maximum speed of 4.5 m s⁻¹, coming from the west and southwest. During that time, firework display 5 was running.

However, even under these conditions, when the

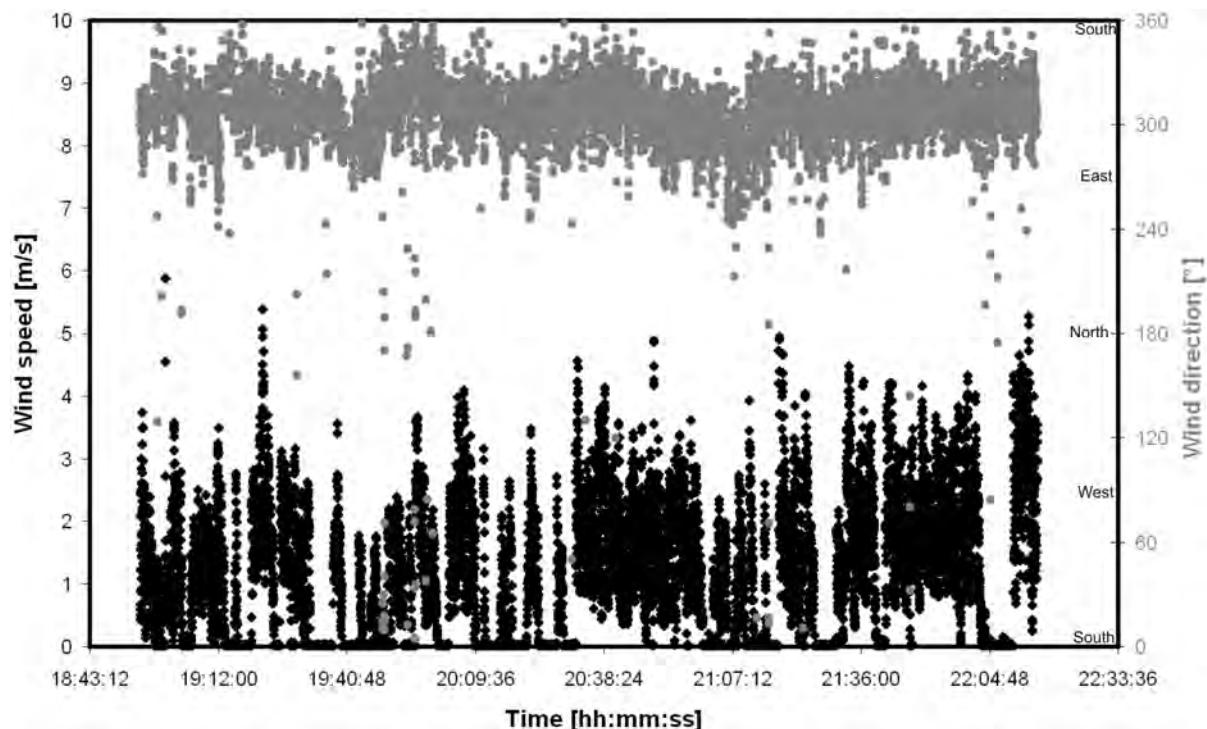


Figure 3. Wind speed and direction on Friday September 5th, 2008, at the Maifeld in Berlin, Germany.

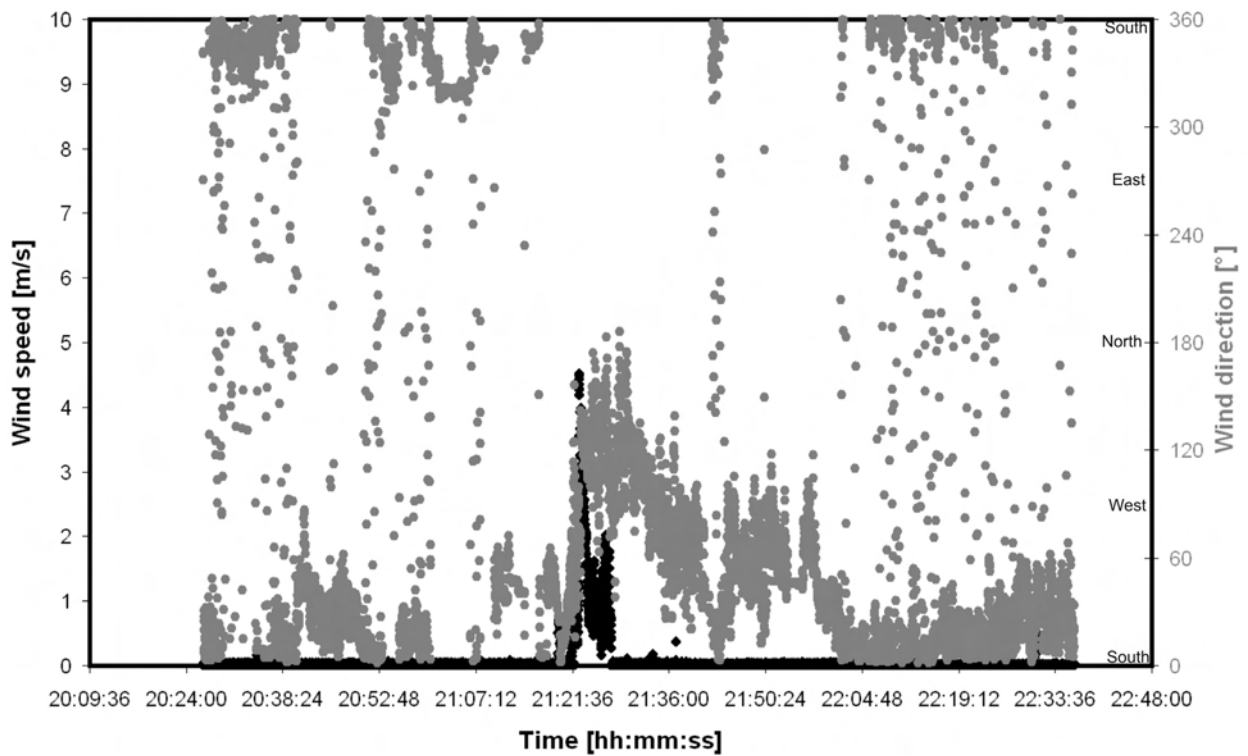


Figure 4. Wind speed and direction on Saturday September 6th, 2008, at the Maifeld in Berlin, Germany.

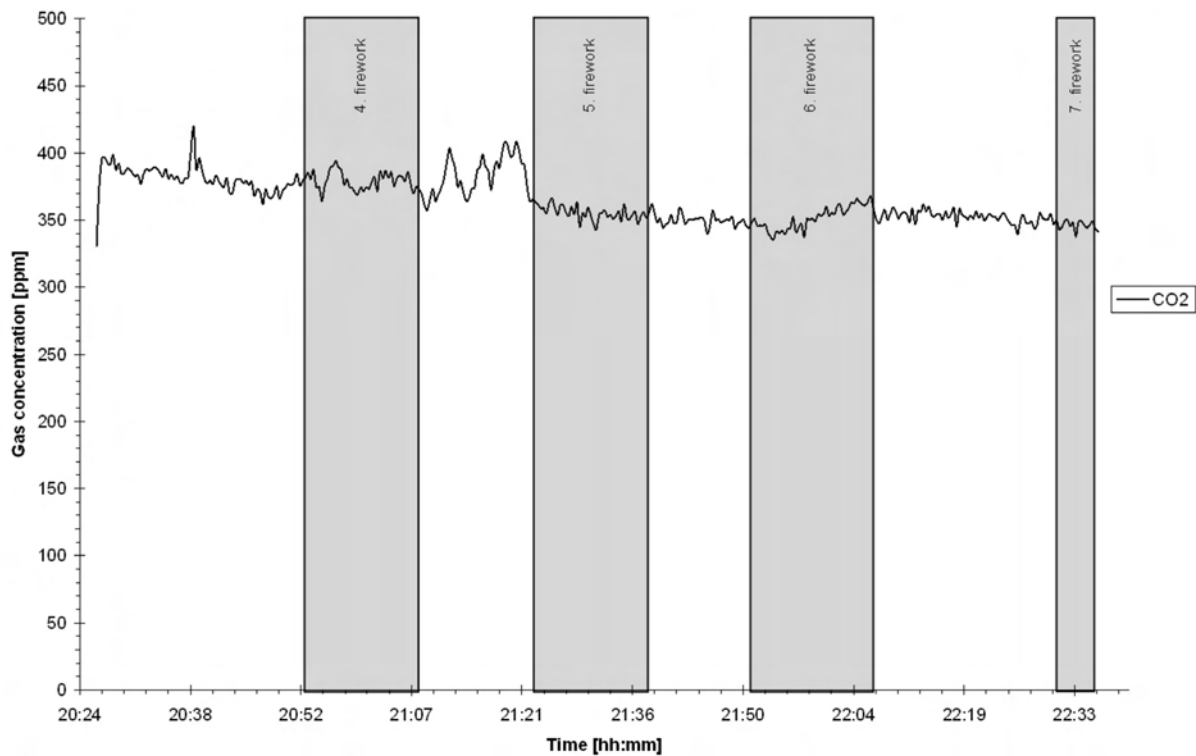


Figure 5. Gas concentration of CO₂ on Saturday September 6, 2008, at the measurement location at a minimum of 110 m distance from the fireworks setup.

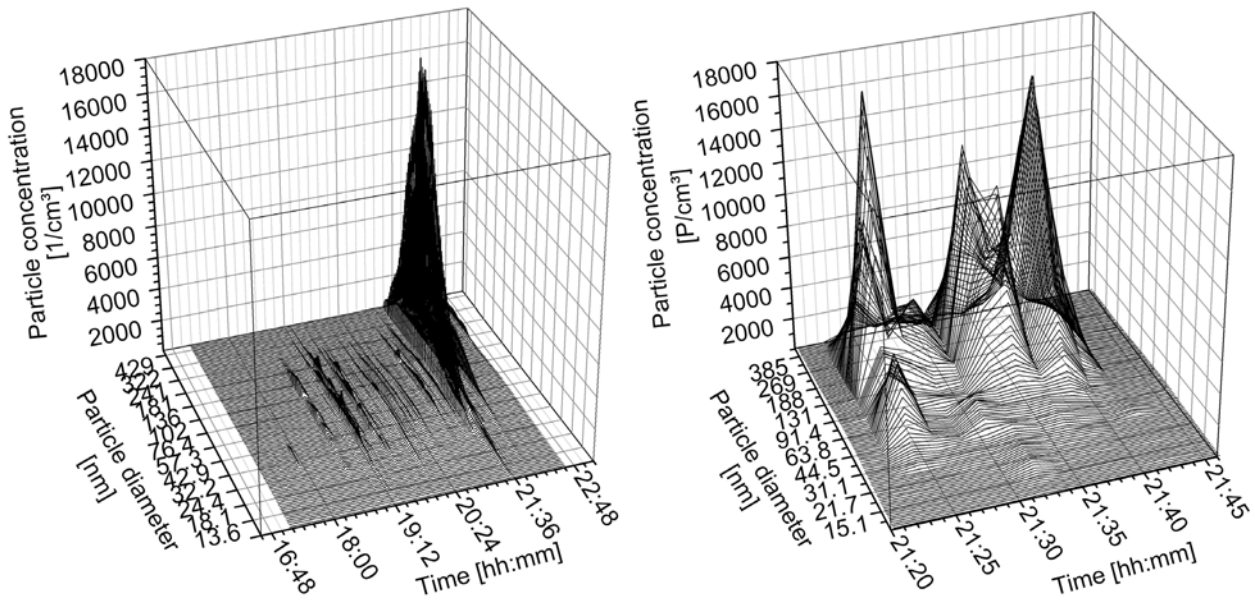


Figure 6. Time-dependent particle size distribution on Saturday September 6th, 2008; left diagram: full spectrum, right side: scale-up of the time interval from 21:20 to 21:45.

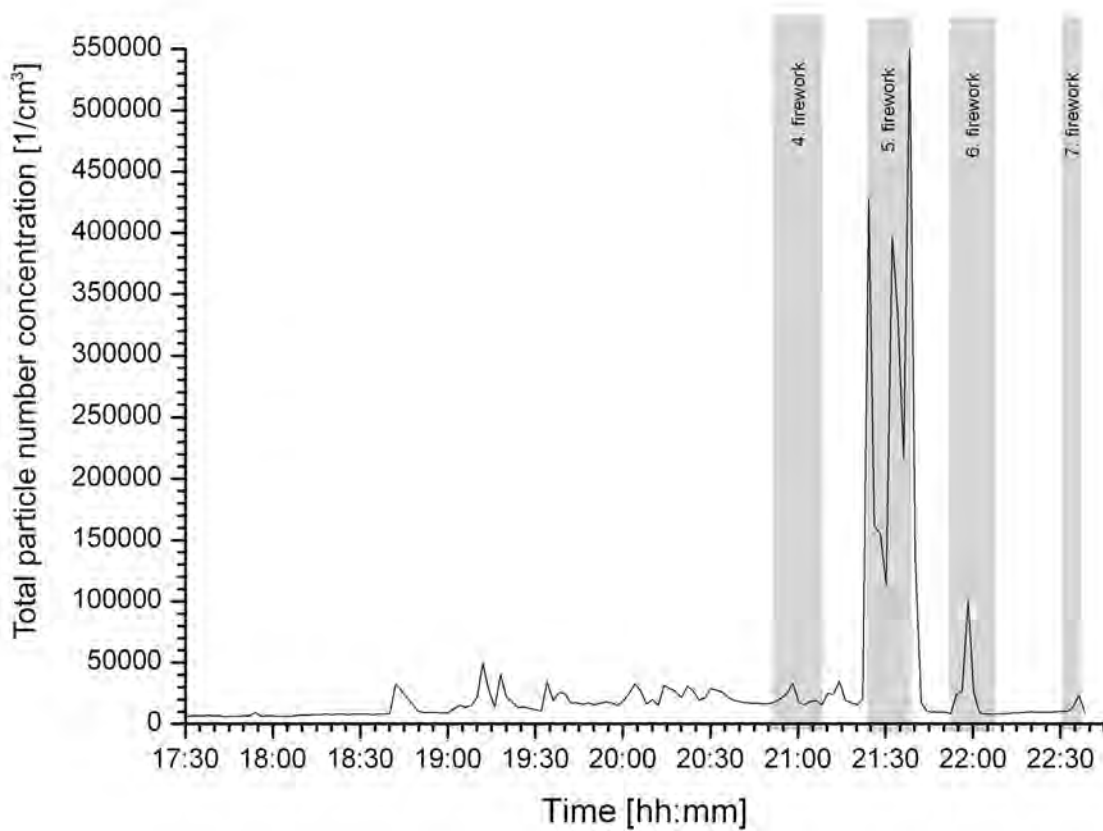


Figure 7. Time-dependent total particle number concentration (<500 nm) on Saturday September 6th, 2008.

fireworks emissions were directly transported to the instrumentation, no significant traces of combustion gases were detected by the FTIR spectrometer. This was due to the large distance from the measurement location to the ignition points (>110 m), leading to dilution effects. In addition, hot reaction gases immediately ascended due to buoyancy forces and were partly dissolved by rain drops. Figure 5 illustrates as an example the time-dependent CO₂ concentration during the evening.

In contrast, significant emissions of particles were detected at the measuring point. The results of the particle measurements are illustrated in Figure 6 to Figure 8. Figure 6 gives the time-dependent particle concentrations for all particle size channels below 500 nm diameter.

The time-dependent total particle number concentration is displayed in Figure 7 and Figure 8.

Measurements during firework display no. 5 (wind was transporting the fume plume to the measuring devices) showed that the particle distribution above background was between 40 nm and 400 nm. It is expected that due to homogeneous

particle formation processes (i.e. combustion of the fireworks) ultrafine particles are predominately created. Concentration maxima occurred at diameters of approximately 145 nm and 170 nm. The total particle number concentration during firework display number 5 reveals a maximum of > 550 000 particles cm⁻³.

To evaluate these data, a conversion to a mass based concentration is necessary. Therefore, as a first approximation, all particles were assumed to be ideal spheres with a standard density of 1200 kg m⁻³ (the real composition and physical structure of the particles are unknown).

The calculated maximum of the total mass concentration was 3.95 mg m⁻³ at 21:38. In addition, the following maximum time-averaged values were measured:

1.58 mg m⁻³ over 15 min, and

0.90 mg m⁻³ over 30 min.

Table 2 contrasts the measured data with (legal) limit and reference values in Germany.

The legal background for occupational safety in Germany is the Labour Protection Law

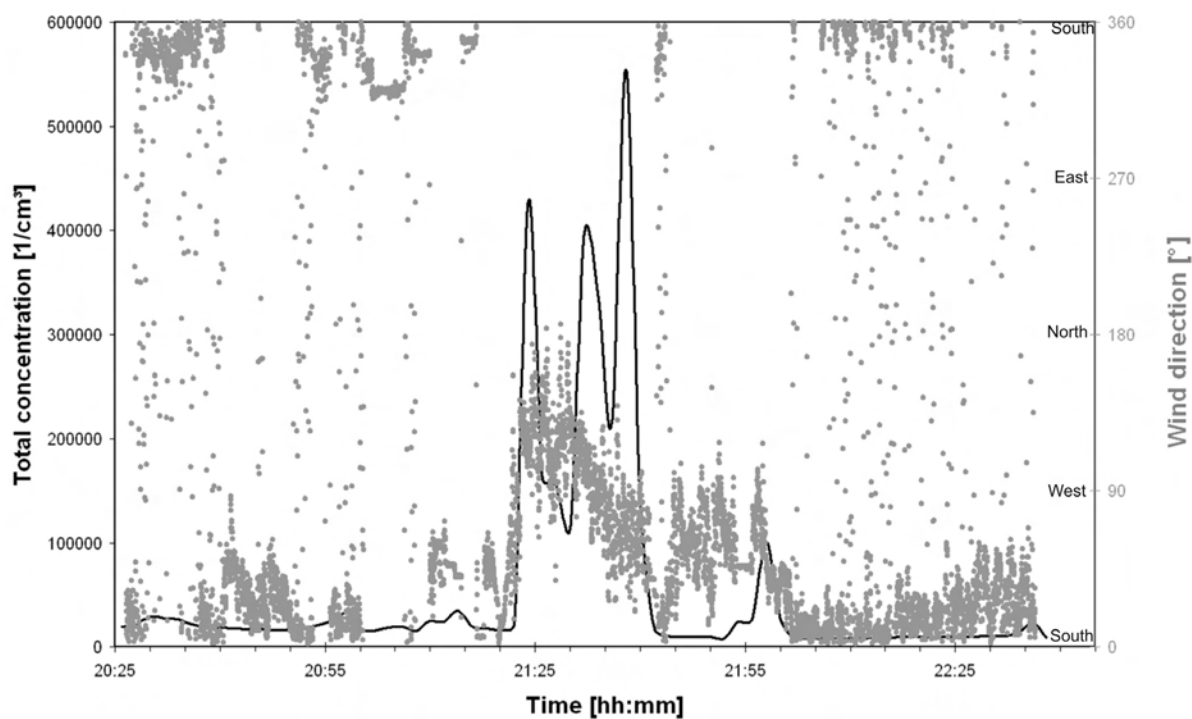


Figure 8. Time-dependent total particle number concentration and wind direction on Saturday September 6th, 2008.

Table 2. Results of particle measurements from Saturday September 6th, 2008, and corresponding (legal) limit and reference values for dusts in Germany.

Maximum measured particle concentration	550 000 particles cm ⁻³ ≈ 3.95 mg m ⁻³
Maximum time-averaged particle concentration (15 min)	1.58 mg m ⁻³
Maximum time-averaged particle concentration (30 min)	0.90 mg m ⁻³
AGW _a for alveolar dust (8 h/day, 40 h/week)	3 mg m ⁻³
AGW _r for respirable dust (8 h/day, 40 h/week)	10 mg m ⁻³
AGW _{STV} (short time value, over 15 min)	AGW _{STV} = 2 × AGW _a = 6 mg m ⁻³
MI (30 min, respirable)	0.45 mg m ⁻³
MI (30 min, particulate matter)	0.3 mg m ⁻³

(Arbeitsschutzgesetz, ArbSchG)¹⁴ and the ancillary Ordinance on Hazardous Substances (Gefahrstoffverordnung, GefStoffV).¹⁵ For activities at work, which cover the handling, liberation or production of hazardous materials, occupational limit values (Arbeitsplatzgrenzwerte, AGW) are binding according to the ArbSchG. The GefStoffV gives a list of hazardous materials, including respirable and alveolar dusts (defined as particle diameters ≤18 μm). Substance dependent AGW are time-averaged concentrations and refer to a working shift, with a typical exposure time of 8 h a day, 5 days a week for the entire working life. They are listed in the Technical Standard TRGS 900.¹⁶ In addition, short time values exist (AGW_{STV}), which replenish the AGW regarding concentration fluctuations. AGW_{STV} limit the shift mean value in terms of magnitude, frequency, and exposure time. AGW_{STV} are the product of the AGW and the overstepping factor (which is 2 in case of dusts; referred to an exposure time of 15 min). Longer exposure times are allowed, as long as the product of the overstepping factor and overstepping time remains the same. The corresponding AGW for respirable and alveolar dusts are presented in Table 2. As a major limitation of the AGW, these values are not valid for dusts which are mutagenic, carcinogenic, allergenic, toxic, soluble, superfine, and coarse particles.

Furthermore, maximum emission values (MI) are given in the VDI guideline 2309¹⁷ and presented for dusts in Table 2. Here the following definitions are set: respirable dusts with a median particle diameter of 25 μm, and particulate matter with a median particle diameter of 10 μm. The given data are not mandatory and represent a very conservative estimation.

The maximum measured particle concentration of 3.95 mg m⁻³ is in good agreement with the data presented by Smith and Dinh.¹⁰

As can be seen from Table 2, the maximum time-averaged particle concentration (over 15 min) of 1.58 mg m⁻³ during the firework display was more than 3 times smaller than the corresponding short time value AGW_{STV} = 6 mg m⁻³, but still of the same magnitude. The same applies for the time-averaged 30 min values. In contrast to this, the measured maximum time-averaged 30 min value of 0.90 mg m⁻³ clearly exceeds the suggested MI value by a factor of 3.

Results towards the emission of sound pressures during the Pyronale® in September 2008 at the Maifeld in Berlin, Germany, are presented in Table 3. An exemplarily unweighted sound pressure versus time history for firework display no. 5 (September 6th, 2009) is illustrated in Figure 9.

Table 3: Results of the sound pressure measurements (L_{max} = maximal unweighted sound pressure; L_{Imax} = time dependent sound pressure at L_{max} ; L_{AImax} = time and A-weighted sound pressure at the L_{max}) for all fireworks during the Pyronale®.

	1. firework	2. firework	3. firework	4. firework	5. firework	6. firework	7. firework
L_{max} dB	157.6	156.8	153.0	147.4	164.6	159.4	150.5
L_{Imax} dB	121.1	121.6	125.5	120.7	120.1	120.6	125.9
L_{AImax} dB	114.6	113.2	115.5	113.2	111.8	113.0	114.5

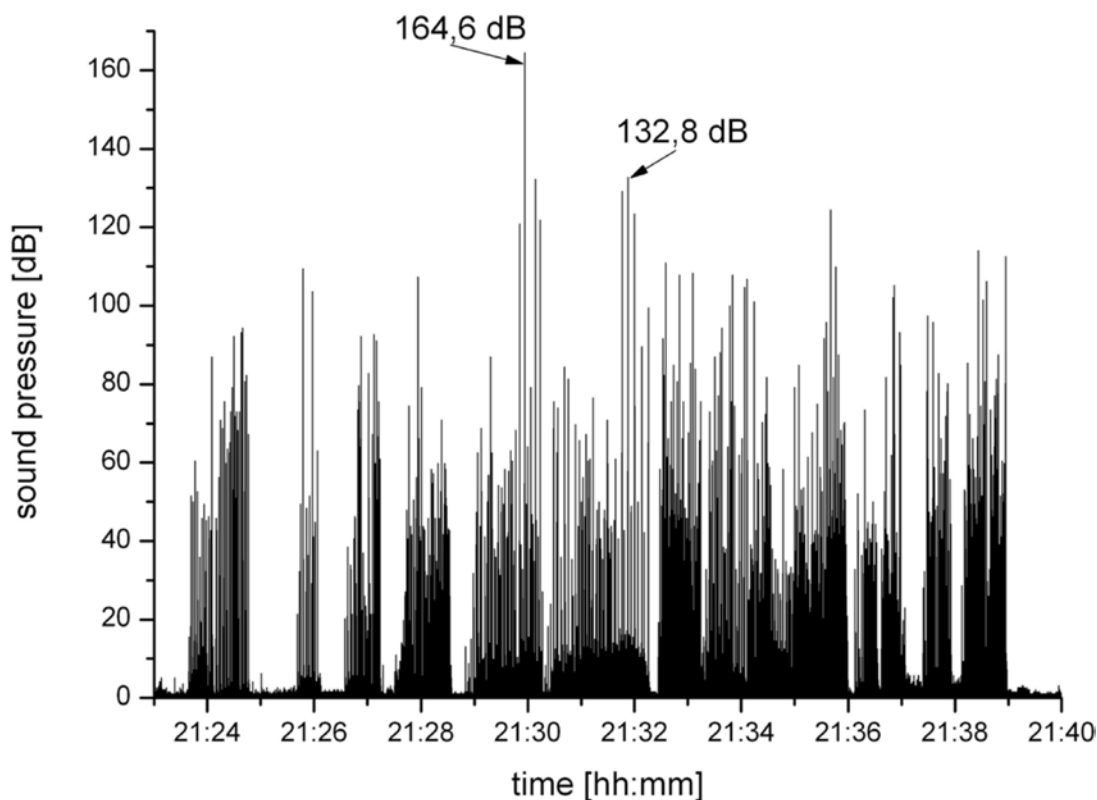


Figure 9. Unweighted sound pressure versus time for firework no. 5.

All fireworks provided very low hazards towards sound pressure impacts at the safety distance to the audience. The maximum sound pressure values of all fireworks did not differ much. The highest maximum value of 115.5 dB(AI) was observed during the third firework display. The lowest maximum value of 111.8 dB(AI) was emitted by firework no. 5.

26th international ADAC-Super-Motocross (indoor)

Table 4 gives time-averaged results of the meteorological data and boundary conditions in the Martin-Schleyer Hall in Stuttgart, Germany.

Additionally, all measured gas concentrations are displayed in Table 5. In terms of combustion gases, the results were quite similar on both days, although the ventilation was turned off on November 14th and turned on November 15th.

Even though the functioning of the pyrotechnic articles took place at an indoor site, very low combustion gas concentrations were measured. Nitrogen oxides were just detectable in low quantities, e.g. NO_2 with a maximum concentration of 19 mg m^{-3} . Only dinitrogen monoxide (N_2O) appeared at levels of up to 54.2 mg m^{-3} , likely emitted by the motor cycles. Furthermore, hydrocarbons like methane (CH_4), and propane

Table 4. Meteorological data of November 14th and November 15th, 2008 inside the Martin-Schleyer Hall in Stuttgart, Germany.

Date (measuring time)	November 14th, 2008 (20:00–21:00)	November 15th, 2008 (20:00–21:00)
Temperature/ $^{\circ}\text{C}$	18.5 ± 0.5	18.5 ± 0.5
Air pressure/hPa	1003	1002
Relative humidity (%)	34–36	35–38
Ventilation on ?	No	Yes

Table 5. Measured gas emissions at the motocross show (Martin-Schleyer Hall, Stuttgart, Germany, November 14th and November 15th, 2008).

Gas	November 14th, 2008			November 15th, 2008		
	Max. concentration/ mg m ⁻³	Max. 10 min average concentration/ mg m ⁻³	Max. 30 min average concentration/ mg m ⁻³	Max. concentration/ mg m ⁻³	Max. 10 min average concentration/ mg m ⁻³	Max. 30 min average concentration/ mg m ⁻³
H₂O	4707	4697	4745	5292	5405	5155
CO₂	1421	1350	1330	1578	1474	1392
CO	37.5	25.9	19.6	29.1	18.5	7.6
NH₃	0.3	0.2	0.1	0.3	0.2	0.1
NO₂	9.3	7.8	7.6	18.9	10.5	8.0
NO	0.0	0.0	0.0	0.0	0.0	0.0
N₂O	42.4	32.4	26.8	54.2	26.8	23.5
SO₂	4.1	1.8	1.3	2.5	1.9	1.1
HCl	3.3	3.4	3.4	3.1	3.8	2.6
HCN	0.8	0.5	0.5	0.8	0.5	0.4
CH₄	1.7	1.6	1.5	1.5	1.3	1.1
C₂H₆	10.9	11.5	10.0	14.1	12.9	9.9
C₃H₈	21.1	16.1	15.4	15.5	17.9	13.9
C₂H₂	5.6	4.0	3.0	7.9	3.2	2.3
C₆H₆	0.0	0.0	0.0	0.0	0.0	0.0

(C₃H₈) with peak concentrations of up to 21 mg m⁻³ were released.

As illustrated in Figure 10 and Figure 11, the SO₂ concentrations increased after the fireworks on both days. To evaluate those concentrations, the WHO AIR Quality Guideline value¹⁸ of 0.5 mg m⁻³ (10 minutes average) is taken into account, since currently no German AGW are published for SO₂.

Whereas on November 14th a maximum SO₂ concentration of 4.1 mg m⁻³ was detected, a significantly lower maximum concentration of about 2.5 mg m⁻³ was observed on November 15th. This effect is explained by the activated hall ventilation on the second day, leading to increased dilution mechanism, as well as possible different compositions of fireworks. In the case of no ventilation, the 10 minute average concentrations constantly exceeded the WHO AIR Quality Guideline value¹⁸ of 0.5 mg m⁻³ more

than 30 minutes after the firework display. Due to the effective ventilation on the second day, a substantial exceeding of the guideline threshold was not observed.

Figure 12 presents the results of the CO measurements on November 14th, 2008. During and shortly after the starting indoor firework displays no relevant CO concentrations were observed. The peaks at 20:20 are likely due to the following motocross race.

On both days, only slightly elevated CO₂ concentrations were observed and could not be traced back to the firework displays.

Figure 13 displays the time and diameter dependent particle concentration on November 14th (left image) and November 15th (right image) in the Martin-Schleyer Hall. The zero-point on the time axis refers to the beginning of the firework display at 20:00. The black points represent measured data,

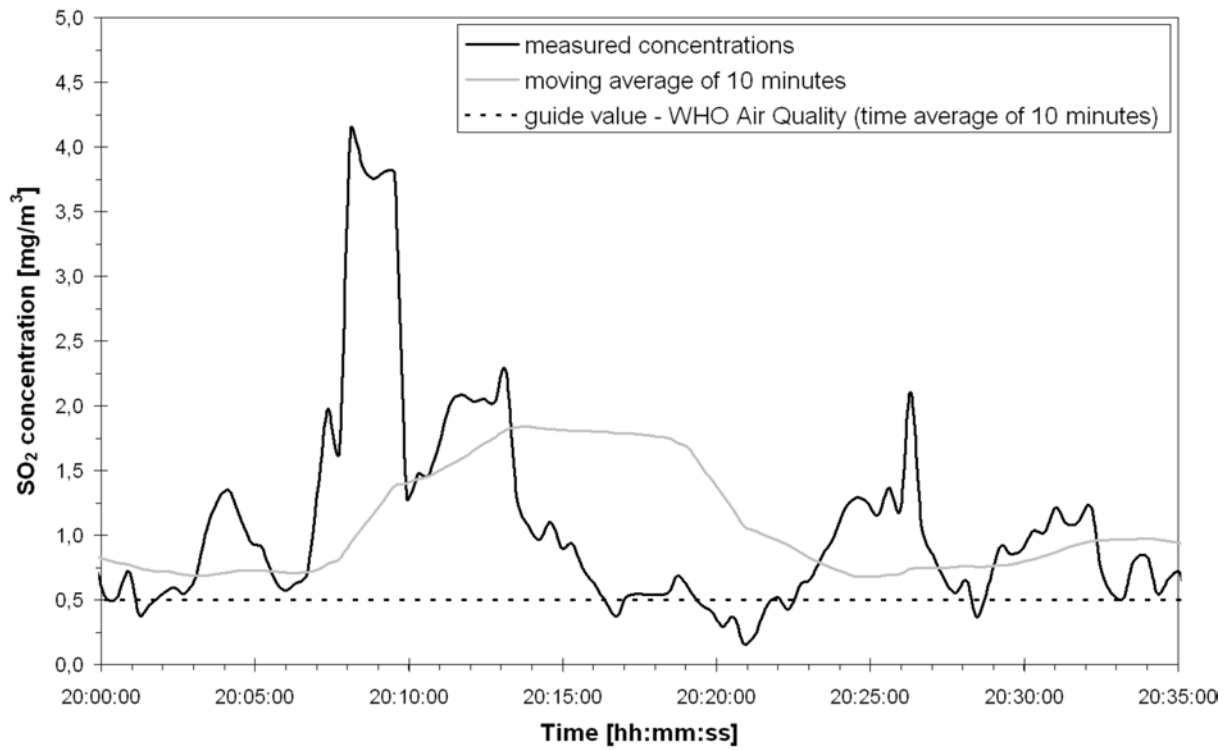


Figure 10. *SO₂ concentration behaviour on November 14th, 2008.*

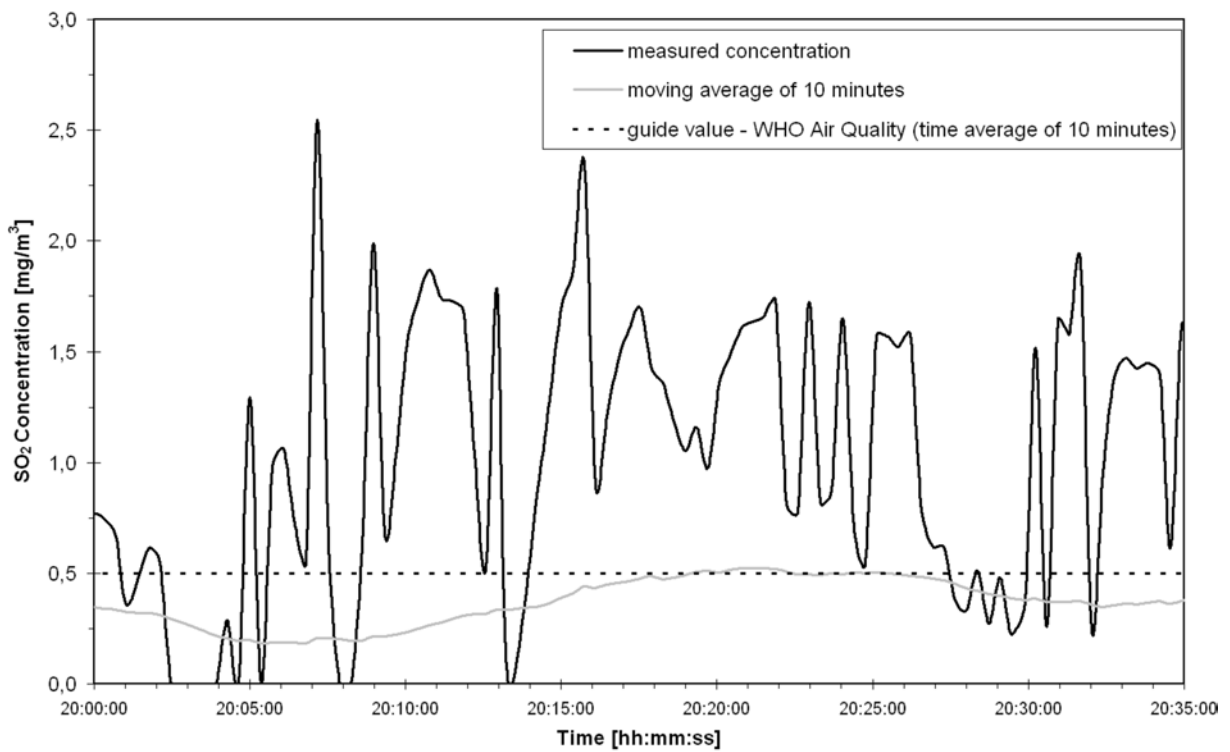


Figure 11. *SO₂ concentration behaviour on November 15th, 2008.*

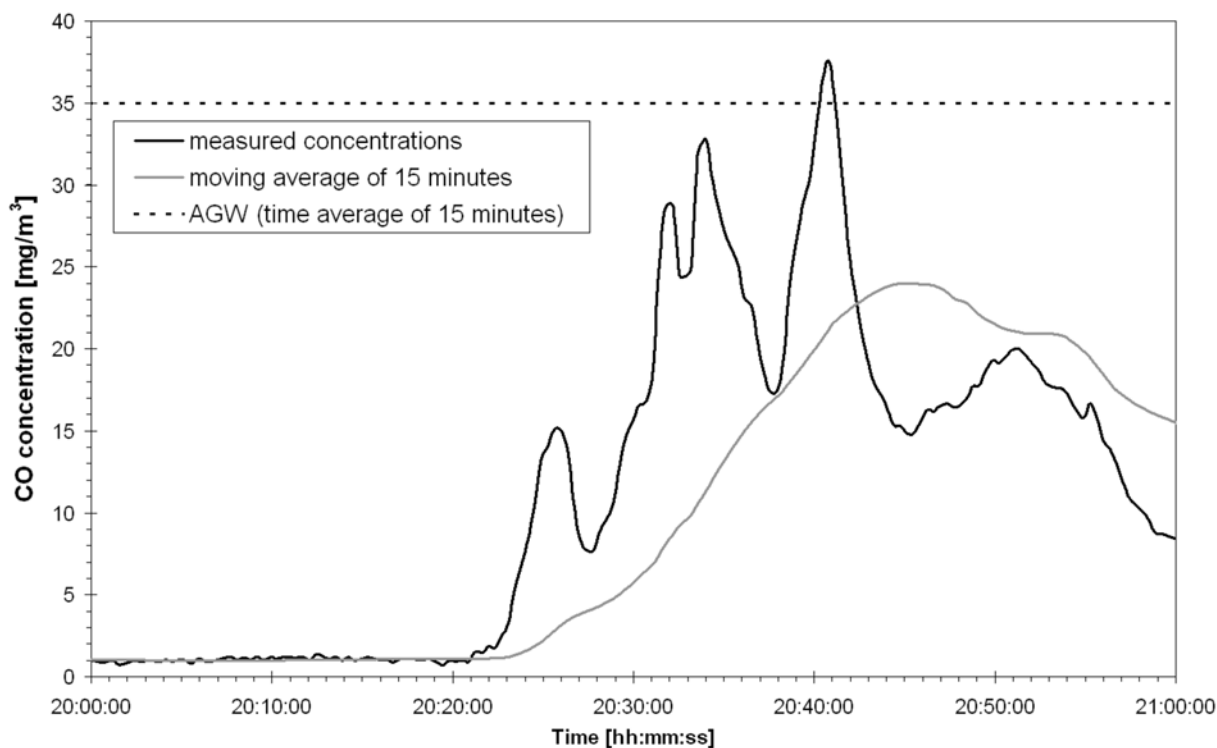


Figure 12. CO concentration behaviour on November 14th, 2008.

whereas the gray areas are interpolated trends.

An integration over all particle size diameters leads to the total particle concentration versus time, as displayed in Figure 14.

Subsequent to the start of the fireworks, particle concentrations increased on both days. Especially on the first day, when the ventilation

system was turned off, the increase in particle concentration occurred rapidly. After reaching the respective concentration maxima shortly after the fireworks, particle concentrations decreased nearly exponentially. Surprisingly, the base level was reached again after an hour, although the motocross races were running. This indicates that nearly all particles in the range from 300–900 nm

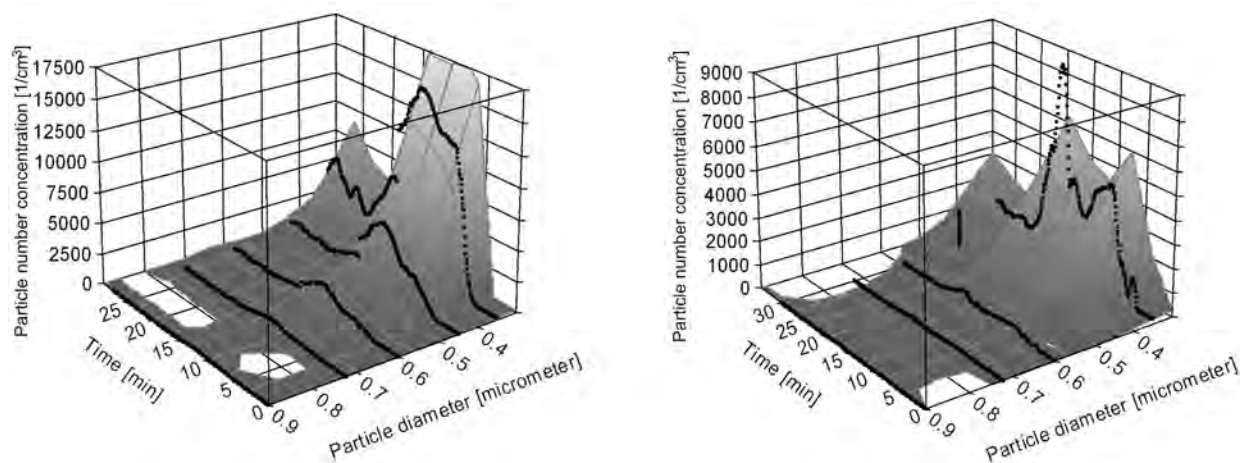


Figure 13. Time-dependent particle size distribution on November 14th, 2008 (left) and November 15th, 2008 (right).

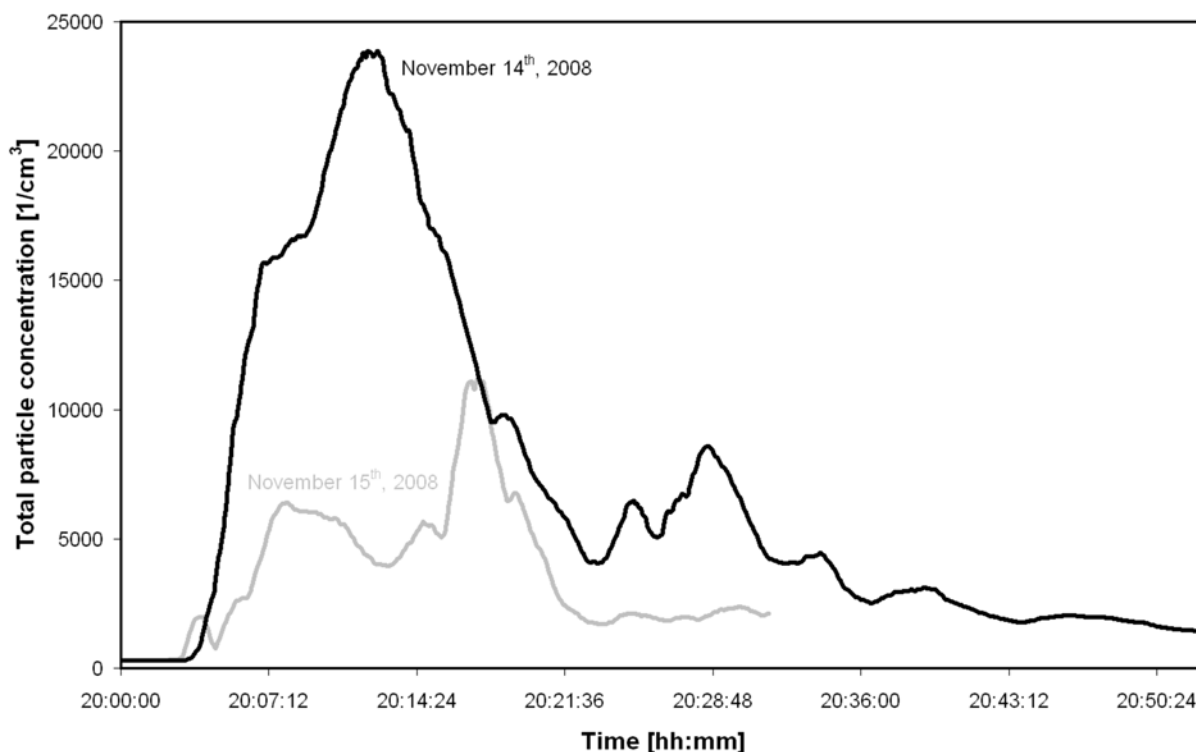


Figure 14. Time-dependent total particle number concentration on November 14th and 15th, 2008.

were emitted by the fireworks and a significant rise of the total particle concentration due to the combustion engines of the motocross bikes was not observed.

The main results of the particle measurements are summarized in Table 6.

Even though the maximum total particle number concentration on November 14th exceeded the one

Table 6. Results of the particle measurements at the opening fireworks of the motocross show on November 14th and 15th and corresponding (legal) limit and reference values for dusts in Germany.

	Nov. 14th, 2008	Nov. 15th, 2008
Maximum measured particle concentration	>23 000 particle cm ⁻³ ≈ 0.41 mg m ⁻³	>11 000 particle cm ⁻³ ≈ 1.18 mg m ⁻³
Maximum time-averaged particle concentration (15 min)	0.31 mg m ⁻³	0.56 mg m ⁻³
Maximum time-averaged particle concentration (30 min)	0.19 mg m ⁻³	0.38 mg m ⁻³
AGW _a for alveolar dust (8 h/day, 40 h/week)	3 mg m ⁻³	
AGW _r for respirable dust (8 h/day, 40 h/week)	10 mg m ⁻³	
AGW _{STV} (short time value, over 15 min)	AGW _{STV} = 2 × AGW _a = 6 mg m ⁻³	
MI (30 min, respirable dust)	0.45 mg m ⁻³	
MI (30 min, particulate matter)	0.3 mg m ⁻³	

on November 15th by a factor of 2, the respective maximum mass-concentration on the first day was lower than on the second day. The reason for this is the difference in particle size distributions. On the second day larger particles were detectable over a slightly longer time period. On both days, maximum particle concentrations did not exceed values of 1.18 mg m^{-3} .

It has to be noted that the appearance of particles with diameters of less than 300 nm was very likely, but due to the limitation of the measurement device in this case, only particles with diameters between 300 nm and $20 \mu\text{m}$ could be observed.

Nevertheless, a substantial hazard to the audience due to aerosol impacts released by the indoor firework displays was not observed during this event.

Summary and conclusions

In this work results of measurements towards the emission of gaseous and solid reaction products, as well as of sound pressure during a large outdoor and indoor firework display are presented.

Depending on the local meteorological conditions, different results were obtained during the two days of the outdoor fireworks. Due to adverse wind conditions, neither gaseous nor solid reaction products (particles) were measured on the first day. The wind direction changed significantly on the second day during one firework show, transporting the plume of reaction products directly towards the measurement technique. Under these conditions massive peak particle concentrations of $>550\,000 \text{ particles cm}^{-3}$ occurred, equivalent to a peak mass concentration of approximately 3.95 mg m^{-3} . The maximum time-averaged particle concentrations (over 15 min and 30 min) during the firework display were more than 3 times lower than the corresponding occupational short time limit values (according to German regulations). However, the measured values were still 3 times higher than the maximum emission values suggested by the VDI guideline 2309, which represent a very conservative estimation.

Even though large increases in particle concentrations were observed during the fireworks, no significant rises in combustion gas concentrations were detected. This is likely due to the long distance from the measurement location

to the ignition point ($>110 \text{ m}$), leading to dilution effects. In addition, hot reaction gases immediately ascended due to buoyancy forces and were partly dissolved by rain drops.

Furthermore, none of the fireworks during the display ever crossed the sound pressure level of 115.5 dB(AI) at the safety distance to the audience.

Measurements during an indoor firework display led to different results. Sulphur dioxide concentrations rose up to a maximum value of 4.1 mg m^{-3} after the fireworks when the ventilation was turned off, and to a maximum value of 2.5 mg m^{-3} with an activated ventilation system inside the hall.

Peaks in carbon monoxide concentrations were likely due to the following motocross race and could not be traced back to the indoor firework displays. Other combustion gas concentrations (e.g. nitrogen dioxide, dinitrogen oxide) appeared at negligible levels.

Caused by different ventilation settings and particle distributions on both evenings, aerosol concentrations exceeded $23\,000 \text{ particles cm}^{-3}$ (equivalent to 0.41 mg m^{-3}) when the ventilation in the hall was turned off, and exceeded particle concentrations of $11\,000 \text{ particles cm}^{-3}$ (equivalent to 1.18 mg m^{-3}) with an activated ventilation system. The highest detected 15 minutes average dust mass concentration of 0.56 mg m^{-3} was nearly 12 times smaller than the corresponding occupational short time limit values (according to German regulations). Due to the used instrumentation at the indoor venue, only particles with diameters between 300 nm and $20 \mu\text{m}$ could be observed. However, it seems likely that smaller particles were emitted, as well.

Sound pressure measurements were not carried out for the indoor firework show.

In conclusion, possible hazards to the public and the environment arising from large firework displays due to harmful or toxic reaction gases seem unlikely, even when the smoke plume reaches the audience. Moreover, the sound pressure impact can be easily controlled by an adequate safety distance, as well. In contrast to this, particulate matter can be transported over long distances and inhalation may lead to adverse health effects due to the potential toxicity of the inhalable particles.

At indoor events, an effective ventilation system can significantly reduce this hazard. This must be taken into account when developing future firework products or designing firework displays.

References

- 1 G. Steinhauser and T. M. Klapötke, “Green Pyrotechnics: A Chemists’ Challenge”, *Angewandte Chemie, International Edition*, Vol. 47, Issue 18, 2008, pp. 3330–3347.
- 2 G. Steinhauser, J. H. Sterba, M. Foster, F. Grass and M. Bichler, “Heavy metals from pyrotechnics in New Year’s Eve snow”, *Atmospheric Environment*, Vol. 42, Issue 37, December 2008, pp. 8616–8622.
- 3 T. Moreno, X. Querol, A. Alastuey, M. C. Minguillón, J. Pey, S. Rodriguez, J. Vicente Miró, C. Felis and W. Gibbons, “Recreational atmospheric pollution episodes: Inhalable metalliferous particles from firework displays”, *Atmospheric Environment*, Vol. 41, Issue 5, February 2007, pp. 913–922.
- 4 D. van der Kamp, I. McKendry, M. Wong and R. Stull, “Lidar ceilometer observations and modeling of a fireworks plume in Vancouver, British Columbia”, *Atmospheric Environment*, Vol. 42, Issue 30, September 2008, pp. 7174–7178.
- 5 Y. Wang, G. Zhuang, C. Xu and Z. An, “The air pollution caused by the burning of fireworks during the lantern festival in Beijing”, *Atmospheric Environment*, Vol. 41, Issue 2, January 2007, pp. 417–431.
- 6 R. Vecchi, V. Bernardoni, D. Cricchio, A. D’Alessandro, P. Fermo, F. Lucarelli, S. Nava, A. Piazzalunga and G. Valli, “The impact of fireworks on airborne particles”, *Atmospheric Environment*, Vol. 42, Issue 6, February 2008, pp. 1121–1132.
- 7 F. Drewnick, S. S. Hings, J. Curtius, G. Eerdekens and J. Williams, “Measurement of fine particulate and gas-phase species during the New Year’s fireworks 2005 in Mainz, Germany”, *Atmospheric Environment*, Vol. 40, Issue 23, July 2006, pp. 4316–4327.
- 8 B. Wehner, A. Wiedensohler and J. Heintzenberg, “Submicrometer aerosol size distributions and mass concentration of the millennium fireworks 2000 in Leipzig, Germany”, *Journal of Aerosol Science*, Vol. 31, Issue 12, December 2000, pp. 1489–1493.
- 9 K. D. Perry, “Effects of Outdoor Pyrotechnic Displays on the Regional Air Quality of Western Washington State”, *Journal of the Air and Waste Management Association*, Vol. 49, 1999, pp. 146–155.
- 10 R. M. Smith and V.-D. Dinh, “Changes in forced expiratory flow due to air pollution from fireworks : Preliminary report”, *Environmental Research*, Vol. 9, Issue 3, June 1975, pp. 321–331.
- 11 G. Hussain and G. J. Rees, “FT-i.r. spectra of gaseous products from the combustion of pyrotechnic mixtures containing carbon”, *Fuel*, Vol. 70, Issue 5, May 1991, pp. 667–669.
- 12 A. Dutschke, C. Lohrer, S. Seeger and L. Kurth, “Gasförmige und feste Reaktionsprodukte beim Abbrand von Indoor-Feuerwerk”, *Chemie Ingenieur Technik*, Vol. 81, Issue 1–2, 2009, pp. 167–176 (in German).
- 13 W. G. Kreyling, M. Semmler-Behnke and W. Möller, “Health implications of nanoparticles”, *Journal of Nanoparticle Research*, Vol. 8, Issue 5, 2006, pp. 543–562.
- 14 BGBl, “Gesetz über die Durchführung von Maßnahmen des Arbeitsschutzes zur Verbesserung der Sicherheit und des Gesundheitsschutzes der Beschäftigten bei der Arbeit (Arbeitsschutzgesetz - ArbSchG)”, *Bundesgesetzblatt I*, 2009 (in German).
- 15 BGBl, “Verordnung zum Schutz vor Gefahrstoffen (Gefahrstoffverordnung - GefStoffV)”, *Bundesgesetzblatt I*, 2005 (in German).
- 16 BAuA, TRGS 900 “Arbeitsplatzgrenzwerte”, *Technische Regeln für Gefahrstoffe (TRGS)*, 2009 (in German).
- 17 *Kommission Reinhaltung der Luft im VDI und DIN – Normenausschuss KRdL*, VDI Guideline 2309 Determination of Maximum Emission Values – Fundamentals, 1983.
- 18 WHO AIR Quality Guidelines, *World Health Organization*, Geneva, Switzerland, 2006.

The Journal of Pyrotechnics Archive

The archive contains downloadable copies of all previous JPyro articles together with copies of other articles published by the Journal of Pyrotechnics. Some of the articles are free to download, but the majority are only available by payment of a per-article fee which will enable perpetual download, or by subscription which will allow access to the entire archive.

The archive will in the future be the primary route to publication.

<http://archives.jpYRO.com>

For more information about obtaining articles from the site, or for multi-article or multi year subscriptions - please visit the archive website, or contact the publishers.

Journal of Pyrotechnics Archive

Dedicated to the advancement of pyrotechnics through the sharing of information

[RSS FEED](#) [COMMENTS](#)

[Home](#) [Information](#) [Sponsorship](#) [Subscriptions](#)

Journal of Pyrotechnics – Issue 28

Posted on January 7, 2010 · [Leave a Comment](#) ([Edit](#))

J28 is now complete and the hard copy of J28 is now in production and will be available shortly. We will update this page when it is published

Welcome to the Journal of Pyrotechnics Archive

Posted on January 1, 2007 · [Leave a Comment](#) ([Edit](#))

Welcome to the online archives of the Journal of Pyrotechnics and the Pyrotechnic Literature Series.

All JPyro articles and the Pyrotechnic Literature Series articles have now been uploaded to this site – indeed, for the Journal of Pyrotechnics articles this site will now be the primary means of publication – with a hard copy omnibus edition available early in the year following electronic publication. This allows us to publish articles quickly and have them available to the pyrotechnic community earlier than by hard copy alone.

When you purchase an article or subscribe to the archive it is essential that you return to the archive from the PayPal page. Please ensure that you complete your transaction with PayPal and return to the archive for your subscription to be activated. When you then go to the paper you have purchased you will see that the “PayPal” button has been replaced with a “Download” button. If you have problems accessing the paper please [email us](#) with details of the purchase (date/time/article number) and we will resolve it as soon as possible.

Notes:

- There are a number of **FREE** downloads on the site – check the categories menu on the right hand side. In general book reviews, comments on previous articles, errata

ARCHIVES

- January 2010
- December 2009
- November 2009
- October 2009
- July 2009
- June 2009
- May 2009
- March 2009
- February 2009
- January 2009
- October 2008
- September 2008
- August 2008
- July 2008
- May 2008
- April 2008
- March 2008
- January 2008
- August 2007
- June 2007
- May 2007
- April 2007
- March 2007
- February 2007
- January 2007

LINKS

- Davas Ltd
- Main JPyro website
- Pyrotechnic Chemistry

HOME


- Archive Homepage
- latest additions to the Archive
- List of all Titles
- List of Current Sponsors
- List of JPyro Board Members

REGISTER/LOGIN

- Log out
- Site Admin
- Contact Us

FORTHCOMING EVENTS

- 19 April:**
 - Pyrotechnic Chemistry Course (all day)



84032 visits since Jan 2007

Hazard Assessment and Effect of Nano-Sized Oxidizer on Sound Level Analysis of Firecrackers

T. L.Thanulingam,^a A. Jeya Rajendran,^b P. Karlmarx,^c K. Subramanian^c and
A. Azhagurajan^c

^a Fireworks Research and Development Centre, Petroleum and Explosives Safety Organisation, Anayoor village, Sivakasi - 626124, India. Email: tlthanulingam@yahoo.co.in

^b Department of Chemistry, Loyola College, Nungambakkam, Chennai-600034, India
Email: jeyarajendran@yahoo.com

^c Department of Mechanical Engineering, MEPCO Schlenk Engineering College, Sivakasi-626005, India

Abstract: Nano-sized sulphur and oxidizers were synthesized by the ball mill method and the size was determined using a particle size analyzer. Pyrotechnic mixtures of compositions using five different oxidizers: potassium nitrate (KNO_3), potassium perchlorate ($KClO_4$), barium nitrate ($Ba(NO_3)_2$), strontium nitrate ($Sr(NO_3)_2$) and bismuth oxide (Bi_2O_3), in different particle sizes, mixed with sulphur (S), aluminium (Al) and boric acid (H_3BO_3), were used to produce sound producing cake-bomb firecrackers for analysis. A bulk density of $0.24\text{--}0.68\text{ g cm}^{-3}$ was maintained for homogeneity of the mixture. The sound level from newly formulated sound producing firecrackers (cake-bombs) showed a linear relationship with the weight of the mixture taken. Decreasing the particle size from micro to nano improves the efficiency of firecrackers using the oxidizers, KNO_3 , $KClO_4$ but not for $Ba(NO_3)_2$, $Sr(NO_3)_2$, or Bi_2O_3 . The analysis of safety characteristic data of thermal and mechanical sensitiveness indicates that the pyrotechnic mixture using the oxidizer $KClO_4$ is highly sensitive to friction and impact. The limiting impact energy (LIE) of pyrotechnic compositions falls in the range of $2.55\text{--}4.51\text{ J}$. LIE of nano materials was less compared to micro materials indicating that as the particle size decreases, the mixture is prone to hazards from impact. Thermal analysis indicates a high temperature for self propagating decomposition making the mixture thermally stable at room temperature.

Keywords: Sound level, pyrotechnic mixture, impact sensitiveness, friction sensitiveness, flash composition, firecrackers.

Introduction

'Fireworks' are a type of pyrotechnic device used for entertainment. The chemicals employed and their compositions vary depending on the type of fireworks being produced. Fireworks are made of an oxidizer, a fuel, and optionally, a colour enhancing chemical and a binder. The choice of fuels and oxidizers can significantly affect activation energy, heat of reaction and the efficiency of energy feedback.¹ The selection of fuel and oxidizer has the potential for having a major influence on the efficiency of the pyrotechnic

mixture. Activation energy, the amount of energy required for an oxidizer to make its oxygen available to react with the fuel, depends on the nature of the oxidizer. Some oxidizers require input of a large amount of energy, while others actually produce energy in the process of releasing their oxygen. There is always an optimum fuel to oxidizer ratio, which produces the fastest burning rate. This corresponds to the situation where the reaction will be essentially complete with little fuel or oxidizer remaining after the reaction.² When the fuel to oxidiser ratio deviates from the optimum value, burn rate is reduced. The burn rate

Article Details

Manuscript Received:-05/10/2009

Publication Date:-22/12/2009

Article No: - 0081_Thanulingam

Final Revisions:-20/12/2009

Archive Reference:-1030

continues to fall as the deviation from optimum increases. During the process of manufacturing fireworks, chemicals are initially mixed to produce a reasonably homogeneous mixture. During these operations impact, friction, spark and heat stimuli may occur and, under certain conditions, one or more stimuli may be enough to cause ignition of the compositions. The sensitiveness of a pyrotechnic mixture depends on, amongst other things, the type, compositions, purity and moisture content of the chemicals used.³ The results from burning a particular pyrotechnic composition depend on various factors. Chemicals used as additives even in small quantities to improve their mechanical properties can alter the combustion process and ignition temperature to lower temperature. The effectiveness of firecrackers depends not only on the compositions of mixtures, but also on factors such as particle size and shape, choice of fuel and oxidizers, fuel to oxidizer ratio, degree of mixing, moisture content, physical form, packing density, presence of additives, local pressure, degree of confinement, degree of consolidation, crystal effects and purity of the chemicals.² The present study assesses the impact and friction sensitiveness of the optimized pyrotechnic mixture for safety considerations and studies the sound level produced from the fireworks by changing the oxidizers and their particle size.

Experimental

Chemicals and materials

The chemicals used for the preparation of the firecrackers were obtained from a firework manufacturing company. The purity and assay of the chemicals were potassium nitrate (KNO_3), potassium chlorate (KClO_4), strontium nitrate ($\text{Sr}(\text{NO}_3)_2$), barium nitrate ($\text{Ba}(\text{NO}_3)_2$) and bismuth trioxide (Bi_2O_3) – 97.6%, sulphur (S) – 99.9%, aluminium (Al) – 99.8% and boric acid (H_3BO_3) – 99% of micron-size and of nano-size. The chemicals used in making fireworks are aluminium powders of grade 999 (200 mesh – 75 microns), KNO_3 , KClO_4 , $\text{Sr}(\text{NO}_3)_2$, $\text{Ba}(\text{NO}_3)_2$, and Bi_2O_3 of 120 mesh (125 microns), S of 100 mesh (150 microns) and H_3BO_3 of 100 mesh (150 microns) sizes. All these chemicals were sieved using a 100-mesh brass sieve. The samples were stored away from light and moisture till they were packed within the paper case of the firecracker unit



Figure 1. Paper case and firecracker taken for analysis. Top: Inner paper case (large); bottom: Firecracker (cake-bomb).

(Figure 1). Kraft paper (brown) with 240 GSM (gram per square meter) thickness which was measured by a GSM meter was used for making the inner shells of the firecrackers. Jute string with gum, of length 130–260 cm, and thin foil papers (cello paper) were used for making firecrackers. Small size paper cases of $15 \times 15 \times 15$ mm (3.375 cm^3) (Figure 1) were used to prepare cake-bomb firecrackers, similar to commercially available firecrackers.

Preparation of nano-size pyrotechnic mixture

The Fritsch, GmbH, ‘Pulverisette 6’ planetary monomill was used for preparing different particle sizes of oxidizers and fuels. 20 g of the material (oxidizer/fuels separately) was placed into a bowl with 100 ml of ethanol, and then 50 tungsten balls were placed in the bowl. The lid was closed and locked. Milling was carried out for 15 min at a speed of 300 rpm. After cooling the bowl for 5 min, milling was again done for 15 min. If the ethanol level became low, some more ethanol was added in order to make the powder in the colloidal state. After grinding for 2 hours the colloidal state powder was transferred to an air-tight container and it was kept safe. To separate the powders

from ethanol the container was kept in the open atmosphere. The powder was collected after evaporating the ethanol.

Measurement of particle size

The particle size was measured using a 'Zetasizer Nano ZS particle size analyzer'. Hydrodynamic or aerodynamic particle size equals the diameter of the sphere that has the same drag coefficient as a given particle. There are several methods for measuring particle size. Some of them are based on light, ultrasound, or electric field, or gravity, or centrifugation. The complexity in defining particle size appears for particles with sizes below a micrometer. When the particle becomes small, the thickness of the interface layer becomes comparable with the particle size. As a result, the position of the particle surface becomes uncertain and practically polydisperse, which means that the particles in an ensemble have different sizes. The statistical distribution of particle size reflects the

polydispersity (Figures 2–5). There is often a need for a certain average particle size for the ensemble of particles. The particle size is measured by taking 0.01 g of the powder in a glass plate and drying it. It is mixed with 50 ml of ethanol and it is sonicated for 2 min. The sonicator works in the frequency range 20 to 50 kHz and the amplitude is set at 31%. After sonication, the solution is poured into the cuvette of the particle size analyzer which is made of polymer to measure the particle size. The bulk packing density was maintained constant for a particular type of oxidizer in order to maintain the homogeneity of the mixture. As the particle size of micro-sized materials was kept the same, the bulk packing density was found to vary from oxidizer to oxidizer.

Firecrackers

Cake-bomb firecrackers were manufactured manually by experienced technicians of the firework manufacturing company for analysis. A flow chart

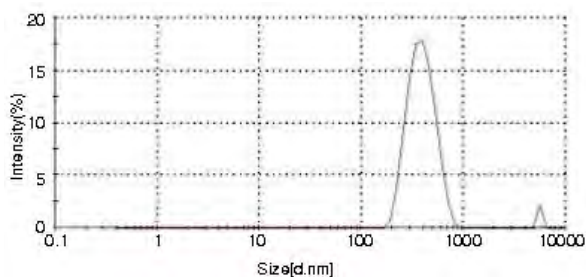


Figure 2. Particle size distribution for KNO_3 .

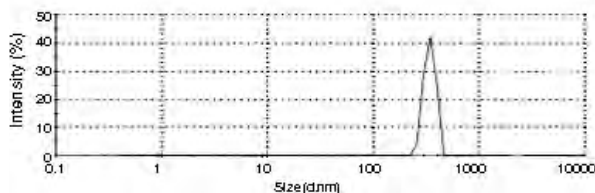


Figure 4. Particle size distribution for sulphur.

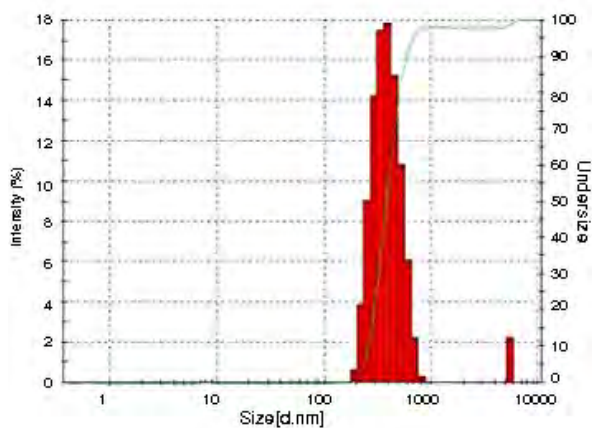


Figure 3. Intensity peak statistics for KNO_3 .

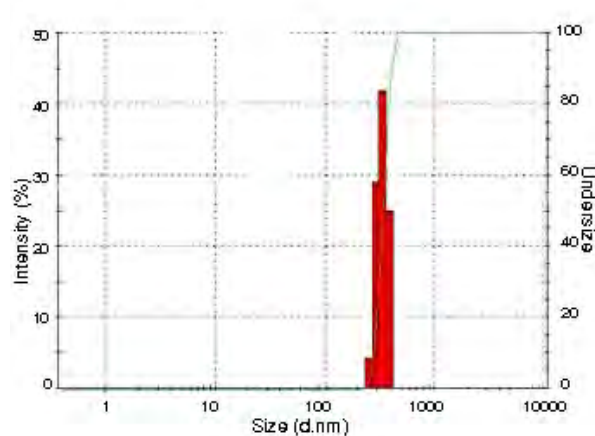
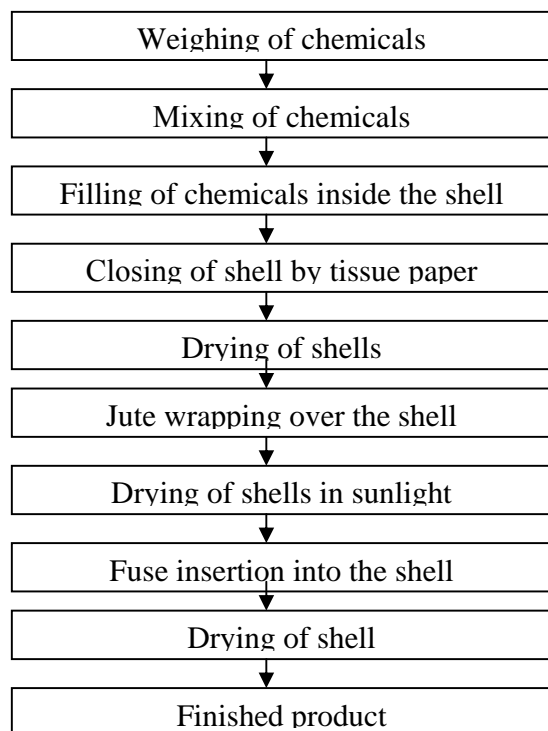


Figure 5. Intensity peak statistics for sulphur.

Table 1. Flow chart for preparing cake-bomb.



for preparing cake-bombs is given in Table 1. The chemical mixtures of $\text{KNO}_3/\text{Al}/\text{S}/\text{H}_3\text{BO}_3$, $\text{KClO}_4/\text{Al}/\text{S}/\text{H}_3\text{BO}_3$, $\text{Sr}(\text{NO}_3)_2/\text{Al}/\text{S}/\text{H}_3\text{BO}_3$, $\text{Ba}(\text{NO}_3)_2/\text{Al}/\text{S}/\text{H}_3\text{BO}_3$, $\text{Bi}_2\text{O}_3/\text{Al}/\text{S}/\text{H}_3\text{BO}_3$ in the molar ratio of 1.28/1.40/1.85/0.02 were sieved separately and mixed thoroughly in non-conducting surfaces like newspaper, rubber mat etc., by sieving through mesh No. 40 (425 microns), four to five times to get a homogeneous mixture of micro-size materials. This chemical mixture was filled inside the paper case of the firecracker unit. Thin foil papers (cello paper) were used to cover the paper case and it was

Table 2. Specification of ball mill.

Sample quantity	Up to 30 g
Voltage	240 volts AC
Weight	63 kg
Output size	0.001 to 1 micron
Operating principle	Impact
Speed	100-650 rpm
Grinding tools	Grinding bowls and grinding balls
Timer	Available selection – make
Grinding jar	Tungsten carbide – 250 ml
Grinding media	Tungsten carbide balls

sealed with gum and dried in atmospheric air. Jute string with gum of length 130–260 cm was wound round the paper case tightly and 3 windings were done, after which it was dried in sunlight for 2 to 3 hours (Figure 1). The fuse wire (100 mm, quick match) was inserted using a brass needle and kept in its place by charcoal powder. Coloured fancy papers were used to cover it for appearance and it was dried for about 24 hours in the sunlight to make the firecrackers ready for testing.

Instruments

Planetary ball mill

The planetary monomill was used for mixing and homogenisation of materials. The grinding mechanism of the planetary monomill is given in Figure 6 and the specifications of the ball mill are given in Table 2. The material was crushed and disintegrated in a grinding bowl by grinding balls. The grinding balls and the material in the grinding bowl were acted upon by the centrifugal forces due to the rotation of the grinding bowl about its own

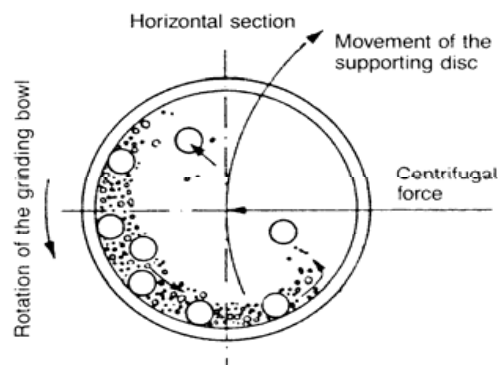


Figure 6. Grinding mechanism.

axis and due to the rotation of the supporting disc. The grinding bowl and the supporting disc rotate in opposite directions, so that the centrifugal forces alternately act in the same and opposite directions. This results in, as a frictional effect, the grinding balls running along the inner wall of the grinding bowl, and as an impact effect, the balls impacting against the opposite wall of the grinding bowl. The bowl is made of tungsten carbide. The bowl consists of 50 balls and these balls are also made of tungsten carbide. The weight of each ball is 8 g and the bowl weight is 5 kg.

Sound level meter

The sound level test was carried out as per the rules of notification of PESO (Petroleum and Explosives Safety Organisation), formerly known as 'Dept. of Explosives', Govt. of India.⁴ The noise level was measured by four sound level monitors using Model No.824L obtained from Larson & Davis, USA and the average values of the four readings were taken as sound level data.⁵ Sound is usually measured in decibels (dB), a logarithmic unit used to describe a ratio of sound pressure [$\log (P_2/P_1)$ dB], or voltage or intensity. When it is used to give the sound level for a single sound rather than a ratio, a reference level is required. The most widely used sound level filter is the A scale, which roughly corresponds to the inverse of the 40 dB (at 1 kHz) equal-loudness curve. Using this filter, the sound level meter is thus less sensitive to very high and very low frequencies. Measurements made on this scale are expressed as dB(A). The C scale is practically linear over several octaves and is thus suitable for subjective measurements only for very high sound levels. Measurements made on this scale are expressed as dB(C). The sound level meters are capable of measuring the noise level in A, C, by flat weightings with slow, fast, impulse detectors. The measurements were taken at 1.2 m elevation from the level of bursting at 4 m distance. The meters were placed in four places such that the angle between them was 90° and the average of these four values was taken as the sound level. A 5 m diameter hard concrete surface

was used for carrying out the sound level test.⁵ A microphone converted sound into electrical power and a decibel meter read out the sound power in watts or dB.

Impact sensitivity measurement

Impact sensitiveness of the pyrotechnic mixture was tested using the BAM method^{6,7} by an impact sensitiveness tester. The design and principles of the equipment are similar to those of the drop fall hammer equipment of the BAM standards. The procedure followed in this study was based on the previously reported method.⁸ The LIE of the sample was calculated using the formula:

$$\text{LIE} = mgh$$

where m = mean of the drop weight (kg), g = acceleration due to gravity (9.81 m s^{-2}), h = height (m).

The validity of the results was tested by calibrating the machine with the LIE of standard substances and the results are given in Table 3. The impact energy measured was within acceptable limits of error (1–2%). Five runs were undertaken to check the reproducibility.

Friction sensitivity measurement

The friction sensitiveness was determined using a Friction Tester by the common test methods of BAM⁴ and it corresponds to the UN Recommendations on the Transport of Dangerous Goods.⁹ The friction test determines whether a pyrotechnic mixture possesses a danger of explosion or reaction when subjected to the effect of friction. When starting a test with materials, a weight was chosen approximately in the middle of the loading range. If two reactions were detected, then the load would be decreased. If no reactions occurred, then the load would be increased. Friction sensitiveness is a relative measurement reported in newtons (N), when ignition or explosion occurs only once in six repetitions.

Thermal analyser

Table 3. *Impact sensitiveness of standards to calibrate the impact sensitiveness apparatus.*

Substance	Reported impact energy (J)	Calculated impact energy (J)	Error (%)
Tetryl (dry)	4	4.05	2
Lead azide (dry)	2.5	2.6	2.5

Thermal analysis (TA), thermogravimetric (TG) and differential thermal analysis (DTA) were carried out using a Perkin-Elmer, Pyris diamond model thermal analyser with a rate of heating of 30 °C min⁻¹ and a temperature range of a standard system of room temperature to 900 °C.

Differential scanning calorimetry

High temperature DSC analysis under ignition conditions was carried out using a Mettler Toledo, model DSC 821, with temperature range of -65 °C to 450 °C and heating rate of 10 °C min⁻¹.

Results and discussion

Sound level analysis

Factors affecting sound level

The sound level produced from firecrackers with different grades of Al, based on the particle size, was studied.⁵ In this work, optimum conditions for making the firecracker cake-bomb were reported to produce a sound level of <125 dB(A)/145 dB(C) peak at 4 m distance, within the allowed level

as prescribed by Govt. of India notification⁴ by using aluminium of 999 (75 micron size) grade, an optimum quantity of pyrotechnic mixture of 1 g in an inner box of specified dimensions made up with kraft paper of GSM 240, bursting strength 2.2 kg cm⁻². The amount of the mixture that produced the sound level depends on the nature of the oxidizers (Table 4). Apart from all these factors, the sound level produced from the fireworks is greatly affected by the composition of the fireworks. In this paper, the sound level produced from the fireworks by varying five different oxidizers of micro and nano-sizes was studied.

Sound producing firecrackers (cake-bomb) were prepared from pyrotechnic mixtures of nano-size and micro-size using different oxidizers similar to commercial firecrackers. Sound level analysis was carried out and the data are given in Table 4. The effect of particle size in producing sound level varies from one oxidizer to another. If KNO₃ is used as oxidizer, decreasing the particle

Table 4. Effect of oxidizer on sound level of firecrackers of nano-sized materials.

Type of oxidizer	Wt. of chemicals/g	Size/ nm	Sound level		Size/ μm	Sound level	
			dB(A) peak	dB(C) peak		dB(A) peak	dB(C) peak
Potassium nitrate	0.25	397	121.1	144.6	250	106.6	131.5
	0.5		123.4	145.9		114.9	139.0
	0.75		130.3	152.9		122.0	144.4
	1.0		131.3	154.0		124.0	146.8
Strontium nitrate	0.25	147	Red flash		250	108.7	130.9
	0.5		Red flash			120.7	143.5
	0.75		Red flash			124.1	146.4
	1.0		Red flash			125.3	148.1
Potassium perchlorate	0.25	320	130.0	152.5	250	127.1	149.9
	0.5		131.8	154.5		130.3	152.7
	0.75		132.8	155.1		132.8	155.4
	1.0		134.2	156.2		134.4	156.5
Barium nitrate	0.25	122	Green flash	124.5	250	Green flash	Green flash
	0.5		101.5			Green flash	Green flash
	0.75		Green flash			Green flash	Green flash
	1.0		Green flash			Green flash	Green flash
Bismuth trioxide	0.25	461	No flash & sound	No flash & sound	250	No flash & sound	No flash & sound
	0.5						
	0.75						
	1.0						

*Inner box dimension: 15 × 15 × 15 mm³ 3.375 cm³; jute length 130 cm, winding: 3ply, GSM 240 g m⁻², bursting strength 2.2 kg cm⁻². Oxidizer/Al/S/H₃BO₃ (mole 1.28/1.40/1.85/0.02).

size from micro- to nano-sized will increase the effectiveness of the pyrotechnic mixture in producing sound. If the particles are nano-sized, 0.5 g of pyrotechnic mixture is sufficient to produce the optimum sound level whereas the same sound level is produced only by using 1 g of micro-sized pyrotechnic mixture (Table 4). It is expected that as the particle size decreases, the pyrotechnic mixture is effective in producing sound. The particle size effect can be considered to be the result of reducing the activation energy, because smaller particles require less energy to be heated to the ignition temperature.² Only atoms on the surface of particles are available to react, and as the particle size is reduced, the fraction of atoms on the surface increases.

If KClO_4 is used as oxidizer, the micro-sized particles produced sound effectively compared to nano-sized particles up to 0.5 g of pyrotechnic mixture (Table 4 and Figure 7) and on further increasing the amount of the mixture, nano-sized pyrotechnic mixture produced sound effectively. In the case of $\text{Sr}(\text{NO}_3)_2$ as oxidizer, firecrackers using the nano-sized pyrotechnic mixture produce no sound and they produce a red colour flash whereas the micro-sized firecrackers produce sound. In the case of $\text{Ba}(\text{NO}_3)_2$ as oxidizer, firecrackers using both nano- and micro-sized pyrotechnic mixtures produce no sound but produce a green flash.

Firecrackers using Bi_2O_3 in micro- and nano-sized

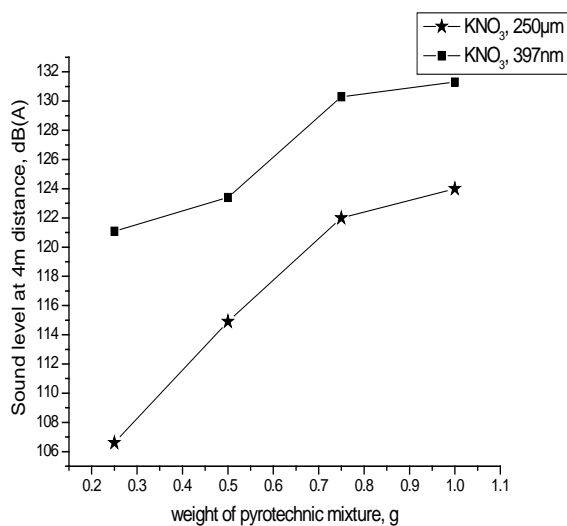


Figure 7. Effect of the amount of pyrotechnic mixture on sound level.

produce neither flash nor sound. Even though oxygen is present, oxides are somewhat inert and the activation energy is not reached to initiate the reaction of oxidizers to release oxygen. Alkali nitrates and chlorate act as effective oxidizers compared to alkaline earth nitrates.

KClO_4 is a strong oxidizer at high temperatures and tends to cake more easily than KNO_3 and needs some anticaking agent. It becomes quite sensitive in contact with other chemicals and ignites very easily by friction.¹ Potassium nitrate alone does not explode even on a strong impact and acts as an oxidizing agent at high temperatures. If it is mixed with charcoal, Al or S, it decomposes and the amount of effective oxygen increases to the maximum value. Barium nitrate can also act as an oxidizer but it cakes to form a hard mass like a stone. The sound level produced from the firecrackers also varies depending on the oxidizer and their particle size which has not been reported earlier (Figures 7–9).

Mechanical sensitivity measurements

Friction sensitivity

The measurements of sensitiveness of the pyrotechnic mixtures $\text{KNO}_3/\text{Al}/\text{S}/\text{H}_3\text{BO}_3$, $\text{KClO}_4/\text{Al}/\text{S}/\text{H}_3\text{BO}_3$, $\text{Sr}(\text{NO}_3)_2/\text{Al}/\text{S}/\text{H}_3\text{BO}_3$, $\text{Ba}(\text{NO}_3)_2/\text{Al}/\text{S}/\text{H}_3\text{BO}_3$, and $\text{Bi}_2\text{O}_3/\text{Al}/\text{S}/\text{H}_3\text{BO}_3$, in the mole ratio 1.28/1.40/1.85/0.02 were carried out (Table 5) to indicate the ease of initiation by an accidental stimulus of the pyrotechnic mixture. The mechanical stress, like friction and impact sensitiveness of the pyrotechnic mixture, was

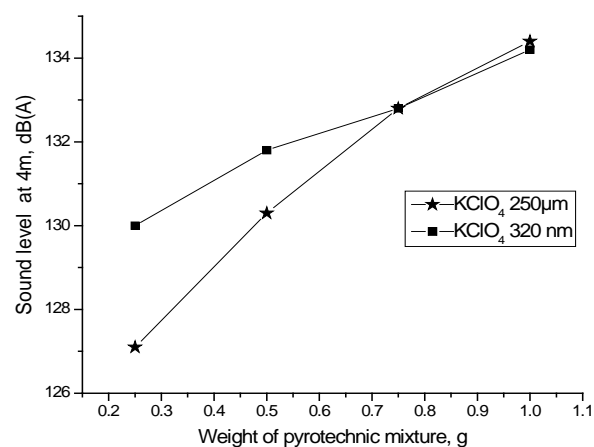


Figure 8. Effect of the amount of pyrotechnic mixture on sound level.

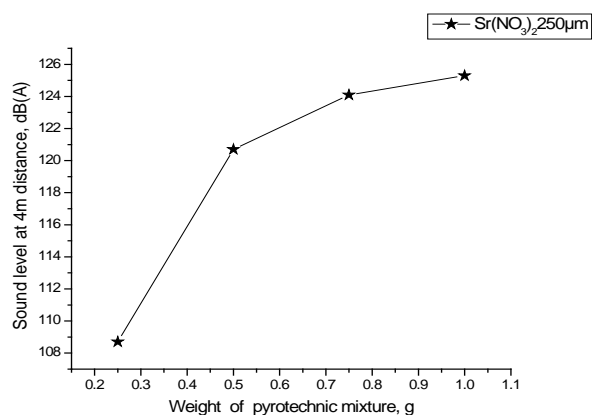


Figure 9. Effect of the amount of pyrotechnic mixture on sound level.

measured.⁸ The friction sensitiveness was found to be >360 N for the pyrotechnic mixtures containing the oxidizers KNO_3 , $\text{Sr}(\text{NO}_3)_2$, $\text{Ba}(\text{NO}_3)_2$ and Bi_2O_3 and 144 N for the mixture containing KClO_4 as oxidizer. High measurements indicate low friction sensitiveness and the pyrotechnic mixture is safer from accidental risk of mechanical stress.⁸ Any material with a limiting load less than 80 N is considered too sensitive for transport of military pyrotechnics. In the case of manufacturing firecrackers, any material that produces a 'Threshold of Initiation' (TIL) greater than 184 N is deemed to be fit for transport.⁹ The friction sensitiveness of the highly sensitive pyrotechnic mixture $\text{KClO}_4/\text{S}/\text{Al}(\text{H}_3\text{BO}_3)$ was found to be 144 N which is <184 N making it too sensitive for transport.

Impact sensitiveness

The impact sensitiveness of the pyrotechnic mixtures was measured in terms of the LIE (Table 5). The limiting impact energy was found

to be 4.51, 2.75, 4.32, 4.12, and 3.53 J for the compositions of the firecrackers containing KNO_3 , KClO_4 , $\text{Sr}(\text{NO}_3)_2$, $\text{Ba}(\text{NO}_3)_2$ and Bi_2O_3 as oxidizers respectively along with $\text{S}/\text{Al}/\text{H}_3\text{BO}_3$, indicating that these compositions were sensitive to impact. If the limiting impact energy is low, the mixture is highly sensitive to impact. The pyrotechnic mixture with oxidizer KClO_4 is considered to be highly sensitive for friction and impact.

Thermal analysis

In order to understand the sensitivity of materials to heat and to determine the relative onset decomposition temperature, thermal analysis of ingredients, oxidisers/ $\text{S}/\text{Al}/\text{H}_3\text{BO}_3$ was carried out (Figures 10, 11). The decomposition reaction of a pyrotechnic mixture containing different oxidizers follows the same mechanism and undergoes a two stage decomposition reaction occurring in the region of 200–300 °C and 500–600 °C. The first peak indicates the decomposition of S as SO_2 and the energy released is used up in initiating the explosion reaction of oxidizers. All the oxidizers are thermally stable for firecrackers at room temperature. The measurements of sensitiveness indicated that KClO_4 is highly sensitive to friction and impact compared to other oxidizers.

DSC Analysis

DSC analysis is used to determine quantitatively the thermodynamic parameters like ΔH and ignition temperature (Table 6). There is no overlap of the endothermic peaks and exothermic peaks. Below 437 °C, there is no exothermic peak and only endothermic peaks were observed.

DSC analysis of KNO_3 shows two endothermic peaks at 121 °C and 141 °C corresponding to the melting point of S and KNO_3 , and one exothermic peak at 353 °C where maximum weight loss occurs

Table 5. Sensitiveness of pyrotechnic mixtures.

Pyrotechnic composition	Particle size		Bulk packing density/ g cm^{-3}		Friction sensitiveness/N		Impact sensitiveness/J	
	(μm)	(nm)	micro	nano	micro	nano	micro	nano
* $\text{KNO}_3/\text{Al}/\text{S}/\text{H}_3\text{BO}_3$	250	397	0.34	0.24	>360	>360	4.51	3.14
* $\text{KClO}_4/\text{Al}/\text{S}/\text{H}_3\text{BO}_3$	250	320	0.41	0.31	144	168	2.75	2.55
* $\text{Sr}(\text{NO}_3)_2/\text{Al}/\text{S}/\text{H}_3\text{BO}_3$	250	147	0.43	0.30	> 360	> 360	4.32	3.92
* $\text{Ba}(\text{NO}_3)_2/\text{Al}/\text{S}/\text{H}_3\text{BO}_3$	250	122	0.47	0.27	> 360	> 360	4.12	3.33
* $\text{Bi}_2\text{O}_3/\text{Al}/\text{S}/\text{H}_3\text{BO}_3$	250	461	0.68	0.67	> 360	> 360	3.53	3.53

*(Oxidizer /Al/S/ H_3BO_3 in the mole ratio 1.28/1.40/1.85/0.02).

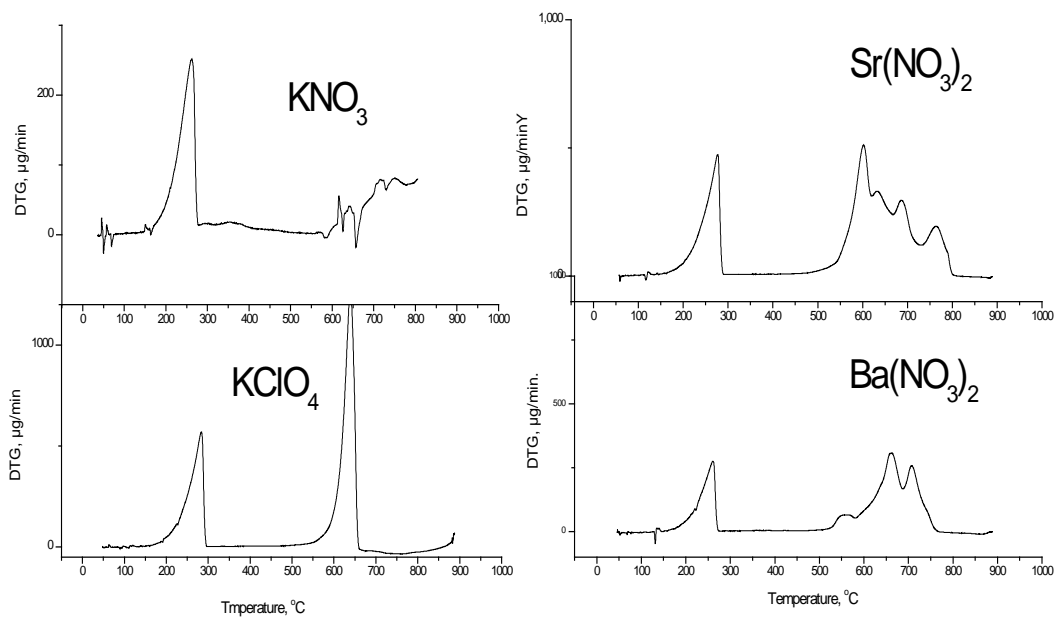


Figure 10. DTG analysis of nano-sized pyrotechnic mixture, oxidisers/S/Al/H₃BO₃.

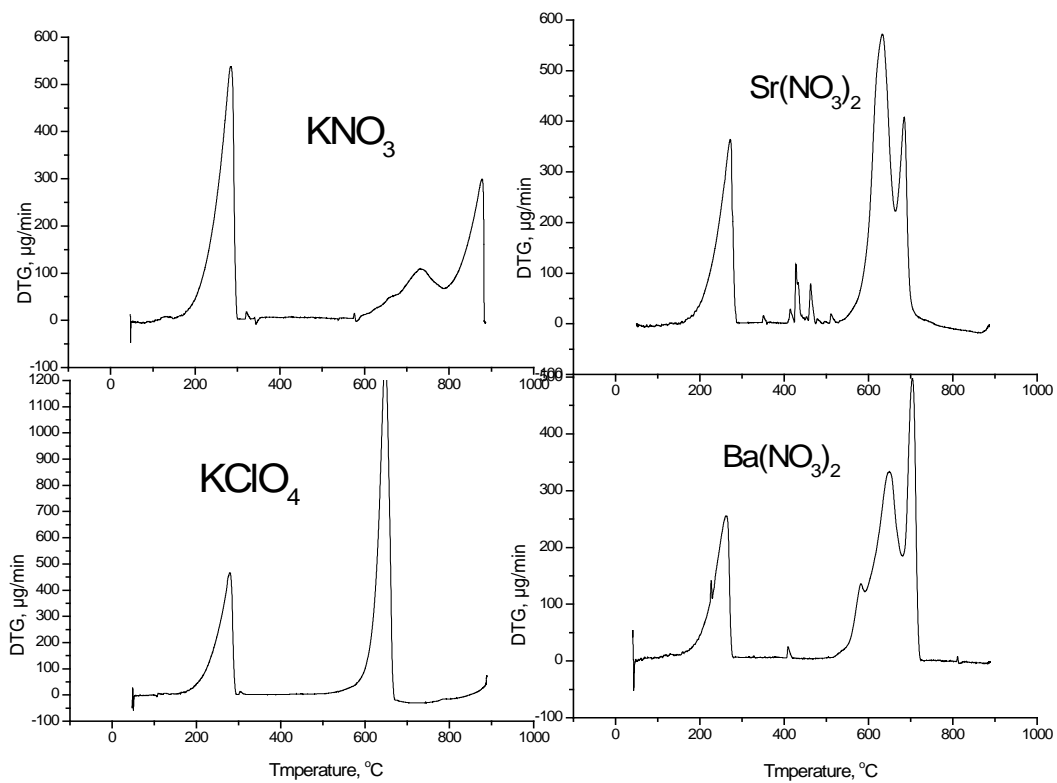


Figure 11. DTG analysis of micro-sized pyrotechnic mixture, oxidisers/S/Al/H₃BO₃.

Table 6 Thermal decomposition parameters by DSC analysis

No	Pyrotechnic composition	Particle size/nm	Onset/°C	Peak/°C	$\Delta H/J\ g^{-1}$	Particle size/ μm	Onset/°C	Peak/°C	$\Delta H/J\ g^{-1}$
1	KNO ₃ /Al/S/ H ₃ BO ₃	397	345.63	363.035	46.793	250	213.75	238.29	17.58
			504.15	58.94	9.19		250.16	258.81	9.10
							341.86	354.90	190.58
							446.13	508.53	42.68
2	KClO ₄ / Al/S/H ₃ BO ₃	147	235.03	248.78	9.30	250	361.73	372.43	16.59
			358.19	372.13	62.59		441.33	559.25	116.85
			446.72	552.57	74.86				
3	Sr(NO ₃) ₂ / Al/S/H ₃ BO ₃	320	343.74	351.67	11.11	250	202.99	281.57	38.15
			412.89	549.04	436.93		335.11	346.78	18.02
4	Ba(NO ₃) ₂ / Al/S/H ₃ BO ₃	122	353.98	366.65	31.80	250	337.41	349.49	19.86–102.9
			508.8	516.88	27.41		576.32	590.00	
5	Bi ₂ O ₃ /Al/S/ H ₃ BO ₃	461	330.39	334.83	5.73	250	330.39	334.83	5.73
			479.35	485.20	19.46		479.35	485.20	19.46
			508.26	527.86	33.44		508.26	527.86	33.44

(Figures 12 and 13). There is no overlapping of exothermic and endothermic peaks. Pyrotechnic mixtures using nano- and micro-sized particles of oxidizers follow the same trend on thermal decomposition but the heat of reaction for nano-sized particles (47 J g⁻¹) is less than that of micro-sized particles (191 J g⁻¹) and the effect of sound level is inversely proportional to the heat

of reaction, as the sound level produced by nano-sized particles is higher than that of micro-sized particles.

DSC analysis of KClO₄ (Figures 14 and 15) shows two endothermic peaks at 117 °C corresponding to the melting point of S and at 307 °C, a well defined solid–solid transition. This solid–solid transition peak makes KClO₄ one of the

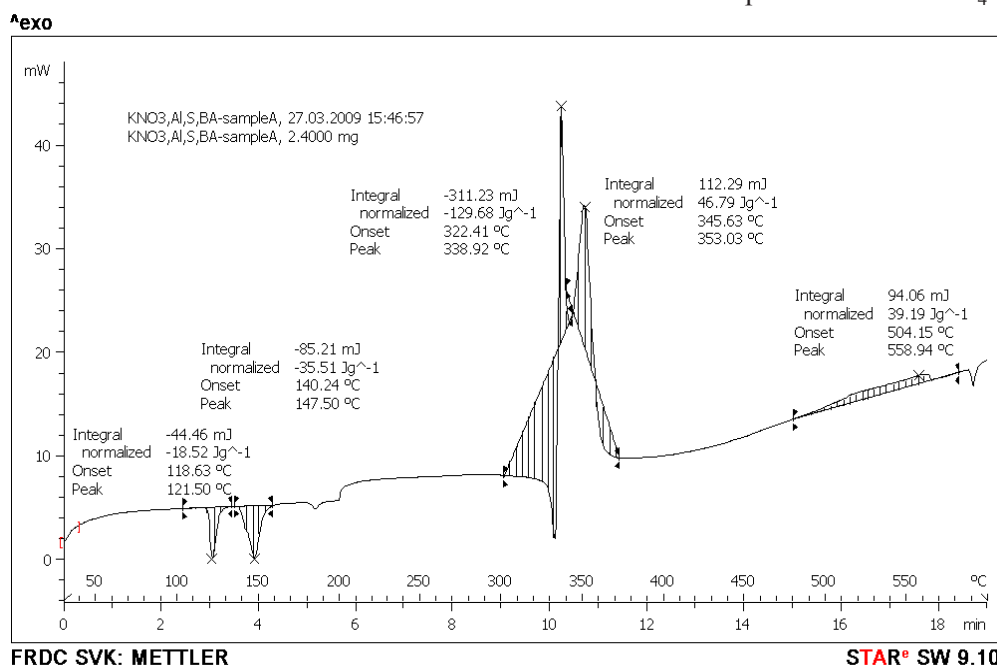


Figure 12. DSC analysis of nano-sized pyrotechnic mixture, KNO₃/S/Al/H₃BO₃.

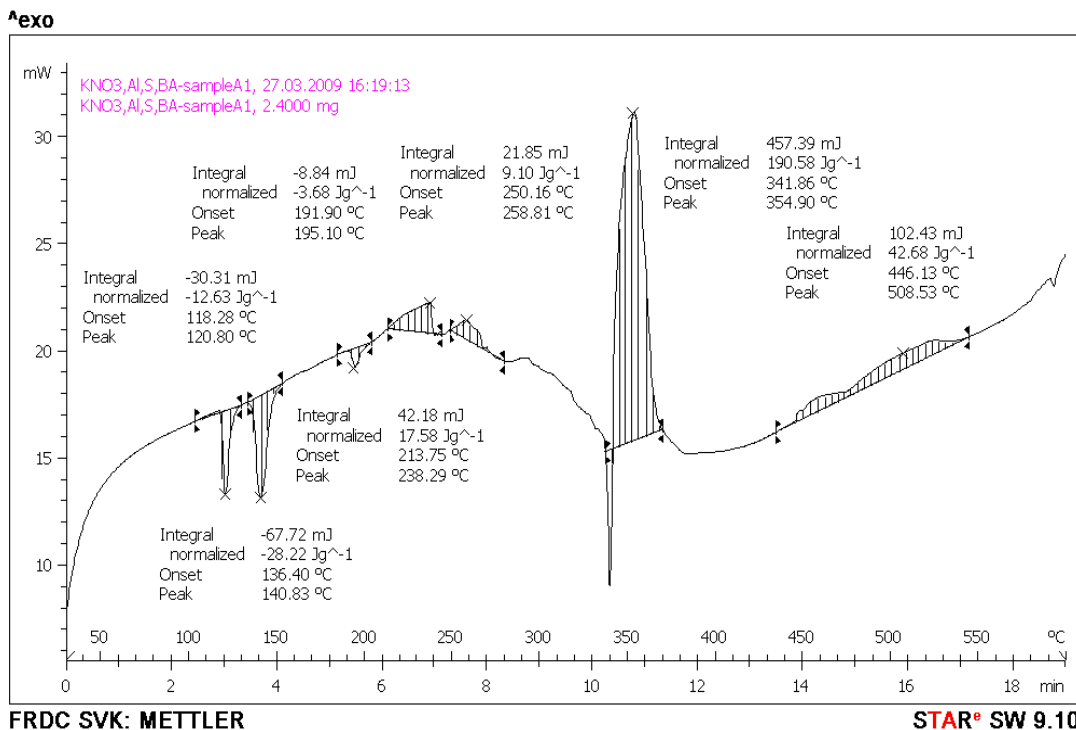


Figure 13. DSC analysis of micro-sized pyrotechnic mixture, $KNO_3/S/Al/H_3BO_3$.

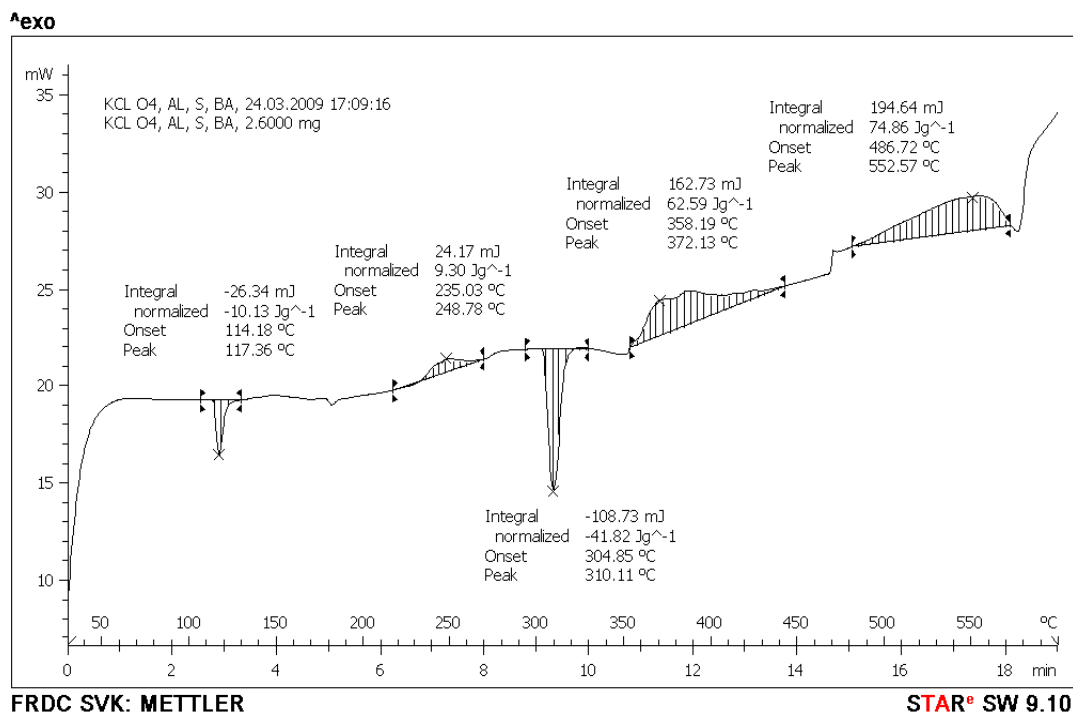


Figure 14. DSC analysis of nano-sized pyrotechnic mixture, $KClO_4/S/Al/H_3BO_3$.

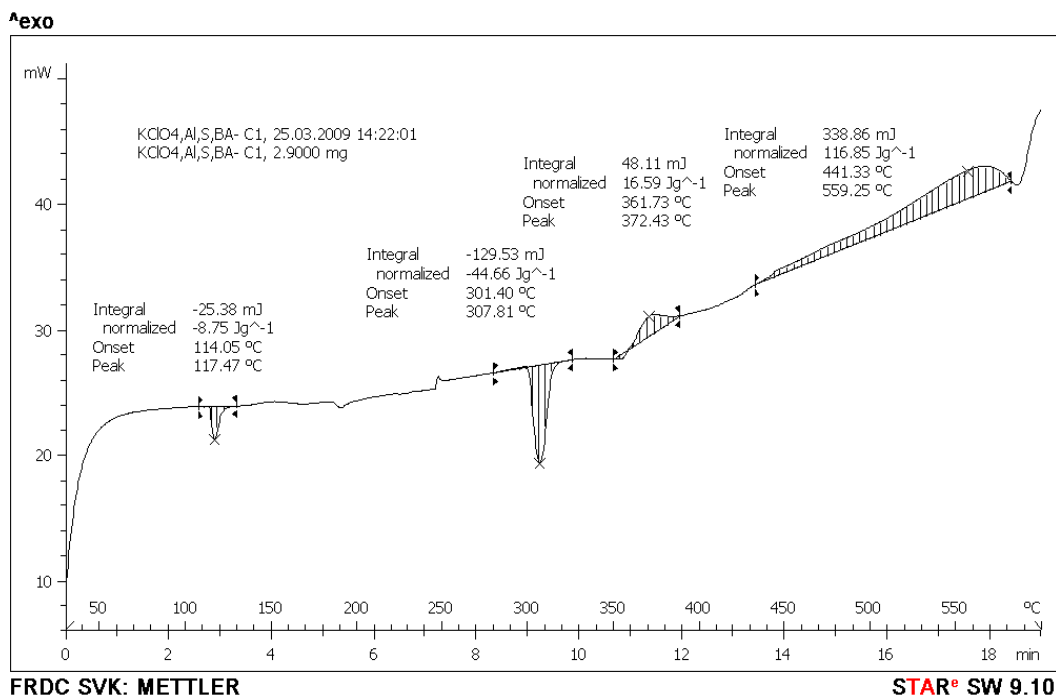


Figure 15. DSC analysis of micro-sized pyrotechnic mixture, $KClO_4/S/Al/H_3BO_3$.

Certified Reference Materials developed by the International Confederation for Thermal Analysis and Calorimetry (ICTAC) for the temperature calibration of DSC and DTA equipment¹⁰ and the area of the solid–solid transition peak could be used as a semi-quantitative estimation of the amount of perchlorate present in a mixture. The exothermic peak at 249 °C represents the oxidation of sulphur into sulphur oxide. The exothermic peaks at 372 °C and 553 °C represent the decomposition where maximum weight loss occurs (Figure 14). The heat of reaction for nano-sized particles (136.9 J g^{-1}) is slightly greater than that of micro-sized particles (132 J g^{-1}) and the effect of sound level is inversely proportional to the heat of reaction, and there is not much difference in the sound level produced by nano-sized and micro-sized particles of $KClO_4$.

In the case of a pyrotechnic mixture with oxidizer $Sr(NO_3)_2$, two endothermic peaks at 117 °C due to the melting of S and at 351 °C correspond to the melting of $Sr(NO_3)_2$ (Figures 16 and 17). The exothermic peaks are observed at 551 °C with heat of reaction 436.99 J g^{-1} for nano-sized materials and at 525.4 °C for micro-sized materials with ΔH of 41.52 J g^{-1} . Though the

positions of the exothermic peak are the same, the nano-materials are not effective in making sound producing firecrackers whereas micro-sized particles are effective in making sound producing firecrackers. The agglomeration of nano-sized particles of $Sr(NO_3)_3$ reduces the efficiency of the firecrackers.

If $Ba(NO_3)_2$ is used as oxidizer in a nano-sized mixture, one endothermic peak at 117 °C and two small exothermic peaks at 366 °C and 516 °C are observed (Figures 18 and 19). But this exothermic peak is immediately followed by an endothermic peak at 583 °C making the pyrotechnic mixture not fit for making sound producing firecrackers in this particular molar ratio. The micro-sized materials give an endothermic peak at 590 °C with no remarkable exothermic peak making the pyrotechnic mixture not fit for firecrackers.

If Bi_2O_3 is used as oxidizer (Figures 20 and 21) a sudden exothermic reaction will not take place even at high temperatures for both micro- and nano-sized materials. Bi_2O_3 can not be used as an effective oxidizer in making sound producing firecrackers.

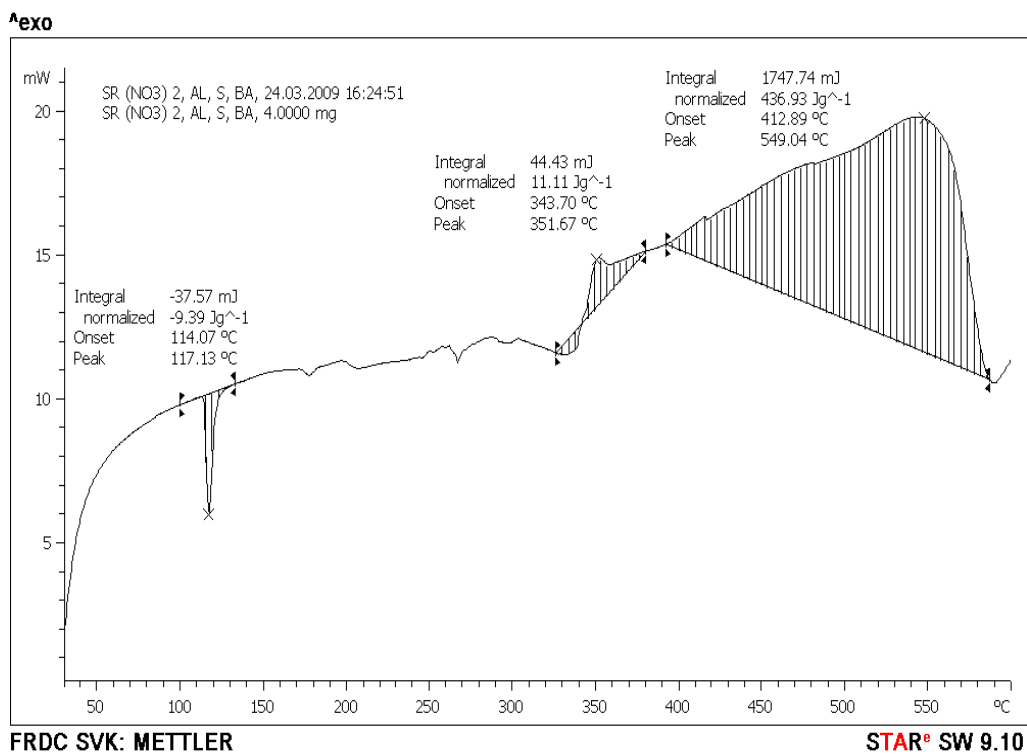


Figure 16. DSC analysis of nano-sized pyrotechnic mixture, $Sr(NO_3)_2/S/Al/H_3BO_3$.

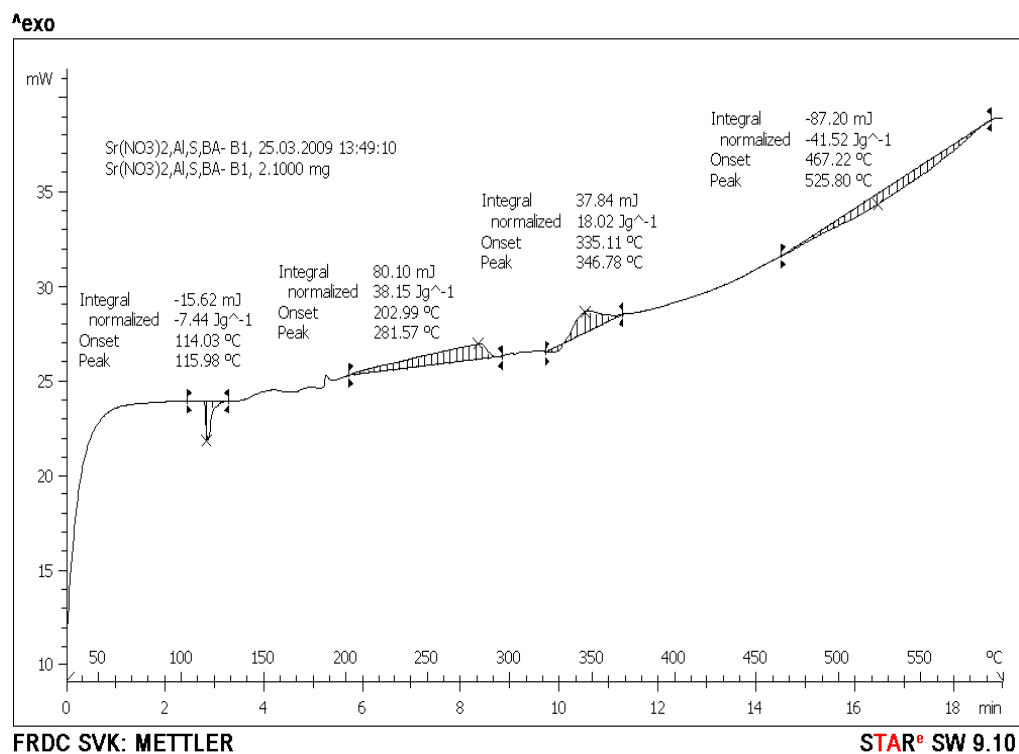


Figure 17. DSC analysis of micro-sized pyrotechnic mixture, $Sr(NO_3)_2/S/Al/H_3BO_3$.

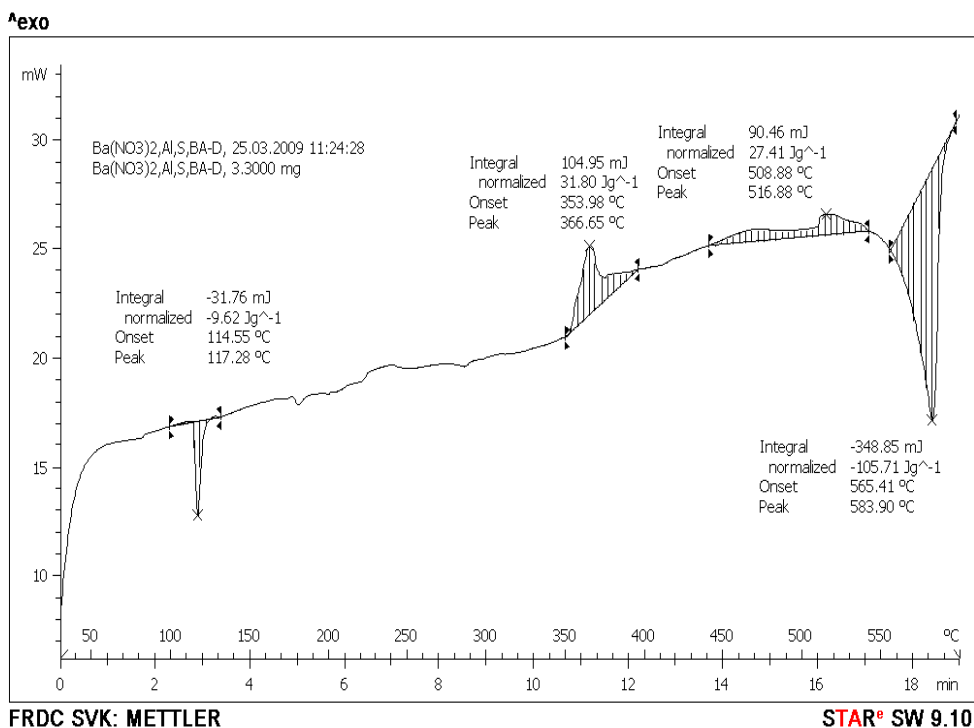


Figure 18. DSC analysis of nano-sized pyrotechnic mixture, $Ba(NO_3)_2/S/Al/H_3BO_3$.

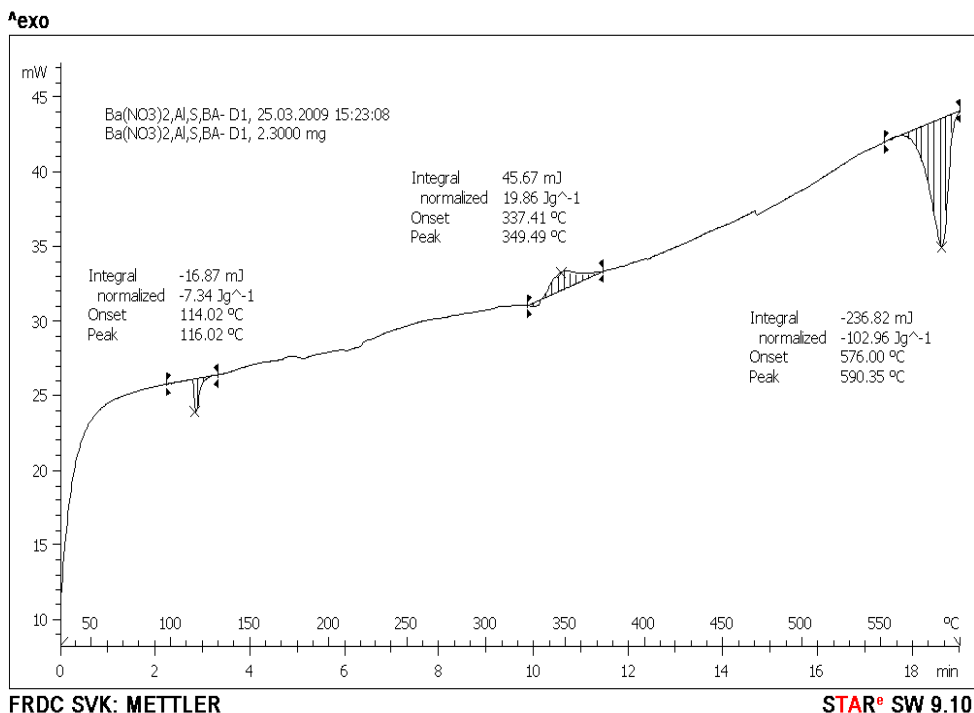


Figure 19. DSC analysis of micro-sized pyrotechnic mixture, $Ba(NO_3)_2/S/Al/H_3BO_3$.

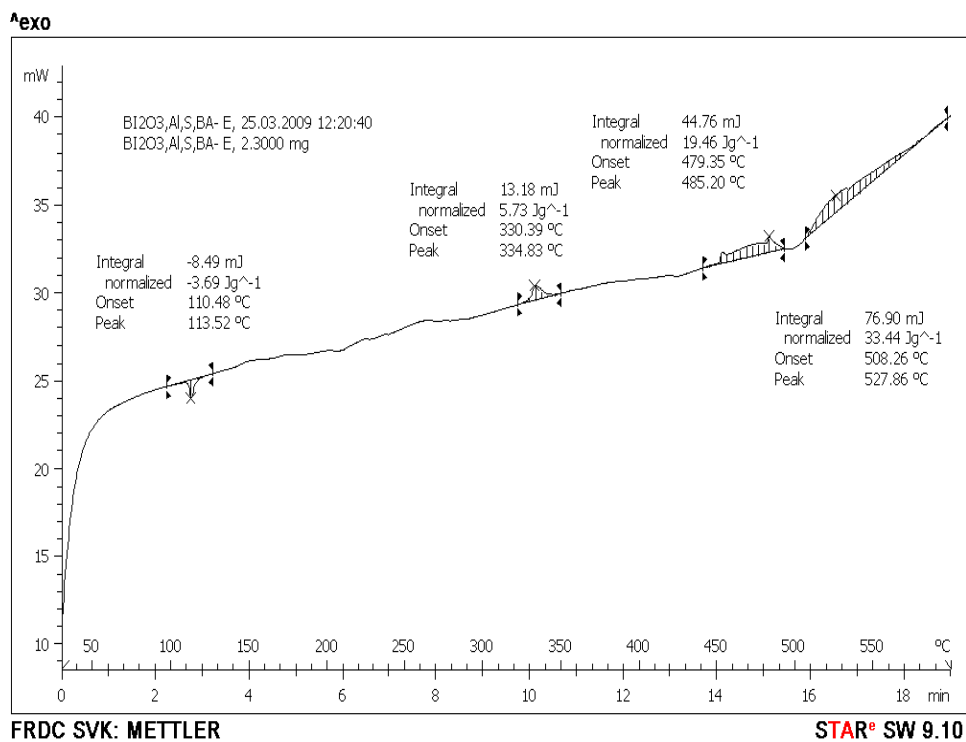


Figure 20. DSC analysis of nano-sized pyrotechnic mixture, Bi₂O₃/S/Al/H₃BO₃.

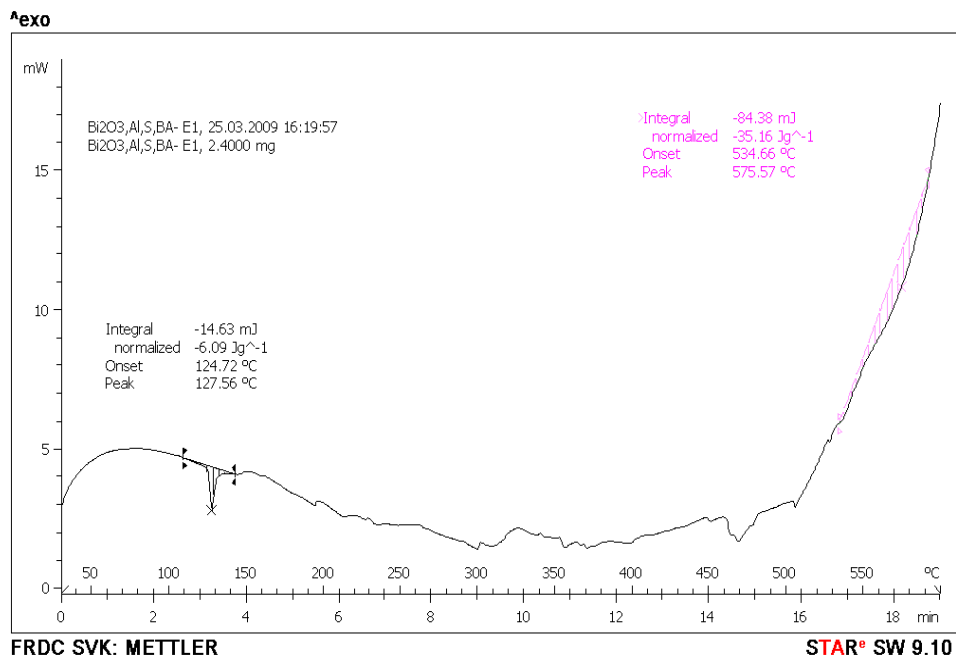


Figure 21. DSC analysis of micro-sized pyrotechnic mixture, Bi₂O₃/S/Al/H₃BO₃.

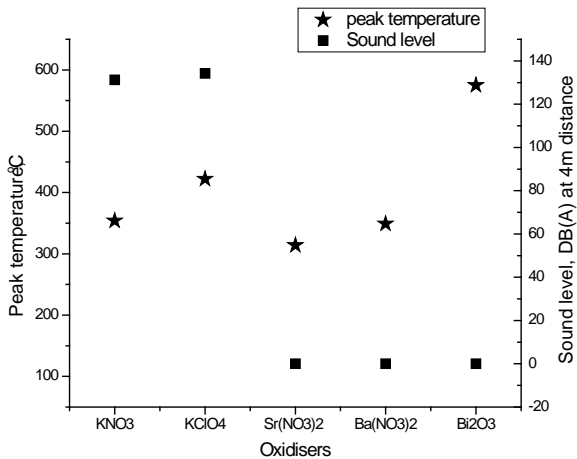


Figure 22. Interrelation between peak temperature and sound level of nano-materials.

Interrelation between sound level and thermal decomposition parameters

The nano-materials of the pyrotechnic mixture (Figures 22–24) reveal that there is an inverse relationship between peak temperature and ΔH , and peak temperature and sound level. A high peak temperature leads to the production of low sound level in the firecrackers. The micro-materials of pyrotechnic mixtures (Figures 24–26) reveal that there is no definite relationship between peak temperature and ΔH in the molar compositions taken for analysis. Figure 24 shows that the peak temperature of nano-materials is high compared to that of micro-materials and the difference between the peak temperature of a pyrotechnic mixture

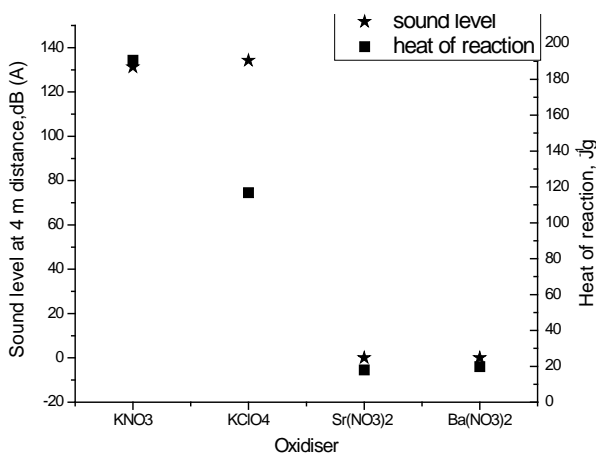


Figure 23. Interrelation between heat of reaction and sound level of nano-materials.

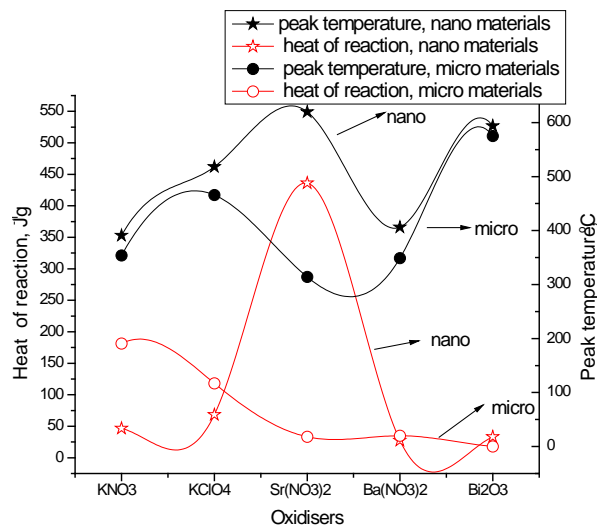


Figure 24. Interrelation between peak temperature and heat of reaction for micro- and nano-oxidizer composition.

using the oxidizer strontium nitrate in nano- and micro-materials is large and the nano-materials do not produce sound which may be due to the formation of agglomeration. In a pyrotechnic mixture with the oxidizer KNO₃ or KClO₄, ΔH_{nano} is less than ΔH_{micro} and nano-materials were found to produce sound effectively. In the case of Sr(NO₃)₂, $\Delta H_{\text{nano}} > \Delta H_{\text{micro}}$ and micro-materials are effective in producing sound. It was observed that the higher the peak temperature, the lower will be ΔH .

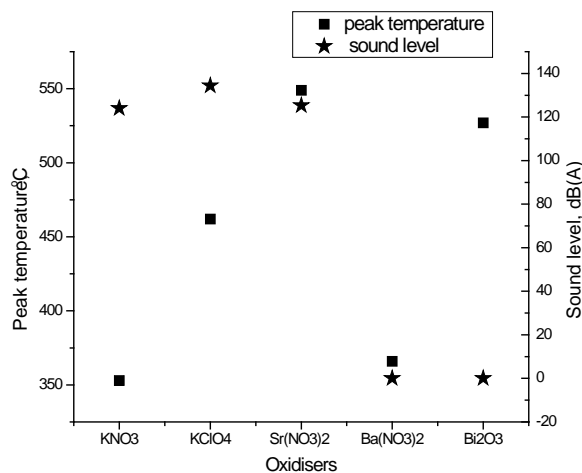


Figure 25. Interrelation between peak temperature and sound level of micro-materials.

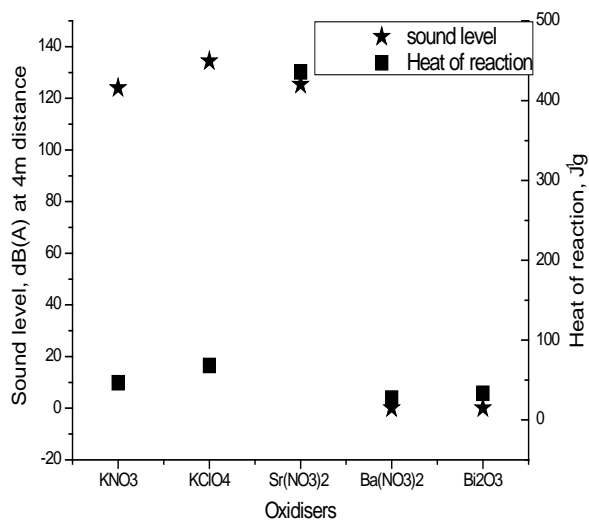


Figure 26. Interrelation between heat of reaction and sound level of micro-materials.

Conclusion

In sound producing cake-bomb firecrackers, pyrotechnic mixtures containing five different oxidizers with S, Al, and H₃BO₃ are used. The effect of different oxidizers in producing sound was studied and it was found that the nature of the oxidizer plays an important role. KClO₄ is a powerful oxidizer, thermally stable but highly sensitive to impact and friction which is not safe for keeping the pyrotechnic mixture as a loose composition and for transport. If the mixture is not used completely in the manufacturing unit, it should be destroyed in an appropriate way. Similarly, Ba(NO₃)₂ is also found to be an effective oxidizer but an anticaking reagent should be used for storing. The pyrotechnic mixture containing KNO₃/S/Al(H₃BO₃) whose inversion temperature is above 400 °C and which is less sensitive to mechanical stress is safe for transport. The composition consisting of 57.5% KNO₃, 20% S, 22% Al and 0.5% H₃BO₃ appears to be an ideal composition in all respects with reduced impact sensitivity, required explosivity and allowed sound pressure level.

Acknowledgements

The authors are highly thankful to ‘The Standard Fire Works Pvt. Ltd.’, Sivakasi, for providing the firecrackers with suitable proportions of pyrotechnic mixtures.

References

- 1 K. Kosanke and B. Kosanke, ‘Pyrotechnic ignition and propagation: A review’, in *Pyrotechnic Chemistry*, Vol. 4, Journal of Pyrotechnics, USA, 2004, Chapter 4, pp. 1–10.
- 2 B. Thomson and A. Wild, ‘Factors affecting the rate of burning of a titanium–strontium nitrate based compositions’, *Proceedings of Pyrochemical International*, United Kingdom, 1975.
- 3 S. Sivaprakasam and M. Surianarayanan, ‘Interrelation between impact, friction, and thermal energy in a pyrotechnic flash reaction’, *Journal of Pyrotechnics*, Vol. 23, 2006, p. 51.
- 4 *Gazette Notification*, 1999, Noise Standards for Firecrackers, G. S. R 682(E).
- 5 A. JeyaRajendran and T. L. Thanulingam, ‘Sound level analysis of firecrackers’ *Journal of Pyrotechnics*, Vol. 27, 2008, pp. 60–76.
- 6 H. Koenen, K. Ide and K. Swart, *Pruefverfahren der Bundesanstalt fuer Materialforschung und -pruefung (BAM)* Vol. 94, 1961, p. 30.
- 7 R. Wharton and J. Harding, ‘An experimental comparison of three documented methods for the evaluation of friction sensitiveness’, *Journal of Energetic Materials*, Vol. 11, 1993, pp. 51–65.
- 8 R. K. Wharton, R. J. Rapley and J. A. Harding, ‘The mechanical sensitiveness of titanium/blackpowder pyrotechnic compositions’, *Propellants, Explosives, Pyrotechnics*, Vol. 18, 1993, pp. 25–28.
- 9 *United Nations: Recommendations on the Transport Dangerous Goods, Manual of tests and criteria*, United Nations, New York, 1990; Vol. ST/SG/AC.10.11/Rev 3.
- 10 M. Fathollahi, S. Pourmortazavi and S. Hosseini, ‘The effect of particle size of KClO₃ in pyrotechnic compositions’, *Combustion and Flame*, Vol. 138, 2004, pp. 304–306.

Ergonomic Hazards in Local Fireworks Factories

Stanley Azzopardi

Centre for Labour Studies, University of Malta

Email: pyrostan@onvol.net

Abstract: *The objective of this paper is to review the practices, postures and workstations in Maltese fireworks factories which may cause back pain and musculoskeletal disorders to fireworkers. Hazards varying from the toxicity of substances used to produce colours and pyro-effects up to ergonomic adversities that such processes impose upon the workers are present in these factories. At fireworks factories, the ergonomic aspects are not considered important and this is mainly attributed to the financial aspects and traditional methods of manufacturing. Rivalry between local fireworks factories fuels this passion which forces the voluntary fireworkers to increase or maintain their yearly production and hence their exposure to such ergonomic hazards. Literature that specifically discusses ergonomics or fireworks manufacturing is readily available, but literature which combines both topics is difficult to find. Even the local legislation, mainly the Explosives Ordinance (Laws of Malta – Chapter 33) and the Occupational Health and Safety Authority Act (Laws of Malta – Chapter 424), do not cross reference each other to provide fireworkers with suitable and systematic guidelines. For this pilot study a questionnaire was designed for use as an investigative tool, to help understand the cause of fireworkers' complaints of aches and pains (if any) during fireworks manufacturing. Results, gathered from 51 licensed fireworkers indicated that the manufacturing processes are the cause of pains located mainly in the upper part of the body. The respondents reported their pains as being frequent or occasional during an average six hour production day. Further discussion argues that these fireworks enthusiasts (the respondents) consider these reported pains as part of their job at the fireworks factories. These illnesses and ailments may be causes of minor and/or major accidents during the processes. These may even end up in injuries, deaths, news sensationalism and resurfacing protests by anti-fireworks citizens.*

Keywords: *fireworks, fireworkers, ergonomic hazards, work practices, time*

Introduction

Ergonomics

The three basic human sciences anatomy, physiology and psychology converge to forge ergonomics to ensure that human beings and technology function in complete harmony. Although ergonomics is widely used during our daily domestic lives, it is far more involved in work settings. Ergonomics helps to increase efficiency, productivity and health and safety.

Local fireworks factories

Fireworks is a Maltese culture which was born decades ago, after the arrival of the Knights of St. John, and nurtured later during the last century.

Village fiestas are organized upon four main pillars – church functions, street decorations, band marches and fireworks. Rivalry between fireworks factories within the same town and also between neighbouring towns holds an important role in the continuous improvement of local fireworks manufacturing.

A total of 38 factories, which are spread across Malta and Gozo, host nearly 1000 licensed enthusiasts. The factories and the manufacturing processes are regulated by the Explosives Ordinance.¹ Each factory is managed by a licensee, who is responsible for the safety of these volunteers and the general manufacturing processes. Maltese fireworks are typical 'Italian type shells',² but

Article Details

Manuscript Received:-02/10/08

Publication Date:07/01/10-

Article No: - 0068

Final Revisions:-06/01/10

Archive Reference:-1039

with innovative fireworks and pyrotechnics. The Maltese fireworkers are much renowned for the 'beraq pront', multibreak colour shells and the more complicated 'murtali tal-loghob'.

Literature review

The local fireworks industry

Esteem and acknowledgment from foreign fireworkers proves that Malta is a sort of Mecca for pyro-enthusiasts from all over the world. Mark Lancaster in 'Fireworks – Principles and Practices' describes Malta as a '*unique place, where fireworks in their purest form are enjoyed for their own sake, by some of the friendliest and skilled pyrotechnists I have ever had the pleasure to meet*'.²

Fireworks and health & safety

The manufacturing process of fireworks is a slow and rigorous one. Dr Takeo Shimizu in his book 'Fireworks – the Art, Science and Technique' published various flowcharts and tables to break down the processes.² Through these the reader can get a glimpse of the variety of tasks which the fireworker will have to undertake once the process of manufacturing has been started.

Although fireworks are part and parcel of our everyday community life, safety in this regard is not inherent in the manufacturing processes. It was only in the last few years that occupational health and safety issues were introduced to the Maltese pyro-community through the courses which have been set up by the Maltese Police Force to grant the A and B licences. But a mere two hour session is really not enough to even introduce the risks associated with the manufacturing of fireworks.

Ergonomic hazards

Although the chemicals at the factories present the highest level of risk and hazards, other risks are omnipresent throughout all the processes. Ergonomic hazards are more prominent at the local factories since these factories are built and run by volunteers. These factories are financed by the money collected from parishioners or fund-raising activities. Investing finance in adequate seating or workstations is considered less important than buying several kilograms of a chemical which will improve the shells' performance. Moreover, studies and writing about the ergonomic hazards in local and foreign firework factories are non-

existent. The author's attempts to find literature about ergonomics and fireworks production proved futile. Comparing fireworking activity with catering activities the author was introduced to conditions which may be caused by fireworks production. Repetitive motion disorders (RMDs) are described by <http://www.medicinenet.com> as 'a family of muscular conditions that result from repeated motions'² and research published by the European Agency for Safety and Health at Work in 2000 states that lower back pain 'is any back pain between the ribs and top of the leg that results from any cause'.²

The European Agency for Safety and Health at Work states that: 'in a stressful environment people might be more sensitive to pain'.² Local firework factories are a stressful environment: all the risks and hazards, the urge to finish the planned works, competition against neighbouring factories and loads of other small issues combine to increase stress upon the workers.

Methodology

The author, being a fireworks enthusiast himself, already had knowledge of manufacturing which helped a lot in the structuring of the questionnaire and discussion of the results. The primary data were collected by means of a survey.* This type of approach helped in presenting insights into the workers' health status during and after fireworks production, the persistence of the ailments and their knowledge of ergonomic hazards at the fireworks factories.

A questionnaire, the most common research instrument, was chosen for the collection of primary data and it consisted of both nominal and ordinal questions. The questionnaire was presented in the Maltese language, so that the respondents would fully understand the technical (on fireworks) questions. The sampling unit consisted of licensed fireworkers irrespective of their age, sex, type of licence and years of experience. Thirteen localities where fireworks factories are located were randomly chosen. Contact points were identified in each locality and through them a sample number of 105 licensed fireworkers was established. Respondents were

* See <http://archives.jpyro.com/?p=1042> for a copy of the survey.

Table 1. Pain reported by respondents.

Pain	Normal range	Overweight	Obese
Lower back	3	7	4
Lower back and calves		1	
Lower back, calves and ankles		1	1
Lower back, calves and knees		1	1
Lower back and knees	1	2	
Knees		2	
Lower and upper back	1	4	2
Upper back	2	2	2
Lower and upper back, calves and ankles			1

asked to self-administer the questionnaire during the months of November–December 2007. Out of 105 distributed questionnaires, 51 returned the questionnaires. The response rate was 48.6%. The non-respondents were not requested to complete the questionnaire.

Results, findings and discussion

The results presented here are a basic statistical occurrence of pains and aches which result from hours of hard labour on the production of fireworks. Moreover the subjects were asked which tasks cause such ailments. Factors such as stress, production time, medical assistance, sick leave and health & safety knowledge were also surveyed.

Profile of sample: age distribution and gender of sample (Q1 & 2)

72.5% of all the subjects, 51 in number, who returned the questionnaire, were under 45 years of age. Male workers are much more common in firework factories than females; this is in accordance with the fact that only one female returned the questionnaire.

Height of sample (Q3)

The subjects were asked about their height, since the benches where these persons work are not adjustable according to height. This information can be used for further studies and experimentation. The single female respondent fell in the lowest height group.

Weight of sample (Q4)

The exact height and weight of each individual in the study was not asked. The interviewees could

choose between different group limits so the approximate body mass index could be calculated for the sample. The sample replies were sorted on an Excel sheet and compared to a body mass index graph and then related to pain reported in the back and lower limbs during fireworks manufacturing. These results indicate that most persons are either overweight or obese and this could be an added complication resulting in back and lower limb pain. However the sample size for normal body mass index was too small to deduce any conclusive results.

Type of licence and years of experience (Q5 & 6)

The type of licence that gives a person the right to perform fireworks is important. 76.5% of the sample hold a B licence, whilst the other 23.6% hold an A licence. Licence A holders are more experienced than Licence B holders; this can be deduced from the fact that all the 12 licence A respondents have placed themselves in the range of 11 years to over 50 years of experience. Positively enough none of the respondents had worked in a fireworks factory for less than one year. This means that their reply is based on at least a year's experience, hence they have come across all the processes at the factories.

Professional or volunteer (Q7)

All the respondents declared that they do not earn their living from manufacturing fireworks. This is consistent with the voluntary work, dedication and passion these men and women put into this art all year round. The main concern at the factories, which are run on a voluntary basis, is the quality and quantity of the shells. Tools and work practices

are not substituted unless the shells produced are better and more numerous even though the systems presently being used are causing ailments due to factors such as repetitive motion, bad postures and restricted work space. Since the work is done on a voluntary basis it takes place during free time (after a normal 40 hour a week job) and this may cause a build up of stress especially during the months of preparation and assembly of the shells.

Employment sector or status (Q8)

The respondents' employment sector or status is here listed in decreasing order: 23 services sector, 15 manufacturing and construction sector, 9 pensioners, 2 in the agriculture and fisheries sector and 2 unemployed. Since 78.4% of the respondents could be exposed to ergonomic hazards such as repetitive work, bad posture at the office, prolonged seating and manual handling during their employment period, and so compromise questions 18a, 18bi, 19, 20 and 21 (where the respondents were asked if any musculoskeletal pains were caused by fireworks manufacturing), question 9 was intended to isolate fireworking activity pain from employment/sports/free time activity pain.

Work, free time or sporting activities related to musculoskeletal pain (Q9)

63% of the respondents do not perform heavy lifting or other work that causes musculoskeletal pain during their work, free time or sports activity. Added to this, the workers could specify at what time the aches or pains are felt, whether it is fireworks production, during salary based work, or during any other activity such as sports or hobbies. This renders the answers for questions 18a, 18bi, 19, 20 and 21 more plausible.

The manufacturing processes and the workers' health

Jobs performed (Q10 & 11)

The subjects were asked to write down the most common three pain-causing jobs from their already marked list. When analyzing the most performed jobs versus the most pain-causing jobs the top five jobs are as follows.

Body movements during tasks (Q12 & 13)

The majority of the workers reported repetitive hand movements using small muscles such as gripping (88.2%), squeezing tightly with the

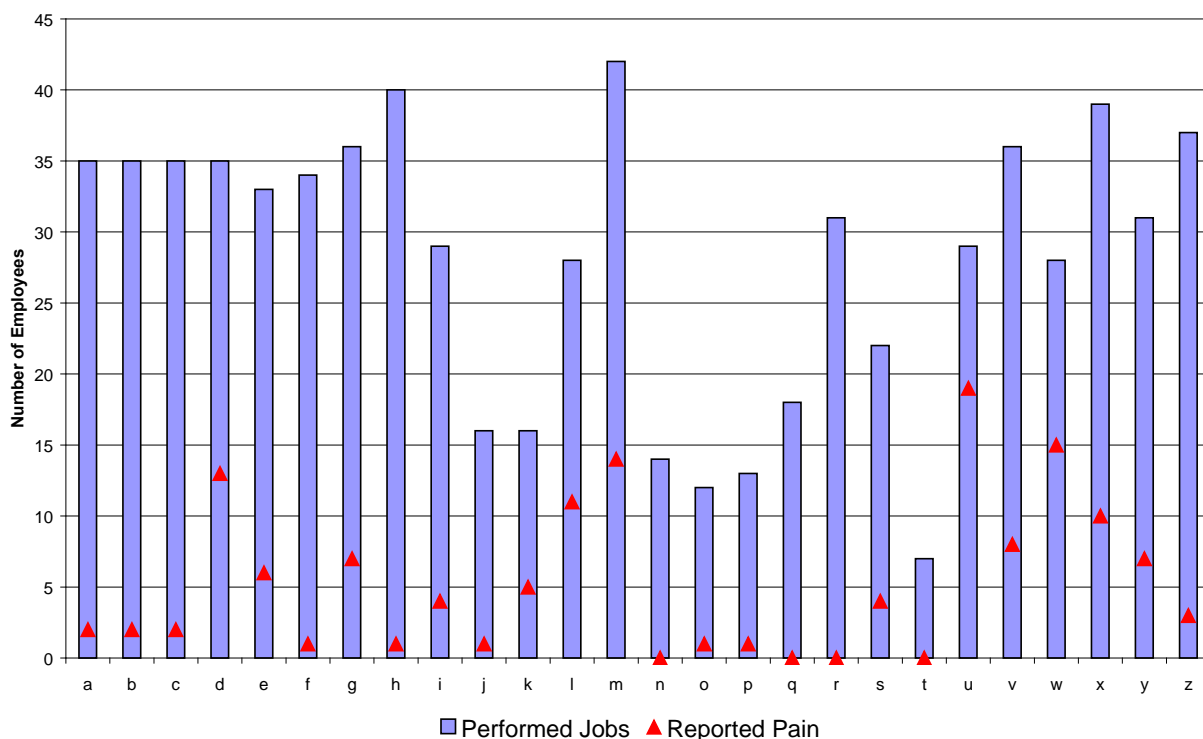


Figure 1. Rate of jobs performed and pain reported for each job. See Appendix for definitions.

Table 2. Table showing most painful job by the most performed.

Code	Job	%
U	Spiking of shells (5" in diameter and bigger)	65.5
W	Assembly of shells	53.6
L	Sieving of black powder	39.3
D	Spiking of beraq casings	37.1
M	Carrying of black powder into sunshine	33.3

fingers (82.4%), and bending of wrist (78.4%). Other tasks require whole body movements such as carrying (76.5%), twisting (72.5%) and bending (54.9%). The least performed task which the subjects recall is pushing (52.9%). This data is very important when collating musculoskeletal ailments to such tasks and also when proposing innovative work processes.

Although there is a balanced reply between reported and non-reported, pain during fireworks manufacturing is mostly reported in finger joints, hands and shoulders. The writer expected a higher incidence of pain in these areas and in the wrist area. However, a psychological factor could be affecting this response; that is the acceptance of such pain as part of their voluntary work.

Stress caused by target date (Q14)

Improving the fireworks' quality and quantity increases stress and tension which may cause the workers to bypass their 'ergonomically safe' work practices and perform undesirable work practices such as working in limited areas on the workbench, working in awkward standing positions and carrying greater loads. These undesirable work practices added to accumulated stress and tension may be the cause of musculoskeletal injuries. Results show that 72% of the sample agrees that the completion of planned fireworks manufacturing processes in due time increases tension and stress.

Workstations (Q15)

It was assumed that the respondents had limited knowledge about the ideal height of their workstations so a question was presented to perceive the respondents' comfort at the workstations in the fireworks factories. 73% of the respondents agreed that their workstations are suitable for their needs.

As already explained in the literature review, the factories are run by donations and such funds are invested in the chemicals, cardboard and other relevant items for the production of shells and not in the workstations. Semi-broken chairs, stools, wooden boxes and other spontaneously invented seating is very common at the factories (Plate 2 and Plate 3). The author recalls a particular factory having a tilted work bench positioned on a slightly sloped concrete platform (Plate 1 below), which implies that the worker has to continuously work in an unlevelled posture. Should the fireworkers be better educated and trained in the best measurements for their workstations, an improvement of the work benches would be definitely seen in the future.

Manufacturing time (Q16 & 17)

Response to these questions can give a glimpse of the average time spent on production during a normal day and total weekly time.

From these results we can derive the exposure time these workers have to ergonomic hazards at their local factories and through further and more



Plate 1. Wooden blocks used to level a working bench at a local fireworks factory. Source: author's own gallery.



Plate 2. Examples of seating at the factories.

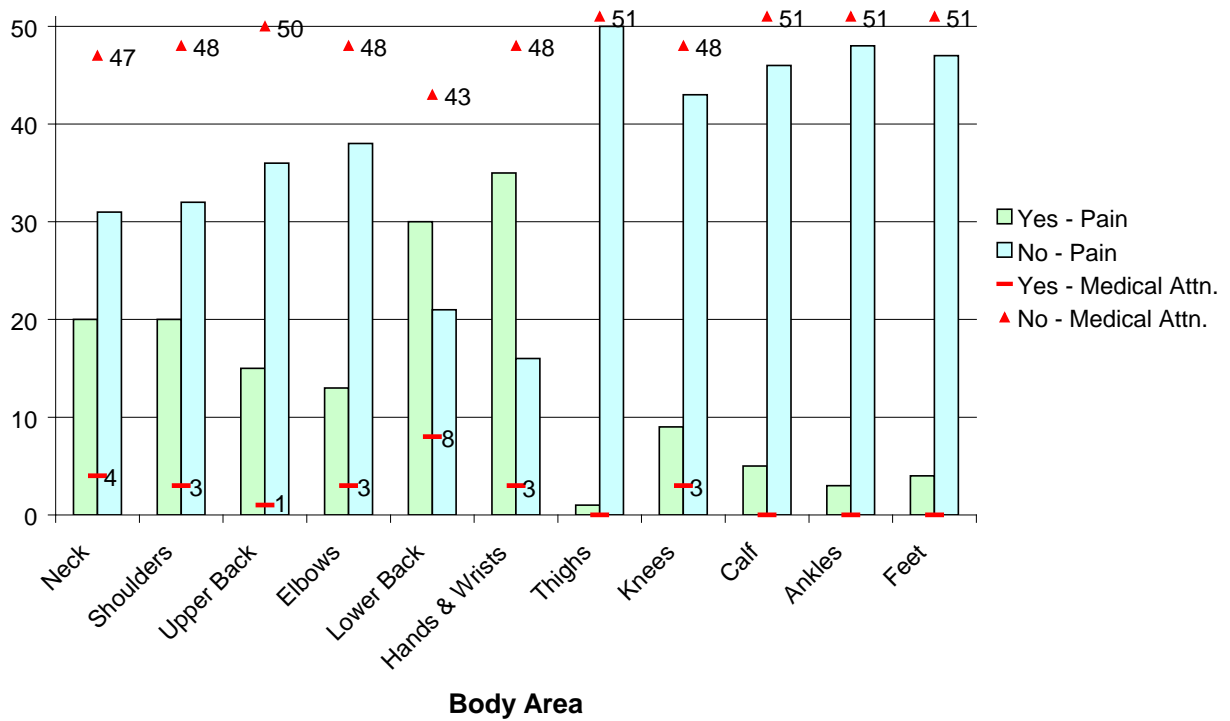


Figure 2. If pain is reported in particular body areas and if medical attention is sought for such pain.

detailed studies a threshold limit value (TLV) or short term exposure level (STEL) can be attributed to each task. Taking into account all data retrieved from these questions we can state that the average working period of a normal production day is 5.48 hours per worker.

Musculoskeletal disorders in specific areas (Q18a & 18bi)

The interviewee was asked whether he experienced any musculoskeletal pain during the past year as a result of his fireworking activity and if he has ever asked for medical advice to cure such problems.

Lower limb pain incidence is very low when compared to pain in the upper torso and upper limbs. Notwithstanding that, some subjects reported discomfort, about which they did not seek medical advice, except for a mere 5.9% that



Plate 3. Other examples of seating found at the factories.

suffered knee problems.

Pain in the hands and wrist was the most highly reported (68.6%) although only 8.6% of these subjects sought medical advice. Here we must reconsider the answers presented in Question 12. In this question the subject is once again being questioned about pain that he/she may recall during certain instances where pain or ache was experienced. The author firmly believes that the answers presented in this question are much more realistic and reaffirm the theory that the voluntary fireworker considers pain as part and parcel of his job.

Figure 2 shows that medical advice is most commonly sought for lower back pain. It is widely known that lower back pain is the major ailment of the European workforce. The findings show that 58.8% of the respondents have suffered some form of lower back pain due to fireworks manufacturing but only 26.7% of these subjects sought medical advice.

The results for elbow pain are more alarming. Although 25.5% of the respondents ticked 'Yes' as their result, 23.1% of these sought professional medical care. This may mean that such aches and pains are much more severe, chronic and annoying than hands and wrist pains. The author recalls mild lower back pain and mild elbow tiredness during the shell spiking process. The author also states that his production time was very low when compared to the long hours of production his comrades used to spend. The most alarming result comes from knee pains. Nine subjects reported knee discomfort and three of them asked for medical advice related to such problems. It is unclear what causes such problems since all three respondents come from different age groups and have different height and weight combinations. When referred to the BMI graph two of the three subjects were found to be overweight and the third one obese. As for the working hours the two overweight respondents reported working from 11–20 hours per week whilst the obese respondent reported working from 6–7 hours per week.

Quantifying aches and pains (Q18bii & 18c)

The subjects were then asked to be more specific on the frequency of their aches. Almost all of the subjects reported 'occasional' or 'frequent' pain.

More specific questions (Q19, 20 & 21)

The subjects were asked if they had experienced any back pain these last three months due to their fireworks manufacturing.

68.6% of the respondents reported negatively, the rest gave a positive answer. This may be due to the fact that during the period this survey was distributed, the processes at the factories did not involve the spiking and/or mounting of the shells, now deemed as the most pain causing jobs at the factories. But other tiring jobs such as sieving black powder and carrying it into the sunshine are regularly conducted throughout these months.

The sample was then asked a further two questions:

- If these tasks have caused severe pain which forces them to stop the production.
- If, even though they suffered severe pain, they have persisted in their production.

The results to both questions are as follows:

- 13.7% of the respondents had to stop the manufacturing due to pain.
- All 7 subjects that 'had to stop due to pain' responded negatively when asked if they have ever persisted on working although in pain.
- 27 subjects responded negatively to both questions.
- 17 subjects noted that they have kept on their production although in pain, but never wanted to stop.

The author once again puts forward the theory that pain is considered by the volunteers as part of their job, hence they accept the muscular pain and keep on persisting with their production. In fact only a small percentage decided to stop work due to their pain.

Sick leave (Q22 & 22a)

In the following question the subjects were asked if they have ever benefited from sick leave due to pain caused during fireworks manufacturing and the duration of such leave.

Four subjects gave a positive answer. Three subjects of these formed part of the sample that had to stop their production because of the pain. The fourth

subject who took sick leave previously reported having kept on working although suffering pain.

The sick leave duration of 50% of the subjects was not longer than 3 days whilst the other 50% were absent from work from 4 to 10 days.

Education – occupational health & safety principles and manual handling (Q23 & 24)

The subjects were asked if they ever received occupational health & safety and/or manual handling training in the context of fireworks production.

It can be clearly noted that the lack of training is spread across all the manufacturing years. A concentration of 'OHS trained' is found in less experienced manufacturers. The author realised that the only official training these fireworkers get on fireworks production is during a special course held prior to the granting of licences A or B.

During this 12 hour course a 2 hour session is allowed for occupational health and safety. During this very short session very basic OHS principles are explained to the attendees and the lecturer almost completely bases his talk on the toxicity of chemicals. He only spends 15 minutes dealing with ergonomics and no training in manual handling at fireworks factories is ever practised.

As previously stated the short course, which is meant to grant a licence for fireworks production, does not include any manual handling training. 56.9% of the sample gave a negative response to the question, thus confirming that they were never given any training in manual handling during fireworks production.

As previously stated the short licence granting course does not include any manual handling training and since the questionnaire was self administered the 22 respondents who chose 'Yes' as their answer must have been misled by the question and confused other manual handling training undertaken at any other place. Hopefully they are putting this training into practice during their fireworks manufacturing. A quick review of these subjects shows that 10 out of 22 perform lifting of heavy items at their place of work in the manufacturing and construction industries.

Conclusion

The manufacturing of fireworks is a local culture which is highly esteemed by the international fireworks community. Nearly 1000 licensed predominantly male voluntary fireworkers put into practice their artisan capabilities at the local fireworks factories across Malta and Gozo. Rivalry between these enthusiasts drives them into strenuous manufacturing processes, which results in spectacular fireworks shows during the summer period. In the attempt to manufacture better shells, these enthusiasts put into practice riskier tasks, in an already hazardous workplace.

The selected sample showed a median height of 1.61–1.70 m (41.18%) with an average weight of 71–80 kg (33.33%) and a very wide range (18 to >65) in age distribution. The majority worked in demanding employment sectors prior to their voluntary tasks (5.48 hours per worker of average extra working time) at the fireworks factories. All of these factors play an important part in the musculoskeletal conditions reported by those voluntarily employed in fireworks factories.

Further studies would be required to provide the statistical significance of the origin of musculoskeletal complaints amongst those 'employed' in such activities following a full day's work in these sectors, although 63% of the respondents did not admit to aches, pains or sporting activities. Firework manufacturing processes require a large number of hand, wrist and upper arm movements. These involve whole body movements such as twisting, bending and both carrying and pushing loads

From an ergonomic perspective the levels of risk from the tasks performed at the fireworks factories increases when conditions such as time and workspace are considered. Reported results show that on an average working day the voluntary workers spend several hours working on a myriad tasks at the factories. The carrying of black powder in the sunshine and spiking of shells larger than 5 inches in diameter were tagged as being the most frequent job and the most tiring job at the factories respectively. Results show that fireworks manufacturing causes most pain in the upper body parts, mainly in the hands and wrists, and this is all attributed to repetitive motions and continuous forces exerted with hands, arms and

upper torso. 72% of the respondents agreed that all of this is made worse due to stress imposed by the multitude of tasks which is to be completed within defined timeframes, the limited time available for manufacturing the fireworks and ever increasing pressure by supporters and sponsors.

Training in posture, manual handling and an improved working environment would go a long way to reducing work-related musculoskeletal conditions at fireworks factories.

References

- 1 Laws of Malta, *Explosives Ordinance*, Chapter 33.
- 2 T. Shimizu, *Fireworks – The Art, Science and Technique*, Pyrotechnica Publications, 3rd edition, Texas, USA, 1981, p. 261.
- 3 R. Lancaster, *Fireworks – Principles and Practices*, Chemical Publishing Company, 3rd edition, New York, USA, 1998.
- 4 T. Shimizu, *Fireworks – The Art, Science and Technique*, Pyrotechnica Publications, 3rd edition, Texas, USA, 1981, pp. 292–297.
- 5 <http://www.medicinenet.com/script/main/art.asp?articlekey=41343&pf=3&page=1>, 26th September 2007
- 6 *Research on Work-Related Low Back Disorders*, European Agency for Safety and Health at Work, Belgium, 2000, p. 12.
- 7 *Research on Work-Related Low Back Disorders*, European Agency for Safety and Health at Work, Belgium, 2000, p. 19.

Bibliography

- E. Contestabile, R. Guilbeault, D. Wilson and B. von Rosen, 'Fireworks Shells Subjected to a Modified Height-to-Detonation Test', *Journal of Pyrotechnics*, Issue No. 20, p. 55, Winter 2004.
- A. Fischer, 'A practical Performance Testing Protocol for Fireworks Mortar Tubes', *Journal of Pyrotechnics*, Issue No. 20, p. 51, Winter 2004.
- Giving Your Own Fireworks Display*, Health and Safety Executive, Crown, 2nd Edition, 2005.
- L. Homan, 'Pulverone-Polverone', *American Fireworks News*, Issue 264, p. 1, September 2003.

<http://www.ergonomics.org.uk>, 11th June 2007

<http://en.wikipedia.org>, 21st and 29th August 2007.

<http://www.ergonomics4schools.com>, 11th June 2007

Laws of Malta, *Protection Against Risks of Back Injury at Work Places Regulations*, Legal Notice 35 of 2003, Chapter 424.

Laws of Malta, *Occupational Health and Safety Authority Act*, Chapter 424.

S. Muscat, *The Magnitude of Back Pain and Musculoskeletal Disorders in the Maltese Catering Industry*, University of Malta, 2006.

S. G. Myatt, 'Observations on the Behavior of Seamed Steel Mortar Tubes', *Journal of Pyrotechnics*, Issue No. 1, p. 6, Summer 1995.

M. Rossol, 'Health Effects from Theatrical Pyrotechnics', *Journal of Pyrotechnics*, Issue No. 3, p. 14, Summer 1996.

J. Theuma, *Awareness of Hazards of Toxic Materials Used in Fireworks*, University of Malta, 2006.

M. A. Williams, 'Modern Rack and Mortar Designs for Professional Fireworks Displays', *Journal of Pyrotechnics*, Issue No. 2, p. 6, Winter 1995.

Working Together on Fireworks Displays, Health and Safety Executive, Crown, 3rd Edition, 2006.

Appendix

List of processes as given on the questionnaire

- A Rolling of beraq casings
- B Rolling of shells casings
- C Filling up and closing of beraq casings.
- D Spiking of beraq
- E Priming of beraq
- F Placing of beraq inside shell casings
- G Cutting of cardboard discs by hand
- H Cutting of cardboard discs by motorized blade
- I Carrying of materials from vehicles to stores

- J Carrying of material from stores to barrel room
- K Putting in and/or taking out material from barrel
- L Sieving of black powder
- M Carrying of black powder filled trays into sunshine
- N Mixing of colour and/or flash compositions
- O Pressing of stars
- P Priming of stars
- Q Placing of stars inside shell casings
- R Closure of shells
- S Pressing of spouettes and/or drivers by hand.
- T Pressing of spouettes and/or drivers by pressing machine
- U Spiking of big shells (5 inches and over in diameter)
- V Spiking of small shells
- W Mounting of multi-break shells
- X Paper gluing of shells
- Y Placing in of lifting charge, shock absorbers and leaders onto shells
- Z Placing of lifting charge and leaders to finale shells
- AA Manufacture of quickmatch
- AB Charging of lances
- AC Preparation works on ground fireworks.
- AD Sieving of charcoal
- AE Others

Book Review: Initiation of Explosives & Pyrotechnic Materials

By: Jean-Rene Duguet – R&D Manager and Consultant in Pyrotechnics.

Preface by: Dr Attie Goosen

Published by: Cultures et Techniques – cultures.techniques@hotmail.fr

ISBN: 978-2-918209-02-7

Price: 50Euros

This small paperback book is packed with information on the chemistry and mechanics of initiation and has extensive chapters on:-

- General outline
- Explosives and Production Processes
- Initiators and Related Devices
- Metrology and Safety

There is extensive detail of the physical characteristics of initiating substances, together with formulations and a good section on sensitivity of various initiating explosives. However the book is somewhat frustrating in so much that the scale and clarity of diagrams and images varies widely, and chemical formulae are inconsistently portrayed. It is also expensive for a 221page paperback (50 Euros) and I felt that I could have certainly lived with a smaller and more consistent typeface throughout if it left more room for bigger diagrams or had reduced the size and price of the book as a result.

Nevertheless I would recommend this book for the bookshelves of practitioners in almost any area of pyrotechnics and explosives – initiation is often poorly understood, and this book does much to inform the reader in this most important subject.

Information for Readers

Editorial Policy

Articles accepted for publication in the *Journal of Pyrotechnics* can be on any technical subject in pyrotechnics. However, a strong preference will be given to articles reporting on research (conducted by professional or serious individual experimenters) and to review articles (either at an advanced or tutorial level). Both long and short articles will be gladly accepted. Also, responsible letters commenting on past Journal articles will be published along with responses by the authors.

Back Issues

Back issues of the Journal will be kept in print permanently as reference material. In addition all past articles and issues are available at the *Journal of Pyrotechnics* - <http://archive.jpYRO.com>.

New Publication Procedures

As announced in Issue 26, the JPYro Board has decided that the Journal will be first published in electronic form and that the hard copy will be published annually. This has been driven by three main factors - the needs of authors to have their papers published in a reasonable timescale, the success of the JPYro archive, and the costs and time required to produce hard copies. In addition the modern publishing and research worlds increasingly rely on early electronic publication to provide information to others in the most timely manner and, as appropriate, to be able to claim Intellectual Property rights on material published (which are taken from the date of publication).

In future articles accepted for publication in the Journal will be published, in the first instance, electronically on the JPYro archive website (<http://archive.jpYRO.com>) within a target timescale of three weeks from acceptance (i.e. when all editing is complete) and eight weeks from original submission. All articles will be dated and published in acceptance order. The timescales rely, of course, on referees and authors responding in a reasonable timescale to any queries raised.

In this way no article will be held up awaiting the collation of all the other material necessary for economic and efficient production of the hard copy. Instead, a hard copy of the Journal will be available to those who require it, in most cases annually - incorporating all the articles published within the previous year - for an additional charge. In addition, the JPYro archive will continue to offer online purchase of single articles from the Journal and other publications, or time-limited access to the entire archive.

If you have any questions regarding the new approach please do contact any of the production team

Publication Frequency

Articles in the *Journal of Pyrotechnics* will appear first electronically at <http://archive.jpYRO.com> and will subsequently be produced in hard copy annually in the early spring of the year following publication.

Subscriptions

The following subscription types are available

- Electronic only - access to the electronic versions of articles published during the subscription period indefinitely
- Electronic and Hard copy - as above + hard copy when published
- Single article access - indefinite access to the specified article
- Access to the entire archive - annual access to the full archive

Sponsors

Individual Sponsor

Gerald Laib

17611 Longview Lane
Olney, MD 20832, USA
phone: 301-744-4358
fax: 301-744-4784

Corporate Sponsors

Allied Specialty Insurance

Rick D'Aprile
10451 Gulf Blvd.
Treasure Island, FL 33706, USA
phone: 800-237-3355
fax: 727-367-1407
email: info@alliedspeciality.com
web: <http://www.alliedspeciality.com>

American Fireworks News

Jack Drewes
HC 67 Box 30
Dingmans Ferry, PA 18328, USA
phone: 570-828-8417
fax: 570-828-8695
email: afn@fireworksnews.com
web: <http://www.fireworksnews.com>

American Pyrotechnics Association

Julie Heckman
4808 Moorland Lane - Ste 109
Bethesda, MD 20814, USA
phone: 301-907-8181
fax: 301-907-9148
email: jheckman@americanpyro.com
web: <http://www.americanpyro.com>

Canadian Explosives Research Laboratory

Dr Phil Lightfoot, Manager
CANMET - 555 Booth St.
Ottawa, ON K1A 0G1, Canada
phone: 613-947-7533
fax: 613-995-1230
email: plightfo@nrca.gc.ca
web: <http://www.nrca.gc.ca/mms/cerl>

Combined Specialities International Inc.

John & Alice Allen
8362 Tamarack Village, Ste. 119
Woodbury, MN 55125, USA
phone: 651-855-0091
fax: 651-855-0088
email: jallen@combinedspecialities.com

Davas Ltd

Tom Smith
8 Aragon Place, Kimbolton, Huntingdon
Cams. UK. PE28 0JD
phone: +44 1480 860124
fax: +44 1480 861125
email: toms@davas.co.uk
web: <http://www.davas.co.uk>

Daveyfire, Inc.

Alan Broca
2121 N California Blvd. Ste. 290
Walnut Creek, CA 94596, USA
phone: 925-926-6414
fax: 925-926-6439
email: info@daveyfire.com

European Pyrotechnic Arts Newsletter

Rob Driessen
Grenadierweg 55
Riemst, B 3770, Belgium
phone: +32-12-210-630
fax: +32-12-210-630
email: epan@pandora.be
web: <http://users.pandora.be/epan>

Fire One

Dan Barker
863 Benner Pike
State College, PA 16801, USA
phone: 814-238-5334
fax: 814-231-0799
email: info@fireone.com
web: <http://www.fireone.com>

Firework Professionals

Anthony Leyland
PO Box 19-912
Christchurch, 8030, New Zealand
phone: +64-3-982-3473
fax: +64-3-982-3474
email: firework@firework.co.nz
web: <http://firework.co.nz>

Fireworks

PO Box 40
Bexhill, Sussex TN40 1GX, England
phone: +44-1424-733-050
fax: +44-1424-733-050
email: editor@fireworks-mag.org
web: <http://www.fireworks-mag.org>

Fireworks and Stage FX America

Joseph R. Bartolotta
PO Box 488
Lakeside, CA 92040, USA
phone: 619-938-8277
fax: 619-938-8273
email: info@fireworksamerica.com
web: <http://www.fireworksamerica.com>

Fireworks Business

Jack Drewes
HC 67 Box 30
Dingmans Ferry, PA 18328, USA
phone: 717-828-8417
fax: 717-828-8695
email: afn@fireworksnews.com
web: <http://www.fireworksnews.com>

Fireworks by Grucci

Phil Grucci
1 Grucci Lane
Brookhaven, NY 11719, USA
phone: 631-286-0088
fax: 631-286-9036
email: philgrucci@aol.com
web: <http://www.grucci.com>

Fullam's Fireworks Inc

Rick Fullam
PO Box 1808 CVSR
Moab, UT 84532, USA
phone: 435-259-2666
email: rfullam_3@yahoo.com

Goex Inc.

Donald McDonald
PO Box 659
Doyline, LA 71023, USA
phone: 318-382-9300
fax: 318-382-9303
email: email@goexpowder.com
web: <http://www.goexpowder.com>

Lantis Fireworks & Lasers

Ken Lantis
PO Box 491
Draper, UT 84020, USA
phone: 801-768-2255
fax: 801-768-2433
email: info@fireworks-lasers.com
web: <http://www.fireworks-lasers.com>

MagicFire Inc

Paul McKinley
PO Box 896
Natick, MA 01760, USA
phone: 508-647-9645
fax: 508-647-9646
email: pyrotech@magicfire.com
web: <http://www.magicfire.com>

Martin-Baker Aircraft Ltd

David Chapman
Lower Rd, Higher Denham
Uxbridge, Middlesex UB9 5AJ
Great Britain
Phone: 44-1895-836-644
FAX: 44-1985-836-686
email: dchapman@martin-baker.co.uk
web: www.martin-baker.com

Martinez Specialities

Phil Martinez
208 Bossard Rd
Groton, NY 13073, USA
phone: 607-898-3053
fax: 607-898-3952
email: mr.squib@clarityconnect.com

Maratamaya Ogatsu Fireworks Co. Ltd.

1-35-35 Oshitate Fuchu
Tokyo, 183-0012, Japan
phone: +81 42-363-6251
fax: +81-42-363-6252
email: hanabi@mof.co.jp
web: <http://www.mof.co.jp>

MP Associates Inc.

PO Box 546
Ione, CA 94640, USA
phone: 209-274-4715
fax: 209-274-4843

Nitrotech Australia Pty. Ltd.

Chris Larkin
PO Box 349
Mount Isa, QLD 4825, Australia
phone: 617-47-44-2290
fax: 617-47-44-3998
email: nitrotech@smartchat.net.au

Precocious Pyrotechnics Inc.

Garry Hanson
4420 278th Ave NW
Belgrade, MN 56312, USA
phone: 320-346-2201
fax: 320-346-2403
email: ppinc@tds.net
web: <http://www.pyro-pro.com>

Pyro Shows Inc.

Lansden Hill
PO Box 1406
LaFollette, TN 37766, USA
phone: 800-662-1331
fax: 423-562-9171
email: info@pyroshows.com
web: <http://pyroshows.com>

Pyrodigital Consultants

Ken Nixon
1074 Wranglers Trail
Pebble Beach, CA 93953, USA
phone: 831-375-9489
fax: 831-375-5255
email: pyrodig@aol.com
web: <http://www.infinityvisions.com/pyrodigital>

PyroLabs Inc.

Ken Kosanke
1775 Blair Road
Whitewater, CO 81527, USA
phone: 970-245-0692
fax: 970-245-0692
email: ken@jpyro.com

RCS Rocket Motor Components Inc.

Gary Rosenfield
2113 W 850 N St
Cedar City, UT 84720, USA
phone: 435-865-7100
fax: 435-865-7120
email: garyr@powernet.net
web: <http://www.rocketmotorparts.com>

RES Speciality Pyrotechnics

Steve Coman
21595 286th St
Belle Plaine, MN 56011, USA
phone: 952-873-3113
fax: 952-873-2859
email: respyro@earthlink.net
web: <http://www.respyro.com>

Rozzi Famous Fireworks

Arthur Rozzi
PO Box 5
Loveland, OH 45140, USA
phone: 513-683-0620
fax: 513-683-2043
email: art@rozzifireworks.com
web: <http://www.rozzifireworks.com>

Service Chemical Inc.

Ben Cutler
2651 Penn Avenue
Hatfield, PA 19440, USA
phone: 215-362-0411
fax: 215-362-2578
email: ben@servicechemical.com
web: <http://www.servicechemical.com>

Spirit of 76 Fireworks

John Bechtold
6401 West Highway 40
Columbia, MO 65202, USA
phone: 573-477-1776
fax: 573-477-1786
email: marketing@76wholesale.com
web: <http://www.76wholesale.com>

Starburst Pyrotechnics & Fireworks Displays Ltd

Bonnie Pon
2nd Fl-Sui Hing Hong Bldg-17, Commissioner St
Johannesburg, Gauteng 2000, South Africa
phone: +27-11-838-7705
fax: +27-11-836-6836
email: info@starburstpyro.co.za
web: <http://www.starburstpyro.co.za>

Weeth and Associates

Charlie Weeth

122 S 17th St

LaCrosse, WI 54601, USA

phone: 608-784-3212

fax: 608-782-2822

email: czweeth@pyro-pages.com

web: <http://www.pyro-pages.com>

Please note

It is our intention in future to maintain an up-to-date list of current sponsors on the JPyro website and not to publish details in the hard-copy edition of the Journal. If there are any changes to your details please email sponsors@jpyro.com.

Events

Now that the Journal of Pyrotecnics is published, primarily, electronically the forthcoming events are available on the archive website <http://archives.jpYRO.com>.

If you have any events you would like included in that list please contact the publisher

Caution

The experimentation with, and the use of, pyrotechnic materials can be dangerous and may require licences or permits in certain countries; it is felt to be important for the reader to be duly cautioned. Without the proper training and experience no one should ever experiment with or use pyrotechnic materials. Also, the amount of information presented in this Journal is not a substitute for necessary training and experience, nor does it remove the relevant application of national or local laws and regulations.

A major effort has been undertaken to review all articles for correctness. However it is possible that errors remain. It is the responsibility of the reader to verify any information herein before applying that information in situations where death, injury or property damage could result.